Deciphering the Biological Basis of Acute Myeloid Leukemia Relapse Using a Novel In-Vitro Study Model

by

Justine Lai

A thesis submitted in partial fulfillment of the requirements for the degree of

Doctor of Philosophy

Department of Medicine
University of Alberta

Abstract

Acute myeloid leukemia (AML) is an aggressive hematologic malignancy associated with a poor clinical outcome that is largely attributed to disease relapses. Treatment options for relapsed AML patients are limited; after relapse, the median survival is only ~6 months. The biology underlying relapse is not well understood, and mechanistic studies of AML relapse are scarce, largely because appropriate study models are lacking. Nonetheless, there are several interrelated hypothetical models linked to the concept of cancer stem cells (CSCs). CSCs, which represent a very small subset of the leukemic cell population, survive the induction/consolidation chemotherapy, and they emerge and re-populate the entire leukemic population (i.e. relapse) after a period of dormancy (i.e. remission). This concept is difficult to prove as the definition of CSCs remains to be elusive and study models are lacking.

The key aim of this study was to examine the validity of the CSC model to explain AML relapse. To identify cancer stem-like (CSL) cells, the SORE6 reporter was employed, which has shown to be useful in detecting/purifying CSL cells; however, this study is the first to use SORE6 to investigate AML. In two *FLT3*-mutated AML cell lines, MOLM-13 and MV4-11, the $SORE6^-$ /$SORE6^+$ dichotomy existed, with $SORE6^+$ cells being significantly more CSL than $SORE6^-$ cells. These two subsets were employed to develop an *in-vitro* model mimicking clinical features of AML relapse. Specifically, after the Ara-C induction of 'zero viability' in which viable cells were undetectable by direct microscopic examination, cells regenerated on day 18±2 of the experiment. These phenomena mimic clinical remission and relapse and are thus labeled *in-vitro* remission and *in-vitro* relapse, respectively. By molecularly barcoding $SORE6^-$ and $SORE6^+$ cells, the relative contributions of original $SORE6^-$ and $SORE6^+$ cells could be determined at *in-vitro* relapse, even if they lose/gain SORE6 activity. Barcode analysis revealed that most *in-vitro* relapse cells were

derived from the original SORE6$^+$ cells and exhibited higher CSL features compared to original SORE6$^+$ cells, even though a proportion of them lost SORE6 activity. Using Myc as the surrogate marker for SORE6$^+$ cells, relapsed patient samples showed an expansion of CSL cells.

Next, different therapeutic agents were tested in the *in-vitro* relapse model to determine if SORE6$^+$ cells are important to all relapses. 5-azacitidine (AZA) or the combination of AZA and Venetoclax (Ven) (i.e. AZA+Ven) were used since these two regimens were recently tested in a large clinical trial, with AZA+Ven being significantly superior to AZA in prolonging disease-free survival. Correlating with the clinical data, *in-vitro* relapse occurred on day 13±1 with AZA, whereas *in-vitro* relapse did not occur at the endpoint (day 30) with AZA+Ven. In contrast to Ara-C, molecular barcoding and flow cytometry analysis of *in-vitro* relapse cells after AZA and AZA+Ven treatment did not show the expansion of SORE6$^+$ cells. Using metabolomic analysis, ornithine decarboxylase (ODC) was identified as a marker for CSL expansion. ODC was upregulated in the Ara-C condition, but not in the AZA and AZA+Ven conditions, correlating with barcoding analysis. Additionally, ODC expression was heterogeneous in a cohort of 12 relapsed AML patient samples; however relapsed samples had a significantly higher level of ODC compared to initial diagnostic specimens.

The utility of the *in-vitro* study model was further examined by investigating the mechanisms underlying the high chemoresistance in SORE6$^+$ cells. The autophagic capacity of SORE6$^+$ cells was examined, as autophagy has been shown to confer chemoresistance. Using standard autophagy assays, SORE6$^+$ cells carried significantly higher autophagic flux after Ara-C treatment, and inhibition of autophagy significantly sensitized SORE6$^+$ cells to Ara-C. Using an autophagy PCR array, ULK2 was identified as an important mediator for the high autophagy capacity in SORE6$^+$ cells. Pharmacologic inhibition of ULK2 significantly sensitized SORE6$^+$,

but not SORE6^{-}, cells to Ara-C. Using the *in-vitro* model for relapse, higher ULK2 expression was found in regenerated AML cells compared to untreated cells, and pharmacological inhibition of ULK2 prevented *in-vitro* relapse. Finally, ULK2 expression was higher in relapsed compared to initial diagnostic AML specimens.

In conclusion, while CSL cells appear to be the major contributors to AML relapse in certain settings, CSL cells may not be uniformly important. While further validation studies are required, the generated *in-vitro* relapse model is useful in developing concepts and hypothetical models to study AML relapse.

Preface

This thesis is an original work by Justine Lai. The studies included in this thesis have received ethics approval for the use of human participants by the Health Research Ethics Board of Alberta (HREBA.CC-21-0253).

A version of Chapter 2 of this thesis has been published as:
Lai J, Shang C, Chen W, Izevbaye I, Chu MP, Sandhu I, Brandwein J, Lai R, Wang P. An In Vitro Model for Acute Myeloid Leukemia Relapse Using the SORE6 Reporter. Int J Mol Sci. 2024; 25(1):496.

A version of Chapter 4 of this thesis has been published as:
Lai J, Yang C, Shang C, Chen W, Chu MP, Brandwein J, Lai R, Wang P. ULK2 Is a Key Pro-Autophagy Protein That Contributes to the High Chemoresistance and Disease Relapse in FLT3-Mutated Acute Myeloid Leukemia. Int J Mol Sci. 2024; 25(1):646.

In these manuscripts, I performed the experiments, analyzed the data, generated figures, and wrote the manuscripts. Co-authors of the manuscripts modified from Chapters 2 and 4 contributed to idea generation, writing and editing of the manuscripts, and obtained resources, including reagents and patient samples.

Metabolomic studies in Chapter 3 were performed in the Metabolomic core facility directed by Dr. Liang Li (Professor, Department of Chemistry, U of Alberta). Glycomic studies were performed using the facilities provided by the Derda Research Group (Department of Chemistry, U of Alberta). I performed the data and statistical analysis.

Acknowledgements

First and foremost, I would like to express my greatest gratitude to my supervisor, Dr. Peng Wang, who has been a great role model for me. Thank you for your patience and guidance throughout these past few years and for always making time to discuss my research despite your clinical obligations. I also would like to thank my co-supervisor, Dr. Joseph Brandwein, and my supervisory member Dr. Ismail Ismail, for providing me the much-needed advice throughout my studies.

Thank you to all of my past and present lab members for your willingness to help, provide advice, and for keeping me company during the long hours in the lab.

My family has been very supportive over the past few years and have been instrumental in my success. Dad, thank you for all of your advice and for sharing your love of science with me. Thank you, Mom, for your continuous encouragement, support, and belief in me. To Aidan and Brendon, thanks for always being able to make me laugh even during times of disappointment.

Table of Contents

List of Tables

Chapter 1

Chapter 3

Chapter 4

List of Figures

Chapter 1

Chapter 2

Chapter 3

Chapter 4

Chapter 5

List of Abbreviations

ALDH	Aldehyde dehydrogenase
AML	Acute myeloid leukemia
Ara-C	Cytarabine
ATG	Autophagy related gene
AZA	5-Azacitidine
AZA+Ven	5-Azacitidine with Venetoclax
CBM	Carbohydrate-binding molecule
CQ	Chloroquine
CR	Complete remission
CSC	Cancer stem cell
CSL	Cancer stem-like
EMT	Epithelial-mesenchymal transition
ESC	Embryonic stem cell
FDA	Food and Drug Administration
FLT3	Fms-like tyrosine kinase 3
GFP	Green fluorescent protein
HCQ	Hydroxychloroquine
HMA	Hypomethylating agent
HSC	Hematopoietic stem cell

IR	*In-vitro* relapse
ITD	Internal tandem duplication
MBP	Maltose-binding protein
ODC	Ornithine decarboxylase
OS	Overall survival
R/R	Relapse/refractory
ROS	Reactive oxygen species
SORE6	Sox2/Oct4 response element
SRR2	Sox2 regulatory region-2
STAT5	Signal transducer and activator of transcription factor 5
TKD	Tyrosine kinase domain
ULK1/2	Unc-51-like kinase 1/2
Ven	Venetoclax

Chapter 1

Introduction

1.1. Acute Myeloid Leukemia (AML)

1.1.1. Definition, incidence and clinical characteristics of AML

Acute myeloid leukemia (AML) is a hematologic malignancy characterized by an accumulation of undifferentiated cells (i.e. blasts) in the bone marrow and/or peripheral blood. A diagnosis of AML is made when the blast count is ≥20%; however, ≥10% blasts are required if an AML-defining genetic alteration is present (e.g. *NPM1* mutation, t(8;21)(q22;q22.1)/*RUNX1* ::*RUNX1T1*) (1, 2). In AML, the blast population shows maturation arrest at the level of myeloblasts, the precursors of granulocytes, red cells, and platelets. Although the pathogenesis of AML is incompletely understood, it is widely accepted that AML leukemogenesis is a multi-step process involving sequential gain-of-function of oncogenes and/or loss-of-function of tumor suppressors. Evidence to support this concept has come from studies using transgenic mouse models as well as various clinical observations. In the transgenic mouse models, it was found that animals expressing specific recurrent genetic mutations identified in AML clinical samples typically do not promptly trigger the development of AML unless a second mutation was introduced (3, 4). The clinical observation that patients diagnosed with myelodysplastic syndromes or myeloproliferative neoplasms can rapidly develop into AML also supports this concept (1). Attention has been focused on two groups of gene mutations: those involved in the deregulations of cell proliferation (Class I mutations, such as *FLT3*) and mutations involved in the inhibition of cell differentiation (Class II, such as *NPM1* (5). Mutations of the so-called Class 3 genes, such as those regulating epigenetics (e.g. *DNMT3A* and *IDH1/2*) are frequently found in AML but their roles in leukemogenesis are yet to be defined. The combined biologic effect of Class I and II mutations leads to the uncontrollable proliferation of blasts in the bone marrow which, if untreated, results in bone marrow failure (6). Patients frequently present with the clinical manifestations of anemia (weakness and shortness of breath), leukopenia (frequent infections) and thrombocytopenia (bleeding) (7). AML also can result in hyperleukocytosis (i.e. white blood cell count >100,000/μL) which may acutely occlude the vasculatures in the lungs and the central nervous system, a highly dangerous scenario (8). Leukemic infiltration of hematologic organs including the spleen, liver and lymph nodes may produce organomegaly and/or lymphadenopathy,

which may be a prominent clinical manifestation at presentation (9, 10). Disseminated intravascular coagulation (commonly called DIC), a well-recognized medical emergency, is most often associated with promyelocytic leukemia characterized by the *t(15;17)* cytogenetic abnormality, a subtype of AML (11).

AML accounts for 80-90% of all adult cases of acute leukemia (12). In the United States, over 20,000 individuals are diagnosed with AML per year, and AML accounts for 1.9% of all cancer deaths that year (5, 13). The overall 5-year relative survival for AML between 2013-2019 was 31.7% (13). For patients that are ≥65 years, prognosis is especially poor; the median survival for these patients is a dismal 6 months (14).

1.1.2. Grouping and risk factors of AML

Given the biological heterogeneity of AML, several classification systems have been generated to provide a unified concept. Historically, AML was classified using the French American British (FAB) system, established in 1976, which is based on blast maturation and differentiation. In this classification system, AML was divided into subtypes, from M0-M7 (15). More recently, a new classification system published by the Who Health Organization (WHO) has been developed based on the existence of pre-existing conditions and associated risk factors (2). This classification system, which was most recently updated in 2022, recognizes several major groups of AML. The first group includes those who have received prior cytotoxic therapy for cancers or other non-neoplastic medical conditions. It is well recognized that patients who have received alkylating agents, nucleoside analogs, topoisomerase II inhibitors, anti-tubulins as well as ionizing radiation are at risk of developing AML, typically with a latency period of 3-7 years (16). The prognosis for therapy-related AML is extremely poor, and the median survival of these patient is approximately 10 months (17).

The second well-recognized group of AML patients are those who have been previously diagnosed with myelodysplastic syndrome or chronic myeloproliferative disorders (such as chronic myeloid leukemia or myelofibrosis). At presentation, the blast count of these patients is typically normal and only slightly elevated. With disease progression, a subset of these patients develops increasing

percentages of blasts in the bone marrow and/or peripheral blood, often associated with the acquisition of additional cytogenetic abnormalities. A diagnosis of AML is made when ≥20% blasts showing features of myeloid differentiation are identified in the bone marrow or blood (18).

The third group include those who carry certain germline mutations that are known to be associated with AML. Perhaps the best-known association in this regard is that of Down syndrome and AML (19).

The fourth group, which is by far the largest group, are cases in which there is no prior exposure to cytotoxic drugs, history of myelodysplasia/chronic myeloproliferative disorder or specific germline mutations. These cases are often referred to as '*de novo* AML'. Notably, many of these cases carry recurrent genetic abnormalities such as those involving the *NPM1* and *FLT3* genes (1). The identification of *NPM1* and *FLT3* mutations carries significant prognostic and therapeutic implications such that these genes are routinely tested in virtually all newly diagnosed AML cases. This group will be further discussed in Section 1.1.3.

The other two groups that are also recognized are 5) myeloid sarcoma (i.e. cases presenting primarily as soft tissue masses) and 6) AML not otherwise specified.

A number of occupational risk factors also have been identified. Workers who have exposure to rubber, paint, pesticides, ethylene oxide, petroleum and ionizing radiation have been found to have a high risk of developing AML (20). Benzene exposure, smoking and obesity also have been found to be associated with a higher risk of AML (20-22).

1.1.3. Common genetic abnormalities in AML

Based on the WHO classification of hematologic neoplasms, a minimum of 20% myeloblasts present in the bone marrow and/or peripheral blood is required for the diagnosis of AML unless an AML-defining genetic alteration is present (2). As mentioned above, within the group of AML with recurrent genetic abnormalities, certain molecular markers or signatures have been found to be prognostically important and thus, they are recognized as distinct entities under this group.

These distinct entities are further grouped as favorable, intermediate, and adverse. As an example, two of the most common AML mutations, *NPM1* and *FLT3*-ITD mutations, are associated with a favorable and intermediate risk, respectively (1). Molecular abnormalities associated with the adverse risk include mutated *TP53, ASLX1* and *RUNX1* (1, 23).

Mutations of the two most common genes, *NPM1* and *FLT3*, will be further elaborated below. A few relatively common recurrent genetic abnormalities are briefly described below:

a. AML with DNMT3A mutations

DNMT3A mutations occur in approximately 20% of AML cases (6). The prognostic significance remains to be controversial, as some studies have associated this mutation with a poor prognosis, while other studies have shown there is no correlation between *DNMT3A* mutations and prognostic classification (24). *DNMT3A* mutations result in aberrant DNA methylation, affecting normal hematopoiesis (25).

b. AML with IDH1/2 mutations

IDH mutations are found in 20% of all AML cases and can occur in either *IDH1* or *IDH2*, both of which encode dehydrogenases (6). These mutations are gain-of-function mutations, resulting in the production of 2-hydroxyglutate, an oncometabolite that interrupts normal hematopoiesis (26). The prognostic significance of *IDH1/2* mutations is not well understood, as some studies have associated these mutations with unfavourable outcomes, while other studies did not show any effect on clinical outcome (27).

c. AML with RUNX1 mutations

RUNX1, a transcription factor regulating HSC differentiation, is mutated in 10-15% of AML patients (28). This mutation, typically appearing as a missense or frameshift mutation, causes impairments in differentiation and ribosome biogenesis (29). AML cases with this mutation are classified as adverse risk by the European LeukemiaNet (1).

d. AML with TP53 mutations

TP53, a well-known tumor suppressor gene involved in apoptosis, senescence, and DNA repair pathways, is mutated in approximately 10% of AML cases or myelodysplastic syndrome (30). This mutation has been shown to act in a dominant-negative effect, inhibiting the activity of wild-type p53 (31). *TP53* mutations in AML are associated with an adverse risk (1).

1.1.4. The biology of leukemogenesis

In addition to their prognostic value, these genetic abnormalities have provided opportunities to further our understanding of the biologic/molecular basis of leukemogenesis. The biology of some of the most common genetic abnormalities in AML, including mutations of *NPM1* and *FLT3*, has been extensively studied. A brief summary of these studies is provided in this section. The biology of FLT3 and its mutations will be detailed in this thesis, in view of the fact that I chose *FLT3*-mutated AML as my study model.

a. FLT3 mutations in AML

FLT3 is a proto-oncogene that encodes a membrane-bound tyrosine kinase, and it is known to play crucial roles in normal hematopoiesis, specifically in the development of B-lymphocytes and hematopoietic stem cells. Accordingly, FLT3 proteins are highly expressed in undifferentiated myeloid and lymphoid cells (32). Homozygous deletion of *FLT3* in mice is not lethal, but these animals were found to have a reduced number of B cell progenitors (33). Gene transcription of *FLT3* is regulated by several proteins including MEIS1, PBX1/3 and MYB (34). Activation of FLT3 is initiated by the binding of FLT3 ligand, a member of the interleukin family, to the extracellular domain of FLT3, which triggers homodimerization of the FLT3 molecules at the cell surface. Consequently, the FLT3 homodimers undergo autophosphorylation, producing a signal cascade that will activate various proliferation and survival pathways including those of PI3K/AKT, MAPK/ERK, RAS and STAT5 (32, 35).

The FLT3 protein consists of 5 functional segments, illustrated in **Figure 1.1** (34-37):

a) **An extracellular domain** that is involved in ligand binding (amino acids 1-541).
b) **A transmembrane domain** that anchors the protein to the cell membrane (amino acids 542-564).

c) **A juxtamembrane domain** which interacts with the tyrosine kinase domain in the absence of the FLT3 ligand to block the ATP binding site, which prevents constitutive activation of FLT3 (amino acids 565-609).

d) **A tyrosine kinase domain and kinase insertion** which interacts with the juxtamembrane domain to prevent activation of FLT3 when FLT3 ligand is absent. This domain contains the activation loop, which shifts FLT3 between the active and inactive conformation (amino acids 610-944).

e) **An intracellular domain** which is located at the C-terminus of the protein. It contains phosphorylation sites that are associated with intracellular proteins involved in propagating the signaling cascade (amino acids 945-993).

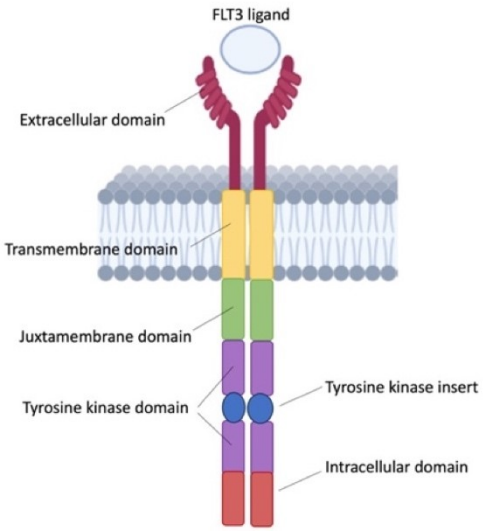

Figure 1.1. Structure of FLT3. FLT3 protein consists of an extracellular domain, transmembrane domain, juxtamembrane domain, a tyrosine kinase domain with a tyrosine kinase insert and an intracellular domain.

Mutations of *FLT3*, occurring in approximately 30% of all AML cases, are one of the most common mutations in AML (32). There are two main types of *FLT3*-mutations found in AML: *FLT3*-ITD (internal tandem duplication) which occurs in ~25% of all AML cases and *FLT3*-TKD (tyrosine kinase domain) which occurs in ~7% of AML cases (32). Detection of *FLT3* mutations is routinely performed in virtually all newly diagnosed AML cases because of the well-documented correlation between these genetic abnormalities and clinical outcome; multiple

clinical studies have shown that patients with *FLT3*-ITD have a significantly lower overall survival and higher rate of relapse compared to those with wild-type *FLT3* (38-40). While the presence of *FLT3*-ITD has a well-documented correlation with clinical outcome, the clinical significance of the less common *FLT3*-TKD is unknown (41).

FLT3-ITD, which results in the generation of a constitutively active tyrosine kinase, is believed to promote leukemogenesis by constitutively activating a host of cellular signaling pathways (42). *FLT3*-ITD is generated as a result of a duplication of the juxtamembrane domain, and these genetic alterations deregulate the function of the juxtamembrane domain, which normally prevents the activation of FLT3 in the absence of FLT3 ligand. Thus, the duplications result in the constitutive activation of FLT3 and its downstream signaling pathways. *FLT3*-ITD is considered to be a driver mutation and a Class I mutation (i.e. promote cell proliferation) (32). In keeping with the concept of multiple hits in leukemogenesis, *FLT3*-ITD transgenic mice were found to develop a form of myeloproliferative disorder, but they did not develop AML (43). However, with the addition of another mutation, *DNMT3A,* AML promptly developed in approximately half of the *FLT3*-ITD transgenic mice (44).

To further support the oncogenic properties of *FLT3*-ITD, the IL-3 dependent murine myeloblast-like cell line, 32D, and the murine pro-B cell line, BA/F3, transfected with *FLT3*-ITD were found to have increased cell proliferation, even without the addition of IL-3, when compared to those transfected with wild-type *FLT3*. Interestingly, transfection of wild-type *FLT3* into these cell lines also can promote the activation of MAPK and AKT but not that of STAT5 (45-47). STAT5 is believed to be a highly important signaling protein in the *FLT3*-ITD-mediated leukemogenesis, as this pathway represents the biggest difference in the activation patterns between BA/F3 cells transfected with wild-type *FLT3* and those transfected with *FLT3*-ITD. Constitutive activation of STAT5 is believed to promote AML leukemogenesis by activating a host of pro-survival and growth pathways and by increasing Myc expression (48, 49).

How *FLT3*-ITD mediates leukemogenesis remains to be incompletely understood. In addition to the constitutive activation of various proliferation pathways, one study suggests that *FLT3*-ITD may promote the survival of AML cells by deregulating autophagy (50). Specifically,

pharmacological and shRNA inhibition of *FLT3* in two *FLT3*-ITD-carrying AML cell lines, MOLM-14 and MV4-11, and *FLT3*-ITD AML patient samples, decreased basal autophagy, and inhibition of autophagy in these cells impeded their survival in a xenograft mouse model. Lastly, *FLT3* was found to be highly expressed in $CD34^{+}CD38^{-}$ cancer stem cells in *FLT3*-ITD-positive AML. *FLT3*-ITD appears to promote the survival of these cells by activating the STAT5/MCL-1, a pro-survival pathway (51).

b. NPM1 mutations

NPM1 mutations are observed in about one-third of all AML cases, making it one of the most common mutations found in AML (52). It is well-documented that *NPM1* mutations confer a favourable clinical outcome (1).

NPM1 is biologically important, as homozygous deletion of this gene is embryonically lethal (53). NPM1, which is highly expressed in normal cells, shuttles between the nucleus and cytoplasm but it is localized most abundantly in the nucleoli (54). It can regulate a wide range of cellular processes. Its key known functions fall into the following categories: DNA repair, chaperoning of histones, stress response, regulation of apoptosis, ribosome synthesis and centrosome duplication (55).

Correlating with its multi-functionality, NPM1 is structurally divided into 4 segments:

a) N-terminal domain is responsible for self-oligomerization, and it functions as a histone chaperone. It mediates the interactions between NPM1 and many other proteins including Fbw7-gamma, a promoter of Myc degradation (56). This domain contains two nuclear export signal (NES) domains (orange boxes - amino acids, 42-49; 94-102).
b) Central domain carries two acidic regions that are responsible for histone and ribosomal binding, as well as two bipartite nuclear localization signal (NLS) regions (green boxes – amino acids 152-157; 190-197).
c) Heterodimerization region carries a basic region (amino acids 189-243) that can bind to DNA and mediate protein-protein interactions. Proteins that bind to this region include p53 and FOXM1.

d) C-terminal region - carries a nucleolar localization domain (NoLS, purple box) that is formed by tryptophan-288 and tryptophan-290.

NPM1 mutations are of great interest in AML, as there is mounting evidence that *NPM1* mutations promote leukemogenesis. Over 55 *NPM1* mutations have been identified (57), and the most common consequence of these mutations is the generation of 4 additional amino acids in the C-terminal, resulting in the loss of the NoLS and the creation of a new NES domain (52). This new NES motif binds more efficiently to the nuclear export protein, exportin 1, compared to the NES motifs normally present in the N-terminal segment (55). As a result, the nucleus and nucleolus are relatively depleted of NPM1, and this nuclear exclusion of NPM1 is believed to be leukemogenic, although the exact underlying mechanism is incompletely understood.

In support of the concept that *NPM1* mutations contribute to leukemogenesis, transgenic mice carrying these mutations were found to develop myeloproliferative disorders, although frank AML was not found (53). In another study using an inducible transgenic mouse model, the animals did develop AML, but only after a relatively long latency time, suggesting that additional gene mutations are necessary (58). In keeping with this concept, development of AML in a transgenic mouse model occurred relatively early when *NPM1* mutations coexist with other mutations such as *FLT3* mutations (4). Taken together, *NPM1* mutations contribute to leukemogenesis, but additional factors are needed.

Several studies have demonstrated that *NPM1* mutations may contribute to leukemogenesis by virtue of eliminating its normal stabilization of Arf, a known tumor suppressor (59). After forming a complex with NPM1, Arf is transported to the nucleolus where it suppresses cell growth and promotes apoptosis (60). When a *NPM1* mutation is generated, the NPM1 mutant along with Arf is mislocalized to the cytoplasm, where Arf is destabilized and is degraded (57). Mutated NPM1 may also contribute to leukemogenesis by inhibiting c-Myc degradation, although there is currently only one study examining the interaction between mutated NPM1 and Myc. This study showed that mutated NPM1 can sequester Fbw7-gamma, which is involved in Myc degradation, in the cytoplasm, resulting in an overall increase in Myc (61).

It is well-documented that *NPM1* mutations correlate with a significantly better clinical outcome, and detection of these genetic abnormalities is routinely done in clinical laboratories to stratify patients in different prognostic categories. Based on the European Leukemia Net guideline, the presence of *NPM1* mutations co-existing with *FLT3* mutations is a key factor for placing patients into a prognostic category. In *FLT3*-ITD AML, the co-existence of *NPM1* mutations down-grades the risk from intermediate to favorable (1). It is unknown why NPM1 mutations, which are believed to be leukemogenic, confers a better clinical outcome.

1.1.5. Treatment of AML

a. Standard Treatment Regimen

Currently, multi-drug chemotherapy is the standard frontline treatment for AML patients (62). Conventionally, the most common regimen consists of a 7-day course of cytarabine (Ara-C) combined with 3 days of an anthracycline (daunorubicin or idarubicin) (63). Ara-C is regarded to be the most effective and universally used chemotherapeutic agent in the treatment of AML. It can become incorporated into DNA, competing with cytidine (64). Once incorporated, Ara-C hinders DNA replication by preventing cytidylate transformation into 2′-deoxycytidylate, inducing miscoding of DNA, and inhibiting the action of DNA polymerase, which can promote apoptosis (65). Thus, Ara-C is only effective against cells that are in S-phase of the cell cycle. Anthracyclines exert anti-mitotic and cytotoxic activity that is independent of the cell cycle. They function by complexing with DNA, inhibiting DNA polymerase and topoisomerase II and generating free radicals that can damage DNA (66, 67). The success of the treatment can be assessed by rates of complete remission (CR), defined primarily as <5% blasts present in the bone marrow or presence of blasts in the blood, and also absolute neutrophil count >1,000/uL and platelet count of 100,000/μL (68). The Ara-C+anthracycline regimen successfully induces CR in 80% of patients classified as favorable risk, 50-60% of patients with intermediate risk, and 40% for adverse risk (69, 70). Patients that achieve remission after frontline treatment (~65-70% overall) receive consolidation therapy after remission to eliminate any residual leukemic cells, which includes intensive chemotherapy and/or allogeneic stem-cell transplantation (71). Consolidation chemotherapy typically consists of 2-4 cycles of Ara-C (62). Allogeneic hematopoietic cell transplantation can reduce the risk of relapse when administered to patients in remission (70). The

high efficacy of this treatment is believed to be related to the graft-versus-leukemia effect, which is the phenomenon in which newly grafted immune cells can recognize and kill leukemic cells (72). However, the transplantation procedure is associated with a very high mortality rate (73). As such, this treatment modality is typically given to patients in the intermediate/adverse risk category. This treatment decision highlights the importance of risk stratification of AML.

b. Targeted therapeutics

Unlike Ara-C and anthracyclines, targeted therapeutics are generally less harsh to the patient, especially elderly patients.

i. FLT3-inhibitors (FLT3i)

Given that *FLT3*-ITD contributes to the leukemogenesis and is associated with a poor prognosis, FLT3i were developed and used to treat patients with *FLT3*-ITD. There are two classes of FLT3i: Type 1 and Type 2 (32). Both classes of FLT3i inhibit the FLT3 receptor by binding to the ATP-binding site of FLT3, preventing autophosphorylation of the FLT3 receptor. Additionally, Type 2 FLT3i also binds adjacent to the ATP-binding site (38). Type 1 FLT3i can bind to both the active and inactive conformation of the FLT3 receptor and can bind to both FLT3-ITD and FLT3-TKD, but it is not specific and can also target kinases other than FLT3. Type 2 FLT3i can only bind to the inactive conformation, rendering it more specific than Type 1 FLT3i (42). However, Type 2 FLT3i can only bind to FLT3-ITD and not FLT3-TKD (36). Type 1 FLT3i include gilteritinib and midostaurin; Type 2 FLT3i includes sorafenib and quizartinib (32).

FLT3i have been shown to significantly improve the patient outcome and are typically used to treat relapsed or refractory AML carrying *FLT3*-ITD AML (36). Two FLT3i, midostaurin and gilteritinib, have been approved for treating AML in the United States, and several more FLT3i are in clinical trials (36). There have been a number of studies showing the efficacy of FLT3i. In one study, patients with relapsed or refractory *FLT3*-ITD AML were treated with gilteritinib, and these patient had higher CR and overall survival (OS) compared to patients that were treated with salvage chemotherapy, with patients in the gilteritinib treatment group having a CR of 34% and a median OS of 9.3 months compared to a CR of 15.3% and a median OS of 5.6 months in the salvage chemotherapy group (74). In a large-scale study involving 727 AML patients, midostaurin

was administered to a group of patients in addition to standard chemotherapy treatment (Ara-C + anthracycline), and midostaurin was continued to be given for an additional 12 months after chemotherapy. Compared to the patients given a placebo, midostaurin treatment resulted in a significant improvement in OS, with an OS of 74.7 months in the midostaurin group compared to 25.6 months in the placebo group. However, midostaurin did not significantly improve CR rate compared to the placebo group, and 50% of patients who achieved CR initially, eventually relapsed (75). This finding highlights a major limitation to the current use of FLT3i: the development of resistance to FLT3i.

In practice, two main classifications of resistance to FLT3i have been found: primary and secondary resistance (38). In the case of primary resistance, the leukemic cells are resistant to FLT3i treatment at initial diagnosis. Primary resistance has been found to exist in ~30% of AML patients carrying *FLT3* mutations (38). Several mechanisms contributing to the development of primary resistance have been proposed. Primary resistance can occur when FLT3-ITD target pathways have become independent of FLT3-ITD signalling prior to FLT3i treatment. To demonstrate this mechanisms, a study found that downstream target pathways of FLT3-ITD, including MAPK, PI3K and STAT5, remained to be activated during treatment of *FLT3*-mutated AML patient samples with FLT3i, suggesting these pathways have become independent of FLT3-ITD signalling (76). *FLT3*-ITD leukemic cells may also be protected from FLT3i by the bone marrow microenvironment. The bone marrow has a high concentration of the enzyme CYP3A4, which has been shown to degrade FLT3i (36). Additionally, the bone marrow contains the growth factor FGF2, which has been shown to contribute to the resistance against the FLT3i quizartinib. FGF2 can promote activation of the MAPK pathway, thus providing a potential mechanism whereby leukemic cells can bypass FLT3 to activate FLT3 downstream pathways (36, 42).

Secondary or adaptive resistance occurs when patients respond initially to a treatment, but resistance develops over time. One potential mechanism whereby secondary resistance develops is through the generation of additional *FLT3* mutations, preventing the binding of FLT3i. A study examining AML patients carrying *FLT3*-ITD that developed resistance to a FLT3i (AC220) contained point mutations in the activation loop of FLT3 that were not present before FLT3i treatment (77). These point mutations can alter the conformation of the activation loop, decreasing

the binding efficacy of FLT3i. Secondary resistance may also develop from mutations in FLT3 downstream targets, making the activation of these pathways independent of FLT3. In support of this proposed mechanism, a study found that when the FLT3 downstream pathways, including AKT and MAPK pathway, were inhibited in FLT3i resistant cells, these cells were partially re-sensitized to FLT3i, demonstrating the vital role FLT3 downstream pathways have in FLT3i resistance (78). In another study, all *FLT3*-mutated AML patients who developed resistance to gilteritinib but did not develop additional *FLT3* mutations were found to have instead developed mutations in the RAS/MAPK pathway (79). Additionally, treatment with chemotherapy has been shown to increase plasma FLT3 ligand concentration (80). The increased FLT3 ligand competes with the FLT3i, resulting in a lower efficacy of FLT3i, and contributing to secondary resistance (42).

While there are very few studies detailing methods to overcome resistance to FLT3i, it has been found that combining FLT3i with treatments that target downstream targets of FLT3 can result in a more effective treatment compared to FLT3i monotherapy. This study combined FLT3i with a treatment that increases PP2A activation, both of which decreases Myc protein expression levels. Co-treatment with these two drugs was found to induce more cell death in *FLT3*-ITD-positive AML cell lines compared to treatment with FLT3i alone (81).

ii. IDH inhibitors

Given that *IDH1/2* mutations occur in 20% of AML patients, IDH inhibitors have been used clinically. Success of IDH inhibitors for the treatment of relapsed/refractory (R/R) AML carrying *IDH* mutations has been shown in a clinical trial, where 7 newly diagnosed patients aged ≥60 years and 19 R/R patients carrying *IDH2* mutations were treated with an IDH inhibitor (Enasidenib) in combination with AZA (82). In this study, CR was achieved in all newly diagnosed patients and in 53% of R/R patients. Currently, there are two IDH inhibitors that have been approved for the treatment of AML patients carrying IDH mutations, including Enasidenib for R/R patients with *IDH2* mutations and Ivosidenib for R/R and newly diagnosed patients unfit for intensive chemotherapy with *IDH1* mutations (83, 84).

iii. CD33 monoclonal antibody (Gemtuzumab ozogamicin)

Since CD33 is found on myeloid cells, this CD33 antibody conjugated with calicheamicin, a cytotoxic agent, specifically targets myeloid cells, where it can induce DNA cleavage (85). This agent was originally approved by the FDA for treating relapsed AML in patients >60 years of age, but this approval was rescinded after a later clinical trial that showed that this agent did not significantly improve the clinical outcome compared to other therapies, and instead, found GO had fatal toxicity (86). Later meta-analysis suggested that GO may improve outcomes for patients also receiving chemotherapy (87).

iv. Venetoclax

Venetoclax, a highly selective Bcl-2 inhibitor, is a better tolerated AML treatment compared to chemotherapy, and thus has been primarily used to treat elderly patients (88). Bcl-2, which is often overexpressed in AML, is an anti-apoptotic protein that sequesters the pro-apoptotic proteins BIM, BID and BAX, promoting the survival of AML cells (89). Venetoclax was tested in a clinical trial as a monotherapy for patients with relapse/refractory AML or who are unfit for intensive chemotherapy; however, the response rate was only 19% (90). This suggests that venetoclax can induce a response in AML, but it may not be the most effective treatment as a monotherapy.

c. Non-targeted biological agents

i. Hypomethylating agents (HMA)

Decitabine and Azacitidine (AZA) are HMAs that have been used to treat AML (91). HMAs demethylate DNA, and in doing so, remove the silencing of tumor suppressor genes which are often hypermethylated in cancer cells. The initial clinical trials using these agents showed some promise in treating AML patients; however, effects were modest. For instance, a clinical trial for AZA in patients aged ≥65 showed an improved median OS for AML patients compared to the conventional regimens (10.4 vs 6.5 months), but this improvement was not significant. AZA did not significantly improve CR rates compared to the conventional regimen group (92). Based on these studies, the use of HMA appears to induce some response for AML, but they are not very effective as a monotherapy.

ii. Venetoclax with HMA (Azacitidine and decitabine)

Given that both Venetoclax and HMAs showed a modest response, it was tested if these treatments could be used in combination to produce a more effective regimen. The use of this regimen for AML treatment has been supported by a large-scale clinical trial that showed improved clinical outcomes in treatment-naïve AML patients that were treated with a combination of Azacitidine with Venetoclax (AZA+Ven) compared to AZA alone (93). Specifically, patients treated with AZA+Ven had an OS of 14.7 months and a CR rate of 66.4% compared to an OS of 9.6 months and a CR rate of 28.3% when treated with AZA alone. Additionally, the median event free survival was 9.8 months in the AZA+Ven group compared to 7.0 months in the AZA group. The success of this regimen led to approval by the FDA to be used as first-line treatment for AML patients unfit for intensive chemotherapy (94).

Interestingly, this treatment has been shown to preferentially target cancer stem-like (CSL) cells (95), a rare subset of cells that are characterized as being drug resistant, which will be further discussed in Section 1.4.

1.1.6. Refractory and relapsed AML

Refractory disease is a situation in which patients never achieve CR following frontline treatment, which occurs in approximately 30% of AML patients (96). Clinically, this is often defined as a failure of lowering the blast count in the bone marrow to below 5% after induction chemotherapy (97). The mechanisms underlying refractory disease are likely due to those causing drug resistance, such as mutations of the therapeutic targets, increased drug metabolism or decreased drug transport into cancer cells (98). In the event that the disease is refractory, treatment is intensified by escalating drug doses and using alternative regimens in order to induce CR. The dose escalation is primarily done with Ara-C, ranging from 1000 to 3000 mg/m^2 administered for 3-6 days (71, 99). This regimen can be used in combination with alternative treatments, including chemotherapy agents such as anthracyclines, etoposide, and fludarabine (63).

In contrast to refractory disease, disease relapse is a situation in which patients develop recurrent disease, defined as the presence of ≥5% blasts in the bone marrow or the presence of blasts in the

peripheral blood, after achieving CR (i.e. <5% blasts in the marrow) (1). Approximately two thirds of patients will achieve remission, and of those patients, around 60% of patients will relapse typically within 18 months after remission (62, 100, 101). **Figure 1.2** demonstrates an example of the timeline of an AML patient from initial diagnosis to relapse. Relapsed diseases are typically resistant to treatments that were used to treat the newly diagnosed disease, and therapeutic options for patients are limited. Currently, the median survival is only ~6 months after relapse, and the overall survival rate for patients who relapse is 10% (101, 102).

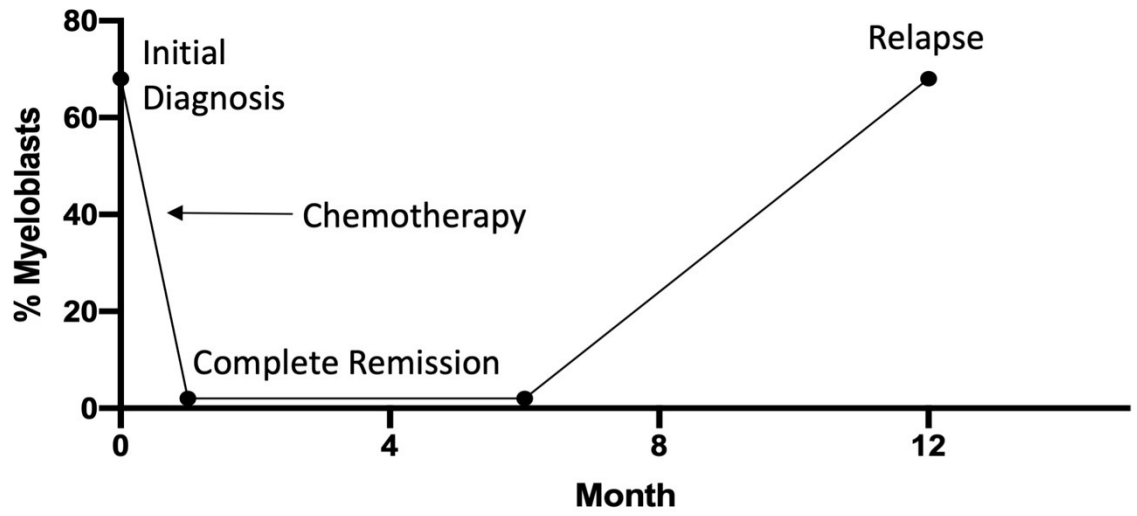

Figure 1.2. Timeline and blast count of an AML patient from initial diagnosis to relapse. Standard frontline treatment was administered, and CR was achieved within one month after diagnosis, with <5% blasts in the bone marrow. Remission lasted for approximately 11 months, at which time relapse occurred.

Although refractory and relapsed AML are likely pathogenetically different, they have been treated the same way. For instance, the DNA methyltransferase inhibitors such as decitabine and AZA have been used as monotherapy or in combination with other chemotherapeutic agents to treat relapsed/refractory AML (103). Allogeneic hematopoietic stem cell transplantation may be an effective treatment for patients with R/R disease, but many patients are not candidates for transplant owing to old age, comorbid conditions and a lack of donors (104). Overall, second remissions can be achieved in 30% to 70% of patients who had relapsed AML, and they are

substantially shorter than that of the first remissions (105). The European prognostic index allows prognostic stratification of relapsed AML into 3 groups. The best group has 70% survival 1 year after relapse and 46% at 5 years, whereas the worst group has 16% and 4%, respectively (106). This scoring system for patients with R/R acute leukemia considers the following factors: 1) duration of the first clinical remission; 2) cytogenetics at initial diagnosis; 3) age at first relapse; 4) whether stem cell transplantation was used before the first relapse.

1.2. Proposed mechanisms for AML relapses

Given the clinical importance of relapses in AML, there have been several studies attempting to uncover the biology underlying relapses. Despite these studies, the molecular basis of how AML relapses is not well understood. However, there have been several models for disease relapses that have been proposed. These models are not mutually exclusive; rather, they focus on different aspects or stages of relapse.

1.2.1. Clonal evolution

The clonal evolution model proposes that leukemic clones present at diagnosis can acquire mutations that provide them a survival advantage, and these clones will persist after treatment, and eventually become the dominant clone at relapse (107). Support from this model comes from studies performing genome sequencing in initially diagnosed and relapsed patient samples. These studies have found that the majority of paired samples at initial diagnosis and relapse within the same patient have a common mutation, suggesting relapsed AML is derived from an initial AML clone (108, 109). Additionally, these studies showed that mutations were typically acquired and lost at relapse compared to initially diagnostic specimens, supporting the acquisition of advantageous mutations proposed in the clonal evolution model.

Clonal evolution has been classified into different patterns, with one common classification categorizing clonal evolution into branching or linear patterns. The branching pattern occurs when the major clone at initial diagnosis is taken over by a new clone at relapse. This pattern is

characterized by the loss of the dominant clone mutations from initial diagnosis at relapse (107). In the linear pattern, the major clone at initial diagnosis acquires new mutations sequentially and the clone with the most advantageous mutations becomes the dominant clone at relapse. In practice, the linear pattern can be identified when the mutations at initial diagnosis, along with new mutations, are present at relapse (107). Evidence for these two patterns have been identified in several AML studies performing whole exome sequencing on paired initial diagnosis and relapse samples (109-111).

The high biological heterogeneity between AML patients at initial diagnosis is also found at relapse, and thus, there are no mutations that are consistently gained at relapse. However, several mutations are more commonly gained, including *FLT3*-ITD, *WT1* mutations, and *KDM6* mutations (111, 112). Additionally, certain mutations are more commonly lost at relapse, including *NRAS, KIT,* and *PTPN11* (111, 113). Mutations that remained stable from initial diagnosis to relapse included *NPM1, DNMT3A* and IDH1/2 (111, 113).

1.2.2. Senescence-like resilient cell model

In contrast to the clonal evolution model, which compares cancer cells at initial diagnosis and relapse, the senescence-like resilient cell model focuses on the biology of cancer cells during CR. This model proposes that when challenged with chemotherapy treatment, select cancer cells can acquire a senescence-like state, which is defined as a cell that ceases cell division but remains to be metabolically active (114). This state of quiescence makes senescence cells resistant to standard cancer treatments that target actively proliferating cells. During the CR phase, these cells remain viable in a dormant state. Eventually, their state of senescence is reversed, and they regain their ability to proliferate, forming the basis of disease relapse.

The major assumption underlying this theory is that cancer cells have the ability to acquire and lose the senescence phenotype. Senescence was initially believed to be an irreversible state that a cell enters when it reaches its replicative limit (115). However, emerging evidence shows that senescence can be induced under conditions of sublethal stress, including chemotherapy treatment (116). A small subset of these senescent cells can reverse the senescence phenotype after a period

of dormancy and return to a state of proliferation (117). These findings support the plausibility of this model.

While this model for disease relapse is plausible, there are few studies supporting it. In one of these studies, patient bone marrow samples collected at nadir (i.e. residual cancer cells after chemotherapy treatment), had an upregulated senescence program compared with initial diagnosis (116). However, it is unclear whether this is a mechanism for disease relapse or refractory disease because the authors did not indicate whether the patients achieved complete remission.

1.2.3. Cancer stem cell model

The cancer stem cell (CSC) model proposes that a tumor is composed of various types of cancer cells that are functionally and phenotypically heterogeneous, existing in a hierarchical model. At the apex of the model are the CSCs, which represent a small percentage of the heterogeneous tumor. CSCs are functionally defined as being able to efficiently xenograft into animals, due to their high tumor initiating capacity (118). CSCs are believed to be pluripotent, carrying both self-renewal properties, while being able to give rise to more differentiated, non-tumorigenic progeny, which make up the bulk of the tumor (119). Thus, CSCs can generate a heterogeneous tumor containing both tumorigenic and non-tumorigenic cells.

Besides their tumorigenic and self-renewal properties, a key characteristic of CSCs is being highly chemoresistant (120-122). Because of their chemoresistance, self-renewal and tumorigenic properties, it is predicted that CSCs can contribute to AML relapses. Specifically, it has been proposed that CSCs can evade chemotherapy, resulting in a small number of undetected CSCs persisting during complete remission. Subsequently, they can leverage their tumorigenic properties to generate a new, more resistant clone of AML. This concept is illustrated in **Figure 1.3.**

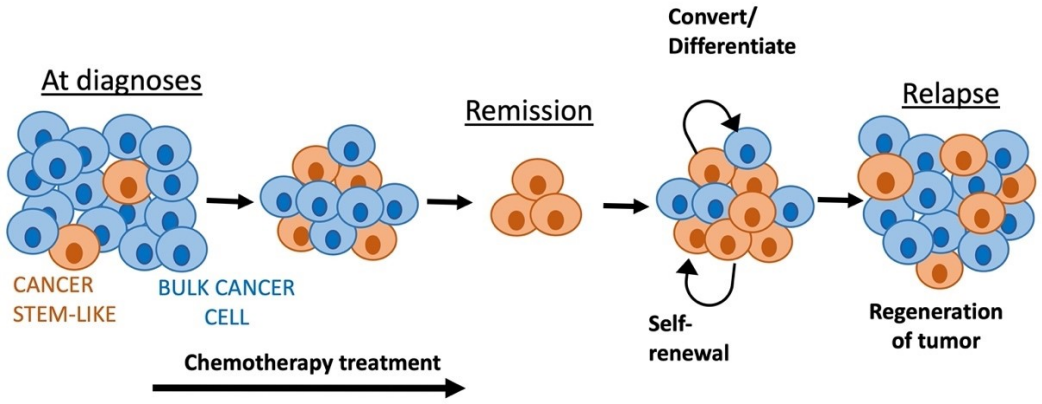

Figure 1.3. Cancer stem cell model for AML relapse. The theory postulates that cancer stem-like cells, which make up a small proportion of all cancer cells, persist after induction chemotherapy due to their high drug resistance. Using their ability to self-renew and differentiate into progeny, they can regenerate the tumor, forming the basis of disease relapse.

One important aspect of the cancer stem cell model is based on the observation that cancer cells are plastic and have the ability to acquire or lose stemness. One of the best examples to demonstrate the concept of cancer cell plasticity is the epithelial-mesenchymal transition (EMT) (123). EMT is a process where epithelial cells acquire morphological changes to become mesenchymal cells. This transition is often accompanied by the acquisition of stem-like properties, including an increased chemoresistance, repressed differentiation, and an aberrant expression of embryonic stem cell proteins (124, 125). Another example of cancer cell plasticity is the ability of non-CSL cells to convert into CSL cells under various stresses, including oxidative stress, and standard cancer treatments, such as ionizing radiation and chemotherapy (126-130). These converted cells had more CSL features, including being significantly more tumorigenic, carrying superior spheroid formation abilities, or upregulating stem cell factors, including Oct4, Sox2, Nanog, Myc and Klf4 (126-130). Taken together, these studies provide strong support that cancer cells can shift between different levels of stemness. This finding is highly relevant to the CSC model for relapse, as it poses another potential mechanism for enrichment of CSL cells during induction chemotherapy. Not only do CSL cells have enhanced chemoresistance properties, but non-CSL cells may also convert to CSL cells when exposed to chemotherapy to further enrich the CSL population.

If the CSC model is shown to be true, it would suggest that eliminating CSCs is critical in preventing patient relapses. There is currently very little evidence showing that CSCs directly contribute to AML relapse; however, some recent, but mainly correlational, evidence is emerging supporting this theory. For instance, AML bone marrow samples that had a high score of CSC-based genes were more likely to relapse than samples with lower expression of the CSC genes, suggesting that a higher number of CSCs is related to a higher chance of relapse (131). Another study compared the proportion of CSCs present in initially diagnostic and relapsed bone marrow specimens and found that the percentage of CSCs, assessed by an *in-vivo* limiting dilution assay, was increased by 9- to 90- fold at relapse (132). Furthermore, another study used paired initially diagnostic and relapse AML bone marrow samples to demonstrate the emergence of two dominant patterns of relapse, both of which highlight the importance of cancer stemness (133). In this study, CSCs were isolated by xenografting in immunodeficient mice. Patient samples and xenografts were genotyped using whole genome sequencing and digital droplet PCR. The genetic profile of relapsed cells was compared to CSCs and bulk cells at diagnosis. In one pattern, relapsed samples predominantly consisted of CSCs, where the clone capable of forming a xenograft at diagnosis was the dominant clone at relapse. In the other pattern, relapsed samples stemmed from bulk cells at initial diagnosis; however, the relapsed cells had acquired a similar gene expression of the relapsed cells from the first pattern, suggesting that despite these cells not originating from the CSC subset, they had acquired stemness. Despite the emergence of two distinct patterns of relapse, both patterns highlight the importance of cancer stemness in the process of relapse. Overall, these studies support that CSCs are associated with relapses, they do not provide direct evidence. The role of cancer stemness in relapse remains to be incompletely understood.

1.3. Cancer stemness

1.3.1. Hematopoietic stem cells

The principles of cancer stemness in leukemia have been guided by the concepts of hematopoiesis and normal hematopoietic stem cells. Hematopoiesis involves a clear hierarchy of cells to generate all lineages of blood cells. At the apex of the hierarchy is the hematopoietic stem cell (HSC), a rare subset of cells that make up only 0.01-0.2% of all bone marrow mononuclear cells, which is the precursor of all blood cells (134). With the ability to self-renew and differentiate, HSCs are capable of maintaining the entire hematopoietic system. The self-renewal ability is unique to HSCs, as more mature cells are not capable of this property. HSCs divide asymmetrically, allowing them to give rise to new HSCs to maintain the stem cell pool, while also generating more differentiated lymphoid and myeloid progenitor cells (135).

The presence of HSCs can be identified using several assays that are based on their enhanced self-renewal capabilities. Using an *in-vitro* model, the colony forming cell assay involves culturing hematopoietic cells in semi-solid mediums. The use of semi-solid mediums allows for a single cell suspension to be formed, which means that every colony formed originated from a single cell (136). Using their abilities to self-renew and differentiate, HSCs are capable of forming colonies. Using *in-vivo* models, the presence of HSCs can be detected by the ability to transplant and maintain the human hematopoietic system in mice (137). In addition to identifying HSCs based on the described assays, cell surface lineage markers have also been used to identify HSCs, with $CD34^{+}CD38^{-}$ being used most frequently as an HSC marker (138). However, these markers are used for enrichment but do not define HSCs, as HSCs have also been found in $CD34^{-}$ fractions (138).

Given that a limited reserve of HSCs give rise to all blood cells throughout the lifespan, these cells require protective mechanisms to promote genomic stability, preventing passing down mutations to their progeny. To this end, HSCs have enhanced DNA repair pathways compared to differentiated cells. A study found that after treatment with a DNA damage inducer, *N*-ethylnitrosourea, HSCs, identified as $CD34^{+}CD38^{low}$, had more efficient DNA repair as assessed

by a comet assay, compared to progenitor ($CD34^+CD38^+$) and mature ($CD34^-$) cells isolated from umbilical cord blood (139).

Many of these properties, including self-renewal, pluripotency, and enhanced DNA repair, are shared with other types of adult stem cells and embryonic stem cells (140). Given that normal tissue is organized in a hierarchical fashion, it is not unexpected that tumors may also carry this same organization, with CSCs residing at the top of the hierarchy, maintaining the tumor.

1.3.2. Definition and characteristics of CSCs and CSL cells

Similar to normal stem cells, the key properties of CSCs include their ability to self-renew and differentiate into more specialized cells, allowing them to produce new bulk cells and new CSCs. CSCs are functionally defined by their ability to engraft cancer when transplanted into mice (118). Studies in AML typically find ≤0.01% of cells that are classified as CSCs, which is based on the number of leukemic cells required to form engraftment in mice (132). However, defining CSCs based on their ability to xenograft may underestimate the frequency of CSCs, due to interspecies differences in microenvironment that may impair the survival of human cells.

Throughout the studies conducted in this thesis, the term cancer stem-like (CSL) cells, rather than CSCs, is used to describe cell subsets carrying high levels of cancer stemness. While the principles underlying CSCs/CSL cells are the same, the definition of CSL cells is less restrictive than that of CSCs. CSL cells are defined as carrying more stem-like features, including tumorigenicity, pluripotency, chemoresistance and spheroid forming ability (141). While CSL cells tend to have enhanced tumorigenic abilities, the ability to engraft is not an absolute requirement for every CSL cell, in contrast to CSCs. Studies typically find ~2-15% of cells are classified as CSLs (122, 142, 143). The reason for using the term CSL cells, instead of CSCs, is related to the fact that there is currently no marker for cancer stemness that only identifies CSCs; rather, the current markers for cancer stemness enrich CSCs. In other words, for all current CSC markers, there are cells within the identified CSC population that are not capable of generating tumor xenografts. As such, throughout my studies, I believe the term CSL cells more accurately represents the cell subset I identified as being more stem-like.

A number of assays have been developed to evaluate CSL characteristics. Tumorigenicity, the ability of a cell to form a heterogeneous tumor, is a characteristic of CSL cells due to their differentiation and self-renewal abilities and can be assessed using xenograft transplantation in mice (141). Additionally, CSCs have been observed to proliferate in a spheroid form, and assays to assess sphere formation typically involve seeding cells at a low density, to further enrich CSCs by selecting cells with high self-renewal properties (141). One of the methods to assess spheroid forming abilities is using the hanging drop assay, where a small number of cells are cultured in drops, allowing for cells to grow in 3D spheres (144). Using this method, a study found that spheres formed using colorectal cell lines were enriched with CSL cells, with higher stemness genes, including Oct4, Sox2, Nanog and Myc, and cell surface markers compared to cells not subjected to the hanging drop assay (145). Resistance to chemotherapy is a well-established characteristic of CSL cells, with this characteristic being a key factor in the CSC theory of relapse. In a number of studies that have isolated CSL cell from bulk cells, the CSL subsets have consistently been more resistant against a number of drugs, including paclitaxel, temozolomide, etoposide, doxorubicin and Ara-C in breast cancer, ovarian cancer, glioblastoma, anaplastic large cell lymphoma, and acute myeloid leukemia (122, 146-150). Moreover, the chemoresistance characteristic in CSL cells has been validated clinically, as the number of CSL cells in pre-treatment patient samples have been found to correlate with chemoresistance in triple negative breast cancer (151). The mechanisms underlying therapy resistance of CSL cells will be discussed in Section 1.3.6.

1.3.3. Origin of CSL cells

The origin of CSCs is currently unknown; however, two main theories have been proposed (152). One theory postulates that CSCs originate from normal stem cells that have acquired the hallmarks of cancers through mutations/epigenetic alteration. In support of this theory, some CSCs have been shown to have immunophenotypic markers and properties similar to normal stem cells. For instance, HSCs have the cell surface marker $CD34^{+}/CD38^{-}$, and this marker has been shown to enrich leukemic stem cells in some settings (153). Many properties are shared by CSCs and adult stem cells, including the ability to self-renew and differentiate. Evidence to support the HSC origin of CSCs comes from a study that traced the clone of origin of AML blast cells to mutated HSCs.

In this study, AML blasts were found to carry both *DNMT3A* and *NPM1* mutations, which are considered to be AML driver mutations. Pre-leukemic HSCs were identified as carrying *DNMT3A* mutations, but *NPM1* mutations were absent, suggesting these mutated HSCs are precursors of all AML cells within this patient (133).

Alternatively, CSCs have been speculated to arise from more differentiated cancer cells or mutated progenitor cells, which de-differentiate, acquiring more CSC characteristics, in order to become CSCs. The feasibility of this theory has been shown by the fact that more mature bulk cells can acquire stemness when exposed to certain stressful environments, such as under oxidative stress or chemotherapy (126, 128-130).

1.3.4. Molecular profile of CSL cells

CSL cells between and within cancer types are heterogeneous, and there is no universal molecular profile of CSL cells. However, there are a number of proteins and signaling pathways that have been associated with cancer stemness.

Several signaling pathways tend to be upregulated in CSL cells, including NF-κB, Wnt-β-catenin, Notch and Hedgehog pathways (154). These pathways promote CSL properties, including self-renewal ability (155). The Notch pathway can regulate CSL phenotype, as supported by a study showing that pharmacological inhibition of this pathway reduced CSL phenotype in glioblastoma neurospheres, which are enriched in CSL cells, and decreased the number of CSL cells *in-vivo* (156).

Another type of key molecule associated with CSL cells is a group of transcription factors that maintain the pluripotency phenotype of embryonic stem cells. These proteins, also known as embryonic stem cell proteins, include Myc, Oct4, Sox2 and Nanog. To highlight the critical role of these proteins to stemness, Takahashi *et al*. showed that the enforced expression of these four transcription factors could reprogram somatic cells into pluripotent stem cells (157). These proteins have also been shown to regulate and maintain stemness of CSL cells. Specifically, Myc, Oct4, Sox2 and Nanog have all been observed to be more highly expressed in various cancer stem

cells compared to bulk cells (122, 158-167). Additionally, knockdown of Sox2, Oct4, or Myc has been shown to decrease characteristics of cancer stemness, including tumorigenicity and chemoresistance, while enforcing the expression of these proteins increased these characteristics (122, 158, 168).

1.3.5. Markers to identify CSL cells

a. Cell surface markers

In order to study the role of CSL cells in relapse, a reliable method to identify CSL cells is required. The first studies of cancer stemness used cell surface markers as a method to enrich CSCs, and since then, there have been a number of studies attempting to identify other cell surface markers. Specifically in AML, these immunophenotypic markers have included $CD34^+/CD38^-$, CD96, CD123 and CD200 (153, 169-171). In these studies, the markers for CSCs have been found to identify cells that have a superior ability to form engraftments in mice. However, these markers have several major limitations. First of all, there is no known biological link between these markers and cancer stemness. Furthermore, several of these markers have been inconsistent in identifying CSCs. For instance, the first CSC marker identified in AML was $CD34^+/CD38^-$, which was shown to enrich leukemic cells capable of engraftment in immunodeficient mice (153). However, the inconsistency of this marker in identifying CSCs has been shown in later studies, with colony forming cells found in $CD34^-$ and $CD38^+$ fractions (172, 173). In another study, CD200 was identified as a marker for CSCs in AML; however, 6/16 AML patient samples showed a low expression of CD200 on blasts, and in these subsets, the CSCs were detected in the $CD200^-$ fraction (170). Additionally, the validity of these markers may be questioned by the absence of evidence showing that knocking down of these proteins decreases stemness, despite the fact that the first of these markers were first discovered several decades ago.

b. Aldehyde dehydrogenase (ALDH)

ALDH, an enzyme that metabolizes aldehydes into carboxylic acids and has a role in cellular detoxification, has been used as a marker for cancer stemness (174). This marker was first found to be elevated in normal stem cells. For instance, using human umbilical cord blood, cells with high ALDH activity were found to be enriched with HSCs (175). ALDH may have a role in

regulating the differentiation of stem cells, promoting the generation of more mature progeny, as pharmacological inhibition of ALDH in HSCs prevented their differentiation (176). Later, ALDH was found to also enrich CSL cells in a number of cancers, including colon cancer, non-small cell lung cancer and AML (177-179). In these studies, cells with high ALDH activity, as measured using a fluorescent based Aldefluor staining assay, were found to have a superior ability in engrafting the cancer in NOD/SCID mice. Since ALDHs are involved in cellular detoxification, their higher expression in CSCs may contribute to the chemoresistance of CSCs. ALDHs can neutralize the toxic effects of aldehydes, which are often intermediates of chemotherapy treatment (180).

There are several limitations of using ALDH as a marker for cancer stemness. Similar to the cell surface markers, the link between ALDH activity and cancer stemness is not completely understood. Additionally, certain tissues express high levels of ALDH, including pancreatic and liver tissue, and because all cells in these tissues express high levels of ALDH, this marker cannot be used to distinguish stem cells and non-stem cells (181).

c. Molecular reporters: SRR2 and SORE6 reporter

Given the limitations of cell surface markers, alternative markers for cancer stemness have been developed. Several reporter systems have recently been developed to detect cells with high levels of cancer stemness. These reporters detect the transcriptional activity of embryonic stem cell proteins, including Sox2, Oct4 and Myc. The basic assumption of using these reporters is that the stemness of cancer cells is proportional to the amount of biologically active embryonic stem cell proteins, including Sox2, Oct4 and Myc. As detailed in Section 1.3.4, this assumption has largely been supported in the literature.

The first of these molecular reporters developed, called the Sox2 regulatory region-2 (SRR2), detects the transcriptional activity of Sox2 (158). The activity of this reporter can easily be detected, as it emits a green fluorescent protein (GFP) or luciferase when it is activated. The use of this reporter in measuring cancer stemness was validated in several study models including breast cancer, anaplastic large cell lymphoma, and esophageal squamous cell carcinoma, where cells that were labelled as CSL cells by the reporter were found to have significantly more stem-

like features, including chemoresistance, tumorigenicity, spheroid forming ability and expression of embryonic stem cell proteins (158, 182, 183). Even though the SRR2 reporter was designed to detect the activity of Sox2, it has been found that Sox2 is not the only transcription factor that is able to drive SRR2 activity. Specifically, a study found that in triple negative breast cancer, both the CSL and non-CSL subsets had no Sox2 expression. To explain why cells with SRR2 activity lacked Sox2 expression, a follow up study found that there were 16 different transcription factors that could bind to the Sox2 binding domain within the SRR2 reporter, many of which were embryonic stem cell proteins, including Myc (158). This finding suggests that multiple embryonic stem cell proteins are involved in driving SRR2 activity and cancer stemness.

A more recently developed reporter for cancer stemness, called the Sox2/Oct4 response element (SORE6) reporter, detects the activity of both Sox2 and Oct4 (121). Similar to the SRR2 reporter, the SORE6 reporter emits a GFP when it is activated. While this reporter has not been used to study AML, there are currently eight publications that have employed the SORE6 reporter in different cancer models, which are summarized in **Table 1.1**. These studies have several factors in common: 1) a minority of cells (~2-20%) from cancer cell lines were SORE6$^+$ at the steady state and 2) SORE6$^+$ cells carry more CSL features, including drug resistance and tumorigenicity (121, 122, 143).

It is important to note that while the SORE6 reporter detects the transcriptional activity of Sox2 and Oct4, there may be other proteins that are able to drive SORE6 activity by binding to the consensus sequence of SORE6, as was found in the case of the SRR2 reporter described above.

A major advantage of these reporter systems as a marker for cancer stemness compared to the cell surface markers discussed above is that these reporters have a molecular basis for stemness, providing a pathway underlying the CSL phenotype that can serve as a starting point to study the biology of cancer stemness. Given this advantage, the SORE6 reporter was used in this study.

Study	Cancer type	Sample type	% SORE6$^+$ at steady state	Characteristics of SORE6$^+$ cells	Additional information
Bano et al. 2023 (184)	Triple negative breast cancer	2 cell lines	Not tested	Not tested	SORE6 activity correlated with ALDH+ cells
Rosas-Cruz et al. 2022 (185)	Breast cancer	2 cell lines	4-9%	Higher expression of DRD1, lower expression of DRD4	
Li et al. 2021 (122)	Anaplastic large cell lymphoma	2 cell lines	~20%	Tumorigenic (colony forming assay), chemoresistant	
Menendez et al. 2020 (186)	Undifferentiated pleomorphic sarcoma	3 cell lines	20-40%	Tumorigenic (xenograft, tumorsphere)	
Padua et al. 2020 (143)	Gastric carcinoma	2 cell lines	8-16%	Tumorigenic (xenograft), drug resistant	No correlation between SORE6$^+$ and current cell membrane markers for gastric CSL cells
Vaddi et al. 2019 (142)	Prostate cancer	3 cell lines	2-20%	Tumorigenic (xenograft, tumorsphere), chemoresistant	
Gao et al. 2018 (187)	Prostate cancer	Cell lines and patient samples	N/A	SORE6$^+$ cells enriched in tumorspheres compared to 2D	Used the SORE6 reporter as a tool to identify presence of CSL in tumor spheres

Tang et al. 2015 (121)	Breast cancer	2 cell lines and Patient Derived Xenograft models	7-15% in cell lines, 7-14% in PDX	Tumorigenic (*in vivo* limiting dilution, tumorsphere), metastatic (Matrigel invasion assay), chemoresistant	

Table 1.1. Summary of published studies using the SORE6 reporter.

1.3.6 Drug resistance mechanisms of CSL

Given that a key characteristic of CSL cells is their enhanced drug resistance, a number of studies have been done examining the mechanisms underlying their drug resistance, which are outlined below.

a. High expression of drug transporter pumps

CSL cells have been reported to have higher levels of the ATP-binding cassette (ABC) transporter family, which can transport drugs out of the cell. In several cancer types, including retinoblastoma, breast cancer, lung cancer, and neuroblastoma, CSL cells expressed higher levels of ABC transporter family genes and showed higher drug efflux compared to non-CSL cells (188, 189). In AML, several of these drug transporters, including MDR1 and BCRP, were upregulated in AML CSL cells (190-192). The expression levels of MDR1 and BCRP have been correlated with poor response to chemotherapy in AML patients (193-195). To date, attempts to treat AML using ABC inhibitors have been unsuccessful (196). This may be due to the upregulation of other transporters or mechanisms of drug resistance to compensate for the inhibition of ABC transporters.

b. Increased resistance to apoptosis

CSL cells have an enhanced ability to resist apoptosis caused by treatments through several mechanisms. First of all, CSL cells have been shown to upregulate anti-apoptotic proteins and pathways, including Bcl-2, PI3K/Akt pathway, and Wnt-β-catenin pathway (152, 197). Moreover, CSL cells can reduce reactive oxygen species (ROS), avoiding DNA damage caused by ROS, and decreasing the likelihood of apoptosis occurring. CSL cells can protect themselves from ROS through a superior ability to synthesize glutathione, an antioxidant (152).

c. Quiescence

CSL cells are believed to be able to enter a quiescent state, where cells are not actively proliferating, but retain the ability to reverse this condition by re-entering the cell cycle. The quiescence of CSL cells has been supported by a study that observed a small subset of cells from a pancreatic adenocarcinoma cell line that were characterized as slow cycling (198). These cells showed higher CSL characteristics, including chemoresistance and tumorigenicity. Similar findings were observed in human ovarian tumor cells, adenocarcinoma cell lines and liver cancer (199-201). Given that conventional cancer treatments target actively proliferating cells, CSL cells in a quiescent state are believed to evade elimination by these treatments. Additionally, the arrested quiescent state allows CSL cells to repair any DNA damage induced by treatments, reducing the likelihood of cell death by apoptosis (202). In fact, CSL cells have been shown to have increased levels of DNA repair proteins, including ATM protein kinase and methyl guanine methyl transferase, further enhancing their ability to repair damage caused by therapeutics (149, 203).

d. Cytoprotective autophagy

Recent evidence has shown that CSL cells upregulate their autophagy when treated with chemotherapeutics, which appears to protect them from treatment (204). The autophagic process and its role as a protective mechanism for CSL cells will be discussed in detail in Section 1.5.

1.4. Metabolomics in cancer

1.4.1. Metabolomics background

Metabolomic reprogramming has been identified as one of the hallmarks of cancer (205). In order to compensate for the increase in energy demand from rapidly proliferating neoplastic cells, these cells need to alter their metabolic pathways. As such, metabolomics, the profiling of small molecules, has emerged as an important technology that can detect the alterations in metabolism of cancer cells. It may be used for biomarker identification as well as to identify potential

therapeutic targets. This analysis can identify cellular pathway by-products, including amino acids, enzymes, organic acids, fatty acids and lipids, and sugars and sugars alcohols (206). The analysis is often performed using mass spectrometry, which can analyze a wide range of metabolites. There are two major types of analysis: untargeted and targeted (207). Untargeted is a comprehensive analysis of all metabolites, but due to this wide range of analysis, it tends to be less sensitive for metabolites in low abundance. Targeted requires a selection of specific pathways but has higher sensitivity than untargeted.

In AML, it has been established that leukemic cells have altered metabolism. The initial metabolomic studies in AML examined the differences in the metabolites between AML patients and healthy controls (208, 209). Serum from AML patients carried increased serum glucose levels and decreased glucogenic amino acids, indicators of high levels of gluconeogenesis (208). Additionally, the AML samples generally carried lower levels of fatty acids and lipids, suggesting that these essential metabolites are being consumed at faster rates compared to healthy controls (206, 208, 209). Moreover, by-products of the tricarboxylic acid (TCA) cycle were often dysregulated in AML samples compared to controls, including higher expression of pyruvate and 2-oxoglutarate, and decreased expression of glycerol-3 phosphate, lactate and citrate, suggesting altered energy production in AML (210).

Several studies have shown the potential of using metabolomics clinically in AML. The expression of some metabolites has been shown to correlate with AML prognosis. For instance, one study identified a panel of six glucose metabolism molecules, where the expression level of these metabolites correlated with prognosis (210). Additionally, high plasma levels of arachidonic acid and its precursors were associated with poor clinical outcome (211).

1.4.2. Metabolomic profile of CSL cells

In a number of cancer types, including AML, glioblastoma, and pancreatic cancer, it has been shown that CSL cells have altered metabolic pathways compared to bulk cancer cells (197, 212, 213). These studies have shown that in contrast to bulk cancer cells, which favor glycolysis for

their energy and nutrient demands (214), CSL cells favor oxidative phosphorylation (197, 212, 213).

In keeping with the altered metabolism of CSL cells, metabolic analysis of CSL cells and bulk cells show that each cell subset has a unique metabolic profile. For instance, a study comparing CSL cells in AML, defined by low reactive-oxygen species levels, and AML blasts derived from primary AML patient samples found 39 of the approximately 100 analyzed metabolites were significantly higher in CSCs compared to blasts (95). These 39 metabolites were involved in the glutathione homeostasis, TCA cycle, and amino acid metabolism. The importance of amino acids to CSL cells was emphasized, as depletion of amino acids decreased CSC viability and colony forming ability, whereas this same treatment had no substantial effect in blasts.

The altered metabolism of CSL cells can provide a potential target for selectively eradicating CSL cells. The AZA+Ven treatment regimen, which was previously introduced in Section 1.1.5., is one of these treatments that can preferentially target CSL cells by disrupting the metabolism of these cells. Specifically, AZA+Ven can target the oxidative phosphorylation pathway and can deplete amino acid levels in CSL cells, and as described above, these pathways are critical for CSL cell survival, but less so for bulk cells (95, 215). However, relapsed CSL cells did not show this decrease in oxidative phosphorylation and amino acids, suggesting these cells may have the ability to reprogram their metabolism (95). As such, this treatment may not be effective for relapsed patients.

1.4.3. Metabolomic profiling in relapsed AML

Currently, there is very little known about how the metabolomic profile evolves in relapsed AML. However, evidence from a small number of studies suggest that metabolic profiles differ between initial diagnosis and relapse AML. In one study, paired initially diagnosed and relapsed bone marrow derived serum samples were collected from 10 patients (206). Metabolomic analysis using gas chromatograph-mass spectrometry showed in general a higher level of metabolite expression in relapsed compared to initially diagnosed samples. Specifically, a number of amino acids (alanine, valine, leucine, glycine, and ornithine), organic acids (succinic acid, malic acid, citric

acid) and fatty acids (palmitic acid, myristic acid) were higher in relapsed samples. In support of this finding, another study performing metabolomic analysis in CSL cells, defined as low reactive oxygen species, found CSL cells from relapsed AML specimens had increased fatty acids, especially arachidonic and eicosapentaenoic acid, compared to CSL cells derived from initially diagnosed specimens (216).

1.5. Autophagy

1.5.1 Autophagy definition and function

Autophagy is a homeostatic mechanism within the cell whereby damaged organelles, protein aggregates and pathogens are digested and recycled (217). Basal levels of autophagy maintain cellular homeostasis, and this process is induced by environmental stress, including hypoxia, oxidative stress, and starvation (218).

There are several autophagy pathways. Macroautophagy, which will hereafter be referred to as autophagy, is the primary and most extensively studied pathway, in which the cell recycles organelles and protein aggregates through the formation of a double membrane vesicle called the autophagosome (217). The autophagosome is built around the molecule to be recycled, and then fuses to a lysosome, resulting in the release of digestion enzymes and the subsequent degradation of the molecules. This thesis will focus on this pathway. Briefly, other autophagy pathways include microautophagy, mitophagy, lipophagy, and chaperone-mediated autophagy. Microautophagy involves a more direct digestion of intracellular components, where lysosomes engulf the molecule (219). There are several specific autophagy pathways, including mitophagy, which is the degradation of mitochondria, lipophagy, which is the selective degradation of lipids, and chaperone-mediated autophagy, which involves the specific degradation of proteins directed by chaperones (220).

The importance of the autophagy pathway is highlighted by the fact that its dysregulation has been associated with a number of pathological conditions, including neurological disorders,

myodegenerative diseases, and cancer (221, 222). In cancer, autophagy has a paradoxical effect as both a tumor suppressor and promoter. The current understanding is that autophagy acts as a tumor suppressor during early stages of tumorigenesis. As the cancer progresses, autophagy becomes a tumor promoting mechanism (223).

1.5.2 Autophagy process

The autophagic process begins with the formation of a double membrane vesicle in the cytoplasm, initially called a phagophore and eventually called an autophagosome once formed, which surrounds the intracellular components for degradation (224). This process is regulated by a number of autophagy-related genes (ATG). To date, 36 ATGs with a role in autophagy have been identified (218). The process of autophagosome formation involves three main steps outlined below and is illustrated in **Figure 1.4** (223, 225, 226).

1. **Pre-initiation**: The autophagic process begins with the activation of the ULK complex, composed of ULK1/2, ATG13, FIP200 and ATG101. This step is regulated by two proteins, mTOR and AMPK, both of which monitor nutrient levels within the cell (227). mTOR inhibits the activation of the ULK complex through the phosphorylation of ULK1/2 (223). In contrast, AMPK activates the ULK complex, either directly by phosphorylating ULK1/2, or indirectly, through the inhibition of mTOR (218, 223). When ULK1/2 is activated, it will phosphorylate other members of the ULK complex, including ATG13 and FIP200 (218).
2. **Initiation**: In this stage, the sequestering vesicle, called the phagophore begins to form, which will eventually become an autophagosome once completed. Additionally, autophagic machinery is recruited to the site of the phagophore. The now activated ULK complex triggers a cascade of events, starting with the phosphorylation and activation of the VPS34-Beclin-1 complex. This complex then recruits WIPI-1/2 and DFCP1, which then recruits the autophagic machinery necessary in building the phagophore, including LC3 and the ATG5-ATG12-ATG16 complex. It is unknown exactly where the phagophore originates from, but the lengthening of the phagophore's lipid membrane involves Atg9, which recruits the required lipids that build the membrane.

3. **Elongation**: The budding membrane of the phagophore is lengthened. This process requires the conversion of LC3 to the active LC3-I, catalyzed by the protease ATG4. Phosphatidylethanolamine (PE), a membrane lipid, is then added to LC3-I, mediated by ATG7 and the ATG5-ATG12-ATG16 complex, producing LC3-II (228). LC3-II is integrated into the lengthening phagophore membrane, where it is responsible for directly or indirectly binding with cargo that will be degraded. The ATG5-ATG12-ATG16 complex is also localized to the budding autophagosome membrane, forming the outer leaf of the autophagosome to help generate the concave shape, but once the autophagosome is fully formed, this complex dissociates from the membrane. The closure of the membrane is mediated by VPS4 and CHMP2A (223).

After the autophagosome is formed, it fuses with a lysosome, producing the autolysosome. This step is mediated by LAMP2 and Rab-7a (218). The hydrolytic enzymes from the lysosome degrade the cargo contained by the autophagosome into fatty acids, amino acids, and nucleotides. The degraded materials are then returned to the cytoplasm to be reused.

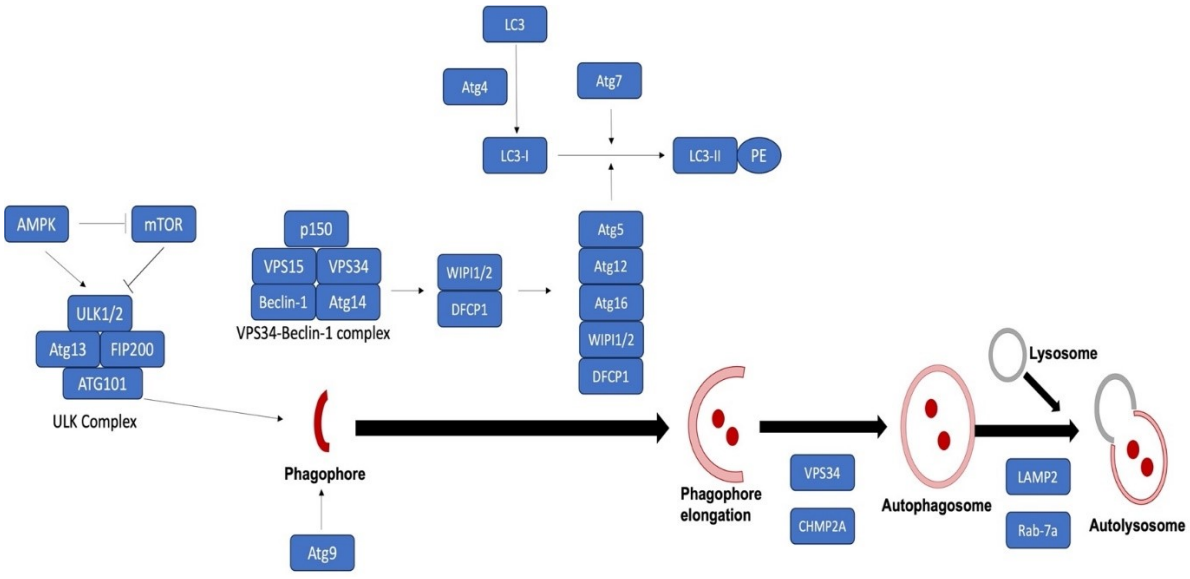

Figure 1.4. The process of autophagy formation. The autophagic process is regulated by AMPK, an autophagy promoter, and mTOR, an autophagy inhibitor. ULK complex, VPS34-Beclin-1 complex and Atg9 recruit components to form the budding phagophore. LC3 is converted into LC3-I and then LC3-II, which is then integrated into the phagophore.

The phagophore becomes an autophagosome upon the closing of the membrane. A lysosome fuses with the autophagosome and degrades the components contained within the autophagosome.

1.5.3 Regulators of autophagy

a. PI3K-Akt-mTOR pathway

This pathway leads to mTOR activation, which as mentioned above, inhibits autophagy. PI3K is activated by a number of molecules, including growth factors, oncogenes, and tumor suppressors. Once activated, PI3K, a catalyst, promotes the production of phosphatidylinosital-3 phosphate, which is necessary for Akt activation (218). Akt indirectly activates mTOR through inhibitory phosphorylation of TSC1/2, an mTOR inhibitor, resulting in decreased autophagy (229).

b. AMPK pathway

AMPK, like mTOR, is a nutrient sensor that is activated based on AMP/ATP levels. When nutrient levels are low, the AMP:ATP ratio increases, resulting in activation of LKB1 and subsequent activation of AMPK. Activated AMPK promotes autophagy both directly and indirectly. AMPK can directly phosphorylate and activate ULK1/2 (230). Additionally, AMPK can phosphorylate TSC2 which inactivates it, which in turn, decreases mTOR, and ultimately promotes autophagy (218).

c. p53

The well-known tumor suppressor p53 has paradoxically been observed to be both an inducer and repressor of autophagy based on its localization. Specifically, when p53 is located in the nucleus, autophagy related genes are transcribed (231). Conversely, p53 localization to the cytoplasm inhibits autophagy by decreasing AMPK activity, which in turn, activates mTOR (232).

d. Bcl-2

Bcl-2, an anti-apoptotic protein, is associated with drug resistance in AML (233). While Bcl-2 is best known for its role in the apoptotic pathway, it has also been implicated in the autophagy pathway, creating a crosstalk between the two pathways. Bcl-2 can directly bind and sequester Beclin-1, preventing the pro-autophagy role of Beclin-1 (234). It has been shown that when

autophagy is induced through cell starvation, this sequestration is inhibited through the phosphorylation of Bcl-2 (235).

e. ULK1/2

ULK1 and ULK2, which are mammalian homologues of ATG1 in yeast, are serine/threonine kinases that have a critical role in autophagy induction (236). In addition to their prominent roles in autophagy, both ULK1 and ULK2 have known functions related to axon formation in neurons (237). These ULK proteins form an autophagy initiation complex with ATG13 and FIP200 (236, 238). Once the complex is formed, ULK proteins are capable of phosphorylating ATG13 and FIP200; however, the significance of this phosphorylation is unknown (239, 240). The activity of the ULK complex is inhibited by mTOR, while conversely, AMPK promotes ULK complex activity, both of which regulate the ULK complex through phosphorylation at different sites (225, 241). ULK1/2 can in turn regulate both mTOR and AMPK through phosphorylation, as well as self-activating through autophosphorylation. Once the ULK complex is activated, it is localized to the pre-autophagosomal structure, where it recruits and phosphorylates several members of the next complex in the cascade, the VPS34 complex, including Beclin-1 and ATG14-L (225, 241).

It is widely believed that the ULK proteins, ULK1 and ULK2, are redundant, as they have high overlap in their structure and function. In humans, *ULK1* is located on chromosome 12 and encodes a protein consisting of 1050 amino acids, whereas *ULK2*, which is located on chromosome 17, encodes a protein consisting of 1036 amino acids (242, 243). Structurally, both proteins contain a N-terminal kinase domain and a C-terminal interacting domain, which interacts with ATG13 and FIP200 (238). The functional overlap between ULK1 and ULK2 have been highlighted by several studies. For instance, in mouse embryonic fibroblasts, knockout of either ULK1 or ULK2 was insufficient to disrupt autophagy, while knockout of both proteins successfully inhibited autophagy (244). Similarly, while mouse knockout of key autophagy genes, such as ATG3, ATG5 and ATG7, caused embryonic lethality, mice could survive knockout of ULK1 or ULK2 separately without significant deficiency in autophagy further suggesting that the overlap of function between ULK1/ULK2 is sufficient to compensate for the loss of its counterpart (238, 245, 246). Indeed, a double mouse knockout of ULK1 and ULK2 caused mice to die within one day after birth (247). Based on these studies, it appears that the overlap in function between ULK1/ULK2 is sufficient to compensate for the loss of its counterpart. However, one recent bioinformatics study suggests

that ULK1 and ULK2 are not completely redundant. This study found that ULK1 and ULK2 differ in several of their interactors. For instance, ULK2, but not ULK1, interacted with p62 and WIPI2, whereas ULK1 interact with ATG4B, ATG14, and MAP1LC3C (236). Additionally, ULK1 and ULK2 had different transcriptional regulators. Despite this finding, there remains to be very little known about the distinction between ULK1 and ULK2.

1.5.4 Dual role of autophagy in cancer

Autophagy has been shown to play a paradoxical role in cancer progression, as there is evidence suggesting that autophagy suppresses and promotes tumorigenesis. The current understanding is that in the initial stages of tumorigenesis, autophagy acts as a tumor suppressor by reducing cancer promoting stressors on cells. However, in later stages of tumorigenesis, autophagy acts as a tumor promoter by increasing survival of cancer cells (248).

a. Tumor suppression effects of autophagy

The autophagic process has been shown to inhibit tumorigenesis, which has been supported by the finding that defective autophagy can promote cancer development. A number of autophagy related genes are frequently mutated in cancer, including frameshift mutations of *ATG2B*, *ATG5* and *ATG12* in colorectal and gastric cancers (249), and monoallelic deletion of *Beclin-1* in ovarian and breast cancers (250), suggesting a tumor suppressor role of these genes and the autophagy pathway. Additionally, the generation of heterozygous *Beclin-1* mutant mice resulted in mice that were more susceptible to tumor formation (250). Furthermore, autophagy induction by overexpressing *Beclin-1* in a breast cancer cell line decreased tumorigenicity (251).

There have been several mechanisms that have been studied to explain how autophagy has a tumor suppressor role.

Autophagy protects cells against genomic instability by reducing stresses on cells (252). It is speculated that if there are defects in the autophagy pathway, then reactive oxygen species and damaged organelles, which would normally be consumed through autophagy, accumulate and promote DNA damage. In support of this mechanism, the impairment of autophagy via the

generation of heterozygous *Beclin-1* mutated mouse kidney epithelial cells increased DNA damage and genomic instability, as measured by levels of γ-H2AX staining and GRP-78 (253).

Additionally, autophagy has a tumor suppression role by decreasing necrosis at tumor sites (254). Necrosis frequently occurs in tumor sites from nutrient and oxygen deprivation. Autophagy can protect cells against these deprivations, suppressing the tumor promoting inflammation that is associated with necrosis (255).

Moreover, autophagy can exert anti-tumor effects by inducing autophagic cell death in cancer cells. Autophagic cell death occurs when excessive autophagy results in the degradation of more organelles than are possible for the cell to survive. Autophagic cell death is caspase independent, and thus, distinct from apoptosis (256). To provide evidence for autophagy cell death, a number of studies have shown that drug-induced autophagy leads to cell death. For example, Hep3B, a hepatoma cell line, treated with the chemotherapeutic etoposide was shown to induce autophagy. Inhibition of autophagy with 3-methyladenine reduced etoposide cell killing (257). Similarly, treatment of the mammary carcinoma cell line MCF-7 with tamoxifen, an estrogen antagonist used to treat breast cancer, resulted in the production of autophagic vacuoles, while inhibition of autophagy using 3-methyladenine decreased cell death by tamoxifen (258).

b. Tumor promoting effects of autophagy

Support for the tumor promoting effects of autophagy has been demonstrated in several studies that have found autophagy inhibition suppresses cancer cell growth. For instance, knockout of FIP200 in murine models resulted in the inhibition of mammary tumor growth (259). A similar finding was observed in pancreatic and lung cancer animal models (255, 260).

Autophagy can promote survival of cancer cells by supplying proliferating cancer cells that have high energy demands with nutrients. Autophagy protects these cells from necrosis that would have been caused by metabolic stress (254).

Autophagy has also been shown to be a tumor promoter by protecting cancer cells against treatment, which may be a mechanism of chemoresistance. In several studies and cancer types,

including AML, cervical cancer, and breast cancer, chemotherapy treatment of cell lines has been shown to induce autophagy. This autophagy was shown to be cytoprotective, as inhibition of autophagy sensitized cancer cells to the treatment (261-263). Similar findings were made in a study using murine models, where chemotherapy combined with autophagy inhibition was more effective in shrinking the tumor than treatment with single agents (264).

These studies have shown that autophagy has tumor promoting effects when examining the entire cancer cell population. However, some recent studies have shown that CSL cells in particular depend on autophagy for their survival, and in fact, autophagy may maintain cancer stemness in CSL cells.

1.5.5. Autophagy may promote cancer stemness

Given the role of autophagy in therapy resistance and the fact that CSL cells are more drug resistant than bulk cells, it has been hypothesized that autophagy may promote stem-like features and survival of CSL cells.

Autophagy has been shown to protect CSL cells from standard cancer therapies. Treatment with these therapies induces more autophagy in CSL cells compared to bulk cells, while inhibition of autophagy sensitizes CSL cells to these treatments. For example, glioma CSL cells, defined as being $CD133^+$, had a higher level of autophagy induction compared to $CD133^-$ cells after being treated with radiation (265). Inhibition of autophagy in $CD133^+$ cells sensitized them to radiation, while inhibition of autophagy did not substantially change the sensitivity of $CD133^-$ cells to radiation. Similarly, a study examining anaplastic large cell lymphoma found that CSL cells have higher autophagic flux in response to Crizotinib, a tyrosine kinase inhibitor being tested in clinical trials for this type of cancer (204). Inhibiting autophagy sensitized these CSL cells to Crizotinib treatment, supporting that autophagy confers cytoprotection against treatment in CSL cells.

Autophagy inhibition has also been found to decrease CSL features. Specifically, CSL cells in ovarian cancer, as defined by the cell surface markers $CD188^+CD44^+$, had decreased spheroid formation, tumorigenicity, and expression of embryonic stem cell proteins after autophagy

inhibition (266). Moreover, in pancreatic cancer cell lines, blocking autophagy via shRNA targeting *ATG5, ATG7* and *Beclin-1* or chloroquine treatment decreased sphere forming ability, chemoresistance and ALDH1 activity in CSL cells (267). Similarly, in osteosarcoma cell lines, inhibition of autophagy via *ATG5/7* shRNA decreased chemoresistance and tumorigenicity in $CD271^+$ CSL cells compared to bulk cancer cells (159).

It is not well understood how autophagy maintains cancer stemness; however, it has been suggested that autophagy allows CSL cells to maintain a dormant state, making them resistant to therapeutics that target proliferating cells (268).

1.5.6. Autophagy as a therapeutic target

Based on the *in-vitro* and *in-vivo* evidence that autophagy has been shown, at least in some cases, to promote cancer cell survival, autophagy inhibition may be used as a cancer treatment.

Autophagy inhibitors can be classified into one of two categories: early-stage and late-stage inhibitors. Early-stage autophagy inhibitors, such as 3-methyladenine, prevent the formation of autophagosomes (269). Late-stage inhibitors, such as chloroquine (CQ) and bafilomycin A1, interfere with the fusion of autophagosomes with lysosomes and subsequent degradation of intracellular components (270). CQ increases the pH of lysosomes, preventing the ability of lysosomal enzymes to degrade intracellular components (271). Bafilomycin A1 prevents lysosomal fusion with autophagosomes through the inhibition of vacuolar-ATPase, an enzyme that is needed for fusion (270).

Currently, autophagy inhibitors have not received FDA approval for cancer treatment. However, CQ and its derivative hydroxychloroquine (HCQ), which have been approved by the FDA to treat malaria, are currently being tested in cancer clinical trials. Phase I/II clinical trials have been conducted in various cancers, including pancreatic cancer, myeloma, breast cancer, prostate cancer, colorectal cancer, lung cancer and AML, either as a monotherapy or in combination with chemotherapy or immunotherapy (272). Studies in breast cancer and pancreatic cancer that used CQ/HCQ as a monotherapy typically did not observe any clinical effects or improvement in

clinical outcomes (273, 274). Using CQ in combination with another drug showed some promising results. For instance, the combination of chloroquine with chemotherapy administered to refractory breast cancer patients showed a response rate of 45% (275). Similarly, the use of chloroquine in combination with the chemotherapeutic gemcitabine to treat pancreatic cancer resulted in a partial response in 33.3% of patients and stable disease in 22.2% of patients, which is superior to the response rate of 10% in patients treated with gemcitabine alone in a previous study (276). Since these studies had small sample sizes, further clinical trial studies need to be done in order to better evaluate the efficacy of chloroquine.

1.6. Hypothesis and Aim of the Study

In this section, I have presented evidence from the literature that cancer stemness is a major contributor to AML relapse. Nonetheless, most of the evidence is relatively indirect, and this difficulty can be largely attributed to a lack of *in-vitro/in-vivo* study models. **The central hypothesis of my PhD studies focused on collecting more direct evidence in support of the role of CSL cells in AML relapse.**

The first objective, which is covered in Chapter 2, was to develop an *in-vitro* model for AML relapse and to use this model to examine the contribution of CSL cells to relapse. To achieve this aim, I first confirmed that the SORE6$^-$/SORE6$^+$ dichotomy exists in two *FLT3*-mutated AML cell lines, MOLM-13 and MV4-11, and provided evidence that SORE6$^+$ cells are significantly more stem-like than SORE6$^-$ cells. Using the SORE6$^-$ and SORE6$^+$ subclones, I successfully developed an *in-vitro* model which shows certain similarities with AML relapse. After the Ara-C induction of 'zero viability' in which viable cells were not detectable by direct microscopic examination using a trypan blue assay, I found regeneration of the cell culture after approximately 2 weeks. These phenomena mimic clinical remission and relapse and are thus labeled *in-vitro* remission and *in-vitro* relapse, respectively. By molecularly barcoding SORE6$^-$ and SORE6$^+$ cells, I was able to track the fate of these cells and determine their relative contributions to the *in-vitro* relapse, even if they lose/gain SORE6 activity. Using flow cytometry to monitor the expression of the GFP (i.e. readout of the SORE6 reporter), I was able to quantify the relative proportion of cells showing

SORE6 reporter activity. By comparing the molecular barcoding results and those of flow cytometry, I was able to assess the degree of conversion between $SORE6^+$ to $SORE6^-$ cells, a phenomenon CSL cells might be expected to do. Using Myc as the surrogate marker for $SORE6^+$ cells, I validated my findings clinically with patient samples.

In Chapter 3, I aimed to address the question of whether CSL cells remained to be the key contributor to relapse when different therapeutic agents were used. 5-azacitidine (AZA) or the combination of AZA and Venetoclax (Ven) (i.e. AZA+Ven) were used since these two regimens were recently tested in a large clinical trial, with AZA+Ven being significantly superior to AZA in prolonging the disease-free survival. Ara-C was included for comparison. The *in-vitro* relapse model could be replicated with both AZA and AZA+Ven treatments. Molecular barcoding and flow cytometry analysis were employed to determine the contribution of CSL cells in these treatment conditions. Metabolomic and glycomic analyses were used to further substantiate the differences between pre-treatment cells and *in-vitro* relapse cells in all treatment conditions. Patient samples were used to validate these findings.

In Chapter 4, I aimed to use my *in-vitro* study model to investigate the mechanisms that might underlie the high chemoresistance in $SORE6^+$ CSL cells. I hypothesized that $SORE6^+$ cells leverage their capability of high autophagic capacity, which has been shown to confer chemoresistance in other cell types. In accordance with the literature, I found evidence of autophagy-mediated chemoresistance in $SORE6^+$ cells. To decipher the mechanisms, I performed an autophagy pathway gene expression array study, to identify an important mediator for the high autophagy capacity in $SORE6^+$ cells. To confirm the role of this target in stemness and relapse, I used my *in-vitro* model to determine if expression of this target was elevated in *in-vitro* relapse cells, and if inhibition of this target could prevent *in-vitro* relapse.

1.7. References

1. Dohner H, Wei AH, Appelbaum FR, Craddock C, DiNardo CD, Dombret H, et al. Diagnosis and management of AML in adults: 2022 recommendations from an international expert panel on behalf of the ELN. Blood. 2022;140(12):1345-77.
2. Khoury JD, Solary E, Abla O, Akkari Y, Alaggio R, Apperley JF, et al. The 5th edition of the World Health Organization Classification of Haematolymphoid Tumours: Myeloid and Histiocytic/Dendritic Neoplasms. Leukemia. 2022;36(7):1703-19.
3. Grisolano JL, O'Neal J, Cain J, Tomasson MH. An activated receptor tyrosine kinase, TEL/PDGFbetaR, cooperates with AML1/ETO to induce acute myeloid leukemia in mice. Proc Natl Acad Sci U S A. 2003;100(16):9506-11.
4. Dovey OM, Cooper JL, Mupo A, Grove CS, Lynn C, Conte N, et al. Molecular synergy underlies the co-occurrence patterns and phenotype of NPM1-mutant acute myeloid leukemia. 2017. p. 1911.
5. De Kouchkovsky I, Abdul-Hay M. Acute myeloid leukemia: a comprehensive review and 2016 update. Blood cancer journal (New York). 2016;6(7):e441.
6. Saultz JN, Garzon R. Acute Myeloid Leukemia: A Concise Review. J Clin Med. 2016;5(3).
7. Estey E, Dohner H. Acute myeloid leukaemia. Lancet. 2006;368(9550):1894-907.
8. Bewersdorf JP, Zeidan AM. Hyperleukocytosis and Leukostasis in Acute Myeloid Leukemia: Can a Better Understanding of the Underlying Molecular Pathophysiology Lead to Novel Treatments? Cells. 2020;9(10).
9. Chang H, Brandwein J, Yi QL, Chun K, Patterson B, Brien B. Extramedullary infiltrates of AML are associated with CD56 expression, 11q23 abnormalities and inferior clinical outcome. Leuk Res. 2004;28(10):1007-11.
10. Pavlovsky S, Eppinger-Helft M, Sackmann Muriel F. Factors that influence the appearance of central nervous system leukemia. Blood. 1973;42(6):935-8.
11. Betancourt-Garcia RD, Castro J, Fernandez AC, Lopez-Enriquez A, Fradera J, Pacheco E. Acquired acute myelogenous leukemia after therapy for acute promyelocytic leukemia with t(15;17): a case report and review of the literature. P R Health Sci J. 2009;28(2):146-50.

12. Ghosh S, Shinde SC, Kumaran GS, Sapre RS, Dhond SR, Badrinath Y, et al. Haematologic and immunophenotypic profile of acute myeloid leukemia: an experience of Tata Memorial Hospital. Indian J Cancer. 2003;40(2):71-6.
13. National Cancer Institute SEER cancer stat facts: leukemia – acute myeloid leukemia (AML). 2023 [cited 2023 October 10]. Available from: https://seer.cancer.gov/statfacts/html/amyl.html.
14. Oran B, Weisdorf DJ. Survival for older patients with acute myeloid leukemia: a population-based study. Haematologica. 2012;97(12):1916-24.
15. Bennett JM, Catovsky D, Daniel MT, Flandrin G, Galton DA, Gralnick HR, et al. Proposals for the classification of the acute leukaemias. French-American-British (FAB) co-operative group. Br J Haematol. 1976;33(4):451-8.
16. Strickland SA, Vey N. Diagnosis and treatment of therapy-related acute myeloid leukemia. Crit Rev Oncol Hematol. 2022;171:103607.
17. Samra B, Richard-Carpentier G, Kadia TM, Ravandi F, Daver N, DiNardo CD, et al. Characteristics and outcomes of patients with therapy-related acute myeloid leukemia with normal karyotype. Blood Cancer J. 2020;10(5):47.
18. Arber DA, Orazi A, Hasserjian R, Thiele J, Borowitz MJ, Le Beau MM, et al. The 2016 revision to the World Health Organization classification of myeloid neoplasms and acute leukemia. Blood. 2016;127(20):2391-405.
19. Caldwell JT, Ge Y, Taub JW. Prognosis and management of acute myeloid leukemia in patients with Down syndrome. Expert Rev Hematol. 2014;7(6):831-40.
20. Tsai RJ, Luckhaupt SE, Schumacher P, Cress RD, Deapen DM, Calvert GM. Acute myeloid leukemia risk by industry and occupation. Leuk Lymphoma. 2014;55(11):2584-91.
21. Li S, Chen L, Jin W, Ma X, Ma Y, Dong F, et al. Influence of body mass index on incidence and prognosis of acute myeloid leukemia and acute promyelocytic leukemia: A meta-analysis. Sci Rep. 2017;7(1):17998.
22. Fircanis S, Merriam P, Khan N, Castillo JJ. The relation between cigarette smoking and risk of acute myeloid leukemia: an updated meta-analysis of epidemiological studies. Am J Hematol. 2014;89(8):E125-32.

23. Greif PA, Konstandin NP, Metzeler KH, Herold T, Pasalic Z, Ksienzyk B, et al. RUNX1 mutations in cytogenetically normal acute myeloid leukemia are associated with a poor prognosis and up-regulation of lymphoid genes. Haematologica. 2012;97(12):1909-15.
24. Yang L, Rau R, Goodell MA. DNMT3A in haematological malignancies. Nat Rev Cancer. 2015;15(3):152-65.
25. Ley TJ, Ding L, Walter MJ, McLellan MD, Lamprecht T, Larson DE, et al. DNMT3A mutations in acute myeloid leukemia. N Engl J Med. 2010;363(25):2424-33.
26. Issa GC, DiNardo CD. Acute myeloid leukemia with IDH1 and IDH2 mutations: 2021 treatment algorithm. Blood Cancer J. 2021;11(6):107.
27. Medeiros BC, Fathi AT, DiNardo CD, Pollyea DA, Chan SM, Swords R. Isocitrate dehydrogenase mutations in myeloid malignancies. Leukemia. 2017;31(2):272-81.
28. DiNardo CD, Cortes JE. Mutations in AML: prognostic and therapeutic implications. Hematology Am Soc Hematol Educ Program. 2016;2016(1):348-55.
29. Mill CP, Fiskus W, DiNardo CD, Birdwell C, Davis JA, Kadia TM, et al. Effective therapy for AML with RUNX1 mutation by cotreatment with inhibitors of protein translation and BCL2. Blood. 2022;139(6):907-21.
30. Grob T, Al Hinai ASA, Sanders MA, Kavelaars FG, Rijken M, Gradowska PL, et al. Molecular characterization of mutant TP53 acute myeloid leukemia and high-risk myelodysplastic syndrome. Blood. 2022;139(15):2347-54.
31. Boettcher S, Miller PG, Sharma R, McConkey M, Leventhal M, Krivtsov AV, et al. A dominant-negative effect drives selection of TP53 missense mutations in myeloid malignancies. Science. 2019;365(6453):599-604.
32. Daver N, Schlenk RF, Russell NH, Levis MJ. Targeting FLT3 mutations in AML: review of current knowledge and evidence. Leukemia. 2019;33(2):299-312.
33. Mackarehtschian K, Hardin JD, Moore KA, Boast S, Goff SP, Lemischka IR. Targeted disruption of the flk2/flt3 gene leads to deficiencies in primitive hematopoietic progenitors. Immunity. 1995;3(1):147-61.
34. Kazi JU, Ronnstrand L. FMS-like Tyrosine Kinase 3/FLT3: From Basic Science to Clinical Implications. Physiol Rev. 2019;99(3):1433-66.
35. Lagunas-Rangel FA, Chavez-Valencia V. FLT3-ITD and its current role in acute myeloid leukaemia. Med Oncol. 2017;34(6):114.

36. Zhao JC, Agarwal S, Ahmad H, Amin K, Bewersdorf JP, Zeidan AM. A review of FLT3 inhibitors in acute myeloid leukemia. Blood Rev. 2021:100905.
37. Pemmaraju N, Kantarjian H, Ravandi F, Cortes J. FLT3 inhibitors in the treatment of acute myeloid leukemia: the start of an era? Cancer. 2011;117(15):3293-304.
38. Kindler T, Lipka DB, Fischer T. FLT3 as a therapeutic target in AML: still challenging after all these years. Blood. 2010;116(24):5089-102.
39. Frohling S, Schlenk RF, Breitruck J, Benner A, Kreitmeier S, Tobis K, et al. Prognostic significance of activating FLT3 mutations in younger adults (16 to 60 years) with acute myeloid leukemia and normal cytogenetics: a study of the AML Study Group Ulm. Blood. 2002;100(13):4372-80.
40. Kottaridis PD, Gale RE, Frew ME, Harrison G, Langabeer SE, Belton AA, et al. The presence of a FLT3 internal tandem duplication in patients with acute myeloid leukemia (AML) adds important prognostic information to cytogenetic risk group and response to the first cycle of chemotherapy: analysis of 854 patients from the United Kingdom Medical Research Council AML 10 and 12 trials. Blood. 2001;98(6):1752-9.
41. Abu-Duhier FM, Goodeve AC, Wilson GA, Care RS, Peake IR, Reilly JT. Identification of novel FLT-3 Asp835 mutations in adult acute myeloid leukaemia. Br J Haematol. 2001;113(4):983-8.
42. Kiyoi H, Kawashima N, Ishikawa Y. FLT3 mutations in acute myeloid leukemia: Therapeutic paradigm beyond inhibitor development. Cancer Sci. 2020;111(2):312-22.
43. Li L, Piloto O, Nguyen HB, Greenberg K, Takamiya K, Racke F, et al. Knock-in of an internal tandem duplication mutation into murine FLT3 confers myeloproliferative disease in a mouse model. Blood. 2008;111(7):3849-58.
44. Poitras JL, Heiser D, Li L, Nguyen B, Nagai K, Duffield AS, et al. Dnmt3a deletion cooperates with the Flt3/ITD mutation to drive leukemogenesis in a murine model. Oncotarget. 2016;7(43):69124-35.
45. Hayakawa F, Towatari M, Kiyoi H, Tanimoto M, Kitamura T, Saito H, et al. Tandem-duplicated Flt3 constitutively activates STAT5 and MAP kinase and introduces autonomous cell growth in IL-3-dependent cell lines. Oncogene. 2000;19(5):624-31.

46. Spiekermann K, Bagrintseva K, Schwab R, Schmieja K, Hiddemann W. Overexpression and constitutive activation of FLT3 induces STAT5 activation in primary acute myeloid leukemia blast cells. Clin Cancer Res. 2003;9(6):2140-50.
47. Seedhouse CH, Pallis M, Grundy M, Shang S, Russell NH. FLT3-ITD expression levels and their effect on STAT5 in AML with and without NPM mutations. Br J Haematol. 2009;147(5):653-61.
48. Harir N, Pecquet C, Kerenyi M, Sonneck K, Kovacic B, Nyga R, et al. Constitutive activation of Stat5 promotes its cytoplasmic localization and association with PI3-kinase in myeloid leukemias. Blood. 2007;109(4):1678-86.
49. Pinz S, Unser S, Rascle A. Signal transducer and activator of transcription STAT5 is recruited to c-Myc super-enhancer. BMC Mol Biol. 2016;17:10.
50. Heydt Q, Larrue C, Saland E, Bertoli S, Sarry JE, Besson A, et al. Oncogenic FLT3-ITD supports autophagy via ATF4 in acute myeloid leukemia. Oncogene. 2018;37(6):787-97.
51. Yoshimoto G, Miyamoto T, Jabbarzadeh-Tabrizi S, Iino T, Rocnik JL, Kikushige Y, et al. FLT3-ITD up-regulates MCL-1 to promote survival of stem cells in acute myeloid leukemia via FLT3-ITD-specific STAT5 activation. Blood. 2009;114(24):5034-43.
52. Falini B, Mecucci C, Tiacci E, Alcalay M, Rosati R, Pasqualucci L, et al. Cytoplasmic nucleophosmin in acute myelogenous leukemia with a normal karyotype. N Engl J Med. 2005;352(3):254-66.
53. Chou SH, Ko BS, Chiou JS, Hsu YC, Tsai MH, Chiu YC, et al. A knock-in Npm1 mutation in mice results in myeloproliferation and implies a perturbation in hematopoietic microenvironment. PloS one. 2012;7(11):e49769.
54. Borer RA, Lehner CF, Eppenberger HM, Nigg EA. Major nucleolar proteins shuttle between nucleus and cytoplasm. Cell. 1989;56(3):379-90.
55. Falini B, Brunetti L, Sportoletti P, Martelli MP. NPM1-mutated acute myeloid leukemia: from bench to bedside. Blood. 2020;136(15):1707-21.
56. Yada M, Hatakeyama S, Kamura T, Nishiyama M, Tsunematsu R, Imaki H, et al. Phosphorylation-dependent degradation of c-Myc is mediated by the F-box protein Fbw7. EMBO J. 2004;23(10):2116-25.
57. Heath EM, Chan SM, Minden MD, Murphy T, Shlush LI, Schimmer AD. Biological and clinical consequences of NPM1 mutations in AML. Leukemia. 2017;31(4):798-807.

58. Vassiliou GS, Cooper JL, Rad R, Li J, Rice S, Uren A, et al. Mutant nucleophosmin and cooperating pathways drive leukemia initiation and progression in mice. Nature genetics. 2011;43(5):470-5.
59. Colombo E, Martinelli P, Zamponi R, Shing DC, Bonetti P, Luzi L, et al. Delocalization and destabilization of the Arf tumor suppressor by the leukemia-associated NPM mutant. Cancer research. 2006;66(6):3044-50.
60. Mitrea DM, Kriwacki RW. On the relationship status for Arf and NPM1 - it's complicated. FEBS J. 2018;285(5):828-31.
61. Bonetti P, Davoli T, Sironi C, Amati B, Pelicci PG, Colombo E. Nucleophosmin and its AML-associated mutant regulate c-Myc turnover through Fbw7 gamma. The Journal of cell biology. 2008;182(1):19-26.
62. Dohner H, Weisdorf DJ, Bloomfield CD. Acute Myeloid Leukemia. N Engl J Med. 2015;373(12):1136-52.
63. Tamamyan G, Kadia T, Ravandi F, Borthakur G, Cortes J, Jabbour E, et al. Frontline treatment of acute myeloid leukemia in adults. Crit Rev Oncol Hematol. 2017;110:20-34.
64. Tomic B, Smoljo T, Lalic H, Dembitz V, Batinic J, Batinic D, et al. Cytarabine-induced differentiation of AML cells depends on Chk1 activation and shares the mechanism with inhibitors of DHODH and pyrimidine synthesis. Sci Rep. 2022;12(1):11344.
65. Emadi A, Karp JE. The clinically relevant pharmacogenomic changes in acute myelogenous leukemia. Pharmacogenomics. 2012;13(11):1257-69.
66. Marinello J, Delcuratolo M, Capranico G. Anthracyclines as Topoisomerase II Poisons: From Early Studies to New Perspectives. Int J Mol Sci. 2018;19(11).
67. Saha M, Das S. Free radical induced activity of an anthracycline analogue and its Mn(II) complex on biological targets through in situ electrochemical generation of semiquinone. Heliyon. 2021;7(8):e07746.
68. Cheson BD, Bennett JM, Kopecky KJ, Buchner T, Willman CL, Estey EH, et al. Revised recommendations of the International Working Group for Diagnosis, Standardization of Response Criteria, Treatment Outcomes, and Reporting Standards for Therapeutic Trials in Acute Myeloid Leukemia. J Clin Oncol. 2003;21(24):4642-9.
69. Fernandez HF, Sun Z, Yao X, Litzow MR, Luger SM, Paietta EM, et al. Anthracycline dose intensification in acute myeloid leukemia. N Engl J Med. 2009;361(13):1249-59.

70. Pelcovits A, Niroula R. Acute Myeloid Leukemia: A Review. R I Med J (2013). 2020;103(3):38-40.
71. Dohner H, Estey E, Grimwade D, Amadori S, Appelbaum FR, Buchner T, et al. Diagnosis and management of AML in adults: 2017 ELN recommendations from an international expert panel. Blood. 2017;129(4):424-47.
72. Loke J, Buka R, Craddock C. Allogeneic Stem Cell Transplantation for Acute Myeloid Leukemia: Who, When, and How? Front Immunol. 2021;12:659595.
73. Saillard C, Darmon M, Bisbal M, Sannini A, Chow-Chine L, Faucher M, et al. Critically ill allogenic HSCT patients in the intensive care unit: a systematic review and meta-analysis of prognostic factors of mortality. Bone Marrow Transplant. 2018;53(10):1233-41.
74. Perl AE, Martinelli G, Cortes JE, Neubauer A, Berman E, Paolini S, et al. Gilteritinib or Chemotherapy for Relapsed or Refractory FLT3-Mutated AML. N Engl J Med. 2019;381(18):1728-40.
75. Stone RM, Mandrekar SJ, Sanford BL, Laumann K, Geyer S, Bloomfield CD, et al. Midostaurin plus Chemotherapy for Acute Myeloid Leukemia with a FLT3 Mutation. N Engl J Med. 2017;377(5):454-64.
76. Knapper S, Mills KI, Gilkes AF, Austin SJ, Walsh V, Burnett AK. The effects of lestaurtinib (CEP701) and PKC412 on primary AML blasts: the induction of cytotoxicity varies with dependence on FLT3 signaling in both FLT3-mutated and wild-type cases. Blood. 2006;108(10):3494-503.
77. Smith CC, Wang Q, Chin CS, Salerno S, Damon LE, Levis MJ, et al. Validation of ITD mutations in FLT3 as a therapeutic target in human acute myeloid leukaemia. Nature. 2012;485(7397):260-3.
78. Piloto O, Wright M, Brown P, Kim KT, Levis M, Small D. Prolonged exposure to FLT3 inhibitors leads to resistance via activation of parallel signaling pathways. Blood. 2007;109(4):1643-52.
79. McMahon CM, Ferng T, Canaani J, Wang ES, Morrissette JJD, Eastburn DJ, et al. Clonal Selection with RAS Pathway Activation Mediates Secondary Clinical Resistance to Selective FLT3 Inhibition in Acute Myeloid Leukemia. Cancer Discov. 2019;9(8):1050-63.
80. Sato T, Yang X, Knapper S, White P, Smith BD, Galkin S, et al. FLT3 ligand impedes the efficacy of FLT3 inhibitors in vitro and in vivo. Blood. 2011;117(12):3286-93.

81. Scarpa M, Singh P, Bailey CM, Lee JK, Kapoor S, Lapidus RG, et al. PP2A-activating Drugs Enhance FLT3 Inhibitor Efficacy through AKT Inhibition-Dependent GSK-3beta-Mediated c-Myc and Pim-1 Proteasomal Degradation. Mol Cancer Ther. 2021;20(4):676-90.
82. Venugopal S, Takahashi K, Daver N, Maiti A, Borthakur G, Loghavi S, et al. Efficacy and safety of enasidenib and azacitidine combination in patients with IDH2 mutated acute myeloid leukemia and not eligible for intensive chemotherapy. Blood Cancer J. 2022;12(1):10.
83. Kim ES. Enasidenib: First Global Approval. Drugs. 2017;77(15):1705-11.
84. Norsworthy KJ, Luo L, Hsu V, Gudi R, Dorff SE, Przepiorka D, et al. FDA Approval Summary: Ivosidenib for Relapsed or Refractory Acute Myeloid Leukemia with an Isocitrate Dehydrogenase-1 Mutation. Clin Cancer Res. 2019;25(11):3205-9.
85. Yamauchi T, Matsuda Y, Tasaki T, Negoro E, Ikegaya S, Takagi K, et al. Induction of DNA strand breaks is critical to predict the cytotoxicity of gemtuzumab ozogamicin against leukemic cells. Cancer Sci. 2012;103(9):1722-9.
86. Modjtahedi H, Ali S, Essapen S. Therapeutic application of monoclonal antibodies in cancer: advances and challenges. Br Med Bull. 2012;104:41-59.
87. Hills RK, Castaigne S, Appelbaum FR, Delaunay J, Petersdorf S, Othus M, et al. Addition of gemtuzumab ozogamicin to induction chemotherapy in adult patients with acute myeloid leukaemia: a meta-analysis of individual patient data from randomised controlled trials. Lancet Oncol. 2014;15(9):986-96.
88. Guerra VA, DiNardo C, Konopleva M. Venetoclax-based therapies for acute myeloid leukemia. Best Pract Res Clin Haematol. 2019;32(2):145-53.
89. Mihalyova J, Jelinek T, Growkova K, Hrdinka M, Simicek M, Hajek R. Venetoclax: A new wave in hematooncology. Exp Hematol. 2018;61:10-25.
90. Konopleva M, Pollyea DA, Potluri J, Chyla B, Hogdal L, Busman T, et al. Efficacy and Biological Correlates of Response in a Phase II Study of Venetoclax Monotherapy in Patients with Acute Myelogenous Leukemia. Cancer Discov. 2016;6(10):1106-17.
91. Leung KK, Nguyen A, Shi T, Tang L, Ni X, Escoubet L, et al. Multiomics of azacitidine-treated AML cells reveals variable and convergent targets that remodel the cell-surface proteome. Proc Natl Acad Sci U S A. 2019;116(2):695-700.

92. Dombret H, Seymour JF, Butrym A, Wierzbowska A, Selleslag D, Jang JH, et al. International phase 3 study of azacitidine vs conventional care regimens in older patients with newly diagnosed AML with >30% blasts. Blood. 2015;126(3):291-9.
93. Wei AH, Montesinos P, Ivanov V, DiNardo CD, Novak J, Laribi K, et al. Venetoclax plus LDAC for newly diagnosed AML ineligible for intensive chemotherapy: a phase 3 randomized placebo-controlled trial. Blood. 2020;135(24):2137-45.
94. Zeidan AM, Pollyea DA, Borate U, Vasconcelos A, Potluri R, Rotter D, et al. Venetoclax plus azacitidine compared with intensive chemotherapy as induction for patients with acute myeloid leukemia: retrospective analysis of an electronic medical record database in the United States. Ann Hematol. 2023;102(4):749-54.
95. Jones CL, Stevens BM, D'Alessandro A, Reisz JA, Culp-Hill R, Nemkov T, et al. Inhibition of Amino Acid Metabolism Selectively Targets Human Leukemia Stem Cells. Cancer Cell. 2018;34(5):724-40 e4.
96. Ram R, Scheid C, Amit O, Chemnitz JM, Moshe Y, Hallek M, et al. Sequential therapy for patients with primary refractory acute myeloid leukemia: a historical prospective analysis of the German and Israeli experience. Haematologica. 2019;104(9):1798-803.
97. DeWolf S, Tallman MS. How I treat relapsed or refractory AML. Blood. 2020;136(9):1023-32.
98. Scholl S, Fleischmann M, Schnetzke U, Heidel FH. Molecular Mechanisms of Resistance to FLT3 Inhibitors in Acute Myeloid Leukemia: Ongoing Challenges and Future Treatments. Cells. 2020;9(11).
99. Bolwell BJ, Cassileth PA, Gale RP. High dose cytarabine: a review. Leukemia. 1988;2(5):253-60.
100. Yilmaz M, Wang F, Loghavi S, Bueso-Ramos C, Gumbs C, Little L, et al. Late relapse in acute myeloid leukemia (AML): clonal evolution or therapy-related leukemia? Blood Cancer J. 2019;9(2):7.
101. Ganzel C, Sun Z, Cripe LD, Fernandez HF, Douer D, Rowe JM, et al. Very poor long-term survival in past and more recent studies for relapsed AML patients: The ECOG-ACRIN experience. Am J Hematol. 2018;93(8):1074-81.
102. Tenold ME, Moskoff BN, Benjamin DJ, Hoeg RT, Rosenberg AS, Abedi M, et al. Outcomes of Adults With Relapsed/Refractory Acute Myeloid Leukemia Treated With

Venetoclax Plus Hypomethylating Agents at a Comprehensive Cancer Center. Front Oncol. 2021;11:649209.
103. Thol F, Schlenk RF, Heuser M, Ganser A. How I treat refractory and early relapsed acute myeloid leukemia. Blood. 2015;126(3):319-27.
104. Deeg HJ, Sandmaier BM. Who is fit for allogeneic transplantation? Blood. 2010;116(23):4762-70.
105. Stanisic S, Kalaycio M. Treatment of refractory and relapsed acute myelogenous leukemia. Expert Rev Anticancer Ther. 2002;2(3):287-95.
106. Breems DA, Van Putten WL, Huijgens PC, Ossenkoppele GJ, Verhoef GE, Verdonck LF, et al. Prognostic index for adult patients with acute myeloid leukemia in first relapse. J Clin Oncol. 2005;23(9):1969-78.
107. Vosberg S, Greif PA. Clonal evolution of acute myeloid leukemia from diagnosis to relapse. Genes Chromosomes Cancer. 2019;58(12):839-49.
108. Kern W, Haferlach T, Schnittger S, Ludwig WD, Hiddemann W, Schoch C. Karyotype instability between diagnosis and relapse in 117 patients with acute myeloid leukemia: implications for resistance against therapy. Leukemia. 2002;16(10):2084-91.
109. Garg M, Nagata Y, Kanojia D, Mayakonda A, Yoshida K, Haridas Keloth S, et al. Profiling of somatic mutations in acute myeloid leukemia with FLT3-ITD at diagnosis and relapse. Blood. 2015;126(22):2491-501.
110. Sood R, Hansen NF, Donovan FX, Carrington B, Bucci D, Maskeri B, et al. Somatic mutational landscape of AML with inv(16) or t(8;21) identifies patterns of clonal evolution in relapse leukemia. Leukemia. 2016;30(2):501-4.
111. Cocciardi S, Dolnik A, Kapp-Schwoerer S, Rucker FG, Lux S, Blatte TJ, et al. Clonal evolution patterns in acute myeloid leukemia with NPM1 mutation. Nat Commun. 2019;10(1):2031.
112. Greif PA, Hartmann L, Vosberg S, Stief SM, Mattes R, Hellmann I, et al. Evolution of Cytogenetically Normal Acute Myeloid Leukemia During Therapy and Relapse: An Exome Sequencing Study of 50 Patients. Clin Cancer Res. 2018;24(7):1716-26.
113. Hollein A, Meggendorfer M, Dicker F, Jeromin S, Nadarajah N, Kern W, et al. NPM1 mutated AML can relapse with wild-type NPM1: persistent clonal hematopoiesis can drive relapse. Blood Adv. 2018;2(22):3118-25.

114. Pluquet O, Abbadie C, Coqueret O. Connecting cancer relapse with senescence. Cancer Lett. 2019;463:50-8.
115. Campisi J. Cellular senescence as a tumor-suppressor mechanism. Trends Cell Biol. 2001;11(11):S27-31.
116. Duy C, Li M, Teater M, Meydan C, Garrett-Bakelman FE, Lee TC, et al. Chemotherapy Induces Senescence-Like Resilient Cells Capable of Initiating AML Recurrence. Cancer Discov. 2021;11(6):1542-61.
117. Saleh T, Tyutyunyk-Massey L, Murray GF, Alotaibi MR, Kawale AS, Elsayed Z, et al. Tumor cell escape from therapy-induced senescence. Biochem Pharmacol. 2019;162:202-12.
118. Park CY, Tseng D, Weissman IL. Cancer stem cell-directed therapies: recent data from the laboratory and clinic. Mol Ther. 2009;17(2):219-30.
119. Meacham CE, Morrison SJ. Tumour heterogeneity and cancer cell plasticity. Nature. 2013;501(7467):328-37.
120. Li X, Lewis MT, Huang J, Gutierrez C, Osborne CK, Wu MF, et al. Intrinsic resistance of tumorigenic breast cancer cells to chemotherapy. J Natl Cancer Inst. 2008;100(9):672-9.
121. Tang B, Raviv A, Esposito D, Flanders KC, Daniel C, Nghiem BT, et al. A flexible reporter system for direct observation and isolation of cancer stem cells. Stem Cell Reports. 2015;4(1):155-69.
122. Li J, Haque M, Shang C, Hassan B, Liu D, Chen W, et al. Identification and Characterization of Cancer Stem-Like Cells in ALK-Positive Anaplastic Large Cell Lymphoma Using the SORE6 Reporter. Curr Issues Mol Biol. 2021;43(2):543-57.
123. Jeon HM, Lee J. MET: roles in epithelial-mesenchymal transition and cancer stemness. Ann Transl Med. 2017;5(1):5.
124. Fischer KR, Durrans A, Lee S, Sheng J, Li F, Wong ST, et al. Epithelial-to-mesenchymal transition is not required for lung metastasis but contributes to chemoresistance. Nature. 2015;527(7579):472-6.
125. Luo W, Li S, Peng B, Ye Y, Deng X, Yao K. Embryonic stem cells markers SOX2, OCT4 and Nanog expression and their correlations with epithelial-mesenchymal transition in nasopharyngeal carcinoma. PLoS One. 2013;8(2):e56324.

126. Gopal K, Gupta N, Zhang H, Alshareef A, Alqahtani H, Bigras G, et al. Oxidative stress induces the acquisition of cancer stem-like phenotype in breast cancer detectable by using a Sox2 regulatory region-2 (SRR2) reporter. Oncotarget. 2016;7(3):3111-27.
127. Lagadec C, Vlashi E, Della Donna L, Dekmezian C, Pajonk F. Radiation-induced reprogramming of breast cancer cells. Stem Cells. 2012;30(5):833-44.
128. Sharma SV, Lee DY, Li B, Quinlan MP, Takahashi F, Maheswaran S, et al. A chromatin-mediated reversible drug-tolerant state in cancer cell subpopulations. Cell. 2010;141(1):69-80.
129. Goldman A, Majumder B, Dhawan A, Ravi S, Goldman D, Kohandel M, et al. Temporally sequenced anticancer drugs overcome adaptive resistance by targeting a vulnerable chemotherapy-induced phenotypic transition. Nat Commun. 2015;6:6139.
130. Wu C, Gupta N, Huang YH, Zhang HF, Alshareef A, Chow A, et al. Oxidative stress enhances tumorigenicity and stem-like features via the activation of the Wnt/beta-catenin/MYC/Sox2 axis in ALK-positive anaplastic large-cell lymphoma. BMC Cancer. 2018;18(1):361.
131. Ng SW, Mitchell A, Kennedy JA, Chen WC, McLeod J, Ibrahimova N, et al. A 17-gene stemness score for rapid determination of risk in acute leukaemia. Nature. 2016;540(7633):433-7.
132. Ho TC, LaMere M, Stevens BM, Ashton JM, Myers JR, O'Dwyer KM, et al. Evolution of acute myelogenous leukemia stem cell properties after treatment and progression. Blood. 2016;128(13):1671-8.
133. Shlush LI, Mitchell A, Heisler L, Abelson S, Ng SWK, Trotman-Grant A, et al. Tracing the origins of relapse in acute myeloid leukaemia to stem cells. Nature. 2017;547(7661):104-8.
134. Pang WW, Price EA, Sahoo D, Beerman I, Maloney WJ, Rossi DJ, et al. Human bone marrow hematopoietic stem cells are increased in frequency and myeloid-biased with age. Proc Natl Acad Sci U S A. 2011;108(50):20012-7.
135. Beckmann J, Scheitza S, Wernet P, Fischer JC, Giebel B. Asymmetric cell division within the human hematopoietic stem and progenitor cell compartment: identification of asymmetrically segregating proteins. Blood. 2007;109(12):5494-501.
136. Bradley TR, Metcalf D. The growth of mouse bone marrow cells in vitro. Aust J Exp Biol Med Sci. 1966;44(3):287-99.

137. Kamel-Reid S, Dick JE. Engraftment of immune-deficient mice with human hematopoietic stem cells. Science. 1988;242(4886):1706-9.
138. Rix B, Maduro AH, Bridge KS, Grey W. Markers for human haematopoietic stem cells: The disconnect between an identification marker and its function. Front Physiol. 2022;13:1009160.
139. Bracker TU, Giebel B, Spanholtz J, Sorg UR, Klein-Hitpass L, Moritz T, et al. Stringent regulation of DNA repair during human hematopoietic differentiation: a gene expression and functional analysis. Stem Cells. 2006;24(3):722-30.
140. Rocha CRR, Lerner LK, Okamoto OK, Marchetto MC, Menck CFM. The role of DNA repair in the pluripotency and differentiation of human stem cells. Mutat Res. 2013;752(1):25-35.
141. Ishiguro T, Ohata H, Sato A, Yamawaki K, Enomoto T, Okamoto K. Tumor-derived spheroids: Relevance to cancer stem cells and clinical applications. Cancer Sci. 2017;108(3):283-9.
142. Vaddi PK, Stamnes MA, Cao H, Chen S. Elimination of SOX2/OCT4-Associated Prostate Cancer Stem Cells Blocks Tumor Development and Enhances Therapeutic Response. Cancers (Basel). 2019;11(9).
143. Pádua D, Barros R, Amaral AL, Mesquita P, Freire AF, Sousa M, et al. A SOX2 Reporter System Identifies Gastric Cancer Stem-Like Cells Sensitive to Monensin. Cancers (Basel). 2020;12(2):20.
144. Foty R. A simple hanging drop cell culture protocol for generation of 3D spheroids. J Vis Exp. 2011(51).
145. Gheytanchi E, Naseri M, Karimi-Busheri F, Atyabi F, Mirsharif ES, Bozorgmehr M, et al. Morphological and molecular characteristics of spheroid formation in HT-29 and Caco-2 colorectal cancer cell lines. Cancer Cell Int. 2021;21(1):204.
146. To K, Fotovati A, Reipas KM, Law JH, Hu K, Wang J, et al. Y-box binding protein-1 induces the expression of CD44 and CD49f leading to enhanced self-renewal, mammosphere growth, and drug resistance. Cancer Res. 2010;70(7):2840-51.
147. Hu L, McArthur C, Jaffe RB. Ovarian cancer stem-like side-population cells are tumourigenic and chemoresistant. Br J Cancer. 2010;102(8):1276-83.

148. Liu T, Cheng W, Lai D, Huang Y, Guo L. Characterization of primary ovarian cancer cells in different culture systems. Oncol Rep. 2010;23(5):1277-84.
149. Liu G, Yuan X, Zeng Z, Tunici P, Ng H, Abdulkadir IR, et al. Analysis of gene expression and chemoresistance of CD133+ cancer stem cells in glioblastoma. Mol Cancer. 2006;5:67.
150. Ishikawa F, Yoshida S, Saito Y, Hijikata A, Kitamura H, Tanaka S, et al. Chemotherapy-resistant human AML stem cells home to and engraft within the bone-marrow endosteal region. Nature biotechnology. 2007;25(11):1315-21.
151. Bousquet G, El Bouchtaoui M, Sophie T, Leboeuf C, de Bazelaire C, Ratajczak P, et al. Targeting autophagic cancer stem-cells to reverse chemoresistance in human triple negative breast cancer. Oncotarget. 2017;8(21):35205-21.
152. Phi LTH, Sari IN, Yang YG, Lee SH, Jun N, Kim KS, et al. Cancer Stem Cells (CSCs) in Drug Resistance and their Therapeutic Implications in Cancer Treatment. Stem Cells Int. 2018;2018:5416923.
153. Lapidot T, Sirard C, Vormoor J, Murdoch B, Hoang T, Caceres-Cortes J, et al. A cell initiating human acute myeloid leukaemia after transplantation into SCID mice. Nature; 1994. p. 4.
154. Murayama T, Gotoh N. Drug resistance mechanisms of cancer stem-like cells and their therapeutic potential as drug targets. Cancer Drug Resist. 2019;2(3):457-70.
155. Borah A, Raveendran S, Rochani A, Maekawa T, Kumar DS. Targeting self-renewal pathways in cancer stem cells: clinical implications for cancer therapy. Oncogenesis. 2015;4(11):e177.
156. Fan X, Khaki L, Zhu TS, Soules ME, Talsma CE, Gul N, et al. NOTCH pathway blockade depletes CD133-positive glioblastoma cells and inhibits growth of tumor neurospheres and xenografts. Stem Cells. 2010;28(1):5-16.
157. Takahashi K, Tanabe K, Ohnuki M, Narita M, Ichisaka T, Tomoda K, et al. Induction of pluripotent stem cells from adult human fibroblasts by defined factors. Cell. 2007;131(5):861-72.
158. Gupta N, Jung K, Wu C, Alshareef A, Alqahtani H, Damaraju S, et al. High Myc expression and transcription activity underlies intra-tumoral heterogeneity in triple-negative breast cancer. Oncotarget. 2017;8(17):28101-15.

159. Zhang D, Zhao Q, Sun H, Yin L, Wu J, Xu J, et al. Defective autophagy leads to the suppression of stem-like features of CD271(+) osteosarcoma cells. J Biomed Sci. 2016;23(1):82.
160. Peng S, Maihle NJ, Huang Y. Pluripotency factors Lin28 and Oct4 identify a sub-population of stem cell-like cells in ovarian cancer. Oncogene. 2010;29(14):2153-9.
161. Zhu P, Wang Y, He L, Huang G, Du Y, Zhang G, et al. ZIC2-dependent OCT4 activation drives self-renewal of human liver cancer stem cells. J Clin Invest. 2015;125(10):3795-808.
162. Gangemi RM, Griffero F, Marubbi D, Perera M, Capra MC, Malatesta P, et al. SOX2 silencing in glioblastoma tumor-initiating cells causes stop of proliferation and loss of tumorigenicity. Stem Cells. 2009;27(1):40-8.
163. Leis O, Eguiara A, Lopez-Arribillaga E, Alberdi MJ, Hernandez-Garcia S, Elorriaga K, et al. Sox2 expression in breast tumours and activation in breast cancer stem cells. Oncogene. 2012;31(11):1354-65.
164. Bourguignon LY, Peyrollier K, Xia W, Gilad E. Hyaluronan-CD44 interaction activates stem cell marker Nanog, Stat-3-mediated MDR1 gene expression, and ankyrin-regulated multidrug efflux in breast and ovarian tumor cells. J Biol Chem. 2008;283(25):17635-51.
165. Jeter CR, Badeaux M, Choy G, Chandra D, Patrawala L, Liu C, et al. Functional evidence that the self-renewal gene NANOG regulates human tumor development. Stem Cells. 2009;27(5):993-1005.
166. Zbinden M, Duquet A, Lorente-Trigos A, Ngwabyt SN, Borges I, Ruiz i Altaba A. NANOG regulates glioma stem cells and is essential in vivo acting in a cross-functional network with GLI1 and p53. EMBO J. 2010;29(15):2659-74.
167. Xu CX, Xu M, Tan L, Yang H, Permuth-Wey J, Kruk PA, et al. MicroRNA miR-214 regulates ovarian cancer cell stemness by targeting p53/Nanog. J Biol Chem. 2012;287(42):34970-8.
168. Beltran AS, Rivenbark AG, Richardson BT, Yuan X, Quian H, Hunt JP, et al. Generation of tumor-initiating cells by exogenous delivery of OCT4 transcription factor. Breast Cancer Res. 2011;13(5):R94.
169. Hanekamp D, Cloos J, Schuurhuis GJ. Leukemic stem cells: identification and clinical application. Springer Science and Business Media LLC; 2017. p. 549.
170. Ho JM, Dobson SM, Voisin V, McLeod J, Kennedy JA, Mitchell A, et al. CD200 expression marks leukemia stem cells in human AML. Blood advances. 2020;4(21):5402-13.

171. Jin L, Lee EM, Ramshaw HS, Busfield SJ, Peoppl AG, Wilkinson L, et al. Monoclonal antibody-mediated targeting of CD123, IL-3 receptor alpha chain, eliminates human acute myeloid leukemic stem cells. Cell Stem Cell. 2009;5(1):31-42.
172. Taussig DC, Miraki-Moud F, Anjos-Afonso F, Pearce DJ, Allen K, Ridler C, et al. Anti-CD38 antibody-mediated clearance of human repopulating cells masks the heterogeneity of leukemia-initiating cells. Blood. 2008;112(3):568-75.
173. Taussig DC, Vargaftig J, Miraki-Moud F, Griessinger E, Sharrock K, Luke T, et al. Leukemia-initiating cells from some acute myeloid leukemia patients with mutated nucleophosmin reside in the CD34(-) fraction. Blood. 2010;115(10):1976-84.
174. Clark DW, Palle K. Aldehyde dehydrogenases in cancer stem cells: potential as therapeutic targets. Ann Transl Med. 2016;4(24):518.
175. Storms RW, Trujillo AP, Springer JB, Shah L, Colvin OM, Ludeman SM, et al. Isolation of primitive human hematopoietic progenitors on the basis of aldehyde dehydrogenase activity. Proc Natl Acad Sci U S A. 1999;96(16):9118-23.
176. Chute JP, Muramoto GG, Whitesides J, Colvin M, Safi R, Chao NJ, et al. Inhibition of aldehyde dehydrogenase and retinoid signaling induces the expansion of human hematopoietic stem cells. Proc Natl Acad Sci U S A. 2006;103(31):11707-12.
177. Huang EH, Hynes MJ, Zhang T, Ginestier C, Dontu G, Appelman H, et al. Aldehyde dehydrogenase 1 is a marker for normal and malignant human colonic stem cells (SC) and tracks SC overpopulation during colon tumorigenesis. Cancer Res. 2009;69(8):3382-9.
178. Jiang F, Qiu Q, Khanna A, Todd NW, Deepak J, Xing L, et al. Aldehyde dehydrogenase 1 is a tumor stem cell-associated marker in lung cancer. Mol Cancer Res. 2009;7(3):330-8.
179. Cheung AM, Wan TS, Leung JC, Chan LY, Huang H, Kwong YL, et al. Aldehyde dehydrogenase activity in leukemic blasts defines a subgroup of acute myeloid leukemia with adverse prognosis and superior NOD/SCID engrafting potential. Leukemia. 2007;21(7):1423-30.
180. Keysar SB, Jimeno A. More than markers: biological significance of cancer stem cell-defining molecules. Mol Cancer Ther. 2010;9(9):2450-7.
181. Ma I, Allan AL. The role of human aldehyde dehydrogenase in normal and cancer stem cells. Stem Cell Rev Rep. 2011;7(2):292-306.

182. Jung K, Gupta N, Wang P, Lewis JT, Gopal K, Wu F, et al. Triple negative breast cancers comprise a highly tumorigenic cell subpopulation detectable by its high responsiveness to a Sox2 regulatory region 2 (SRR2) reporter. Oncotarget. 2015;6(12):10366-73.
183. Zhang HF, Wu C, Alshareef A, Gupta N, Zhao Q, Xu XE, et al. The PI3K/AKT/c-MYC Axis Promotes the Acquisition of Cancer Stem-Like Features in Esophageal Squamous Cell Carcinoma. Stem Cells. 2016;34(8):2040-51.
184. Bano A, Stevens JH, Modi PS, Gustafsson JA, Strom AM. Estrogen Receptor beta4 Regulates Chemotherapy Resistance and Induces Cancer Stem Cells in Triple Negative Breast Cancer. Int J Mol Sci. 2023;24(6).
185. Rosas-Cruz A, Salinas-Jazmin N, Valdes-Rives A, Velasco-Velazquez MA. DRD1 and DRD4 are differentially expressed in breast tumors and breast cancer stem cells: pharmacological implications. Transl Cancer Res. 2022;11(11):3941-50.
186. Menendez ST, Rey V, Martinez-Cruzado L, Gonzalez MV, Morales-Molina A, Santos L, et al. SOX2 Expression and Transcriptional Activity Identifies a Subpopulation of Cancer Stem Cells in Sarcoma with Prognostic Implications. Cancers (Basel). 2020;12(4).
187. Gao W, Wu D, Wang Y, Wang Z, Zou C, Dai Y, et al. Development of a novel and economical agar-based non-adherent three-dimensional culture method for enrichment of cancer stem-like cells. Stem Cell Res Ther. 2018;9(1):243.
188. Hirschmann-Jax C, Foster AE, Wulf GG, Nuchtern JG, Jax TW, Gobel U, et al. A distinct "side population" of cells with high drug efflux capacity in human tumor cells. Proc Natl Acad Sci U S A. 2004;101(39):14228-33.
189. Seigel GM, Campbell LM, Narayan M, Gonzalez-Fernandez F. Cancer stem cell characteristics in retinoblastoma. Mol Vis. 2005;11:729-37.
190. de Figueiredo-Pontes LL, Pintao MC, Oliveira LC, Dalmazzo LF, Jacomo RH, Garcia AB, et al. Determination of P-glycoprotein, MDR-related protein 1, breast cancer resistance protein, and lung-resistance protein expression in leukemic stem cells of acute myeloid leukemia. Cytometry B Clin Cytom. 2008;74(3):163-8.
191. Vasconcelos FC, de Souza PS, Hancio T, de Faria FCC, Maia RC. Update on drug transporter proteins in acute myeloid leukemia: Pathological implication and clinical setting. Crit Rev Oncol Hematol. 2021;160:103281.

192. Raaijmakers MH, de Grouw EP, Heuver LH, van der Reijden BA, Jansen JH, Scheper RJ, et al. Breast cancer resistance protein in drug resistance of primitive CD34+38- cells in acute myeloid leukemia. Clin Cancer Res. 2005;11(6):2436-44.
193. Wuchter C, Leonid K, Ruppert V, Schrappe M, Buchner T, Schoch C, et al. Clinical significance of P-glycoprotein expression and function for response to induction chemotherapy, relapse rate and overall survival in acute leukemia. Haematologica. 2000;85(7):711-21.
194. Schaich M, Soucek S, Thiede C, Ehninger G, Illmer T, Group SAS. MDR1 and MRP1 gene expression are independent predictors for treatment outcome in adult acute myeloid leukaemia. Br J Haematol. 2005;128(3):324-32.
195. Benderra Z, Faussat AM, Sayada L, Perrot JY, Chaoui D, Marie JP, et al. Breast cancer resistance protein and P-glycoprotein in 149 adult acute myeloid leukemias. Clin Cancer Res. 2004;10(23):7896-902.
196. Cripe LD, Uno H, Paietta EM, Litzow MR, Ketterling RP, Bennett JM, et al. Zosuquidar, a novel modulator of P-glycoprotein, does not improve the outcome of older patients with newly diagnosed acute myeloid leukemia: a randomized, placebo-controlled trial of the Eastern Cooperative Oncology Group 3999. Blood. 2010;116(20):4077-85.
197. Lagadinou ED, Sach A, Callahan K, Rossi RM, Neering SJ, Minhajuddin M, et al. BCL-2 inhibition targets oxidative phosphorylation and selectively eradicates quiescent human leukemia stem cells. Cell Stem Cell. 2013;12(3):329-41.
198. Dembinski JL, Krauss S. Characterization and functional analysis of a slow cycling stem cell-like subpopulation in pancreas adenocarcinoma. Clin Exp Metastasis. 2009;26(7):611-23.
199. Gao MQ, Choi YP, Kang S, Youn JH, Cho NH. CD24+ cells from hierarchically organized ovarian cancer are enriched in cancer stem cells. Oncogene. 2010;29(18):2672-80.
200. Vincent Z, Urakami K, Maruyama K, Yamaguchi K, Kusuhara M. CD133-positive cancer stem cells from Colo205 human colon adenocarcinoma cell line show resistance to chemotherapy and display a specific metabolomic profile. Genes Cancer. 2014;5(7-8):250-60.
201. Haraguchi N, Ishii H, Mimori K, Tanaka F, Ohkuma M, Kim HM, et al. CD13 is a therapeutic target in human liver cancer stem cells. J Clin Invest. 2010;120(9):3326-39.
202. Skvortsov S, Debbage P, Lukas P, Skvortsova I. Crosstalk between DNA repair and cancer stem cell (CSC) associated intracellular pathways. Semin Cancer Biol. 2015;31:36-42.

203. Facchino S, Abdouh M, Chatoo W, Bernier G. BMI1 confers radioresistance to normal and cancerous neural stem cells through recruitment of the DNA damage response machinery. J Neurosci. 2010;30(30):10096-111.
204. Shang C, Hassan B, Haque M, Song Y, Li J, Liu D, et al. Crizotinib Resistance Mediated by Autophagy Is Higher in the Stem-Like Cell Subset in ALK-Positive Anaplastic Large Cell Lymphoma, and This Effect Is MYC-Dependent. Cancers (Basel). 2021;13(2).
205. Hanahan D. Hallmarks of Cancer: New Dimensions. Cancer Discov. 2022;12(1):31-46.
206. Kim HK, Son SY, Oh JS, Song YN, Byun JM, Koh Y, et al. Metabolic Profiling during Acute Myeloid Leukemia Progression Using Paired Clinical Bone Marrow Serum Samples. Metabolites. 2021;11(9).
207. Bingol K. Recent Advances in Targeted and Untargeted Metabolomics by NMR and MS/NMR Methods. High Throughput. 2018;7(2).
208. Wang Y, Zhang L, Chen WL, Wang JH, Li N, Li JM, et al. Rapid diagnosis and prognosis of de novo acute myeloid leukemia by serum metabonomic analysis. J Proteome Res. 2013;12(10):4393-401.
209. Musharraf SG, Siddiqui AJ, Shamsi T, Choudhary MI, Rahman AU. Serum metabonomics of acute leukemia using nuclear magnetic resonance spectroscopy. Sci Rep. 2016;6:30693.
210. Chen WL, Wang JH, Zhao AH, Xu X, Wang YH, Chen TL, et al. A distinct glucose metabolism signature of acute myeloid leukemia with prognostic value. Blood. 2014;124(10):1645-54.
211. Pabst T, Kortz L, Fiedler GM, Ceglarek U, Idle JR, Beyoğlu D. The plasma lipidome in acute myeloid leukemia at diagnosis in relation to clinical disease features. BBA Clinical. 2017;7:105-14.
212. Janiszewska M, Suva ML, Riggi N, Houtkooper RH, Auwerx J, Clement-Schatlo V, et al. Imp2 controls oxidative phosphorylation and is crucial for preserving glioblastoma cancer stem cells. Genes Dev. 2012;26(17):1926-44.
213. Viale A, Pettazzoni P, Lyssiotis CA, Ying H, Sanchez N, Marchesini M, et al. Oncogene ablation-resistant pancreatic cancer cells depend on mitochondrial function. Nature. 2014;514(7524):628-32.
214. Warburg O. On the origin of cancer cells. Science. 1956;123(3191):309-14.

215. Pollyea DA, Stevens BM, Jones CL, Winters A, Pei S, Minhajuddin M, et al. Venetoclax with azacitidine disrupts energy metabolism and targets leukemia stem cells in patients with acute myeloid leukemia. Nat Med. 2018;24(12):1859-66.
216. Culp-Hill R, Stevens BM, Jones CL, Pei S, Dzieciatkowska M, Minhajuddin M, et al. Therapy-Resistant Acute Myeloid Leukemia Stem Cells Are Resensitized to Venetoclax + Azacitidine by Targeting Fatty Acid Desaturases 1 and 2. Metabolites. 2023;13(4).
217. Mizushima N, Ohsumi Y, Yoshimori T. Autophagosome formation in mammalian cells. Cell Struct Funct. 2002;27(6):421-9.
218. Panda PK, Mukhopadhyay S, Das DN, Sinha N, Naik PP, Bhutia SK. Mechanism of autophagic regulation in carcinogenesis and cancer therapeutics. Semin Cell Dev Biol. 2015;39:43-55.
219. Li WW, Li J, Bao JK. Microautophagy: lesser-known self-eating. Cell Mol Life Sci. 2012;69(7):1125-36.
220. Xie Y, Li J, Kang R, Tang D. Interplay Between Lipid Metabolism and Autophagy. Front Cell Dev Biol. 2020;8:431.
221. Kroemer G. Autophagy: a druggable process that is deregulated in aging and human disease. J Clin Invest. 2015;125(1):1-4.
222. Levine B, Kroemer G. Autophagy in the pathogenesis of disease. Cell. 2008;132(1):27-42.
223. Chavez-Dominguez R, Perez-Medina M, Lopez-Gonzalez JS, Galicia-Velasco M, Aguilar-Cazares D. The Double-Edge Sword of Autophagy in Cancer: From Tumor Suppression to Pro-tumor Activity. Front Oncol. 2020;10:578418.
224. Feng Y, He D, Yao Z, Klionsky DJ. The machinery of macroautophagy. Cell Res. 2014;24(1):24-41.
225. Alers S, Loffler AS, Wesselborg S, Stork B. The incredible ULKs. Cell Commun Signal. 2012;10(1):7.
226. Smith AG, Macleod KF. Autophagy, cancer stem cells and drug resistance. J Pathol. 2019;247(5):708-18.
227. Hardie DG, Ross FA, Hawley SA. AMPK: a nutrient and energy sensor that maintains energy homeostasis. Nat Rev Mol Cell Biol. 2012;13(4):251-62.

228. Yang Z, Klionsky DJ. An overview of the molecular mechanism of autophagy. Curr Top Microbiol Immunol. 2009;335:1-32.
229. Dan HC, Ebbs A, Pasparakis M, Van Dyke T, Basseres DS, Baldwin AS. Akt-dependent activation of mTORC1 complex involves phosphorylation of mTOR (mammalian target of rapamycin) by IkappaB kinase alpha (IKKalpha). J Biol Chem. 2014;289(36):25227-40.
230. Egan D, Kim J, Shaw RJ, Guan KL. The autophagy initiating kinase ULK1 is regulated via opposing phosphorylation by AMPK and mTOR. Autophagy. 2011;7(6):643-4.
231. Shim D, Duan L, Maki CG. P53-regulated autophagy and its impact on drug resistance and cell fate. Cancer Drug Resist. 2021;4(1):85-95.
232. Tasdemir E, Maiuri MC, Galluzzi L, Vitale I, Djavaheri-Mergny M, D'Amelio M, et al. Regulation of autophagy by cytoplasmic p53. Nat Cell Biol. 2008;10(6):676-87.
233. Kobyakova M, Lomovskaya Y, Senotov A, Lomovsky A, Minaychev V, Fadeeva I, et al. The Increase in the Drug Resistance of Acute Myeloid Leukemia THP-1 Cells in High-Density Cell Culture Is Associated with Inflammatory-like Activation and Anti-Apoptotic Bcl-2 Proteins. Int J Mol Sci. 2022;23(14).
234. Pattingre S, Tassa A, Qu X, Garuti R, Liang XH, Mizushima N, et al. Bcl-2 antiapoptotic proteins inhibit Beclin 1-dependent autophagy. Cell. 2005;122(6):927-39.
235. Wei Y, Pattingre S, Sinha S, Bassik M, Levine B. JNK1-mediated phosphorylation of Bcl-2 regulates starvation-induced autophagy. Mol Cell. 2008;30(6):678-88.
236. Demeter A, Romero-Mulero MC, Csabai L, Olbei M, Sudhakar P, Haerty W, et al. ULK1 and ULK2 are less redundant than previously thought: computational analysis uncovers distinct regulation and functions of these autophagy induction proteins. Sci Rep. 2020;10(1):10940.
237. Wang B, Iyengar R, Li-Harms X, Joo JH, Wright C, Lavado A, et al. The autophagy-inducing kinases, ULK1 and ULK2, regulate axon guidance in the developing mouse forebrain via a noncanonical pathway. Autophagy. 2018;14(5):796-811.
238. Wong PM, Puente C, Ganley IG, Jiang X. The ULK1 complex: sensing nutrient signals for autophagy activation. Autophagy. 2013;9(2):124-37.
239. Chan EY, Longatti A, McKnight NC, Tooze SA. Kinase-inactivated ULK proteins inhibit autophagy via their conserved C-terminal domains using an Atg13-independent mechanism. Mol Cell Biol. 2009;29(1):157-71.

240. Jung CH, Jun CB, Ro SH, Kim YM, Otto NM, Cao J, et al. ULK-Atg13-FIP200 complexes mediate mTOR signaling to the autophagy machinery. Mol Biol Cell. 2009;20(7):1992-2003.
241. Zachari M, Ganley IG. The mammalian ULK1 complex and autophagy initiation. Essays Biochem. 2017;61(6):585-96.
242. Randhawa R, Sehgal M, Singh TR, Duseja A, Changotra H. Unc-51 like kinase 1 (ULK1) in silico analysis for biomarker identification: a vital component of autophagy. Gene. 2015;562(1):40-9.
243. Shin SH, Lee EJ, Chun J, Hyun S, Kang SS. ULK2 Ser 1027 Phosphorylation by PKA Regulates Its Nuclear Localization Occurring through Karyopherin Beta 2 Recognition of a PY-NLS Motif. PLoS One. 2015;10(6):e0127784.
244. Lee EJ, Tournier C. The requirement of uncoordinated 51-like kinase 1 (ULK1) and ULK2 in the regulation of autophagy. Autophagy. 2011;7(7):689-95.
245. Cheong H, Lindsten T, Wu J, Lu C, Thompson CB. Ammonia-induced autophagy is independent of ULK1/ULK2 kinases. Proc Natl Acad Sci U S A. 2011;108(27):11121-6.
246. Kundu M, Lindsten T, Yang CY, Wu J, Zhao F, Zhang J, et al. Ulk1 plays a critical role in the autophagic clearance of mitochondria and ribosomes during reticulocyte maturation. Blood. 2008;112(4):1493-502.
247. Cheong H, Wu J, Gonzales LK, Guttentag SH, Thompson CB, Lindsten T. Analysis of a lung defect in autophagy-deficient mouse strains. Autophagy. 2014;10(1):45-56.
248. Singh SS, Vats S, Chia AY, Tan TZ, Deng S, Ong MS, et al. Dual role of autophagy in hallmarks of cancer. Oncogene. 2018;37(9):1142-58.
249. Kang MR, Kim MS, Oh JE, Kim YR, Song SY, Kim SS, et al. Frameshift mutations of autophagy-related genes ATG2B, ATG5, ATG9B and ATG12 in gastric and colorectal cancers with microsatellite instability. J Pathol. 2009;217(5):702-6.
250. Qu X, Yu J, Bhagat G, Furuya N, Hibshoosh H, Troxel A, et al. Promotion of tumorigenesis by heterozygous disruption of the beclin 1 autophagy gene. J Clin Invest. 2003;112(12):1809-20.
251. Liang XH, Jackson S, Seaman M, Brown K, Kempkes B, Hibshoosh H, et al. Induction of autophagy and inhibition of tumorigenesis by beclin 1. Nature. 1999;402(6762):672-6.

252. Vessoni AT, Filippi-Chiela EC, Menck CF, Lenz G. Autophagy and genomic integrity. Cell Death Differ. 2013;20(11):1444-54.
253. Mathew R, Kongara S, Beaudoin B, Karp CM, Bray K, Degenhardt K, et al. Autophagy suppresses tumor progression by limiting chromosomal instability. Genes Dev. 2007;21(11):1367-81.
254. Degenhardt K, Mathew R, Beaudoin B, Bray K, Anderson D, Chen G, et al. Autophagy promotes tumor cell survival and restricts necrosis, inflammation, and tumorigenesis. Cancer Cell. 2006;10(1):51-64.
255. Yang S, Wang X, Contino G, Liesa M, Sahin E, Ying H, et al. Pancreatic cancers require autophagy for tumor growth. Genes Dev. 2011;25(7):717-29.
256. Levine B, Yuan J. Autophagy in cell death: an innocent convict? J Clin Invest. 2005;115(10):2679-88.
257. Yoo SH, Yoon YG, Lee JS, Song YS, Oh JS, Park BS, et al. Etoposide induces a mixed type of programmed cell death and overcomes the resistance conferred by Bcl-2 in Hep3B hepatoma cells. Int J Oncol. 2012;41(4):1443-54.
258. Bursch W, Ellinger A, Kienzl H, Torok L, Pandey S, Sikorska M, et al. Active cell death induced by the anti-estrogens tamoxifen and ICI 164 384 in human mammary carcinoma cells (MCF-7) in culture: the role of autophagy. Carcinogenesis. 1996;17(8):1595-607.
259. Wei H, Wei S, Gan B, Peng X, Zou W, Guan JL. Suppression of autophagy by FIP200 deletion inhibits mammary tumorigenesis. Genes Dev. 2011;25(14):1510-27.
260. Guo JY, Karsli-Uzunbas G, Mathew R, Aisner SC, Kamphorst JJ, Strohecker AM, et al. Autophagy suppresses progression of K-ras-induced lung tumors to oncocytomas and maintains lipid homeostasis. Genes Dev. 2013;27(13):1447-61.
261. Bosnjak M, Ristic B, Arsikin K, Mircic A, Suzin-Zivkovic V, Perovic V, et al. Inhibition of mTOR-dependent autophagy sensitizes leukemic cells to cytarabine-induced apoptotic death. PLoS One. 2014;9(4):e94374.
262. Bano N, Ansari MI, Kainat KM, Singh VK, Sharma PK. Chloroquine synergizes doxorubicin efficacy in cervical cancer cells through flux impairment and down regulation of proteins involved in the fusion of autophagosomes to lysosomes. Biochem Biophys Res Commun. 2023;656:131-8.

263. Qadir MA, Kwok B, Dragowska WH, To KH, Le D, Bally MB, et al. Macroautophagy inhibition sensitizes tamoxifen-resistant breast cancer cells and enhances mitochondrial depolarization. Breast Cancer Res Treat. 2008;112(3):389-403.
264. Zhu Y, Huang S, Chen S, Chen J, Wang Z, Wang Y, et al. SOX2 promotes chemoresistance, cancer stem cells properties, and epithelial-mesenchymal transition by beta-catenin and Beclin1/autophagy signaling in colorectal cancer. Cell Death Dis. 2021;12(5):449.
265. Lomonaco SL, Finniss S, Xiang C, Decarvalho A, Umansky F, Kalkanis SN, et al. The induction of autophagy by gamma-radiation contributes to the radioresistance of glioma stem cells. Int J Cancer. 2009;125(3):717-22.
266. Pagotto A, Pilotto G, Mazzoldi EL, Nicoletto MO, Frezzini S, Pasto A, et al. Autophagy inhibition reduces chemoresistance and tumorigenic potential of human ovarian cancer stem cells. Cell Death Dis. 2017;8(7):e2943.
267. Yang MC, Wang HC, Hou YC, Tung HL, Chiu TJ, Shan YS. Blockade of autophagy reduces pancreatic cancer stem cell activity and potentiates the tumoricidal effect of gemcitabine. Mol Cancer. 2015;14:179.
268. Akkoc Y, Peker N, Akcay A, Gozuacik D. Autophagy and Cancer Dormancy. Front Oncol. 2021;11:627023.
269. Wu YT, Tan HL, Shui G, Bauvy C, Huang Q, Wenk MR, et al. Dual role of 3-methyladenine in modulation of autophagy via different temporal patterns of inhibition on class I and III phosphoinositide 3-kinase. J Biol Chem. 2010;285(14):10850-61.
270. Mauthe M, Orhon I, Rocchi C, Zhou X, Luhr M, Hijlkema KJ, et al. Chloroquine inhibits autophagic flux by decreasing autophagosome-lysosome fusion. Autophagy. 2018;14(8):1435-55.
271. Zeng J, Shirihai OS, Grinstaff MW. Modulating lysosomal pH: a molecular and nanoscale materials design perspective. J Life Sci (Westlake Village). 2020;2(4):25-37.
272. Mohsen S, Sobash PT, Algwaiz GF, Nasef N, Al-Zeidaneen SA, Karim NA. Autophagy Agents in Clinical Trials for Cancer Therapy: A Brief Review. Curr Oncol. 2022;29(3):1695-708.
273. Arnaout A, Robertson SJ, Pond GR, Lee H, Jeong A, Ianni L, et al. A randomized, double-blind, window of opportunity trial evaluating the effects of chloroquine in breast cancer patients. Breast Cancer Res Treat. 2019;178(2):327-35.

274. Wolpin BM, Rubinson DA, Wang X, Chan JA, Cleary JM, Enzinger PC, et al. Phase II and pharmacodynamic study of autophagy inhibition using hydroxychloroquine in patients with metastatic pancreatic adenocarcinoma. Oncologist. 2014;19(6):637-8.
275. Anand K, Niravath P, Patel T, Ensor J, Rodriguez A, Boone T, et al. A Phase II Study of the Efficacy and Safety of Chloroquine in Combination With Taxanes in the Treatment of Patients With Advanced or Metastatic Anthracycline-refractory Breast Cancer. Clin Breast Cancer. 2021;21(3):199-204.
276. Samaras P, Tusup M, Nguyen-Kim TDL, Seifert B, Bachmann H, von Moos R, et al. Phase I study of a chloroquine-gemcitabine combination in patients with metastatic or unresectable pancreatic cancer. Cancer Chemother Pharmacol. 2017;80(5):1005-12.

Chapter 2

An *in-vitro* model using the SORE6 reporter for acute myeloid leukemia relapse

A version of this chapter has been published as:

Lai J, Shang C, Chen W, Izevbaye I, Chu MP, Sandhu I, Brandwein J, Lai R, Wang P. An In Vitro Model for Acute Myeloid Leukemia Relapse Using the SORE6 Reporter. Int J Mol Sci. 2024; 25(1):496.

2.1. Introduction

Acute myeloid leukemia (AML), defined by an accumulation of myeloblasts in the bone marrow and/or peripheral blood, is a type of highly aggressive hematologic cancer associated with a poor clinical outcome. Despite recent therapeutic advance, the 5-year survival rate for AML patients receiving treatment with a curative intent is approximately 30% (1). Refractory disease, defined as a failure to achieve complete remission, occurs in approximately 30% of all treated AML patients (2). In patients who achieve complete remission after the initial treatment, disease relapses develop in 40-50% of those who are aged <65 years and in the vast majority of patients who are aged ≥65 years (3, 4). Treatment options for patients who develop relapses are limited; only ~10% of these patients survive >3 years after the diagnosis of relapse is made (5). To improve the overall outlook of AML patients, new treatments for AML relapse are needed.

The molecular basis of AML relapse has not been extensively studied, partly due to the relative paucity of *in-vitro* study models that can be readily established in conventional research laboratories. Several hypothetical models have been postulated. In the clonal evolution model, it is believed that small subclones of AML cells present at diagnosis acquire gene mutations that allow them to survive the initial chemotherapy (6). In another model, it has been proposed that the initial chemotherapy sends a subset of AML cells to a senescence-like state, which protects these cells during a period of dormancy that precedes relapse (7). The cancer stem cell model postulates the existence of a very small subset of cancer cells carrying stem-like features, such as a high level of chemoresistance, tumorigenicity and self-renewal capacity. These few cells survive the initial treatment and eventually contribute to disease relapses after a period of dormancy. A modified version of the cancer stem cell model is related to the concept of cancer cell plasticity, in which a subset of bulk cancer cells acquires cancer stemness. Regardless of which model is important, relapse AML cells exhibit a higher level of chemoresistance to the initial treatments compared to the original cell population, thereby explaining why the initial treatments are typically ineffective for relapse. Overall, evidence supporting any of these models is relatively scarce. In support of the cancer stem cell model, it was found that relapse AML cells from patient samples contained higher proportions of cancer stem cells that were quantified by using an *in-vivo* limiting dilution assay (8). In another study, the expression of the cancer stem cell gene signature in AML blasts was

found to correlate with a relatively high risk of disease relapse (9). Nonetheless, these evidence are relatively indirect.

Aberrant expression of embryonic stem cell proteins such as Sox2, Oct4 and Myc has been shown in many cancer types, and the expression of these proteins in various cancer models has been found to significantly correlate with cancer stem-like (CSL) features and a poor clinical outcome (10-14). The Sox2/Oct4 response element (SORE6) reporter system, designed to detect the transcriptional activity of these two proteins, has been successfully employed to identify/purify CSL cells in a few solid and hematologic cancer models (11, 15, 16). Our group has recently reported that a small cell subset of ALK-positive anaplastic large cell lymphoma express SORE6 reporter activity, which can be readily quantified based on the expression of green fluorescent protein (GFP) detectable by using flow cytometry (11). Importantly, purified $SORE6^+$ cells showed significantly more CSL features, including spheroid forming ability and chemoresistance, compared to their $SORE6^-$ counterparts. The SORE6 reporter has never been used in AML studies.

In this study, we aimed to test the importance of CSL cells in the context of AML relapse. We first asked if the SORE6 reporter can be used to identify/purify CSL cells in AML cell lines. After the SORE6 reporter was confirmed to be useful in identifying/purifying CSL cells in AML cell lines, we leveraged the $SORE6^-$/$SORE6^+$ dichotomy to generate an *in-vitro* study model that mimics key features of AML relapse. In view of the molecular diversity of AML, we focused our studies on AML cells with a specific molecular aberrancy, namely FLT3 mutations.

2.2. Materials and Methods

2.2.1. Cell culture

Two *FLT3*-mutated AML cell lines, MV4-11 and MOLM-13 (17), were cultured in Roswell Park Memorial Institute (RPMI) 1640 (Invitrogen, Waltham, MA, USA) supplemented with 10% fetal bovine serum (Gibco, Waltham, MA, USA) and 1% penicillin/streptomycin (Gibco). Cells

transduced with the SORE6 reporter, carrying a puromycin selection marker, were cultured in the presence of 0.25 μg/mL puromycin (Gibco).

2.2.2. Generation of SORE6$^-$ and SORE6$^+$ subsets

The SORE6-mCMVo-dsCop-GFP-PURO (SORE6) reporter and mCMVp-dsCopGFP-PURO (mCMV) plasmids were kind gifts from Dr. Lalage Wakefield (National Cancer Institute, Bethesda, MD, USA) (15). Short hairpin RNA (shRNA) plasmid for Myc was purchased from MilliporeSigma (Burlington, MA, USA). AML cell lines underwent lentiviral transduction with these plasmids as described previously (18).

SORE6 activity was quantified by measuring the level of GFP expression using flow cytometry. Cells transduced with mCMV were used to establish the cut-off. SORE6$^-$ and SORE6$^+$ cell subsets were generated using flow cytometric cell sorting (Sony MA900, New York, NY, USA). Cells expressing relatively high GFP (i.e. top ~4-8%) were purified and cultured into the SORE6$^+$ subset, and cells expressing no detectable GFP (i.e. the bottom ~4-8%) were purified and cultured into the SORE6$^-$ subset. All experiments performed in this study employed SORE6$^+$ cells showing ≥75% GFP positivity and SORE6$^-$ cells showing <5% GFP detectable by flow cytometry.

2.2.3. Antibodies and drug treatments

Primary antibodies used in western blot studies included anti-MYC (Y69, #ab32072), anti-Sox2 (EPR3131; #ab92494) and anti-Oct4 (#ab19857), which were purchased from Abcam (Cambridge, MA, USA), anti-β-actin (#sc-47778) from Santa Cruz Biotechnology (Santa Cruz, CA, USA), anti-FLT3 (8F2, #3462) from Cell Signaling (Danvers, MA, USA), and anti-p-STAT5 (Tyr694, #9359) from Cell Signaling. Additionally, anti-myeloperoxidase (A1F4; #MA5-42397) from Invitrogen (Waltham, MA, USA) and anti-MYC mentioned above were used in immunostaining experiments. Gilteritinib (ASP2215, #S7754) was purchased from Selleckchem (Houston, TX, USA) and Ara-C (PHR1787) was purchased from Sigma-Aldrich (St Louis, MO, USA). Venetoclax was gifted by Abbvie.

2.2.4. Polymerase chain reaction

Genomic DNA extraction was performed using PureLink® Genomic DNA mini kit (Invitrogen) based on the manufacturer's protocol. PCR reactions to detect cell barcoding were performed using the CloneTracker 4-barcode-plus cell labeling kit (Cellecta) following the manufacturer's protocol. PCR reactions to detect SORE6 were done using SYBR Green Real-Time PCR Master Mixes, as indicated by the manufacturer (ThermoFisher Scientific, Waltham, MA, USA). Bands were visualized by gel electrophoresis with a 3% agarose gel. Primer sequences were as followed:
SORE6: F-5'-ACAATGGCCTTGGTGCAG-3′ & R-5′-TGCACCAAGGCCATTGTAA-3′ ;
GAPDH: F-5-GGTCTCCTCTGACTTCAACAGCG-3 & R-5-
ACCACCCTGTTGCTGTAGCCAA-3.

2.2.5. Hanging drop assay

100,000 cells were seeded in 1 mL of culture media. 10 µL drops were pipetted onto the lid of a cell culture dish. Spheroid formation was assessed after 48 hours using a light microscope. The criteria for spheroid formation were that viable cells were clustered together in a sphere. Every well will contain one of these two types of cell clumps - 1) true spheroid - Well-defined, tightly packed, spherical cell mass (**Figure 2.1a**) irregularly shaped, loosely bound cell clumps (**Figure 2.1b**). On high magnification, the true spheroids consist of viable-appearing cells as shown by their refractile appearance as opposed to cell debris in the non-viable cell clumps. 15 drops were randomly selected for analysis per plate.

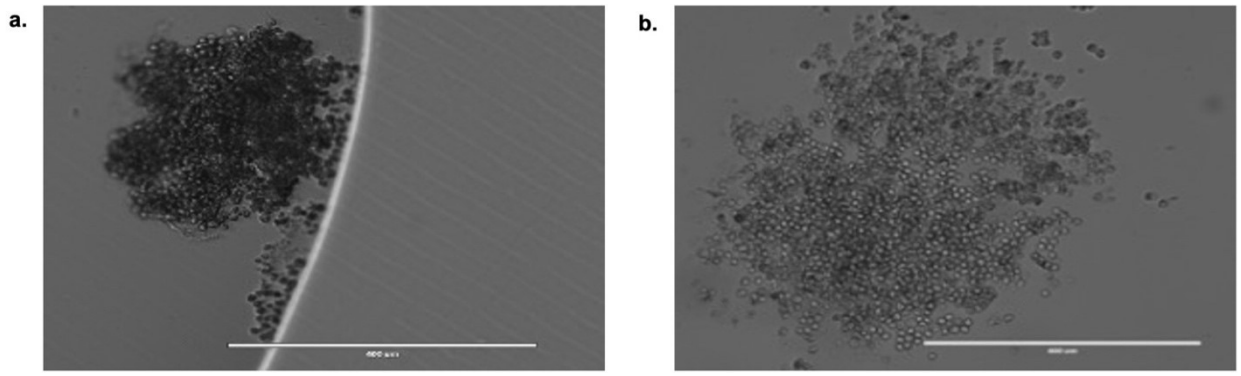

Figure 2.1. Image of a spheroid and non-spheroid in the hanging drop assay. (a) Example of a true spheroid with a well-defined, tightly packed spherical cell mass. (b) Example of a non-spheroid, with loosely bound cell clumps. Imaged with a bright-field microscope (40x).

2.2.6. Cell viability assay

Cells were plated with a concentration of 250,000 cells/mL using media with 5% fetal bovine serum in 24-well plates. Cell viability was assessed using trypan blue exclusion. IC50 was calculated by GraphPad Prism software (GraphPad Software, San Diego, CA, USA).

2.2.7. Western blot

Cell pellets were lysed with RIPA buffer (MilliporeSigma, Burlington, MA, USA), with protease and phosphatase inhibitors (MilliporeSigma). Proteins were separated on a 10-15% polyacrylamide SDS-PAGE gel, transferred to a nitrocellulose membrane (GE Healthcare, Velizy-Villacoublay, France), and then incubated with primary antibodies. The membrane was then incubated with horseradish peroxidase-conjugated secondary antibodies. Bands were visualized with an Odyssey® Infrared Imaging System (LI-COR, Lincoln, NE, USA).

2.2.8. DNA pull-down assay

DNA pull-down was performed as described previously (11). The sequence of the SORE6 probe was:

5′-BiosgCCCTTTTGCATTACAATGTCTTTTGCATTACAATGTCTTTTGCATTACAATG-3′. A mutant DNA probe was used as the negative control.

2.2.9. Barcode labeling of SORE6 Sorted Cells

The CloneTracker 4-barcode-plus cell labeling kit (Cellecta, Mountain View, CA, USA) was employed to track cell fate. Barcodes were transduced into purified SORE6^{+} and SORE6^{-} cells by following the manufacturer's protocol. For the remainder of this manuscript, the barcode used for SORE6^{-} cells was labeled barcode #1, while that for SORE6^{+} cells was labeled barcode #2. The unique sequence in each barcode was detectable by polymerase chain reaction and a set of primers supplied by Cellecta. Both barcodes also carried red fluorescence protein to allow the identification of cells with successful transduction of the barcodes. The barcodes were stably expressed in both cell populations over the course of 4 weeks of our experiments, with >95% of cells expressing RFP that was detectable by flow cytometry.

2.2.10. *In-vitro* AML relapse model

MOLM-13 and MV4-11 cells were plated to a concentration of 150,000 cells/mL in T25 flasks. Cells were treated with Ara-C for two days, at which point media without Ara-C was added to the culture. The lowest doses that induced '*in-vitro* remission', defined by the absence of trypan blue-negative cells after three observations, were found to be 100 nM for MOLM-13 and 250 nM for MV4-11. Immediately after the induction of '*in-vitro* remission', we performed flow cytometry and quantified the number of viable cells. Using the forward scatter/size scatter gating strategy, we found a median of ~300 cells/mL (i.e., ~0.2% viability). To detect regeneration, 200 µL of the cell culture was removed for trypan blue cell counting every two days, and the cell culture was replenished with 200 µL of fresh culture media. Once the cell density reached the same level as the original density (labeled as 'IR'), cell culture was split in half and topped up with fresh culture media every two days.

2.2.11. Patient samples

Nine initially diagnostic and nine relapsed AML bone marrow aspirates stored in liquid nitrogen were retrieved retrospectively from the University of Alberta Hospital. Formalin-fixed/paraffin-embedded bone marrow clot sections representing the initially diagnostic sample as well as the relapse samples from one *FLT3*-mutated AML patient was also retrieved retrospectively from the University of Alberta Hospital. The use of these patient samples was approved by the Health Research Ethics Board of Alberta (HREBA.CC-21-0253).

2.2.12. Immunohistochemistry

After deparaffinization and rehydration of the tissue, antigen retrieval was performed using an EDTA buffer (Sigma-Aldrich). Slides were incubated overnight at 4°C with an anti-Myc antibody (abcam). Sections were blocked with 3% hydrogen peroxide and were then incubated with Dako EnVision+ System HRP Labelled Polymer secondary antibody (Agilent, Santa Clara, CA, USA) at room temperature for one hour. Dako DAB+ Chromagen (Agilent) was used to develop the sections. Antigen retrieval was then repeated using citrate buffer (Sigma-Aldrich). Sections were incubated with anti-myeloperoxidase antibody (Invitrogen) overnight at 4°C. After secondary antibody incubation with Dako EnVision+ System HRP Labelled Polymer, slides were developed with AEC peroxidase (Enzo Life Sciences, ENZ-43825, Farmingdale, NY, US). Slides were coverslipped with an aqueous mounting medium. To score slides, blasts were identified as being myeloperoxidase weak/negative and by their morphology. Areas with predominantly immature cells relatively devoid of erythroid cells were chosen for evaluation. Megakaryocytes were similarly excluded based on their morphology.

2.2.13. Statistical analysis

Statistical analyses were performed using GraphPad Prism 8 (Graphpad Software Inc. LaJolla, Ca, USA). P-values were calculated using two-tailed Student's t-test.

2.3. Results

2.3.1. SORE6 activity is expressed in a small subset of cells in two *FLT3*-mutated AML cell lines

We first examined if MOLM-13 and MV4-11 carry any detectable SORE6 reporter activity. Following lentiviral transduction of the reporter into these two cell lines, we found that they both contained a small proportion of SORE6$^+$ cells, with the expression of GFP being detectable by flow cytometry in 7% and 11% of cells, respectively (**Figure 2.2a**). Using a lentiviral vector carrying the *red fluorescence protein* gene, we found that the efficiency of lentiviral gene transduction for both cell lines was approximately 80% (results not shown).

We then purified SORE6$^-$ and SORE6$^+$ from both cell lines stably transduced with the SORE6 reporter, as illustrated in **Figure 2.2b**. To confirm that the GFP-negativity in SORE6$^-$ cells was not due to insufficient SORE6 integration into the genome, we performed PCR using a SORE6 primer set. As shown in **Figure 2.2c**, the SORE6 amplicons were readily detectable in both cell subsets. By performing flow cytometry every 2 weeks for a total of 8 weeks, we assessed the stability of SORE6 activity in both SORE6$^-$ and SORE6$^+$ cells. We found that GFP expression was consistently negative in SORE6$^-$ cells from both cell lines, whereas SORE6$^+$ cells derived from MOLM-13 and MV4-11 showed GFP expression in 80-95% and 75-85% of the cell population, respectively (**Figure 2.2d**).

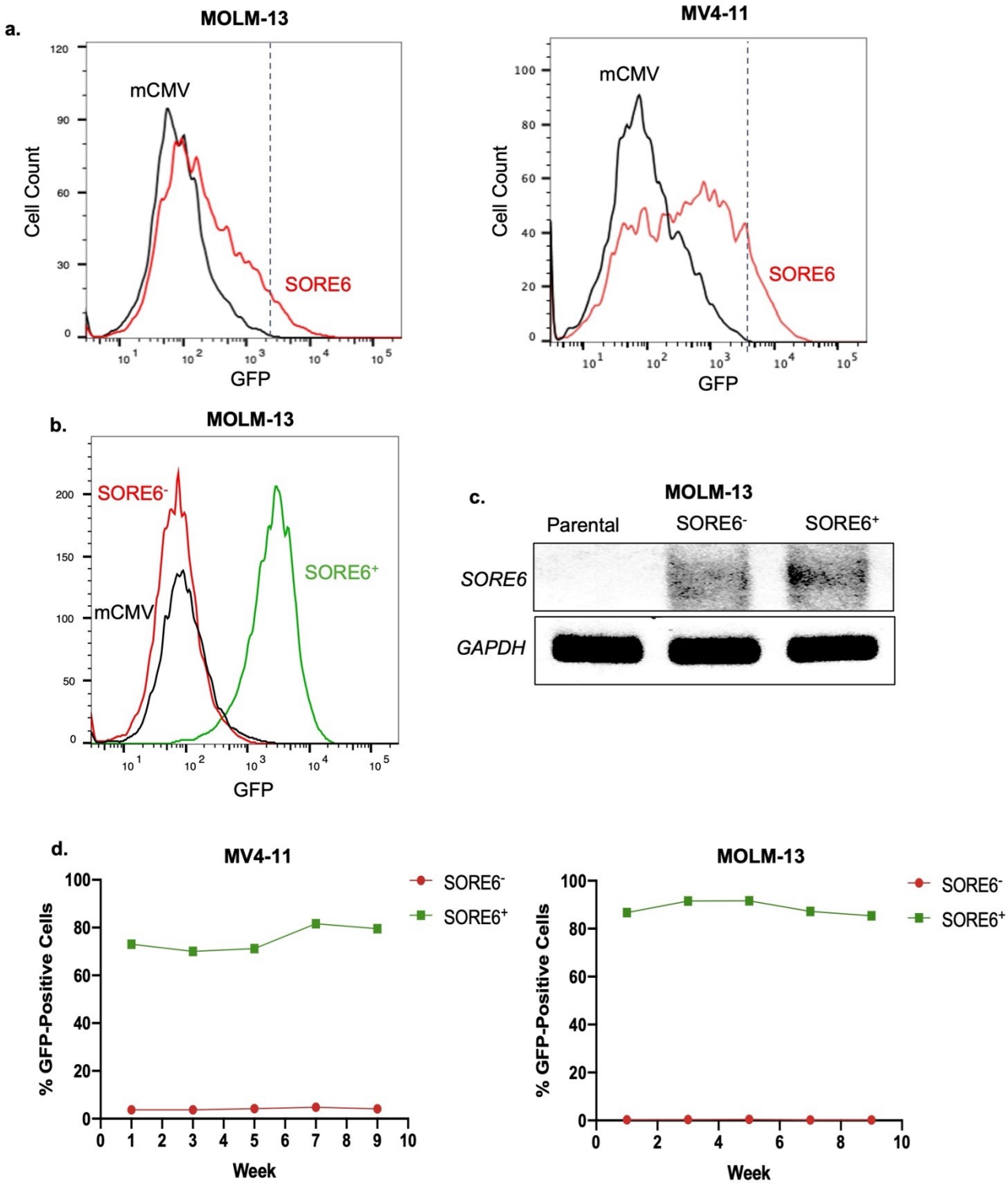
a.
MOLM-13
mCMV
SORE6
Cell Count
GFP
MV4-11
mCMV
SORE6
Cell Count
GFP
b.
MOLM-13
SORE6-
SORE6+
mCMV
GFP
c.
MOLM-13
Parental
SORE6-
SORE6+
SORE6
GAPDH
d.
MV4-11
SORE6-
SORE6+
% GFP-Positive Cells
Week
MOLM-13
SORE6-
SORE6+
% GFP-Positive Cells
Week

Figure 2.2. SORE6 activity is expressed in a small subset of *FLT3*-mutated AML cell lines. (a) The SORE6 reporter was transduced into two *FLT3*-mutated AML cell lines (MOLM-13 and MV4-11). The percentage of cells positive for GFP was assessed by flow cytometry seven days after the transduction. Cells transduced with mCMV were used to establish the cut-off. (b) MOLM-13 cells transduced with SORE6 were sorted using flow cytometry to generate a SORE6$^-$ cell subset with 0.2% GFP and a SORE6$^+$ cell subset with 99.0% GFP. (c) PCR was performed to detect the level of SORE6 integration in untransduced MOLM-13 cells, MOLM-13 SORE6$^-$ cell subset and MOLM-13 SORE6$^+$ cell subset. GAPDH was used as a loading control. Approximately equal levels of SORE6 amplicons were detectable in SORE6$^-$ and SORE6$^+$ cell subsets, but not in untransduced cells. (d) Percentage of SORE6$^+$ cells measured by flow cytometry analysis of GFP in SORE6$^-$ and SORE6$^+$ subsets in MOLM-13 and MV4-11 cells. GFP was analyzed over a period of 8 weeks, starting at one week post transfection. Cells transfected with mCMV were used as a control.

2.3.2. SORE6$^+$ cells have more CSL characteristics than SORE6$^-$ cells

To compare SORE6$^-$ and SORE6$^+$ cells phenotypically, these cell subsets were subjected to the hanging drop assay (19). As shown in **Figure 2.3a**, SORE6$^+$ cells derived from MV4-11 formed a significantly higher number of spheroids compared to their SORE6$^-$ counterparts (80.3% versus 37.3%, p<.001). Similar findings were observed for these two cell subsets derived from MOLM-13 (71.7% versus 31.7%, p=.006).

We next examined whether the SORE6-positivity in these two AML cell lines correlates with other CSL features such as chemoresistance. As illustrated in **Figure 2.3b**, when cells were exposed to increasing dosages of Ara-C in the presence of only 5% growth-supporting serum, SORE6$^+$ cells showed significantly higher IC50 (i.e. inhibitory concentration at 50%) than SORE6$^-$ cells. Specifically, the IC50 of SORE6$^-$ cells derived from MV4-11 cells was 27.9 nM, as compared to 119.7 nM for SORE6$^+$ cells (p<.001). The IC50 of SORE6$^-$ cells derived from MOLM-13 was 32.0 nM, as compared to 87.3 nM for SORE6$^+$ cells (p<.0001).

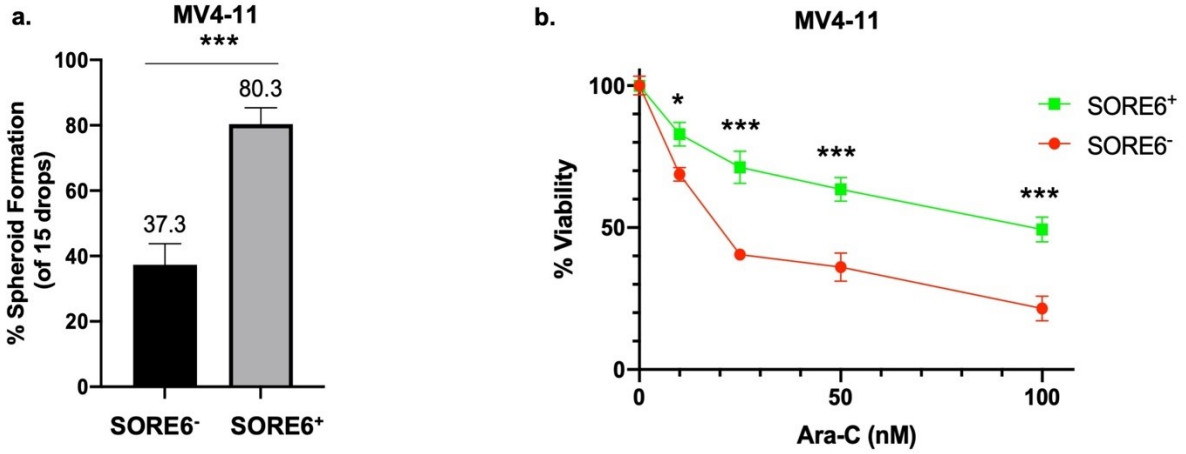

Figure 2.3. SORE6$^+$ cells have more cancer stem-like features. (a) Percentage of spheroids formed from the hanging drop assay in MV4-11 SORE6$^-$ and SORE6$^+$ cell subsets. Drops were counted as a spheroid (well-defined, tightly packed, spherical cell mass) or a non-spheroid (irregularly shaped, loosely bound cell clumps). Results shown are based on three independent experiments; 15 drops were imaged in each experiment. (b) Cell viabilities of SORE6$^-$ and SORE6$^+$ cell subsets derived from MV4-11 cell line treated with increasing doses of Ara-C for 24 hours. Cell viability assays were performed in triplicates (Trypan Blue). Results shown as mean ± standard deviation. * $p < 0.05$, ** $p < 0.01$, *** $p < 0.001$, Student's t test.

2.3.3. SORE6$^+$ cells are more resistant to low-dose Ara-C and Venetoclax (LDAC+Ven) compared to SORE6$^-$ cells

LDAC+Ven has recently been adopted to be a front-line therapy for elderly patients diagnosed with AML, including those with *FLT3*-mutated AML (20). As shown in **Figure 2.4a**, in the presence of a relatively low-dose of Ara-C, which was arbitrarily set as 50% below the IC50 dose level of the parental cell line stably transduced with SORE6 (i.e. 10 nM), SORE6$^+$ were found to be significantly more resistant to Venetoclax than SORE6$^-$ cells (10.9 nM versus 3.7 nM, p=.006). To further explore this phenomenon, we employed western blots to examine the protein expression of Bcl-2, the target of Venetoclax, in the two cell subsets. As shown in **Figure 2.4b**, treatment of 10 nM of Ara-C induced a dramatic decrease in the Bcl-2 protein level in SORE6$^+$ but not SORE6$^-$

cells. These findings suggest that the resistance of SORE6$^+$ cells to LDAC+Ven may be related to the preferential downregulation of the Bcl-2 proteins by low-dose Ara-C in this cell subset.

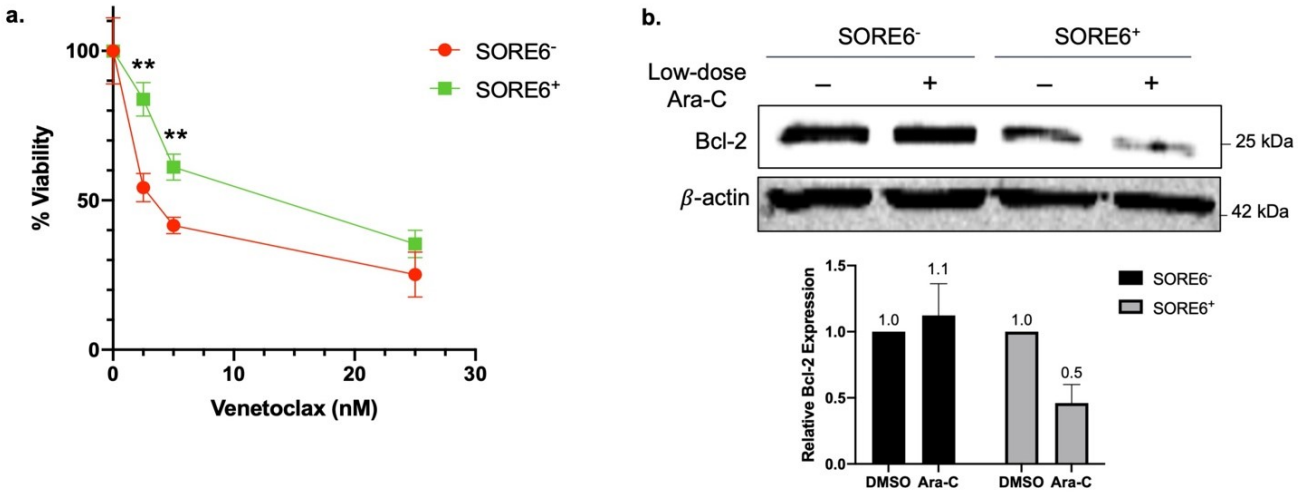

Figure 2.4. SORE6$^+$ cells are more resistant to Venetoclax + Low-Dose Ara-C. (a) Cell viabilities of MOLM-13 SORE6$^+$ and SORE6$^-$ cells after treatment of different doses of Venetoclax (0, 5, 10 and 25 nM) in combination with low dose (10 nM) Ara-C for 24 hours. (b) Western blot of MOLM-13 SORE6$^+$ and SORE6$^-$ cells after treatment with low dose (10 nM) Ara-C compared to DMSO for 24 hours. Data from three independent experiments are shown in the bar graph.

2.3.4. SORE6 activity is Myc-dependent

Since SORE6 was designed to detect the transcriptional activity of Sox2 and Oct4, we assessed their protein expression using western blots. In both AML cell lines, there was no/minimal Sox2 and Oct4 detected compared to SupM2, a lymphoma cell line (**Figure 2.5a**). Myc, another embryonic stem cell protein, was readily detectable in both SORE6$^-$ as well as SORE6$^+$ cells (**Figure 2.5a**). However, the Myc level was substantially higher in SORE6$^+$ cells (**Figure 2.5b**). To test if Myc directly contributes to the relatively high SORE6 activity in SORE6$^+$ cells, we inhibited Myc using shRNA. As shown in **Figure 2.5c-d**, shRNA inhibition of Myc in SORE6$^+$ cells derived from MOLM-13 resulted in a dramatic reduction in the mean % of GFP$^+$ cells from

72.1 to 18.7% (triplicate experiments, $p<.0001$). Likewise, pharmacological inhibition of Myc using 50 μM of 10058-F4 reduced the mean % of GFP^+ cells after 24 hours from 95.4% to 58.6% ($p=0.002$) (**Figure 2.5e-f**). To directly show that Myc is capable of binding to the Sox2/Oct4 promoter region of the SORE6 reporter, we performed a pull-down assay using the DNA-binding consensus sequence of SORE6 as the probe. As shown in **Figure 2.5g**, SORE6 binding by Myc was observed.

We then asked if the phenotypic differences between the $SORE6^-$ and $SORE6^+$ cells may also be attributed to differences in key cellular signaling pathways. Using western blots, we assessed the expression of phospho-ERK (Thr202/Tyr204), phospho-Akt (Ser473), and phospho-STAT5 (pSTAT5) (Tyr694). Except for pSTAT5, we found no appreciable differences. The level of pSTAT5 was substantially higher in $SORE6^+$ cells (**Figure 2.5b**). Since previous publications have shown that FLT3 can upregulate pSTAT5 when *FLT3* is mutated (21), we compared the FLT3 protein expression between the cell subsets, and we found that the FLT3 level was appreciably higher in $SORE6^+$ cells. We then asked if FLT3 contributes to the SORE6 activity in $SORE6^+$ cells. As shown in **Figure 2.6a**, pharmacological inhibition of FLT3 using 50 nM of Gilteritinib for 24 hours significantly decreased the % of $SORE6^+$ cells (80.6% versus 17.9%, $p<.0001$). Interestingly, Gilteritinib treatment also substantially decreased the Myc protein level (**Figure 2.6b**). The finding Gilteritinib decreased the Myc protein level suggests that FLT3 may contribute to SORE6 activity and cancer stemness by upregulating Myc.

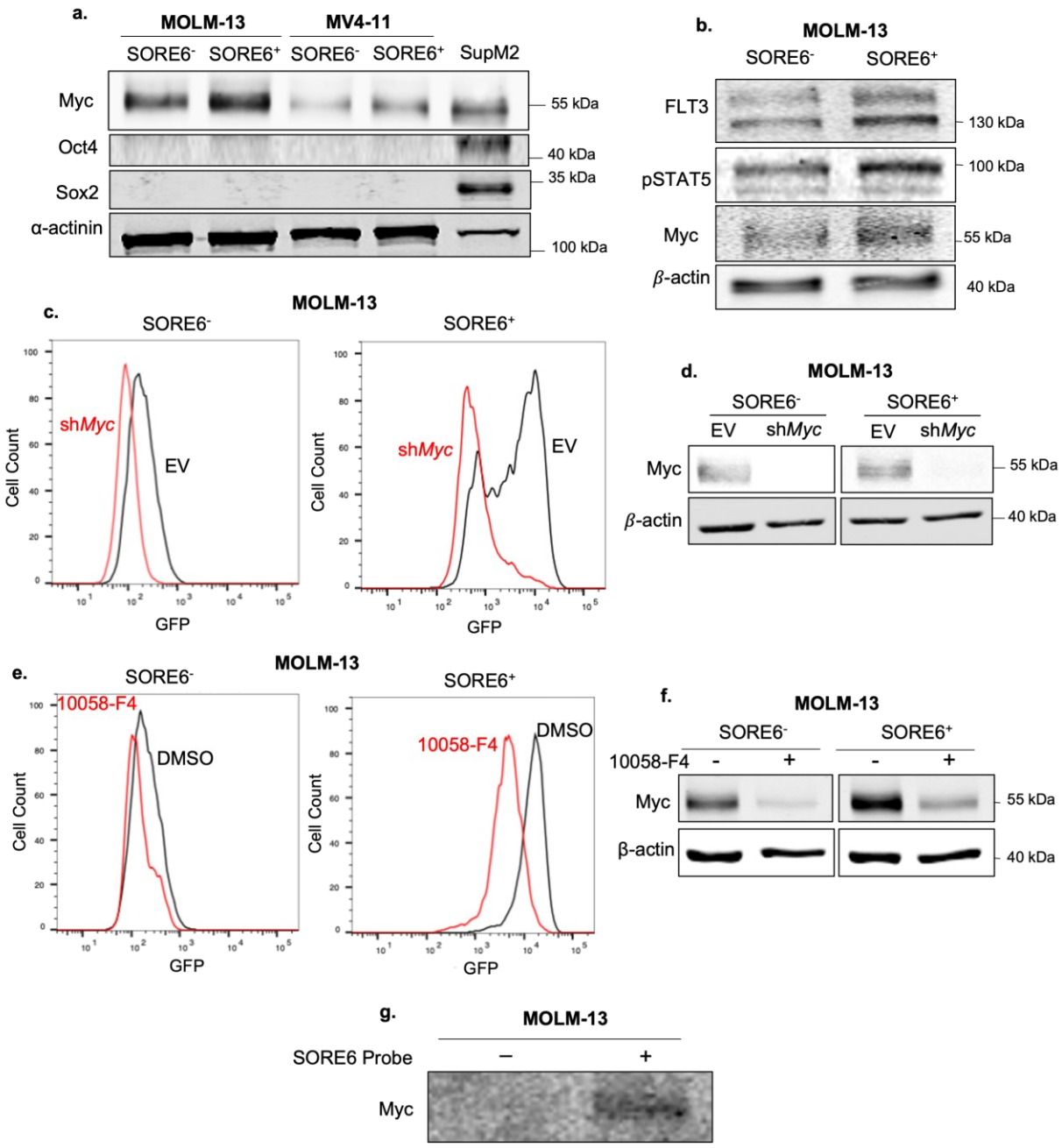
a.
MOLM-13
MV4-11
SORE6-
SORE6+
SORE6-
SORE6+
SupM2
Myc
Oct4
Sox2
α-actinin
55 kDa
40 kDa
35 kDa
100 kDa
b.
MOLM-13
SORE6-
SORE6+
FLT3
pSTAT5
Myc
β-actin
130 kDa
100 kDa
55 kDa
40 kDa
c.
MOLM-13
SORE6-
SORE6+
shMyc
EV
Cell Count
GFP
d.
MOLM-13
SORE6-
SORE6+
EV
shMyc
EV
shMyc
Myc
β-actin
55 kDa
40 kDa
e.
MOLM-13
SORE6-
SORE6+
10058-F4
DMSO
Cell Count
GFP
f.
MOLM-13
SORE6-
SORE6+
10058-F4
-
+
-
+
Myc
β-actin
55 kDa
40 kDa
g.
MOLM-13
SORE6 Probe
–
+
Myc

Figure 2.5. Myc is a regulator of SORE6 activity. (a) Protein expression level of Sox2, Oct4 and Myc in SORE6$^-$ and SORE6$^+$ subsets derived from MOLM-13 and MV4-11 at steady state, assessed by western blots. SupM2 cells were used as a positive control for Sox2 and Oct4. Myc/β-actin ratio was normalized to SORE6$^-$ subsets. (b) Western blot analysis of p-STAT5, FLT3 and Myc in MOLM-13 SORE6$^-$ and SORE6$^+$ subsets. (c) Flow cytometry analysis of GFP after shMyc (red) in MOLM-13 SORE6$^-$ and SORE6$^+$ cells, with empty vector (EV) (black) used as a negative control. (d) Western blot to confirm the efficacy of the inhibition of Myc by shRNA. (e) Flow cytometry analysis of GFP in SORE6$^-$ and SORE6$^+$ cells after Myc pharmacological inhibitor (10058-F4) treatment for 24 hours. Treatment with 10058-F4 (red) was compared to treatment with DMSO (black). (f) Western blot to confirm the efficacy of the inhibition of Myc by pharmacological inhibition with 10058-F4. (g) DNA pull-down of Myc using a biotin-labeled SORE6 probe. A mutant DNA probe was used as the negative control.

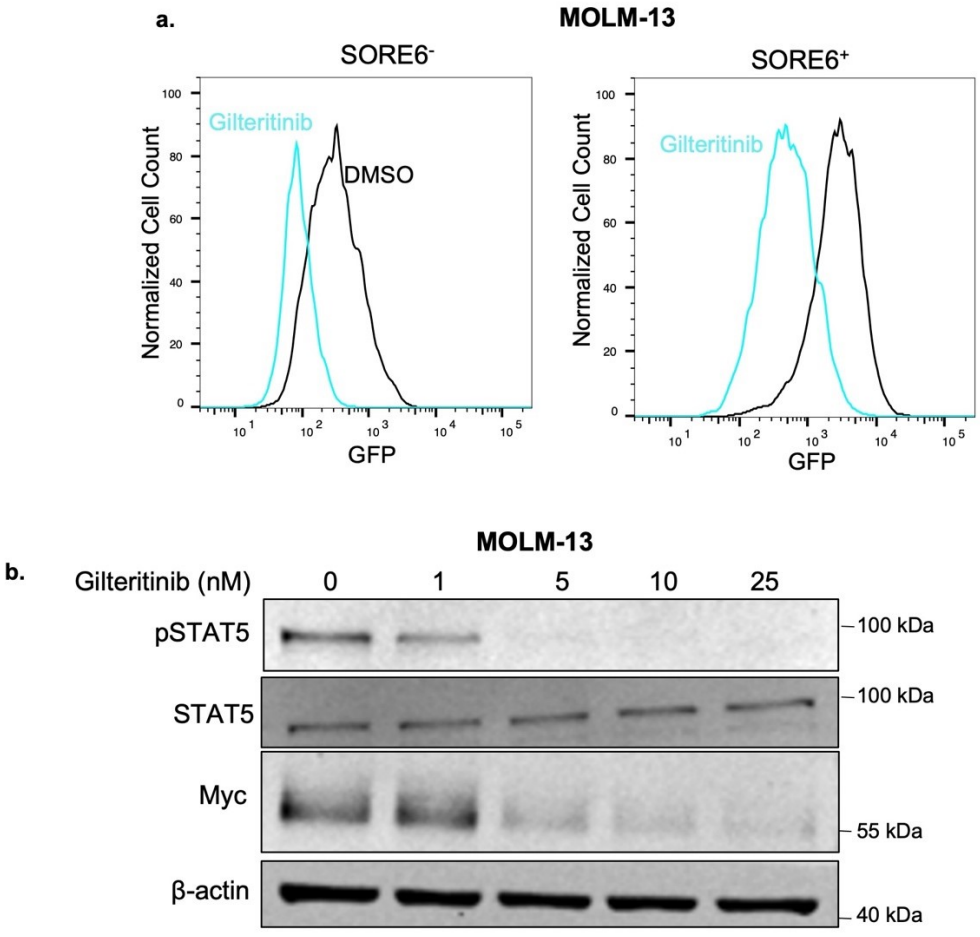

Figure 2.6. FLT3 may regulate SORE6 activity via Myc. (a) Flow cytometry analysis of GFP in MOLM-13 SORE6$^-$ and SORE6$^+$ cells after treatment with 50 nM of Gilteritinib (in blue) for 24 hours compared to a DMSO control (in black). (b) Western blot analysis after increasing doses of Gilteritinib in MOLM-13 cells for 24 hours. Downregulation of pSTAT5 confirmed the efficacy of inhibition of FLT3.

2.3.5. Generation of an *in-vitro* model to study AML relapses using SORE6$^-$/SORE6$^+$ cells

In view of the hypothesis that CSL cells contribute to AML relapse and our finding that SORE6$^+$ cells have CSL properties, we attempted to establish an *in-vitro* model to study AML relapse by using a mixture of SORE6$^-$/SORE6$^+$cells derived from the two *FLT3*-mutated AML cell lines. Purified SORE6$^-$ and SORE6$^+$ cells derived from MOLM-13 or MV4-11 were pooled in a 9:1 ratio to approximate the ratio of these two cell subsets at the steady state. The SORE6$^-$/SORE6$^+$ cell mixture was treated with Ara-C to achieve the '*in-vitro* remission' state, defined by the absence of trypan blue-negative cells after three observations. The minimal dose of Ara-C required to induce *in-vitro* remission in MOLM-13 and MV4-11 was 100 nM and 250 nM, respectively. Based on triplicate experiments using MV4-11 cells, *in-vitro* remission was achieved on day 2±1 of the experiment, and on day 12±2, viable cells (i.e. trypan blue-negative) were first detectable (**Figure 2.7a**). On day 16±3 of the experiment, the number of cells reached the original number at the initiation of the experiments (labeled as *in-vitro* relapse (IR)). The endpoint of this experiment was arbitrarily set as 10 days after IR.

If the hypothesis that CSL cells contribute to AML relapse is correct, we expect that SORE6$^+$ cells are the predominant cell type in the regenerated cell population. Since there is a possibility that SORE6$^+$ cells in the regeneration may originate from SORE6$^-$ cells (i.e. conversion due to cancer plasticity), we repeated the experiments using SORE6$^-$ and SORE6$^+$ cells that had been separately molecularly barcoded. Triplicate experiments were performed using both AML cell lines and representative results from MV4-11 are demonstrated. As shown in **Figure 2.7b**, at IR, the mean SORE6$^+$ cells measured by flow cytometry was 54.1±10.1%, compared to 13.0±4.7% before Ara-C treatment. At the endpoint, the mean %SORE6$^+$ was 68.0±3.0%. Then, using PCR to detect the

molecular barcodes, we assessed the ratio of the original SORE6$^-$/SORE6$^+$ cells present in the resurrected cell population. As shown in **Figure 2.7c**, band 2 (top band), which was used to label the original SORE6$^+$ cells, was relatively weak compared to that of band 1 (lower band, original SORE6$^-$ cells) at the beginning of the experiment. In contrast, the band 2 was slightly stronger than band 1 at IR. Using densitometry, the mean band2:total band intensity (band1+band2) ratio at the beginning of the experiment was 0.19±0.02, compared to 0.72±0.08 at IR and 0.92±0.02 at the endpoint. As shown in **Figure 2.7d**, using flow cytometry, the SORE6$^+$:total cell ratios at IR and endpoint were significantly lower than the band2:total band intensity ratios at these two time points, suggesting that a small subset of SORE6$^+$ cells had converted/differentiated during this course of the experiment. Similar experiments were repeated using MOLM-13 cells, and similar results were obtained.

We next asked if the resurrected cells at the endpoint possessed higher CSL features. Specifically, they are significantly more resistant to Ara-C compared to untreated SORE6$^+$ cells (IC50 140.2 versus 98.9 nM, p=.007). Regenerated cells at the endpoint also formed a significantly higher number of spheroids in the hanging drop assays compared to SORE6$^+$ cells (88.3 versus 68.0%, p<.001). These results suggest that the regenerated cells had acquired a significantly higher CSL phenotype, despite the occurrence of conversion into SORE6$^-$ cells in a proportion of cells.

2.3.6. A small number of viable cells is detectable during *in-vitro* remission

In order to explain how cells could recover from a state of no detectable viable cells, we analyzed the number of viable cells during the *'in-vitro* remission stage' using flow cytometry, a more sensitive quantification method compared to the trypan blue assay. Using a forward scatter/side scatter gating strategy to quantify viable cells, we counted the cell number two days after 'zero-viability' was induced (day 4 of the experiment) and continued to perform flow cytometry every four days until viable cells were detectable by trypan blue. Two days after 'zero-viability' stage, showed a median of 206 viable cells/mL (i.e. 0.2% viability). Between day 4-12 of the experiment, the number of viable cells changed minimally, with a median of 206 to 521 cells/mL detected during this time frame, suggesting a period of limited cell proliferation (**Figure 2.7e**). However,

between day 12-16 of the experiment, the cell count increased from a median of 521 to 2092, which is more consistent with the doubling time of this cell line (i.e. 32-48 hours) (22, 23).

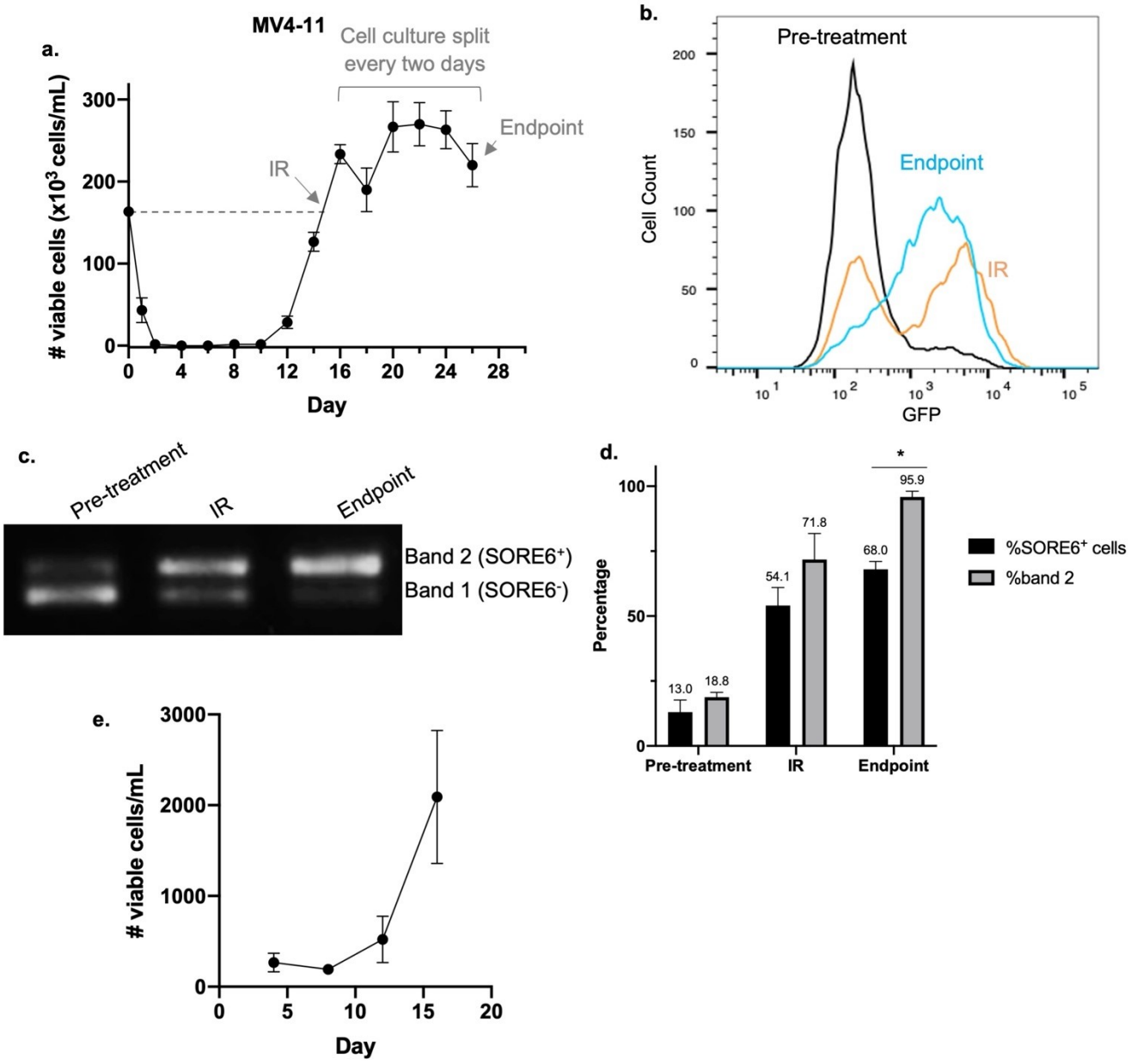

Figure 2.7. Cells regenerated after Ara-C treatment are enriched with SORE6$^+$ cells. (a) MV4-11 SORE6$^-$ and SORE6$^+$ cells pooled to a ratio of 9:1 were treated with 250 nM of Ara-C for two days. Viable cells were detected 10 days after '*in-vitro* remission' was achieved. After an additional four days, the number of viable cells returned to the original

number at the initiation of the experiments (i.e. *in-vitro* relapse (IR)). Cells were then split every 2 days, until being harvested 10 days after IR (i.e. endpoint). Cell viability assays were performed in triplicates and assessed by Trypan Blue. (b) Flow cytometry analysis of GFP assessing SORE6 activity in MV4-11 cells at pre-treatment, IR, and endpoint. (c) Relative proportion of PCR amplicons of band 1 (original SORE6$^-$) and band 2 (original SORE6$^+$) in MV4-11 cells at pre-treatment, IR, and endpoint. (d) Comparison of SORE6$^+$:total cell ratio assessed by flow cytometry analysis and band2:total band intensity ratio by densitometry of PCR amplicons in cells at pre-treatment, IR, and endpoint. Triplicate experiments were performed. Results shown as mean±standard deviation. * $p < 0.05$; Student's *t* test. (e) Number of viable cells during *in-vitro* remission, quantified by a forward scatter/side scatter gating strategy.

2.3.7. Relapsed patient samples have more stem-like cells than initially diagnosed samples

Lastly, we aimed to collect evidence to support the importance of SORE6$^+$ cells in clinical samples. Since Myc is a key driver of SORE6 activity, we used immunodetection of Myc as a surrogate marker for SORE6 activity. We examined Myc protein level by western blot in a panel of nine initially diagnosed and nine relapsed bone marrow specimens. We quantified the Myc expression with densitometry analysis and normalized the values to blast count. Overall, relapsed samples had a significantly higher level of Myc expression, with a 23-fold upregulation in mean Myc expression level in the relapsed panel compared to the initial diagnostic panel (p=.02). Additionally, immunostaining of Myc was performed on bone marrow clot sections from a patient with both initially diagnosed and relapsed samples. In order to minimize the inclusion of early myeloid precursors in the evaluation, we performed double immunostaining using Myc and myeloperoxidase, and strongly myeloperoxidase-positive cells were excluded from being counted as blasts. As illustrated in **Figure 2.8**, we found that Myc-positive blasts were significantly higher in the relapsed bone marrow sample.

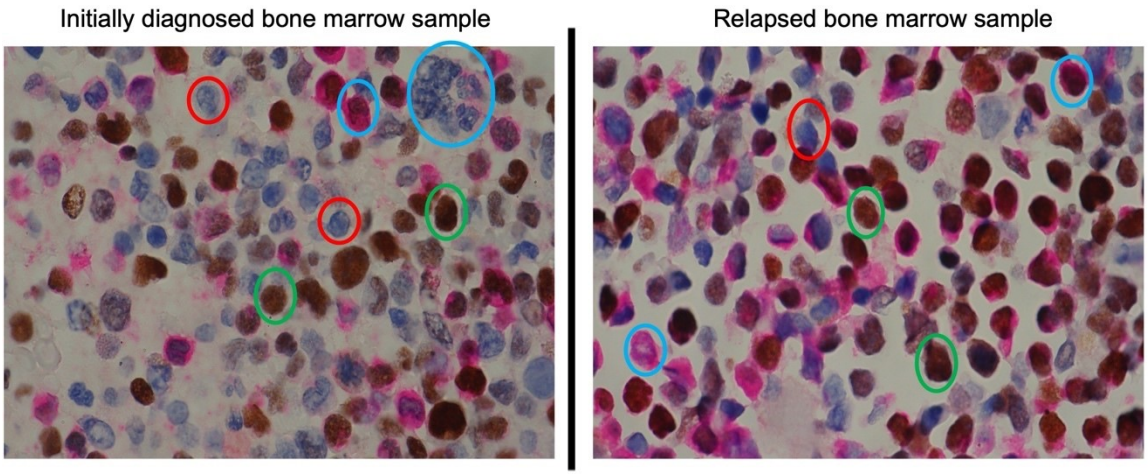

Figure 2.8. Relapsed bone marrow samples have a higher percentage of Myc-positive cells compared to initially diagnosed bone marrow samples. Double immunostaining of Myc (brown) and myeloperoxidase (pink) was performed in paired initially diagnosed and relapsed AML bone marrow clot sections from the same patient. Blasts were identified by their morphology and as having weak/negative myeloperoxidase expression. Blasts were counted as either being Myc-positive (example circled in green) or Myc-negative (example circled in red). Examples of non-blast cells are circled in blue. For this patient, the mean % of Myc-positive blasts was 87.7% in the relapsed samples, as compared to 49.2% Myc-positive blasts in the initially diagnosed sample ($p<0.0001$).

2.4. Discussion

Disease relapse poses one of the most important clinical challenges for treating AML patients. Concepts related to clonal evolution, senescence, and cancer stem cells/CSL cells have been postulated to be potentially important. Nonetheless, due to the paucity of study models, evidence supporting the relevance of these concepts is relatively scarce and circumstantial. Thus, one of our main research goals was to establish an *in-vitro* experimental model that mimics key characteristics of AML relapse. We have described our *in-vitro* model that is primarily based on the use of the SORE6 reporter to identify/purify CSL cells. The substantial duration and limited cell proliferation of the Ara-C-induced '*in-vitro* remission' and the subsequent regeneration mimic disease remission and relapse of AML, respectively. The relatively high chemoresistance in the resurrected

cell population also mirrors the clinical observation that relapsed diseases are highly resistant to frontline chemotherapeutic agents such as Ara-C. This study model can be readily established in a conventional research laboratory, so long as SORE6$^-$/SORE6$^+$ cell subsets can be obtained/generated.

The concept that the reporter activity of SORE6 correlates with cancer stemness has been demonstrated in a number of solid tumors and hematologic cancers (11, 15, 16, 24). Common themes of all published SORE6 studies are as follows: 1) only a minority of cells (~2-20%) in various cancer cell lines were identified as SORE6$^+$ at the steady state and 2) SORE6$^+$ cells carried more CSL features, including tumorigenicity and chemoresistance, compared to SORE6$^-$cells. The design of SORE6 was built on the assumption that cancer stemness is associated with the transcriptional activity of two embryonic stem cell proteins, Sox2 and Oct4. This approach is in contrast with that used in most of the previously published studies on cancer stemness, which are based on the expression of specific cell-surface proteins carrying no known functional link to cancer stemness. Experimental inhibition of Sox2, Oct4 or Myc can lead to significant decreases to the CSL phenotypes in cancer cells (10, 11, 25, 26). To our knowledge, this current study represents the first to use the SORE6 reporter to study AML. Our finding that SORE6 activity significantly correlated with cancer stemness are in line with those of other SORE6 studies. In contrast with a few other SORE6 studies, we found that Myc, rather than Sox2 or Oct4, is the key regulator of the SORE6 reporter activity in FLT3-mutated AML cells. Similar findings were observed in a study examining triple negative breast cancer using a molecular reporter similar to SORE6, called the SRR2 reporter, which detects the transcriptional activity of Sox2. In this study, 16 different transcription factors, including Myc, were found to bind to the SRR2 consensus sequence (10). Thus, the redundancy of these consensus sequences may explain how SORE6 activity is observed despite the lack of detectable Sox2/Oct4 expression in AML cells.

Leveraging molecular barcoding, we directly addressed the question of whether CSL cells are major contributors of AML relapses. Analysis of the barcoded SORE6$^-$ and SORE6$^+$ cells after resurrection led us to conclude that CSL cells are the major contributors to AML relapses. Firstly, while SORE6$^+$ cells accounted for approximately 10% of the cell population at the beginning of the experiments, the proportion of original SORE6$^+$ cells increased to approximately 70% and 90%

at IR and the endpoint, respectively. The progressive increase in the proportion of SORE6$^+$ cells during the *in-vitro* relapse suggests that most SORE6$^-$ cells that emerged after the resurrection did not survive at the endpoint. Based on this observation, it is tempting to hypothesize that AML relapse may involve two distinct phases: 1) the initial emergence from the '*in-vitro* remission' condition, and 2) a subsequent clonal expansion of cell clones that are primarily derivatives of SORE6$^+$ cells.

The term 'cancer plasticity' has been used to describe the ability of cancer cells to acquire stemness (27). One example is epithelial-mesenchymal transition (EMT), in which exposure of various insults to epithelial cells can change their morphology to that of mesenchymal cells, which is accompanied by an increase in chemoresistance and the aberrant expression of various embryonic stem cell proteins (28-30). Using a Sox2 reporter (i.e. SRR2), our group has previously demonstrated the acquisition of stemness in breast cancer and lymphoma cells exposed to oxidative stress (10, 31). We asked if cancer plasticity occurs in our AML model. If a substantial degree of cancer plasticity occurred, the %SORE6$^+$cells (by flow cytometry) in the resurrected cell population should be appreciably higher than the % of cells derived from the original SORE6$^+$ cells (by barcoding). Our finding that the derivatives of the original SORE6$^+$ cells account for >90% at the endpoint (by barcoding) argues against the importance of cancer plasticity in this model. However, based on the observation that the %SORE6$^+$ cells (GFP by flow cytometry) was less than the % of original SORE6$^+$ cells (by barcoding), a small proportion of SORE6$^+$ cells (15-20%) may have differentiated.

In conclusion, we described the establishment of an *in-vitro* model for AML relapse based on the SORE6$^-$/SORE6$^+$ dichotomy. This model has characteristics that mimic the clinical features of AML relapse. Using this model, we have provided evidence to support the importance of CSL cells in AML relapse. Further research using this model may facilitate the identification of cellular pathways and therapeutic targets for AML relapse.

2.5. References

1. Vetrie D, Helgason GV, Copland M. The leukaemia stem cell: similarities, differences and clinical prospects in CML and AML. Nature reviewsCancer. 2020;20(3):158-73.
2. Ram R, Scheid C, Amit O, Chemnitz JM, Moshe Y, Hallek M, et al. Sequential therapy for patients with primary refractory acute myeloid leukemia: a historical prospective analysis of the German and Israeli experience. Haematologica. 2019;104(9):1798-803.
3. Dohner H, Weisdorf DJ, Bloomfield CD. Acute Myeloid Leukemia. N Engl J Med. 2015;373(12):1136-52.
4. Thol F, Ganser A. Treatment of Relapsed Acute Myeloid Leukemia. Curr Treat Options Oncol. 2020;21(8):66.
5. Bose P, Vachhani P, Cortes JE. Treatment of Relapsed/Refractory Acute Myeloid Leukemia. Curr Treat Options Oncol. 2017;18(3):17.
6. Vosberg S, Greif PA. Clonal evolution of acute myeloid leukemia from diagnosis to relapse. Genes Chromosomes Cancer. 2019;58(12):839-49.
7. Duy C, Li M, Teater M, Meydan C, Garrett-Bakelman FE, Lee TC, et al. Chemotherapy Induces Senescence-Like Resilient Cells Capable of Initiating AML Recurrence. Cancer Discov. 2021;11(6):1542-61.
8. Ho TC, LaMere M, Stevens BM, Ashton JM, Myers JR, O'Dwyer KM, et al. Evolution of acute myelogenous leukemia stem cell properties after treatment and progression. Blood. 2016;128(13):1671-8.
9. Ng SW, Mitchell A, Kennedy JA, Chen WC, McLeod J, Ibrahimova N, et al. A 17-gene stemness score for rapid determination of risk in acute leukaemia. Nature. 2016;540(7633):433-7.
10. Gupta N, Jung K, Wu C, Alshareef A, Alqahtani H, Damaraju S, et al. High Myc expression and transcription activity underlies intra-tumoral heterogeneity in triple-negative breast cancer. Oncotarget. 2017;8(17):28101-15.
11. Li J, Haque M, Shang C, Hassan B, Liu D, Chen W, et al. Identification and Characterization of Cancer Stem-Like Cells in ALK-Positive Anaplastic Large Cell Lymphoma Using the SORE6 Reporter. Curr Issues Mol Biol. 2021;43(2):543-57.

12. Sholl LM, Barletta JA, Yeap BY, Chirieac LR, Hornick JL. Sox2 protein expression is an independent poor prognostic indicator in stage I lung adenocarcinoma. Am J Surg Pathol. 2010;34(8):1193-8.
13. He W, Li K, Wang F, Qin YR, Fan QX. Expression of OCT4 in human esophageal squamous cell carcinoma is significantly associated with poorer prognosis. World J Gastroenterol. 2012;18(7):712-9.
14. Ohanian M, Rozovski U, Kanagal-Shamanna R, Abruzzo LV, Loghavi S, Kadia T, et al. MYC protein expression is an important prognostic factor in acute myeloid leukemia. Leuk Lymphoma. 2019;60(1):37-48.
15. Tang B, Raviv A, Esposito D, Flanders KC, Daniel C, Nghiem BT, et al. A flexible reporter system for direct observation and isolation of cancer stem cells. Stem Cell Reports. 2015;4(1):155-69.
16. Pádua D, Barros R, Amaral AL, Mesquita P, Freire AF, Sousa M, et al. A SOX2 Reporter System Identifies Gastric Cancer Stem-Like Cells Sensitive to Monensin. Cancers (Basel). 2020;12(2):20.
17. Quentmeier H, Reinhardt J, Zaborski M, Drexler HG. FLT3 mutations in acute myeloid leukemia cell lines. Leukemia. 2003;17(1):120-4.
18. Shang C, Hassan B, Haque M, Song Y, Li J, Liu D, et al. Crizotinib Resistance Mediated by Autophagy Is Higher in the Stem-Like Cell Subset in ALK-Positive Anaplastic Large Cell Lymphoma, and This Effect Is MYC-Dependent. Cancers (Basel). 2021;13(2).
19. Gheytanchi E, Naseri M, Karimi-Busheri F, Atyabi F, Mirsharif ES, Bozorgmehr M, et al. Morphological and molecular characteristics of spheroid formation in HT-29 and Caco-2 colorectal cancer cell lines. Cancer Cell Int. 2021;21(1):204.
20. Wei AH, Montesinos P, Ivanov V, DiNardo CD, Novak J, Laribi K, et al. Venetoclax plus LDAC for newly diagnosed AML ineligible for intensive chemotherapy: a phase 3 randomized placebo-controlled trial. Blood. 2020;135(24):2137-45.
21. Spiekermann K, Bagrintseva K, Schwab R, Schmieja K, Hiddemann W. Overexpression and constitutive activation of FLT3 induces STAT5 activation in primary acute myeloid leukemia blast cells. Clin Cancer Res. 2003;9(6):2140-50.

22. Kersey JH, Wang D, Oberto M. Resistance of t(4;11) (MLL-AF4 fusion gene) leukemias to stress-induced cell death: possible mechanism for extensive extramedullary accumulation of cells and poor prognosis. Leukemia. 1998;12(10):1561-4.
23. Shan X, Fung JJ, Kosaka A, Danet-Desnoyers G, Reproducibility Project: Cancer B. Replication Study: Inhibition of BET recruitment to chromatin as an effective treatment for MLL-fusion leukaemia. Elife. 2017;6.
24. Vaddi PK, Stamnes MA, Cao H, Chen S. Elimination of SOX2/OCT4-Associated Prostate Cancer Stem Cells Blocks Tumor Development and Enhances Therapeutic Response. Cancers (Basel). 2019;11(9).
25. Beltran AS, Rivenbark AG, Richardson BT, Yuan X, Quian H, Hunt JP, et al. Generation of tumor-initiating cells by exogenous delivery of OCT4 transcription factor. Breast Cancer Res. 2011;13(5):R94.
26. Herreros-Villanueva M, Zhang JS, Koenig A, Abel EV, Smyrk TC, Bamlet WR, et al. SOX2 promotes dedifferentiation and imparts stem cell-like features to pancreatic cancer cells. Oncogenesis. 2013;2(8):e61.
27. Meacham CE, Morrison SJ. Tumour heterogeneity and cancer cell plasticity. Nature. 2013;501(7467):328-37.
28. Luo W, Li S, Peng B, Ye Y, Deng X, Yao K. Embryonic stem cells markers SOX2, OCT4 and Nanog expression and their correlations with epithelial-mesenchymal transition in nasopharyngeal carcinoma. PLoS One. 2013;8(2):e56324.
29. Fischer KR, Durrans A, Lee S, Sheng J, Li F, Wong ST, et al. Epithelial-to-mesenchymal transition is not required for lung metastasis but contributes to chemoresistance. Nature. 2015;527(7579):472-6.
30. Jeon HM, Lee J. MET: roles in epithelial-mesenchymal transition and cancer stemness. Ann Transl Med. 2017;5(1):5.
31. Wu C, Gupta N, Huang YH, Zhang HF, Alshareef A, Chow A, et al. Oxidative stress enhances tumorigenicity and stem-like features via the activation of the Wnt/beta-catenin/MYC/Sox2 axis in ALK-positive anaplastic large-cell lymphoma. BMC Cancer. 2018;18(1):361.

Chapter 3

The role of SORE6-positive cancer stem-like cells in acute myeloid leukemia relapse is dependent on the type of therapeutic agent

3.1. Introduction

Despite recent therapeutic advances, acute myeloid leukemia (AML) remains to carry a very poor clinical outcome. One of the major factors contributing to this poor outcome is disease relapse, which affects approximately two thirds of AML patients who achieve complete remission (1). Treatment options for patients who experience relapse are limited; the median survival time after relapse is only ~6 months (2). In order to develop more effective treatments for AML relapse, an improved understanding of its biological basis is of paramount importance.

While the mechanisms underlying AML relapse are not well understood, several theories have been postulated and described in the literature. The clonal evolution model based on the Darwinian concept of 'survival-of-the-fittest' is one of the first models proposed. In this model, subclones of cancer cells are believed to acquire additional mutations which provide them with advantages in surviving the harsh environment imposed by the induction/consolidation chemotherapy; these subclones will then expand and eventually contribute to clinically evident disease relapse (3). Another model is based on the assumption that subsets of cancer cells are equipped with the ability to enter a reversible senescence-like state during the induction/consolidation chemotherapy, which typically targets the rapidly proliferating cells; after a period of dormancy, these cells escape from this senescence-like state, enter a proliferative phase which forms the basis of disease relapse (4). The cancer stem cell (CSC) model hypothesizes that CSCs, a rare subset of the tumor population carrying higher chemoresistance and tumor initiating capabilities, are the major contributors to AML relapse. Leveraging their superior chemoresistance, these cells are believed to survive the initial chemotherapy, and subsequently remain undetectable at complete remission due to their rarity. Eventually, these cells use their tumorigenic abilities to expand and result in relapse.

There is accumulating evidence supporting the CSC model in AML. In one study, CSCs, defined by their high tumorigenicity detectable in an *in-vivo* limiting dilution assay, were found to be significantly higher in frequency in relapsed bone marrow patient samples as compared to the pre-treatment bone marrow patient samples (5). In another study, AML with higher expressions of CSC-associated genes in the pre-treatment bone marrow specimens had a significantly higher likelihood to experience disease relapse (6). Nonetheless, there is also evidence AML relapse may

result from expansion of bulk cells rather than CSC. Specifically, in a study where paired initially diagnostic and relapsed bone marrow samples were examined by using whole genome sequencing and digital droplet PCR, the authors found cases in which relapsed samples stemmed from bulk cells which had acquired a gene expression pattern similar to that of CSCs (7).

One possible explanation for the conflicting evidence of both bulk and CSC cells expansion at relapse is related to the use of different treatment regimens. While multi-drug chemotherapy is the standard frontline treatment for AML, consisting of a 7-day course of Ara-C with 3 days of an anthracycline (8), a number of alternative treatments have been developed. These treatments are generally less harsh to the patient and have been designed to target specific molecular abnormalities or used to treat patients that are unfit for intensive chemotherapy. While CSCs are generally shown to be more drug resistant, some of these therapies have been found to preferentially target CSCs. For example, treatment with the hypomethylating agent, azacitidine (AZA) in combination with a Bcl-2 inhibitor, Venetoclax (Ven), which is currently being used to treat AML patients unfit for intensive chemotherapy, has been found to more effectively eradicate CSCs over bulk cells by targeting metabolic pathways, such as the oxidative phosphorylation pathway, that are preferentially used by CSCs (9-11). This evidence supports the concept that relapse patterns may be affected by the type of treatment. However, this concept could not be directly tested, in part due to the lack of experimental models for AML relapse.

To further study the biology of AML relapse, I have recently generated an *in-vitro* model in which expansion of the cancer stem-like (CSL) cells characterized by SORE6 reporter activity was found to be the primary contributor to the *in-vitro* relapse (IR) in AML cell lines treated with cytarabine (Ara-C). Using this *in-vitro* model, I tested if the expansion of CSL cells is a universal phenomenon when different doses and types of chemotherapeutic agent are used.

3.2. Materials and Methods

3.2.1. Generation of SORE6$^-$ and SORE6$^+$ cell subsets and cell culture

SORE6$^-$ and SORE6$^+$ cell subsets were generated for two *FLT3*-mutated cell lines, MOLM-13 and MV4-11. Cell lines underwent lentiviral transduction with the SORE6-mCMVo-dsCop-GFP-PURO (SORE6) reporter (National Cancer Institute, NIH, Bethesda, MD, USA) (12). SORE6 activity, detectable by green fluorescent protein (GFP) expression, was assessed using flow cytometry. SORE6$^-$ and SORE6$^+$ subsets were purified using a flow cytometric cell sorter (Sony MA900) based on their GFP expression. All cells transduced with the SORE6 reporter were cultured in RPMI media supplemented with 10% fetal bovine serum in the presence of 0.25 μg/mL puromycin.

3.2.2. Antibodies and drug treatments

Primary antibodies used in western blot studies included anti-MYC (Y69, #ab32072), purchased from Abcam (Cambridge, MA, USA), anti-β-actin (#sc-47778) from Santa Cruz Biotechnology (Santa Cruz, CA, USA), anti-FLT3 (8F2, #3462), anti-p-STAT5 (Tyr694, #9359) and anti-ODC1 (485, #ab193338) were purchased from Cell Signaling (Danvers, MA, USA). Venetoclax was gifted by Abbvie, and Azacitidine, Ara-C, and 10058-F4 were purchased from Selleckchem.

3.2.3. *In-vitro* AML relapse model

MOLM-13 and MV4-11 cells were plated to a concentration of 150,000 cells/mL in T25 flasks. Cells were treated with Ara-C for two days, at which point fresh medium without Ara-C was added to the culture in a 1:1 ratio. The lowest doses that induced '*in-vitro* remission', defined by the absence of trypan blue-negative cells after three observations, were found to be 500 nM for MOLM-13 and 750 nM for MV4-11. To detect cell regeneration, 200 μL of the cell culture was removed for trypan blue cell counting every two days, and the cell culture was replenished with

200 µL of fresh culture media. The point at which viable cells were first detected was labelled as 'first viability (FV).' Once the cell density reached the same level as the original density (labeled as '*in-vitro* relapse' or 'IR'), cells were harvested for analysis.

3.2.4. Barcode labeling of SORE6 Sorted Cells

The CloneTracker 4-barcode-plus cell labeling kit (Cellecta, Mountain View, CA, USA) was employed to track cell fate. Barcodes were transduced into purified $SORE6^+$ and $SORE6^-$ cells by following the manufacturer's protocol. For the remainder of this manuscript, the barcode used for $SORE6^-$ cells was named barcode #1, while that for $SORE6^+$cells was labeled barcode #2. The unique sequence in each barcode was detectable by polymerase chain reaction and a set of primers supplied by Cellecta. Both barcodes also carried a *red fluorescence protein* gene to allow the identification of cells with successful transduction of the barcodes. The barcodes were stably expressed in both cell populations over the course of 4 weeks of our experiments, with >95% of cells expressing RFP that was detectable by flow cytometry.

3.2.5. Polymerase chain reaction

Genomic DNA extraction was performed using PureLink® Genomic DNA mini kit (Invitrogen, Waltham, MA, USA) based on the manufacturer's protocol. PCR reactions to detect cell barcoding were performed using the CloneTracker 4-barcode-plus cell labeling kit (Cellecta) following the manufacturer's protocol. Bands were visualized by gel electrophoresis with a 3% agarose gel.

3.2.6. Western blot studies

Cell pellets were lysed with RIPA buffer (MilliporeSigma, Burlington, MA, USA), with protease and phosphatase inhibitors (MilliporeSigma). Proteins were separated on a 10% polyacrylamide SDS-PAGE gel, transferred to a nitrocellulose membrane (GE Healthcare, Velizy-Villacoublay, France), and then incubated with primary antibodies. The membrane was then incubated with

horseradish peroxidase-conjugated secondary antibodies. Bands were visualized with an Odyssey® Infrared Imaging System (LI-COR, Lincoln, NE, USA).

3.2.7. Metabolomic analysis

Metabolomic analysis was performed at the Metabolomics Innovation Centre, U of Alberta. Cells were pelleted and flash frozen using liquid nitrogen. Metabolites were extracted using ceramic beads and methanol to homogenize samples. Samples were then centrifuged, and the solvent was isolated and dried to yield sample extracts. Samples were split into two aliquots, with one aliquot from each sample being pooled, and this pooled sample was used as the reference. Chemical isotope labelling was then performed, with the individual samples labelled with $^{12}C_2$ and the pooled sample labelled with $^{13}C_2$, using a Dansyl-labeling kit (Nova Medical Testing Inc., Edmonton, AB, Canada), as indicated by the manufacturer's protocol. The $^{12}C_2$ sample was mixed with the $^{13}C_2$ pooled sample and were then analyzed with LC-MS. Untargeted 1-channel (amine/phenol) analysis was performed using an Agilent 1290 LC and an Agilent 6546 Q-TOF mass spectrometer. The relative quantification of each metabolite was detected by comparing the ^{12}C-peak from the individual samples with the ^{13}C-peak from the reference. Metabolites were identified by comparing retention time and mass indicated by the peaks with two labelled metabolite libraries (CIL Library and LI Library).

3.2.8. Glycomic analysis

Barcoded phage plasmids ligated with lectins were generated by the Derda research group at the University of Alberta. 1 million phages were incubated with 1 million cells in order for lectins to bind to sialic acids on cell surfaces. Three separate lectin-phage conjugates were generated: carbohydrate-binding molecule (CBM), Siglec-7 and maltose-binding protein (MBP). MBP, a protein found on bacteria but not mammalian cells (13), was used as a negative control. Following binding, cell-phage mix was washed, and then RNase A and Proteinase K were added to the mixture. The mixture was centrifuged, and the supernatant containing the DNA product was

collected. The DNA product was amplified using qPCR, with the primers targeting the DNA barcode on the phage. Deep sequencing of the PCR product was performed at the Molecular Biology Service Unit, University of Alberta, using an Illumina NextSeq500 system.

3.2.9. Patient samples

22 initially diagnosed and 12 relapsed AML bone marrow aspirates that were stored in liquid nitrogen were collected retrospectively from the University of Alberta Hospital. The use of these patient samples was approved by the Health Research Ethics Board of Alberta (HREBA.CC-21-0253_REN1; date of approval July 7, 2022).

3.2.10. Statistical analysis

Statistical analyses were performed using GraphPad Prism 8 (Graphpad Software Inc. LaJolla, Ca, USA). P-values were calculated using two-tailed Student's t-test.

3.3. Results

3.3.1. Zero viability *and in-vitro* relapse induced by Ara-C, AZA and AZA+Ven

Firstly, I established whether *in-vitro* remission followed by *in-vitro* relapse could be achieved using different therapeutic agents. Ara-C was the only therapeutic agent tested during my initial characterization of the *in-vitro* model (Chapter 2). For simplicity, the lowest dose of drugs needed to induce *in-vitro* remission, where no viable cells were detected, was labeled the 'optimal dose'. As shown in **Figure 3.1**, 750 nM of Ara-C was found to be the optimal dose for MV4-11, which occurred on day 2. With this dosage, the first detectable viable cells, labelled as 'first viability (FV)', occurred on day 12±1 and the *in-vitro* relapse (IR) (i.e. when the number of relapsed cells

was equal to that at the beginning of experiments) was detected on day 18±2. This pattern is similar to that described in Chapter 2.

The experiments were then repeated using AZA or AZA+Ven, two frontline regimens used primarily for AML patients who cannot tolerate Ara-C-based regimens due to old age or comorbid conditions. These regimens were compared in a recent large clinical trial, and AZA+Ven was found to be superior to AZA, with the overall survival being longer with the combination treatment (14.7 versus 9.6 months, $p<0.001$) (14). Using the *in-vitro* model, the optimal dose for AZA was found to be 10 μM, and that of Ven was 25 nM. Using the same dosing strategy used in the clinical trial (14), the AZA+Ven treatment consists of the optimal dose of AZA and that of Ven (i.e. 10 μM of AZA and 25 nM of Ven). As shown in **Figure 3.1**, MV4-11 cells treated with 10 μM of AZA or 25 nM of Ven, *in-vitro* remission was consistently achieved on day 2; FV was detectable on day 7±1 for both drugs, and IR was reached on day 13±1 and day 20±2, respectively. No FV was observed in cells treated with the optimal dose of AZA+Ven on day 30, the experimental endpoint. These findings correlate with the conclusion from the clinical trial that AZA+Ven showed significantly higher clinical efficacy (14).

Given that FLT3-inhibitors are used to treat *FLT3*-mutated AML, I also tested one of the FLT3 inhibitors (i.e. Gilteritinib) in the *in-vitro* model. MV4-11 cells were treated with 20, 40 and 60 nM of Gilteritinib. As shown in **Figure 3.2,** 20 nM of Gilteritinib was insufficient in inducing *in-vitro* remission. While 40 and 60 nM of Gilteritinib did induce *in-vitro* remission, FV was not observed on day 30. Gilteritinib treatment was not further studied since *in-vitro* relapse did not occur.

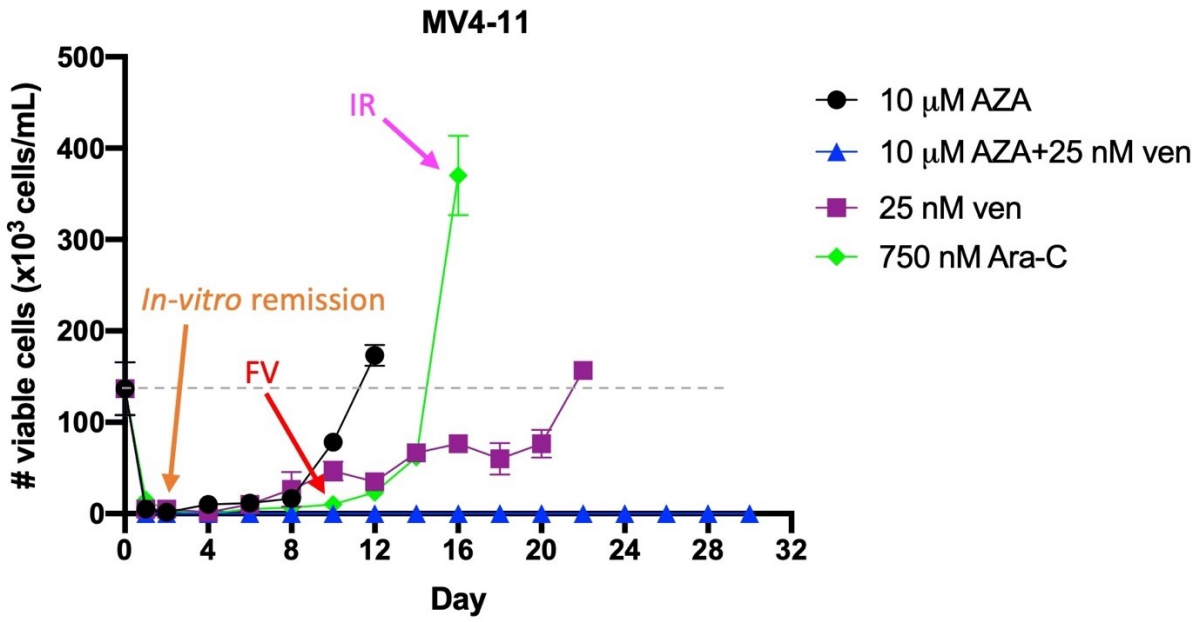

Figure 3.1. *In-vitro* relapse model using four different treatments. MV4-11 SORE6$^-$ and SORE6$^+$ cells pooled to a ratio of 9:1 were treated with 10 μM AZA, 25 nM Venetoclax, 10 μM AZA with 25 nM Venetoclax, or 750 nM of Ara-C, for two days. All 4 treatments induced "*in-vitro* remission" on day 2 of the experiment, where no viable cells were detected. Viable cells were counted every two days using Trypan Blue. The red arrow shows the point where viable cells were first detected after treatment, labelled as 'FV', for the Ara-C condition. The first measurement that reaches or exceeds the original cell number at the initiation of the experiments was labelled as 'IR' (blue arrow), at which point cells were no longer counted. Cell viability assays were performed in triplicates and assessed by trypan blue.

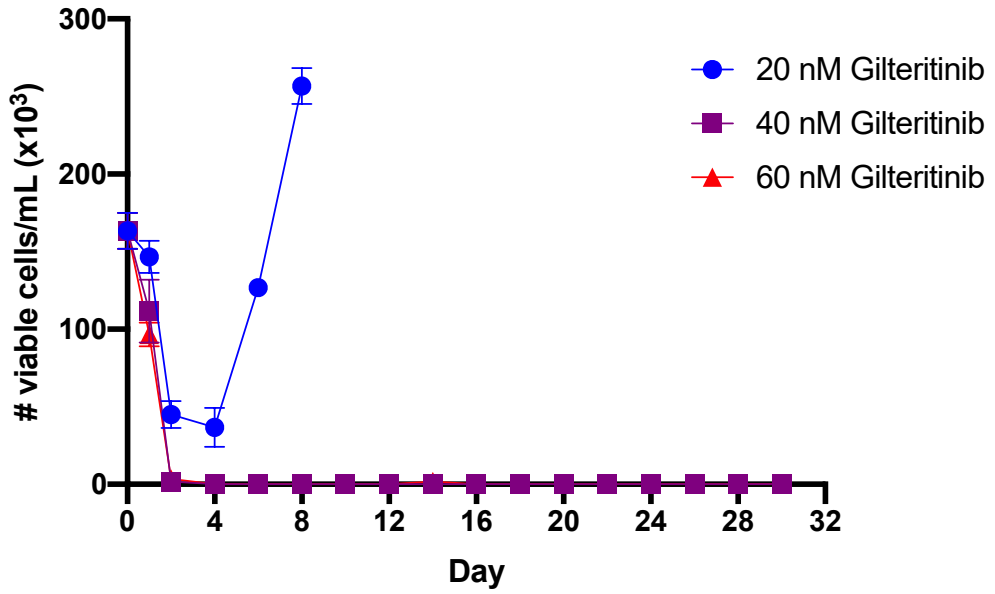

Figure 3.2. *In-vitro* relapse model with Gilteritinib. MV4-11 SORE6$^-$ and SORE6$^+$ cells were mixed to a proportion of 9:1 and treated with 20 nM, 40 nM, and 60 nM Gilteritinib for 2 days. 20 nM was not sufficient to induce zero viability. 40 nM and 60 nM of Gilteritinib resulted in zero viability after two days, but no viable cells were detected at the end of the experiment.

3.3.2. Characteristics of IR when suboptimal drug doses are used

In addition to examining whether the use of different therapeutic agents would affect the contribution of SORE6$^+$ cells to *in-vitro* relapse, I also examined whether exposing cells to suboptimal doses would affect the role of SORE6$^+$ cells to *in-vitro* relapse. A range of suboptimal doses were tested for each of the four treatment regimens used in section 3.3.1. The *in-vitro* relapse patterns for suboptimal doses are summarized as followed:

a) Ara-C (**Figure 3.3a**), five suboptimal doses (675, 563, 375, 188 and 94 nM, representing 10%, 25%, 50%, 75% and 82.5% reduction, respectively) of Ara-C were used, in addition to the optimal dose of 750 nM). IR was reached earlier in a dose-dependent manner (i.e. day 11±1 at 94 nM of Ara-C, day 13±1 at 188 nM of Ara-C, day 17±2 at 375 and 563 nM of Ara-C). Both 750 and 675 nM doses reached the IR on day 18±2.

b) AZA (**Figure 3.3b**): three doses (9, 7.5 and 5 μM, representing 10%, 25% and 50% reduction of the optimal dose) of AZA were tested, in addition to the optimal dose of 10 μM. In contrast with Ara-C, the days IR was reached were not appreciably different among these suboptimal doses (i.e. day 13±1 for 10 μM, day 13±2 for 9 μM, and day 11±1 for both 7.5 and 5 μM).

c) AZA+Ven (**Figure 3.3c**): Mild reduction of the dosage (i.e. 9 μM of AZA + 23 nM of Ven, 10% reduction) did not result in any appreciable degree of expansion; no viable cells were detected at the end of the experiment (day 30). Moderate reduction of the dosage (8 μM AZA + 19 nM Ven, 25% reduction) resulted in FV on day 19±3 and IR was reached relatively late (i.e. day 24±3). Reduction of dosages at 50% (5 μM of AZA and 12.5 nM of Ven) led to FV on day 14±2 and IR was reached on day 19±3.

d) Ven alone (**Figure 3.3d**): The results of Ven alone are included for completeness. Similar to Ara-C, IR was reached earlier in a dose-dependent manner, with IR being reached on day 20±2 with 25 nM Ven (optimal dose), day 17±1 with 23 and 19 nM Ven (10% and 25% dose reduction), and day 15±1 with 13 nM Ven (50% dose reduction).

In summary, graded dose reductions of the four treatments led to different patterns of the *in-vitro* relapse model. In the following section, these patterns are correlated with the presence/absence of CSL expansion.

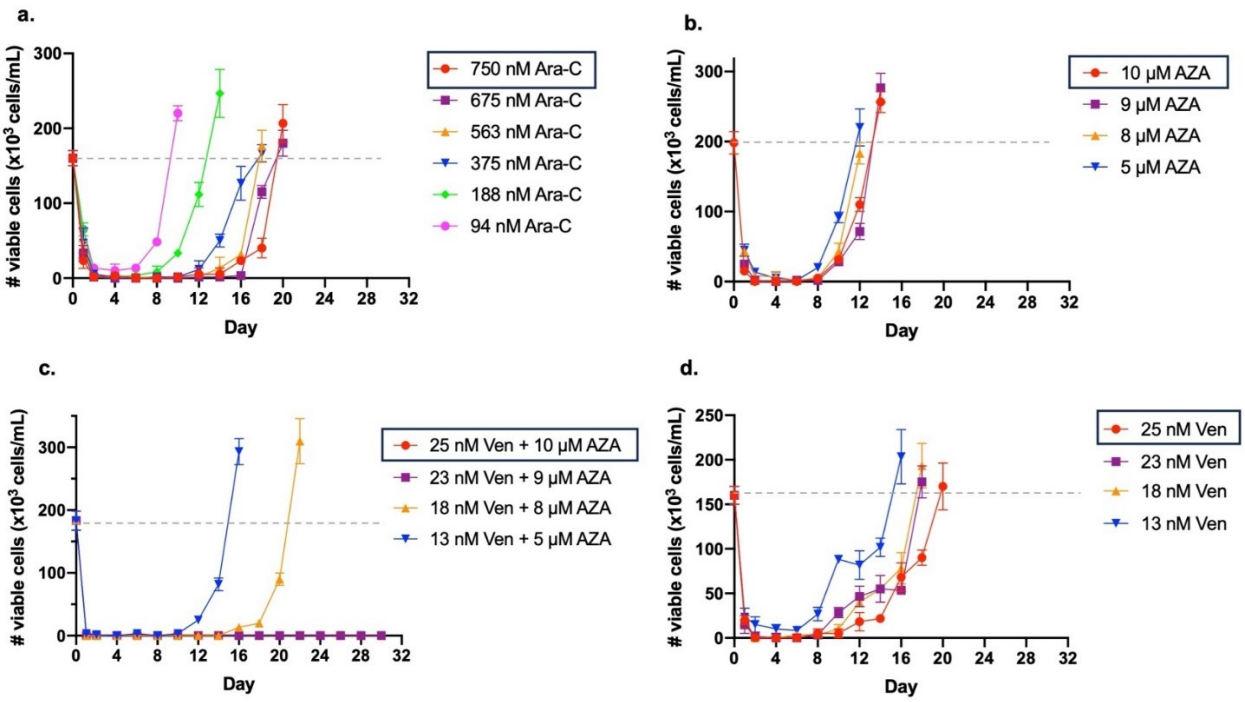

Figure 3.3. *In-vitro* relapse with suboptimal doses of the four treatments. Barcoded MV4-11 SORE6$^-$ and SORE6$^+$ cells mixed to a ratio of 9:1 were treated with (a) 750, 675, 563, 375, 188 and 94 nM Ara-C, (b) 10, 9, 8, 5 μM AZA, (c) 25+10, 23+9, 19+8 and 13+5 nM Ven+μM AZA, and (d) 25, 23, 19, 13 nM Ven for two days. Viable cells were counted every two days using trypan blue. Gray dotted lines depict number of viable cells required for IR to be attained. Optimal doses are boxed.

3.3.3. The importance of CSL cell expansion varies with different chemotherapeutic agents

In Chapter 2, I tracked the relative contribution of SORE6$^-$ and SORE6$^+$ cells during IR using molecular barcoding. To assess if there was a SORE6$^-$/SORE6$^+$ conversion, flow cytometry to assess GFP expression (i.e. the readout of the SORE6 reporter) was employed. Using this experimental approach, the relative contribution of the SORE6$^+$ CSL cells in IR and whether SORE6$^-$/SORE6$^+$ conversion occurred was assessed for the graded doses of different treatments. At the beginning of the experiments, purified SORE6$^-$ and purified SORE6$^+$ cells were mixed in a 9:1 ratio, in order to mimic the ratio identified in unsorted cells. Results are summarized in **Figure 3.4a-d**.

a) Ara-C (**Figure 3.4a**): IR cells treated with 750 nM of Ara-C were highly enriched in SORE6^{+} CSL cells at the expense of the SORE6^{-} bulk cells; this finding was consistent with the results illustrated in Chapter 2. Interestingly, IR cells treated with low doses of Ara-C were also enriched in SORE6^{+} CSL cells. By flow cytometry, most of the IR cells were GFP^{+}. With the exception of the 675 nM dose, there was no significant difference in SORE6^{+} cells by flow cytometry and molecular barcoding, suggesting that in general, no substantial SORE6^{-}/SORE6^{+} conversion or differentiation occurred.

b) AZA (**Figure 3.4b**): By molecular barcoding, IR cells treated with 10 μM (optimal dose) of AZA were enriched in SORE6^{-} bulk cells at the expense of the SORE6^{+} CSL cells. Specifically, compared to the pre-treatment sample, SORE6^{+} cells appeared to be preferentially suppressed at the optimal dose. IR cells treated with lower doses showed lesser degree of SORE6^{+} suppression compared to that of the optimal dose. In keeping with these findings, flow cytometry studies showed a mild but appreciable reduction of GFP^{+} cells compared to the pre-treatment sample. Comparing flow cytometry and molecular barcoding results also suggest that there was no significant SORE6^{-}/SORE6^{+} phenotypic conversion.

c) AZA+Ven (**Figure 3.4c**): IR cells treated with varying degrees of dose reduction showed the distinct loss of SORE6^{+} cells. Accordingly, most of the IR cells at IR were GFP^{-} cells detectable by flow cytometry.

d) Ven alone (**Figure 3.4d**): For completeness, the results of Ven alone are included. By flow cytometry, IR cells treated with varying degrees of dose reductions showed slightly higher proportions of GFP^{+} cells compared to that in the pre-treatment cell population. However, by molecular barcoding, the percentage of SORE6^{+} cells was significantly higher than the GFP^{+} cells, suggesting some degree of differentiation from SORE6^{+} to SORE6^{-} cells.

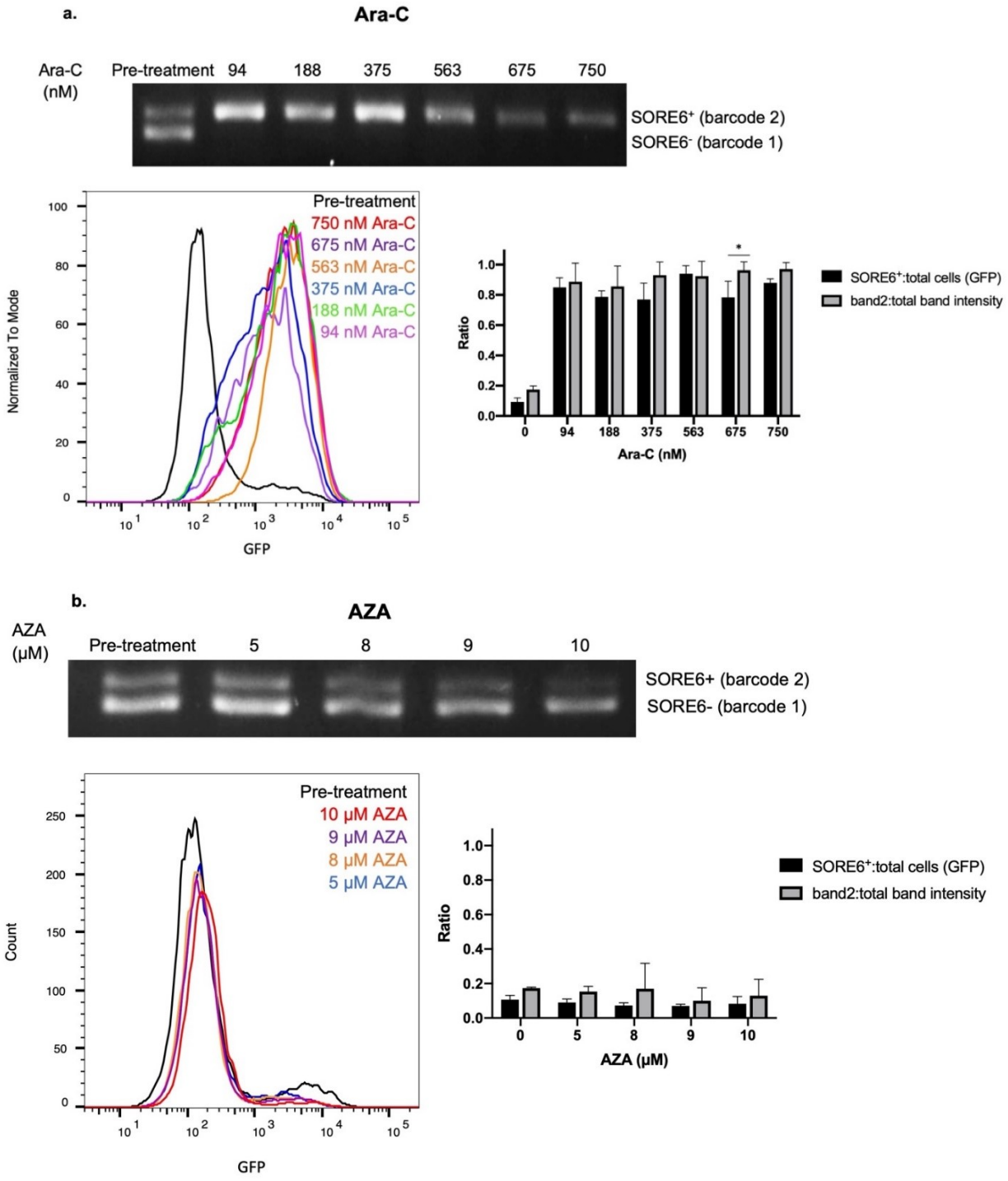
a.
Ara-C
Ara-C (nM)
Pre-treatment
94
188
375
563
675
750
SORE6+ (barcode 2)
SORE6- (barcode 1)
Pre-treatment
750 nM Ara-C
675 nM Ara-C
563 nM Ara-C
375 nM Ara-C
188 nM Ara-C
94 nM Ara-C
Normalized To Mode
GFP
Ratio
Ara-C (nM)
SORE6+:total cells (GFP)
band2:total band intensity
b.
AZA
AZA (μM)
Pre-treatment
5
8
9
10
SORE6+ (barcode 2)
SORE6- (barcode 1)
Pre-treatment
10 μM AZA
9 μM AZA
8 μM AZA
5 μM AZA
Count
GFP
Ratio
AZA (μM)
SORE6+:total cells (GFP)
band2:total band intensity

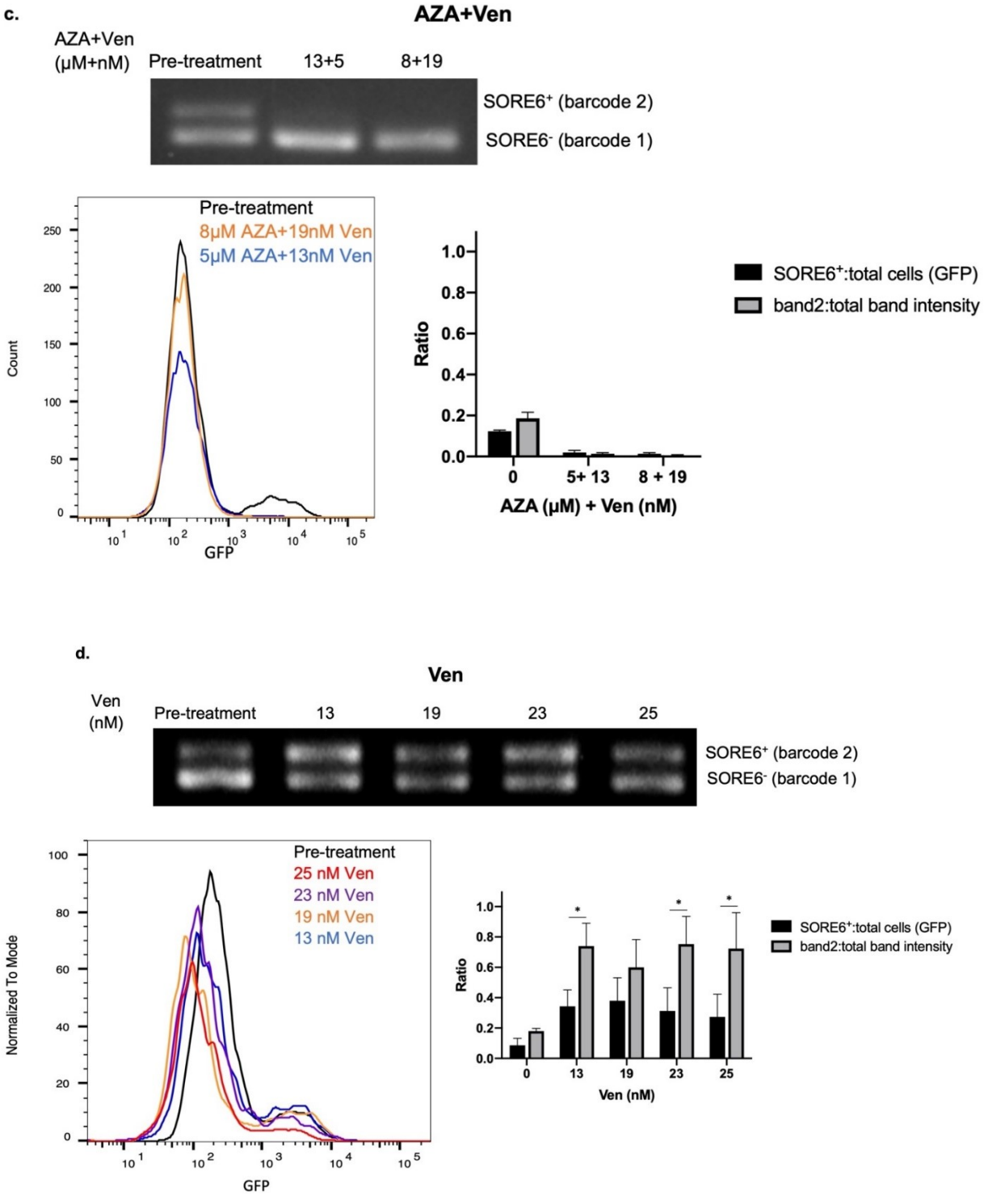
c.
AZA+Ven
AZA+Ven
(μM+nM)
Pre-treatment
13+5
8+19
SORE6+ (barcode 2)
SORE6- (barcode 1)
Pre-treatment
8μM AZA+19nM Ven
5μM AZA+13nM Ven
Count
GFP
Ratio
0
5+ 13
8 + 19
AZA (μM) + Ven (nM)
SORE6+:total cells (GFP)
band2:total band intensity
d.
Ven
Ven
(nM)
Pre-treatment
13
19
23
25
SORE6+ (barcode 2)
SORE6- (barcode 1)
Pre-treatment
25 nM Ven
23 nM Ven
19 nM Ven
13 nM Ven
Normalized To Mode
GFP
Ratio
Ven (nM)
SORE6+:total cells (GFP)
band2:total band intensity

Figure 3.4. The importance of CSL cell expansion variers with different chemotherapeutic agents. Barcoded MV4-11 SORE6$^-$ and SORE6$^+$ cells mixed in a ratio of 9:1 were treated for two days with (a) 750, 675, 563, 375, 188 and 94 nM Ara-C, (b) 10, 9, 8, 5 μM AZA, (c) 25+10, 23+9, 19+8 and 13+5 nM Ven+μM AZA, and (d) 25, 23, 19, 13 nM Ven. Cells that reached IR were subjected to barcoding and flow cytometry analysis. Relative proportion of PCR amplicons of barcode 1 (SORE6$^-$) and barcode 2 (SORE6$^+$) and flow cytometry analysis of GFP assessing SORE6 activity are shown. GFP and barcode 2 percentages are summarized in the bar charts. Error bars show standard deviation; *p*-value calculated using a student's *t*-test, where *p<.05.

3.3.4. Myc inhibition correlates with the contribution of SORE6$^+$ CSL cells in IR

As mentioned above, AZA+Ven is the most efficient in suppressing SORE6$^+$ CSL cells. While AZA showed evidence of CSL suppression, this effect was not as complete as that of AZA+Ven (evidenced by both molecular barcoding and flow cytometry data). Ara-C and Ven showed less efficacy against CSL cells.

Based on the results presented, I expected AZA+Ven (followed by AZA) to suppress the expression of Myc, which as shown in Chapter 2, is a driver of the SORE6 reporter activity and cancer stemness in these *FLT3*-mutated AML cells. As shown in **Figure 3.5**, treatment with AZA+Ven for 4 hours dramatically decreased the expression of Myc. In addition, the FLT3/pSTAT5 axis, which was found to upregulate Myc (15, 16), was also substantially downregulated. AZA partially downregulated Myc but exerted no appreciable effects on the FLT3/pSTAT5 axis. Ara-C and Ven showed no appreciable decrease in Myc or FLT3/pSTAT5.

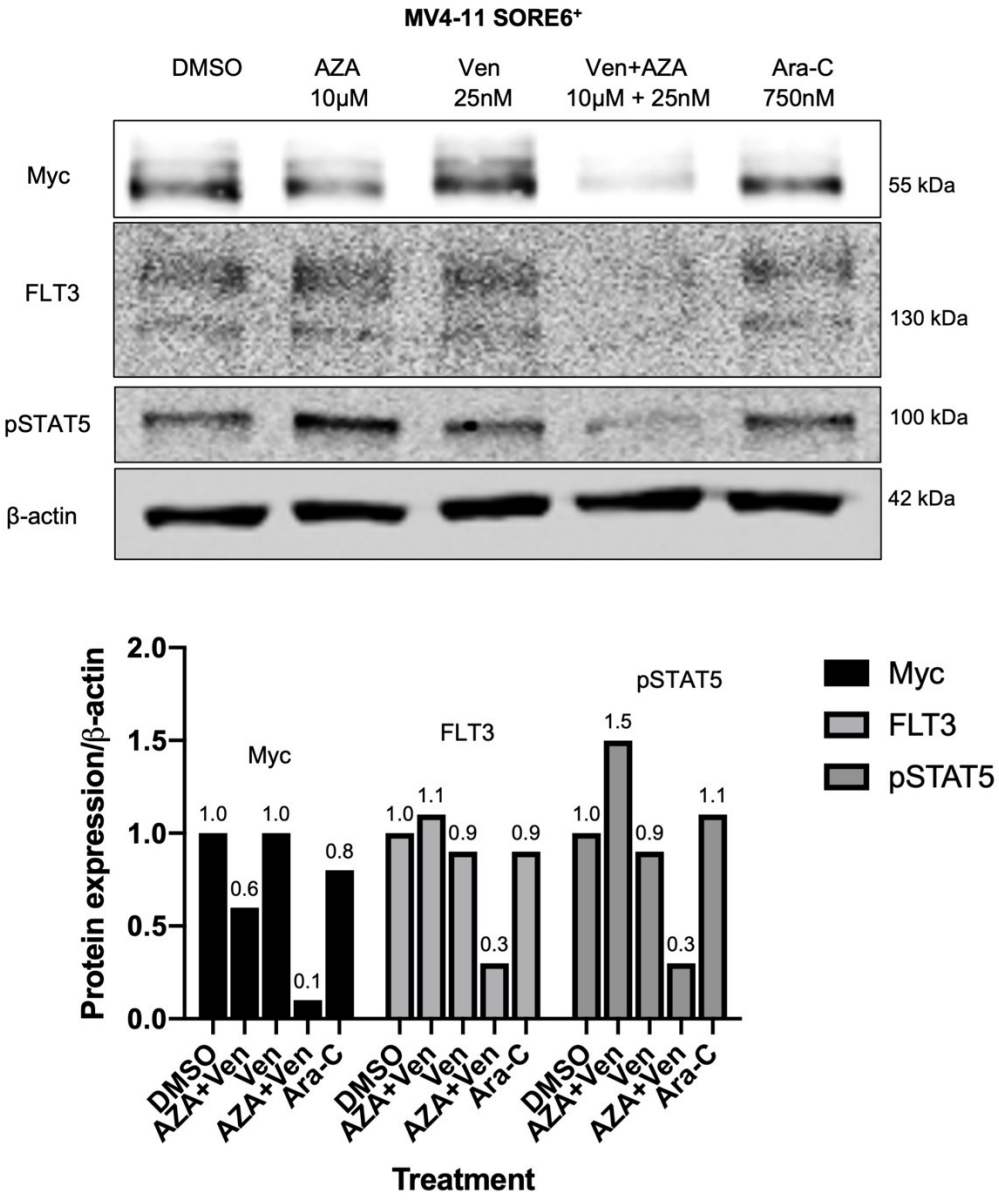

Figure 3.5. Myc inhibition correlates with the contribution of SORE6$^+$ CSL cells in IR. Protein expression level of FLT3, p-STAT5, Myc in MV4-11 SORE6$^+$ cells treated with 10 μM AZA, 25 nM Ven, 10 μM AZA with 25 nM Ven, or 750 nM Ara-C for 4 hours. Densitometry analysis for each protein was normalized to β-actin.

3.3.5. IR cells rich in SORE6$^+$ cells have distinct biological signatures

Using the *in-vitro* model, I have demonstrated that the cell regeneration during IR may involve the expansion of SORE6$^+$ cells (as in the case of Ara-C) or the expansion of SORE6$^-$ cells (as in the case of AZA or suboptimal doses of AZA+Ven). To substantiate this dichotomy based on whether the expansion of SORE6$^+$ cells is a dominant factor during IR, I sought additional correlations.

a. Metabolomics data

I hypothesize that the two different patterns of IR (i.e. with or without the expansion of SORE6$^+$ cells) may correlate with distinct metabolic signatures. Since SORE6$^+$ cells were most 'preserved' with the Ara-C treatment, I focused on initial large scale metabolomics profiling studies comparing IR cells and the pre-treatment cells in the Ara-C treatment group. Samples extracted from cells treated with the optimal dose for MOLM-13 (i.e. 500 nM of Ara-C) and for MV4-11 (i.e. 750 nM of Ara-C) were included, with the pre-treatment cells serving as the comparison. Four runs were carried out for each sample. A total of 21 statistically significant targets common to both cell lines were identified (**Table 3.1**). Among the targets showing the most significant differences, targets in the ornithine/spermine pathway (**illustrated in Figure 3.6**) stood out. Since ornithine decarboxylase (ODC) is the rate-limiting enzyme in this pathway (17), I then tested if a high ODC level is a surrogate marker for the expansion of SORE6$^+$ CSL cells.

As shown in **Figure 3.7a**, western blot studies to measure ODC showed that the levels of ODC generally correlated with whether the expansion of SORE6$^+$ CSL cells was involved. Specifically, in cells treated with Ara-C, ODC was found to be highly expressed at IR at all tested doses. In contrast, in all other situations where the expansion of SORE6$^+$ cells was not as prominent as Ara-C, such as AZA, Ven and AZA+Ven (suboptimal dose), there was either a downregulation of ODC or no appreciable change compared to the pre-treatment condition. These findings are in support of the concept that AML relapses are biologically heterogeneous. My results suggest that the upregulation of ODC and the ODC/spermidine/spermine pathway may be a signature for IR involving the expansion of SORE6$^+$ CSL cells.

	MOLM-13		MV4-11	
Compound	Fold Change (IR/pre-treatment)	p-value	Fold Change (IR/pre-treatment)	p-value
Kynurenine	1.230	0.003	1.211	0.001
Ornithine	2.916	0.000	2.507	0.000
N(gamma)-Acetyldiaminobutyric acid	1.437	0.000	1.598	0.000
Isomer 1 of DL-2-Aminooctanoic acid	1.851	0.002	1.294	0.000
Isomer 1 of N(6)-Methyllysine	2.099	0.014	1.313	0.037
Glutamyl-Valine	1.442	0.003	1.215	0.002
Gamma-glutamyl-ornithine	1.338	0.009	1.548	0.009
Xanthine	3.395	0.002	2.427	0.002
Choline	1.323	0.000	1.734	0.000
(R)-1-Aminopropan-2-ol	2.098	0.003	1.280	0.019
5,10-Methylenetetrahydrofolic acid	1.264	0.000	1.535	0.000
4-Aminobutyraldehyde	2.458	0.001	2.412	0.000
Spermine	3.516	0.023	1.521	0.007
N-Formimino-L-glutamic acid	1.887	0.002	1.348	0.036
Kynurenine	1.230	0.003	1.211	0.001
Isomer 1 of 4,6-Dihydroxyquinoline	2.901	0.022	3.800	0.008
3-Aminopropanal	1.205	0.040	1.219	0.027

5-Aminopentanal	1.947	0.001	1.341	0.000
4-Chloro-L-lysine	5.471	0.001	2.256	0.000
2-Amino-2-methyl-1,3-propanediol	2.418	0.002	2.366	0.000
5-Hydroxydopamine	2.814	0.001	1.598	0.000

Table 3.1. **Metabolites upregulated in *in-vitro* relapse compared to pre-treatment cells.** From a metabolomic analysis, these 21 targets were significantly higher in *in-vitro* relapse compared to pre-treatment samples in both MOLM-13 and MV4-11 cell lines. Metabolites highlighted in orange are part of the ornithine/putrescine/spermidine/spermine pathway.

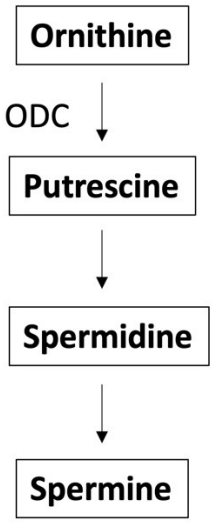

Figure 3.6. Diagram of the ornithine/putrescine/spermidine/spermine pathway.

b) Glycomics data

In addition to the metabolic studies, I examined the expression configurations of cell-surface sialic acids, as recognized by a panel of lectins, courtesy of Dr. Ratmir Derda's laboratory (Department of Chemistry, U of Alberta). AML cells from pre-treatment and IR cells were tested. Details of the

method have been previously published (18). Briefly, engineered bacterial phages were ligated with various lectins, each of which recognizes specific configuration of sialic acids. The identity of each lectin can be detected by using DNA sequencing since each bacterial phage is engineered to carry a DNA barcode. Once lectins were bound by the sialic acids on the cell surface, cells were harvested, processed, and sent for DNA sequencing, and the abundance of various lectins bound on the cell surface can be accurately determined. A few recent publications have demonstrated the biological significance of alterations to sialic acid configurations. For instance, aberrant sialylation has been associated with cancer (19), and a recent paper has shown different sialic acid configurations in cancer stem cells compared to bulk cancer cells in breast cancer (20).

IR MV4-11 cells treated with 750 nM of Ara-C, 10 μM of AZA and 25 nM of Ven were examined. As IR did not occur with cells treated with AZA+Ven, this arm was not included in this study. Two lectin-phage conjugates, CBM and Siglec-7, were employed in the analysis. Both lectins were normalized against MBP, a lectin serving as the internal control.

Levels of CBM and Siglec-7 for each treatment condition are summarized in the heat map shown in **Figure 3.7b**. Compared to untreated cells, IR cells treated with Ara-C showed the most substantial reduction in binding in both CBM and Siglec-7, those treated with Ven showed moderate reduction in Siglec-7 and no change in CBM, and those treated with AZA showed slight reduction in both CBM and Siglec-7. This result provides further evidence that the characteristics of cells at IR differ based on treatment type. IR cells in the Ara-C condition showed the most reduction in binding, correlating with the highest proportion of $SORE6^{+}$ cells at IR in this condition.

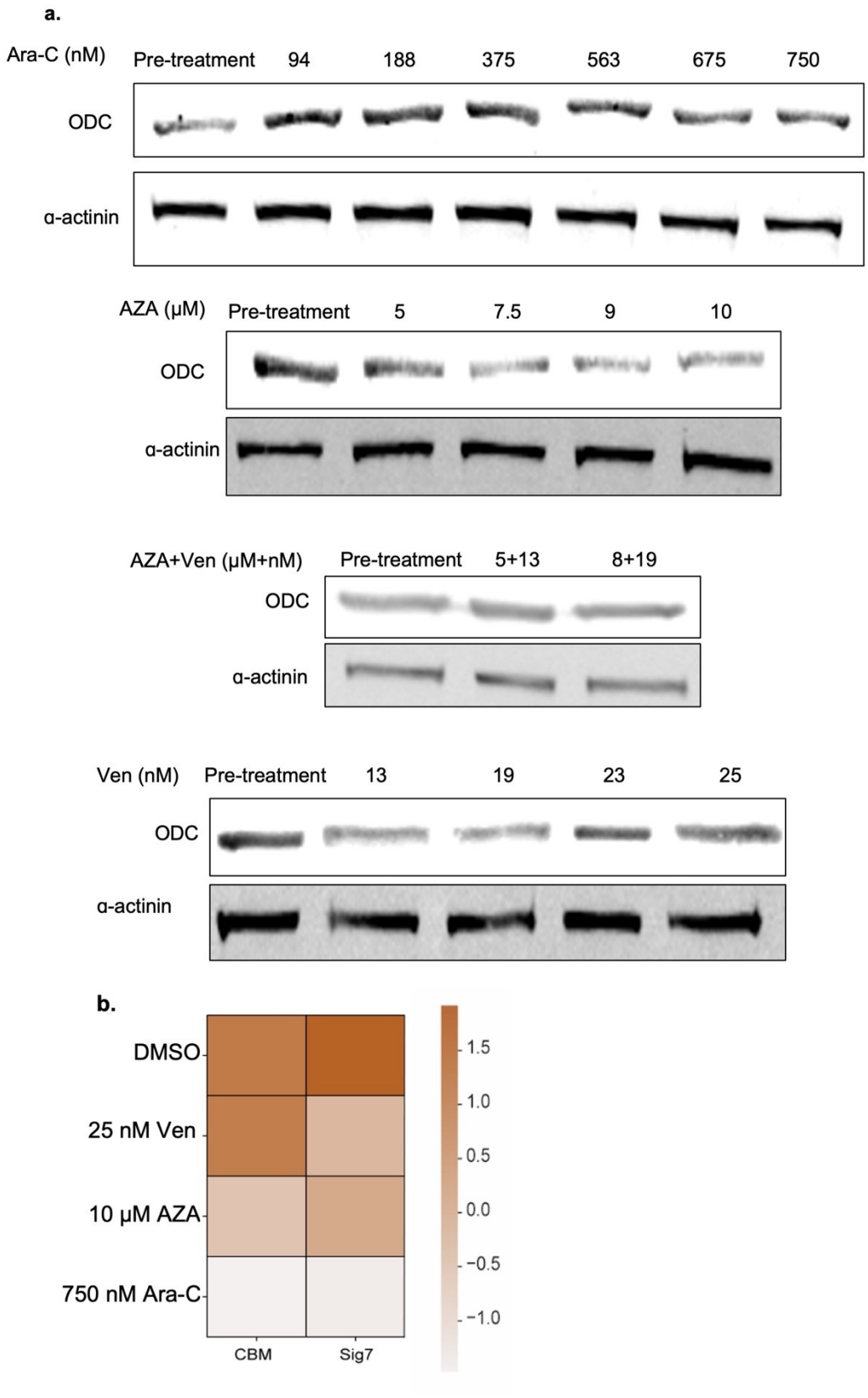
a.
Ara-C (nM)
Pre-treatment
94
188
375
563
675
750
ODC
α-actinin
AZA (μM)
Pre-treatment
5
7.5
9
10
ODC
α-actinin
AZA+Ven (μM+nM)
Pre-treatment
5+13
8+19
ODC
α-actinin
Ven (nM)
Pre-treatment
13
19
23
25
ODC
α-actinin
b.
DMSO
25 nM Ven
10 μM AZA
750 nM Ara-C
CBM
Sig7
1.5
1.0
0.5
0.0
−0.5
−1.0

Figure 3.7. IR cells after different treatments have distinct biological signatures. (a) Protein expression of ODC levels assessed by western blots in MV4-11 IR cells treated with Ara-C, AZA, Ven and AZA+Ven. (b) Heat map showing binding levels of CBM and Siglec-7 with sialic acids on cells treated with 25 nM Ven, 10 μM AZA and 750 nM Ara-C. All lectins are normalized to MBP, which serves as the internal control.

3.3.6. A panel of relapsed patient samples had significantly higher levels of ODC compared to initially diagnosed specimens

To provide clinical validation, we examined the expression level of ODC by western blot in a panel of 22 initially diagnosed and 12 relapsed AML bone marrow specimens. After normalizing the densitometry analysis to the blast count in the bone marrow, we categorized the samples as either ODC-high or ODC-low, where the cut-off was chosen as a natural separation between all samples. As shown in **Figure 3.8**, ODC expression was heterogenous in both groups, with 9/12 (75.0%) relapsed samples and 7/22 (31.8%) initially diagnosed samples categorized as ODC-high; however, the panel of relapsed samples showed a significantly higher proportion of ODC-high samples compared to the initially diagnosed group (p=.03; Fisher's exact test).

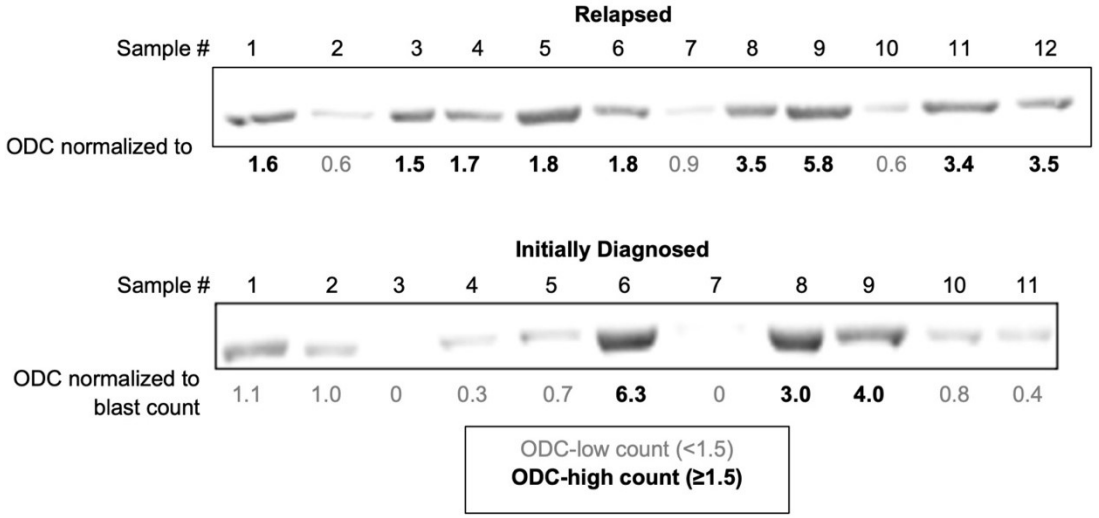

	ODC-low	ODC-high	Total
Relapsed	3	9	12
Initially diagnosed	15	7	22

p=.03

Figure 3.8. Relapsed AML bone marrow specimens showed higher ODC expression compared to initially diagnosed bone marrow specimens. Results from western blot studies and densitometry analysis of a panel of 22 initially diagnosed (11 shown above) and 12 relapsed specimens. The densitometry data of the ODC bands was normalized to the blast count.

3.4. Discussion

In this chapter, I addressed the question of whether expansion of the SORE6$^+$ CSL cells is a consistent finding for AML relapse. Using my *in-vitro* relapse model, IR cells treated with the optimal and suboptimal doses of four therapeutic agents/regimens were correlated with the expansion of the SORE6$^+$ CSL cell subset, traceable by molecular barcoding. The results generated are rather unexpected, since the expansion of SORE6$^+$ cells is highly dependent on the type of therapeutic agents employed; dosages did not appear to be key factor in this regard. The results are summarized in **Table 3.1**. Of the four treatments tested, expansion of SORE6$^+$ CSL cells was most pronounced with Ara-C. In contrast, the expansion of SORE6$^+$ CSL cells during IR was less pronounced with Ven and was not observed with the other 2 treatments (AZA and AZA+Ven). Thus, IR appears to be biologically heterogeneous. In one scenario, IR is characterized by an expansion of SORE6$^+$ CSL cells; in another scenario, IR is characterized by SORE6$^-$ cells. The former group also can be subdivided into two subgroups: the expansion of SORE6$^+$ cells with (i.e. Ven) or without (i.e. Ara-C) the persistence of SORE6$^-$ cells.

	CSL expansion during IR	IR pattern	Suppression of Myc	ODC expression	COMMENT
Ara-C	Yes	*In-vitro* remission reached when the optimal dose was used. IR reached earlier with suboptimal doses	No	Increased	SORE6$^-$ but not SORE6$^+$ cells killed effectively, and this correlates with a lack of Myc inhibition by Ara-C.
Ven	Partial expansion of SORE6$^+$ cells.	*In-vitro* remission reached when the optimal dose was used. IR reached earlier with suboptimal doses	No	Decreased	Partial effects on both SORE6$^-$ and SORE6$^+$ cells. There is evidence of SORE6$^-$ → SORE6$^+$ conversion during IR.
AZA	No	*In-vitro* remission reached when the optimal dose was used. IR reached relatively early with all doses	Weakly	Decreased	IR cells are mostly SORE6$^-$ cells. No evidence of expansion of SORE6$^+$ cells during IR, suggesting that AZA inhibits SORE6$^+$ better than SORE6$^-$ cells.
AZA +Ven	No	*In-vitro* remission reached when the optimal and suboptimal doses were used. IR reached only when at least 25% reduction of the dose	Strong suppression. FLT3 and STAT5 are also suppressed	No change	Excellent in suppressing SORE6$^+$ CSL cells.

Table 3.2 Summary of the inhibitory effect on SORE6$^-$ and SORE6$^+$ by the four treatments

The observation that CSL cell expansion is a prominent event during IR in the Ara-C group strongly suggests that Ara-C preferentially kills and/or severely damages the regenerative ability of the SORE6$^-$ bulk cells, whereas at least a subset of the SORE6$^+$ CSL cells is relatively untouched. To explain this possibility, the mode of action of Ara-C was reviewed. Cytarabine is a pyrimidine analog. Specifically, once it is converted into the triphosphate form within the cell, it

competes with cytidine to be incorporated into DNA (21). Once incorporated into DNA, the sugar moiety of Ara-C hinders DNA replication. Thus, this drug targets cells in S phase the most. Based on the cancer stem cell model, CSL cells are a contributing factor to relapse by virtue of their ability to reduce proliferation and achieve quiescence, enhance their DNA repair, and increase removal of drugs and toxic chemicals such as reactive oxygen species (22). Thus, it is perceivable that CSL cells in my *in-vitro* study model go into a quiescence state during the time of *in-vitro* remission, which typically last for over 10 days after the elimination of detectable viable cells (assessed by trypan blue). Indeed, as shown in Chapter 2*,* using flow cytometry, the number of viable cells was assessed during the approximately 10 days of zero viability, where 200-500 viable cells/mL were found, and this cell number remained relatively stable throughout this time period. This observation is in keeping with the quiescence concept.

Venetoclax, a Bcl-2 inhibitor, was proposed to treat AML partly because the anti-apoptotic protein Bcl-2 has been reported to be elevated in CSL cells in a few studies (23, 24). Nonetheless, in my *in-vitro* model, Venetoclax appears to have inhibitory effects on both SORE6$^-$ bulk cells and SORE6$^+$ CSL cells, but it is not sufficiently potent in eradicating either of them, as both cell subsets were represented in the IR cell population. In view of the observation that SORE6$^+$ cells were proportionally higher in IR than in the pre-treatment samples, a 'partial' SORE6$^+$ cell expansion must have occurred. Another interesting observation is that there was evidence of SORE6$^+$ to SORE6$^-$ conversion, since the % of GFP-positive cells remained to be approximately 30% while the proportions of SORE6$^+$ cells were approximately 70% by barcoding (**Figure 3.4d**).

AZA is designed to reverse epigenetic silencing of genes that otherwise can produce suppressors of leukemogenesis. It functions by being incorporated into RNA, hindering mRNA synthesis, and ultimately resulting in apoptosis (25). Since AZA targets an enzyme, the actual biochemical effects in individual cancer cells are variable, depending on the pre-treatment epigenetic landscape. Nonetheless, in one recent study using the multi-omics approach, the authors found that the cellular pathways most prominently impacted by AZA are shared by all 4 AML cell lines they examined, despite the observations that AZA induced diverse effects at the individual gene and protein level in these cell lines (26); these common effects are most common related to downregulation of metabolism and upregulation of immune defense. Since CSL cells have been shown to have

heightened metabolism, AZA may have inhibited SORE6^{+} CSL cells in my study model via downregulation of the metabolism.

Based on the discussion thus far, it is perceivable that AZA+Ven carries better therapeutic efficacy than Ven or AZA alone, since the combination likely can kill or severely injure CSL cell in my model by attacking both the Bcl-2 and the metabolic pathway. This combination of targeting may have explained the effective eradication of SORE6^{+} CSL cells. The combination of these drugs also may have exerted additive or synergistic effects on the inhibition of SORE6^{-} cells, and this may have explained the relatively long delay of the IR even at 25% reduction of the dosages.

Probably one of the most interesting questions that evolves from this study is related to the nature of SORE6^{-} cells responsible for IR in the AZA and AZA+Ven groups. I believe that there are at least two possibilities. In the first scenario, a very small subset of SORE6^{-} cells carry stem-like features, which are driven by proteins that escape the detection of the SORE6 reporter. I suspect that the implicated proteins may be other proteins involved in the maintenance of stemness, which can be detected if appropriate reporters are introduced into these cells. To test this possibility, future studies may involve transduction of additional reporters into SORE6^{-} cells, such as reporters for the Wnt canonical pathway. In another scenario, a very small subset of SORE6^{-} cells quickly acquire stemness which provide them with the ability to withstand the high level of chemoresistance and enter/exit a state of dormancy, two key features of disease relapse. Comparative studies of SORE6^{-} cells harvested at pre-treatment, immediately post-treatment, *in-vitro* remission, and IR will shed light into this question.

Lastly, I am rather surprised by the overall alignment among the pattern of IR, whether the expansion of SORE6^{+} CSL is involved, the efficiency of Myc inhibition, and the metabolomics/glycomics patterns in the 4 treatment groups. I believe that results from this study support the concepts that AML relapse is not a homogeneous disease, and it involves a number of relatively distinct molecular pathways. With further characterization, it might be possible that AML relapse is defined by the predominant metabolic pathways utilized for clonal expansion. These very metabolic pathways also might be directly or indirectly responsible for the other

distinctive phenotype displayed by the IR cells, such as their glycosylation patterns, which may in turn regulate their immune evasion.

3.5. References

1. Dohner H, Weisdorf DJ, Bloomfield CD. Acute Myeloid Leukemia. N Engl J Med. 2015;373(12):1136-52.
2. Tenold ME, Moskoff BN, Benjamin DJ, Hoeg RT, Rosenberg AS, Abedi M, et al. Outcomes of Adults With Relapsed/Refractory Acute Myeloid Leukemia Treated With Venetoclax Plus Hypomethylating Agents at a Comprehensive Cancer Center. Front Oncol. 2021;11:649209.
3. Vosberg S, Greif PA. Clonal evolution of acute myeloid leukemia from diagnosis to relapse. Genes Chromosomes Cancer. 2019;58(12):839-49.
4. Duy C, Li M, Teater M, Meydan C, Garrett-Bakelman FE, Lee TC, et al. Chemotherapy Induces Senescence-Like Resilient Cells Capable of Initiating AML Recurrence. Cancer Discov. 2021;11(6):1542-61.
5. Ho TC, LaMere M, Stevens BM, Ashton JM, Myers JR, O'Dwyer KM, et al. Evolution of acute myelogenous leukemia stem cell properties after treatment and progression. Blood. 2016;128(13):1671-8.
6. Ng SW, Mitchell A, Kennedy JA, Chen WC, McLeod J, Ibrahimova N, et al. A 17-gene stemness score for rapid determination of risk in acute leukaemia. Nature. 2016;540(7633):433-7.
7. Shlush LI, Mitchell A, Heisler L, Abelson S, Ng SWK, Trotman-Grant A, et al. Tracing the origins of relapse in acute myeloid leukaemia to stem cells. Nature. 2017;547(7661):104-8.
8. Tamamyan G, Kadia T, Ravandi F, Borthakur G, Cortes J, Jabbour E, et al. Frontline treatment of acute myeloid leukemia in adults. Crit Rev Oncol Hematol. 2017;110:20-34.
9. Zeidan AM, Pollyea DA, Borate U, Vasconcelos A, Potluri R, Rotter D, et al. Venetoclax plus azacitidine compared with intensive chemotherapy as induction for patients with acute myeloid leukemia: retrospective analysis of an electronic medical record database in the United States. Ann Hematol. 2023;102(4):749-54.

10. Jones CL, Stevens BM, D'Alessandro A, Reisz JA, Culp-Hill R, Nemkov T, et al. Inhibition of Amino Acid Metabolism Selectively Targets Human Leukemia Stem Cells. Cancer Cell. 2018;34(5):724-40 e4.
11. Pollyea DA, Stevens BM, Jones CL, Winters A, Pei S, Minhajuddin M, et al. Venetoclax with azacitidine disrupts energy metabolism and targets leukemia stem cells in patients with acute myeloid leukemia. Nat Med. 2018;24(12):1859-66.
12. Tang B, Raviv A, Esposito D, Flanders KC, Daniel C, Nghiem BT, et al. A flexible reporter system for direct observation and isolation of cancer stem cells. Stem Cell Reports. 2015;4(1):155-69.
13. Wassenberg D, Liebl W, Jaenicke R. Maltose-binding protein from the hyperthermophilic bacterium Thermotoga maritima: stability and binding properties. J Mol Biol. 2000;295(2):279-88.
14. DiNardo CD, Jonas BA, Pullarkat V, Thirman MJ, Garcia JS, Wei AH, et al. Azacitidine and Venetoclax in Previously Untreated Acute Myeloid Leukemia. N Engl J Med. 2020;383(7):617-29.
15. Seedhouse CH, Pallis M, Grundy M, Shang S, Russell NH. FLT3-ITD expression levels and their effect on STAT5 in AML with and without NPM mutations. Br J Haematol. 2009;147(5):653-61.
16. Pinz S, Unser S, Rascle A. Signal transducer and activator of transcription STAT5 is recruited to c-Myc super-enhancer. BMC Mol Biol. 2016;17:10.
17. Shantz LM, Pegg AE. Translational regulation of ornithine decarboxylase and other enzymes of the polyamine pathway. Int J Biochem Cell Biol. 1999;31(1):107-22.
18. Lin CL, Sojitra M, Carpenter EJ, Hayhoe ES, Sarkar S, Volker EA, et al. Chemoenzymatic synthesis of genetically-encoded multivalent liquid N-glycan arrays. Nat Commun. 2023;14(1):5237.
19. Pinho SS, Reis CA. Glycosylation in cancer: mechanisms and clinical implications. Nat Rev Cancer. 2015;15(9):540-55.
20. Walker MR, Goel HL, Mukhopadhyay D, Chhoy P, Karner ER, Clark JL, et al. O-linked alpha2,3 sialylation defines stem cell populations in breast cancer. Sci Adv. 2022;8(1):eabj9513.
21. Emadi A, Karp JE. The clinically relevant pharmacogenomic changes in acute myelogenous leukemia. Pharmacogenomics. 2012;13(11):1257-69.

22. Fajardo-Orduna GR, Ledesma-Martinez E, Aguiniga-Sanchez I, Mora-Garcia ML, Weiss-Steider B, Santiago-Osorio E. Inhibitors of Chemoresistance Pathways in Combination with Ara-C to Overcome Multidrug Resistance in AML. A Mini Review. Int J Mol Sci. 2021;22(9).
23. Tothova E, Fricova M, Stecova N, Kafkova A, Elbertova A. High expression of Bcl-2 protein in acute myeloid leukemia cells is associated with poor response to chemotherapy. Neoplasma. 2002;49(3):141-4.
24. Venditti A, Del Poeta G, Maurillo L, Buccisano F, Del Principe MI, Mazzone C, et al. Combined analysis of bcl-2 and MDR1 proteins in 256 cases of acute myeloid leukemia. Haematologica. 2004;89(8):934-9.
25. Aimiuwu J, Wang H, Chen P, Xie Z, Wang J, Liu S, et al. RNA-dependent inhibition of ribonucleotide reductase is a major pathway for 5-azacytidine activity in acute myeloid leukemia. Blood. 2012;119(22):5229-38.
26. Leung KK, Nguyen A, Shi T, Tang L, Ni X, Escoubet L, et al. Multiomics of azacitidine-treated AML cells reveals variable and convergent targets that remodel the cell-surface proteome. Proc Natl Acad Sci U S A. 2019;116(2):695-700.

Chapter 4

ULK2 is a key pro-autophagy protein that contributes to the high chemoresistance and disease relapse in *FLT3*-mutated AML

A version of this chapter has been published as:

Lai J, Yang C, Shang C, Chen W, Chu MP, Brandwein J, Lai R, Wang P. ULK2 Is a Key Pro-Autophagy Protein That Contributes to the High Chemoresistance and Disease Relapse in FLT3-Mutated Acute Myeloid Leukemia. Int J Mol Sci. 2024; 25(1):646.

4.1. Introduction

Acute myeloid leukemia (AML) is an aggressive hematologic malignancy carrying a 5-year overall survival rate of only 30% (1). Chemoresistance, which contributes to the development of refractory and relapsed diseases, remains to be a significant challenge in the treatment of AML patients. Refractory disease, typically defined by a failure to induce complete remission, occurs in approximately 30% of patients who are treated with a curative intent (2). Relapsed disease, typically defined by disease recurrence after a period of complete remission, occurs in approximately 50% of patients treated with a curative intent (3). The mechanisms underlying AML relapse remain to be elusive, partly due to a lack of appropriate *in-vitro* study models. Nonetheless, one of the hypotheses is that a very small proportion of treatment-resistant cells survive the initial chemotherapy, and after a period of remission, these cells provide the seeds for the return of full-blown disease. Accumulating evidence has suggested that this small cell subset is enriched with cancer stem cells or cancer stem-like (CSL) cells. In this regard, a few prior studies have shown that CSL cells have significantly higher drug resistance compared to bulk cancer cells (4, 5). Our group has recently studied the role of CSL cells in AML relapse using the SORE6 reporter. We detected/purified a small subset of SORE6$^+$ cells in two *FLT3*-mutated AML cell lines and found that SORE6$^+$ cells have significantly higher CSL phenotype than the bulk SORE6$^-$ cells. Leveraging this SORE6$^-$/SORE6$^+$ dichotomy, we developed an *in-vitro* AML relapse model, in which Ara-C treatment could induce a stage of '*in-vitro* remission, where no viable cells could be identified using trypan blue, and this stage was eventually followed by regeneration of AML cells. Importantly, the regenerated cells were found to be enriched in SORE6$^+$ cells, a finding that is supportive of the role of CSL cells in AML relapse (6).

The mechanisms underlying the high chemoresistance in CSL cells are incompletely understood, although there have been several possibilities suggested, including the upregulation of transporters (e.g. MDR1) to export cytotoxic drugs (7) and that of anti-apoptotic proteins such as Bcl-2 (8). More recently, much attention was given to heightened macro-autophagy (hereafter referred to as "autophagy") in CSL cells as a key mechanism of chemoresistance. Autophagy, a process whereby intracellular components are degraded and recycled, has been shown to be cytoprotective in cancer cells. There is also accumulating evidence that autophagy is closely linked to cancer stemness.

Specifically, a study using ovarian cancer cells showed that inhibition of autophagy using chloroquine or ATG5 knockout effectively decreased the CSL features, including spheroid formation, tumorigenicity, and the expression of stem cell markers Sox2, Nanog, and Oct4, in a small cell subset characterized by the $CD188^{+}CD44^{+}$ immunophenotype (9). Additionally, AML CSL cells, defined as $CD34^{+}/ROS^{low}$, have been shown to have elevated autophagy compared to $CD34^{+}/ROS^{high}$ cells, and inhibition of autophagy in AML CSL cells resulted in decreased engraftment in mice (10). In another AML study, CSL cells, defined as $CD34^{+}CD38^{-}$, were shown to have heightened autophagy and increased chemoresistance upon treatment with JQ1, an epigenetic modifying agent proposed to treat AML (11). In view of the new evidence supporting a link between autophagy and AML CSL cells, we asked if autophagy contributes to the high chemoresistance in $SORE6^{+}$ cells and the *in-vitro* relapse in our AML study model. If so, it might be possible to utilize our *in-vitro* model to decipher the molecular events underlying the heightened autophagic response in the $SORE6^{+}$ CSL cells.

In this study, we aimed to decipher the role of autophagy in the chemoresistance of CSL cells and 'in vitro relapse', and to use our study model to explore the mechanisms underlying the autophagy-mediated chemoresistance and 'in vitro relapse' of $SORE6^{+}$ cells. We first determined that there is a significantly higher chemotherapy-induced autophagic response in $SORE6^{+}$ cells, as compared to $SORE6^{-}$ cells. Using chloroquine, an autophagy inhibitor, we found evidence that the heightened autophagic response in $SORE6^{+}$ cells directly contributes to their higher chemoresistance and their relatively efficient regeneration in our *in-vitro* model. Using an autophagy pathway-specific array, we then identified ULK2 as the key molecule underlying the enhanced autophagy response in $SORE6^{+}$ cells.

4.2. Materials and Methods

4.2.1. Generation of $SORE6^{-}$ and $SORE6^{+}$ cell subsets

$SORE6^{-}$ and $SORE6^{+}$ cell subsets were generated for two *FLT3*-mutated cell lines, MOLM-13 (CVCL_2119; DSMZ, Braunschweig, Germany) and MV4-11 (CVCL_0064; ATCC, Manassas, VA, USA). Cell lines underwent lentiviral transduction with the SORE6-mCMVo-dsCop-GFP-

PURO (SORE6) reporter (National Cancer Institute, NIH, Bethesda, MD, USA) [45]. SORE6 activity, detectable by green fluorescent protein (GFP) expression, was assessed using flow cytometry. SORE6$^-$ and SORE6$^+$ subsets were purified using a flow cytometric cell sorter (Sony MA900, Sony Biotechnology, San Jose, CA, USA) based on their GFP expression. All cells transduced with the SORE6 reporter were cultured in RPMI 1640 media supplemented with 10% fetal bovine serum in the presence of 0.25 μg/mL puromycin.

4.2.2. Antibodies and drug treatments

Primary antibodies used in western blot studies included anti-LC3B antibody (#L7543) from Sigma-Aldrich (Burlington, MA, USA), anti-MYC (Y69, #ab32072) from Abcam (Cambridge, MA, USA), anti-ULK1 (D8H5, #8054) from Cell Signaling Technology (Danvers, MA, USA), anti-ULK2 (#PA5-22173) from ThermoFisher Scientific (Waltham, MA, USA), and anti-β-actin (#sc-47778) from Santa Cruz Biotechnology (Santa Cruz, CA, USA). MRT68921 (#S7949), chloroquine (#S6999), and Ara-C (U-19920A, #S1648) were purchased from Selleckchem (Houston, TX, USA). IRDye 800CW goat anti-rabbit IgG (#926-32213, 1:40000) and anti-mouse IgG (#926-32212, 1:40000) were used as the secondary antibody (LI-COR Biosciences, Lincoln, NE, USA).

4.2.3. Western blot

Cell pellets were lysed with RIPA buffer (MilliporeSigma, Burlington, MA, USA), with protease and phosphatase inhibitors (MilliporeSigma). Proteins were separated on a 10-15% polyacrylamide SDS-PAGE gel, transferred to a nitrocellulose membrane (GE Healthcare, Velizy-Villacoublay, France), and then incubated with primary antibodies. The membrane was then incubated with horseradish peroxidase-conjugated secondary antibodies. Bands were visualized with an Odyssey® Infrared Imaging System (LI-COR, Lincoln, NE, USA).

4.2.4. Autophagy assay red detection kit

Cells were incubated with autophagy probe dye (BioRad, Hercules, CA, USA) for 30 minutes at room temperature. The fluorescence from the dye was detected by flow cytometry using BD LSRFortessa X-20 (BD, Franklin Lakes, NJ, USA) as indicated by the manufacturer.

4.2.5. Cell viability assay

Cells were plated with a concentration of 250,000 cells/mL using media with 5% fetal bovine serum in 24-well plates. Cell viability was assessed using trypan blue exclusion. Viable cells, defined as trypan blue-negative cells, were counted by direct microscopic examination. IC50 was calculated by GraphPad Prism software (GraphPad Software, San Diego, CA, USA).

4.2.6. RNA extraction and quantitative real-time polymerase chain reaction

RNA was extracted from cell lines using the RNeasy Plus Mini Kit (Qiagen, Valencia, CA, USA) as indicated by the manufacturer's protocol. cDNA conversion of RNA was performed with the High Capacity cDNA Reverse Transcription Kit (Invitrogen, Waltham, MA, USA). Quantitative real-time polymerase chain reaction (qRT-PCR) was done using the Power SYBR™ Green Master Mix (ThermoFisher Scientific, Waltham, MA, USA) with the following primers: ULK1 F-5-CCTCGCCAAGTCTCAGACGC-3 & R-5-CCCCACCGTTGCAGTACTCC-3; ULK2 F-5-CTCCTCAGGTTCTCCAGTGC-3 & R-5-TTGGTGGGAGAAGTTCCAAG-3; GAPDH F-5-GGAGCGAGATCCCTCCAAAAT-3 & R-5-GGCTGTTGTCATACTTCTCATGG-3. The PCR reactions were quantified using the QuantStudio™ 5 (ThermoFisher Scientific). Gene expression was normalized to GAPDH expression.

4.2.7. Autophagy PCR array

cDNA used for the autophagy array was generated as described above (Section 4.2.6). The RT2 Profiler™ PCR Human Autophagy Array (PAHS-084Z, Qiagen, Germantown, MD, USA) was

employed as indicated by the manufacturer to analyze gene expression in 84 autophagy related genes.

4.2.8. *In-vitro* AML relapse model

We have generated an *in-vitro* model for disease relapses previously (6). Cells were plated to a concentration of 150,000 cells/mL and were treated with 500 nM Ara-C for two days, which induced '*in-vitro* remission,' defined by the absence of trypan blue-negative cells. After two days of treatment, media without Ara-C was added to the culture. To detect regeneration, 200 µL of the cell culture was removed for trypan blue cell counting every two days, and the cell culture was replenished with 200 µL of fresh culture media. The end of the experiment was arbitrarily set as day 32, and if no viable cells were detected at this point, the cells were considered to be unable to regenerate.

4.2.9. Patient samples

Two bone marrow aspirates representing the initial diagnostic sample as well as the relapse samples from two *FLT3*-mutated AML patients were retrieved retrospectively from the University of Alberta Hospital. The use of these patient samples was approved by the Health Research Ethics Board of Alberta (HREBA.CC-21-0253_REN1; date of approval July 7, 2022).

4.2.10. Statistical analysis

Statistical analyses were performed using GraphPad Prism 8 (Graphpad Software Inc. La Jolla, Ca, USA). P-values were calculated using two-tailed Student's t-test.

4.3. Results

4.3.1. SORE6$^+$ cells exhibited higher autophagy flux than SORE6$^-$ cells

We recently found that purified SORE6$^+$ cells derived from MOLM-13 and MV4-11, two AML cell lines carrying *FLT3*-ITD, displayed significantly higher CSL phenotype (such as resistance to Ara-C) compared to SORE6$^-$ cells (Chapter 2). Using SORE6$^-$/SORE6$^+$ cells derived from MOLM-13, the Ara-C inhibitory concentration at 50% (IC50) for SORE6$^+$ cells was 172.9 nM, which is significantly higher than that of their SORE6$^-$ counterparts (61.0 nM, p<.0001) (**Figure 4.1a**). Similar results were obtained when SORE6$^+$/SORE6$^-$ cells derived from MV4-11 were used (61.8 versus 29.0 nM, p<.001).

Since autophagy has been shown to contribute to chemoresistance in cancer cells, we asked whether the autophagic flux in SORE6$^+$ cells is higher than that in SORE6$^-$ cells. To assess the autophagy response, we employed western blots to quantify the LC3-II:LC3:I protein ratio before and after Ara-C treatment. SORE6$^-$/SORE6$^+$ cells derived from MOLM-13 were used initially. In the presence of chloroquine, SORE6$^+$ cells derived from MOLM-13 showed substantially higher accumulation of LC3-II than SORE6$^-$ cells. In a triplicate experiment, densitometric quantification of the LC3-II and LC3-I bands revealed that SORE6$^+$ cells exhibited a mean of 2.1-fold increase in the LC3-II:LC3-I ratio upon treatment of 5 nM of Ara-C for 24 hours (p=.02), whereas the same treatment did not induce any significant change in SORE6$^-$ cells (**Figure 4.1b**). Similar results were obtained when 10 nM of Ara-C was used. To substantiate these observations, we also measured the autophagic response using a fluorescence signal-based assay. As shown in **Figure 4.1c**, treatment with Ara-C at 5 or 10 nM induced significantly higher autophagy in SORE6$^+$ cells compared to SORE6$^-$ cells. These experiments were then repeated by using SORE6$^-$/SORE6$^+$ cells derived from MV4-11, and similar results were obtained.

4.3.2. Inhibition of autophagy sensitizes SORE6$^+$ cells to Ara-C

We then asked if autophagy directly contributes to the higher chemoresistance in SORE6$^+$ cells. As shown in **Figure 4.2a**, addition of chloroquine significantly decreased the IC50 from 179.3 to

57.5 nM (p=.009). In contrast, chloroquine treatment did not significantly change the IC50 in SORE6$^-$ cells. Similar results were observed with SORE6$^-$/SORE6$^+$cells derived from MV4-11, with the Ara-C IC50 in SORE6$^+$ cells decreasing from 65.1 to 14.6 nM when chloroquine was added (p<.0001), while no significant decrease in the IC50 of SORE6$^-$ cells was observed with the addition of chloroquine.

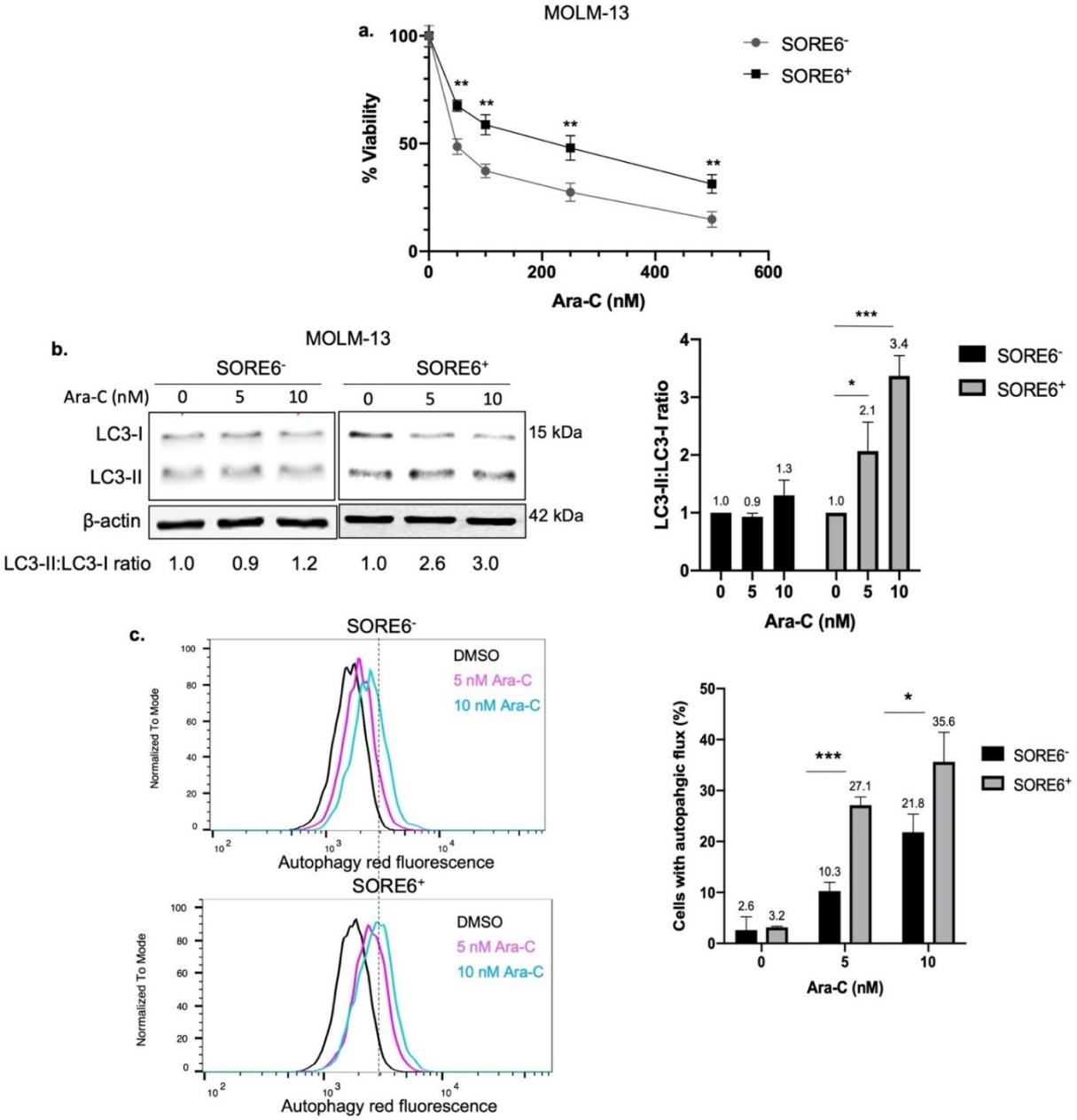

Figure 4.1. SORE6$^+$ cells exhibited higher autophagic flux in response to Ara-C. (a) Cell viability of MOLM-13 SORE6$^-$ and SORE6$^+$ cells after treatment with increasing doses of Ara-C for 24 hours. Cell viability was assessed using trypan blue and was performed in triplicates. (b) Western blots of LC3 in MOLM-13 SORE6$^-$ and SORE6$^+$ cells after treatment with 0, 5, or 10 nM of Ara-C, with 10 μM of chloroquine for 24 hours. LC3-II and LC3-I bands were quantified by densitometry analysis using ImageJ. Data from three independent experiments are shown in the bar graph. (c) Flow cytometric analysis of MOLM-13 SORE6$^-$ and SORE6$^+$ cells subjected to the Autophagy Assay Red Detection Kit after treatment with 0, 5, or 10 nM of Ara-C for 24 hours. Data shown as mean ± standard deviation. P-value calculated using a student's *t*-test, where *p<.05, **p<.01, ***p< .001.

4.3.3. Inhibition of autophagy prolongs time to *in-vitro* relapse

We have recently generated an *in-vitro* model with features mimicking AML relapse (Chapter 2). Specifically, an '*in-vitro* remission' state, defined by the absence of trypan blue-negative cells induced by the lowest dose of Ara-C on three independent observations, is followed by regeneration of AML cells (i.e. *in-vitro* relapse) after a period of time. In this model, the regenerated cells are highly enriched with SORE6$^+$ cells, suggesting these CSL cells are the major contributors to the '*in-vitro* relapse'. Given our findings that autophagy protects SORE6$^+$ cells from Ara-C treatment, we asked if autophagy contributes to the '*in-vitro* relapse'. As illustrated in **Figure 4.2b**, inhibition of autophagy using chloroquine significantly increased the duration of '*in-vitro* remission'. Specifically, treatment with chloroquine in combination with Ara-C increased the time for cells to regenerate in a dose-dependent manner, i.e. reach pre-treatment levels of viability, from 14 days when treated with Ara-C alone to 18 days when treated with Ara-C combined with 20 μM chloroquine and 28 days when treated with Ara-C combined with 50 μM chloroquine.

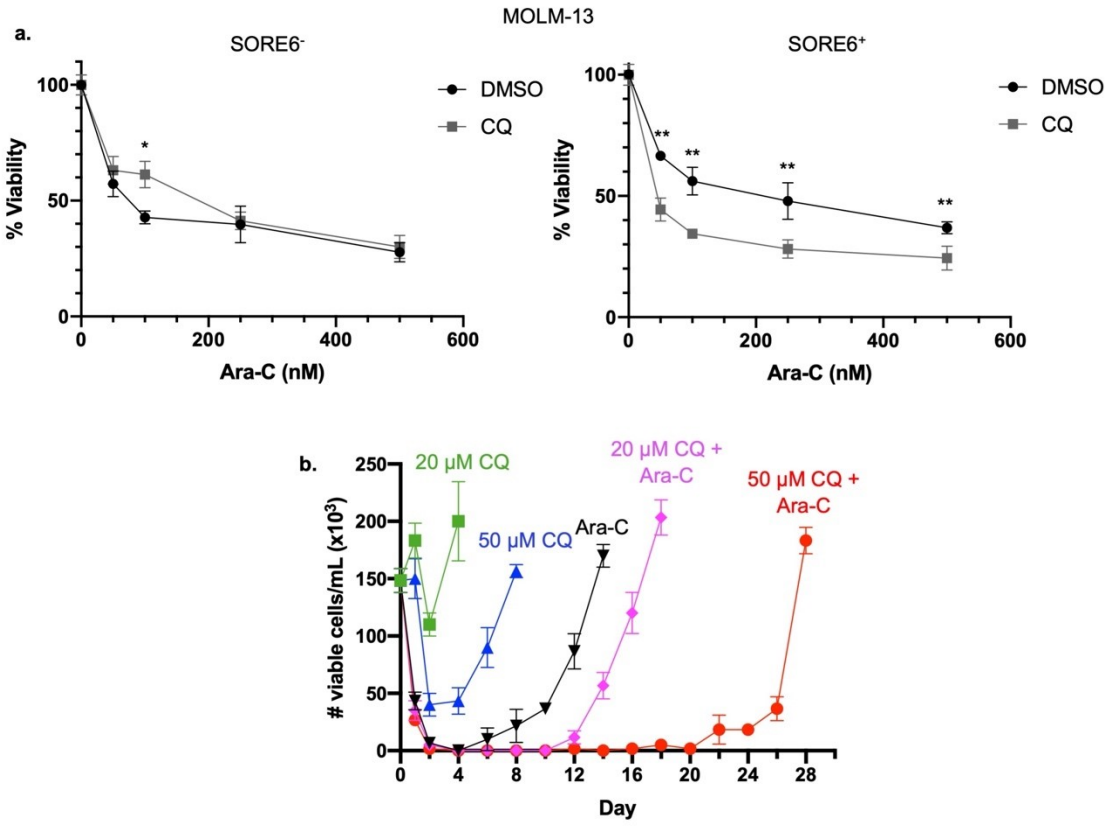

Figure 4.2. Inhibiting autophagy sensitizes SORE6$^+$ cells to Ara-C treatment. (a) Cell viability of MOLM-13 SORE6$^-$ and SORE6$^+$ cells subjected to increasing doses of Ara-C, with or without 10 µM of chloroquine, for 24 hours. Cell viability, assessed by trypan blue, was normalized to cells treated with DMSO, and three independent experiments were performed. Data reported as mean ± standard deviation. * denotes $p<.05$, ** $p<.01$, student's *t* test. (b) Cell viability assessed by trypan blue in MV4-11 cells subjected to the *in-vitro* relapse model treated with 500 nM Ara-C alone, 20 or 50 µM CQ alone, or combination of Ara-C + 20 or 50 µM CQ.

4.3.4. ULK2 is a key regulator of the autophagy flux in SORE6$^+$ cells

To decipher the molecular basis underlying the relatively high autophagy capacity of SORE6$^+$ cells, we employed a commercially available oligonucleotide array that includes 84 autophagy-related genes. We first identified the differential gene expression in both SORE6$^-$ and SORE6$^+$

cells before and after they were treated with 10 nM of Ara-C, a level with which we observed a substantial difference in the autophagy response between these two cell subsets. We then compared the gene lists from the two cell subsets. We found that *ULK2* was the most differentially expressed gene between SORE6$^+$ and SORE6$^-$ cells after Ara-C treatment, with 13.4-fold higher expression in Ara-C treated SORE6$^+$compared to SORE6$^-$ cells. The full list of analyzed genes and fold up- and down-regulation between untreated and Ara-C treated subsets is shown in **Table 4.1.**

In view of the known importance of ULK1, a homologue of ULK2, in the autophagy pathway (12), and our finding that *ULK2* is the most differentially expressed gene between the two cell subsets treated with Ara-C, we focused the remainder of this study on ULK2. Firstly, we validated the upregulation of *ULK2* induced by Ara-C using quantitative RT-PCR. Since ULK1 and ULK2 have been shown to have substantial structural similarities and functional redundancy, we included ULK1 for comparison. As shown in **Figure 4.3a**, after subjecting SORE6$^-$/SORE6$^+$ cells derived from MOLM-13 to 10 nM of Ara-C for 24 hours, *ULK2* expression was found to be significantly higher in SORE6$^+$ cells (mean = 5.3 fold, p=.02). In comparison, no significant change in *ULK2* expression was observed in SORE6$^-$ cells. The expression of *ULK1* was also found to be significantly increased in SORE6$^+$ cells, although the increment was relatively small (i.e. 2.1-fold) compared to that of *ULK2* (i.e. 5.3-fold).

We then performed western blot to analyze ULK1/2 protein expression in SORE6$^-$/SORE6$^+$ cells at steady state and after treatment with Ara-C. As shown in **Figure 4.3b**, ULK2 was substantially higher in SORE6$^+$ cells at steady state, whereas no substantial differences were observed in ULK1. As illustrated in **Figure 4.3c**, we found that ULK2 was substantially upregulated in SORE6$^+$ cells treated with 10 nM Ara-C. In contrast, ULK2 was not appreciably changed in SORE6$^-$ cells treated with Ara-C. Changes in ULK1 induced by Ara-C in both cell subsets were relatively minimal. Taken together, these findings have highlighted the Ara-C-induced upregulation of ULK2, but not ULK1, suggesting that ULK2 might be a key contributor to the preferentially robust autophagy response in SORE6$^+$ cells. Similar experiments were performed in MV4-11 cells, and similar findings were made.

SORE6$^+$/SORE6$^-$ No Ara-C		SORE6$^+$/SORE6$^-$ With 10 nM Ara-C	
Gene	**Fold Up- or Down-Regulation**	**Gene**	**Fold Up- or Down-Regulation**
ESR1	10.90	***ULK2***	13.90
FAS	9.19	*INS*	9.03
PTEN	9.08	*SNCA*	8.37
SNCA	8.55	*IFNG*	7.89
MAPK14	8.47	*APP*	7.61
APP	8.07	*TMEM74*	7.20
IFNG	7.26	*DAPK1*	5.03
CTSS	6.83	*TGM2*	4.37
ATG10	6.79	*IGF1*	3.42
BNIP3	6.76	*ESR1*	3.41
MAP1LC3B	6.73	*ATG9B*	3.15
TMEM74	6.65	*BNIP3*	2.51
AKT1	6.62	*CTSS*	2.44
DAPK1	6.26	*MAP1LC3A*	2.25
ULK2	5.67	*ATG10*	2.15
INS	5.09	*RAB24*	2.14
TGM2	5.04	*PIK3R4*	1.99
CDKN2A	4.60	*BAK1*	1.87
RAB24	4.19	*HTT*	1.76
ATG9B	4.01	*ATG16L2*	1.69
CTSB	3.90	*CTSD*	1.68
MTOR	3.76	*SQSTM1*	1.67
GABARAPL2	3.51	*NFKB1*	1.60
MAP1LC3A	3.28	*HSPA8*	1.56
BAK1	3.26	*EIF4G1*	1.55
PIK3R4	3.10	*GABARAPL1*	1.51
MAPK8	3.02	*DRAM1*	1.48
ATG7	2.89	*AMBRA1*	1.46
HSP90AA1	2.35	*UVRAG*	1.46
BID	2.32	*MAPK14*	1.46
ATG4B	2.25	*CTSB*	1.45
HSPA8	2.09	*GAA*	1.44
IGF1	2.06	*BCL2L1*	1.43
EIF4G1	2.04	*RPS6KB1*	1.42
ATG12	1.99	*TGFB1*	1.42
CASP8	1.98	*NPC1*	1.41
ATG5	1.94	*CASP8*	1.41

EIF2AK3	1.87	*IRGM*	1.41
AMBRA1	1.87	*LAMP1*	1.40
BCL2L1	1.79	*PIK3C3*	1.40
DRAM1	1.70	*ATG4C*	1.37
RPS6KB1	1.65	*PRKAA1*	1.37
GABARAPL1	1.63	*HSP90AA1*	1.36
WIPI1	1.62	*HDAC1*	1.36
PRKAA1	1.51	*BECN1*	1.35
ATG16L1	1.51	*ATG4B*	1.34
ATG16L2	1.50	*ATG7*	1.34
PIK3C3	1.49	*MAP1LC3B*	1.34
CASP3	1.49	*PIK3CG*	1.33
PIK3CG	1.41	*PTEN*	1.33
FADD	1.38	*MTOR*	1.32
IRGM	1.37	*ATG16L1*	1.30
NPC1	1.35	*TP53*	1.29
ATG4D	1.33	*ATG9A*	1.29
HTT	1.30	*CLN3*	1.28
SQSTM1	1.30	*EIF2AK3*	1.26
ATG3	1.28	*FADD*	1.25
NFKB1	1.22	*ATG5*	1.25
ATG4C	1.20	*TNFSF10*	1.24
BECN1	1.17	*HGS*	1.22
DRAM2	1.14	*WIPI1*	1.21
GAA	1.14	*GABARAPL2*	1.20
ATG4A	1.14	*CASP3*	1.20
BAD	1.10	*ATG12*	1.19
CXCR4	1.09	*ATG4A*	1.18
TP53	1.08	*ULK1*	1.16
UVRAG	1.08	*HDAC6*	1.14
HDAC1	1.07	*BID*	1.13
RB1	1.06	*RB1*	1.12
HDAC6	1.01	*MAPK8*	1.07
BAX	-1.02	*BCL2*	1.07
LAMP1	-1.03	*AKT1*	1.06
ULK1	-1.08	*CXCR4*	1.06
CLN3	-1.08	*BAX*	1.05
CTSD	-1.14	*DRAM2*	1.05
ATG9A	-1.15	*ATG3*	1.05
TNFSF10	-1.21	*BAD*	1.02
GABARAP	-1.26	*RGS19*	1.01

CDKN1B	-1.33	*ATG4D*	-1.02
BCL2	-1.35	*CDKN1B*	-1.02
TGFB1	-1.35	*GABARAP*	-1.03
HGS	-1.36	*TNF*	-1.42
RGS19	-1.38	*CDKN2A*	-1.46
TNF	-1.42	*FAS*	-3.32

Table 4.1. List of differential gene expression for all genes analyzed by the oligonucleotide array. The fold up- and down- regulation is indicated for MOLM-13 SORE6^{+} compared to SORE6^{-} cells, with and without Ara-C treatment.

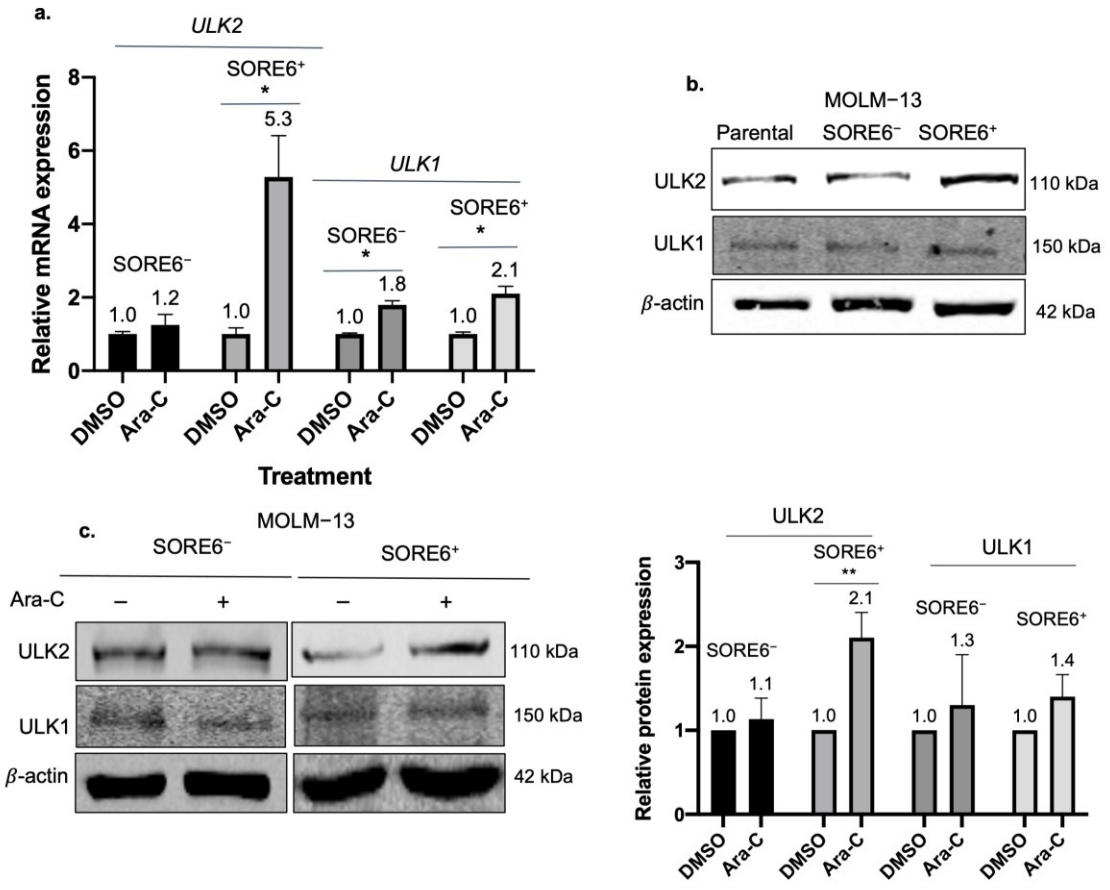

Figure 4.3. ULK2 is significantly upregulated after Ara-C treatment in SORE6$^+$ cells. (a) Gene expression level of *ULK2* or *ULK1* in MOLM-13 SORE6$^-$ and SORE6$^+$ cells after Ara-C treatment for 24 hours, normalized to cells treated with DMSO. Data reported as mean ± standard deviation (triplicate experiments). * denotes $p< 0.05$, ** denotes $p<.01$, student's *t* test. (b) Western blot analysis of ULK2 and ULK1 in MOLM-13 parental cells and SORE6$^-$ and SORE6$^+$ cell subsets at steady state. (c) Western blot analysis of ULK2 and ULK1 in MOLM-13 SORE6$^-$ and SORE6$^+$ subsets after treatment with 10 nM Ara-C for 24 hours, as compared to DMSO treatment. Data from three independent experiments are shown in graph.

4.3.5. ULK2 inhibition sensitizes SORE6$^+$ cells to Ara-C treatment

We further evaluated whether ULK2 plays a direct role in conferring the higher Ara-C resistance and autophagy flux in SORE6$^+$ cells. ULK1/2 activity was inhibited by using the pharmacologic agent MRT68921 (13). As shown in **Figure 4.4a**, the expression of ULK2 was dramatically decreased by MRT68921 in a dose-dependent manner. As shown in **Figure 4.4b**, pharmacological inhibition of ULK2 in SORE6$^+$ cells derived from MOLM-13 led to a significant reduction in their IC50 to Ara-C (194.0 to 88.0 nM, p=.003). In contrast, the same treatment did not significantly change the IC50 in SORE6$^-$ cells.

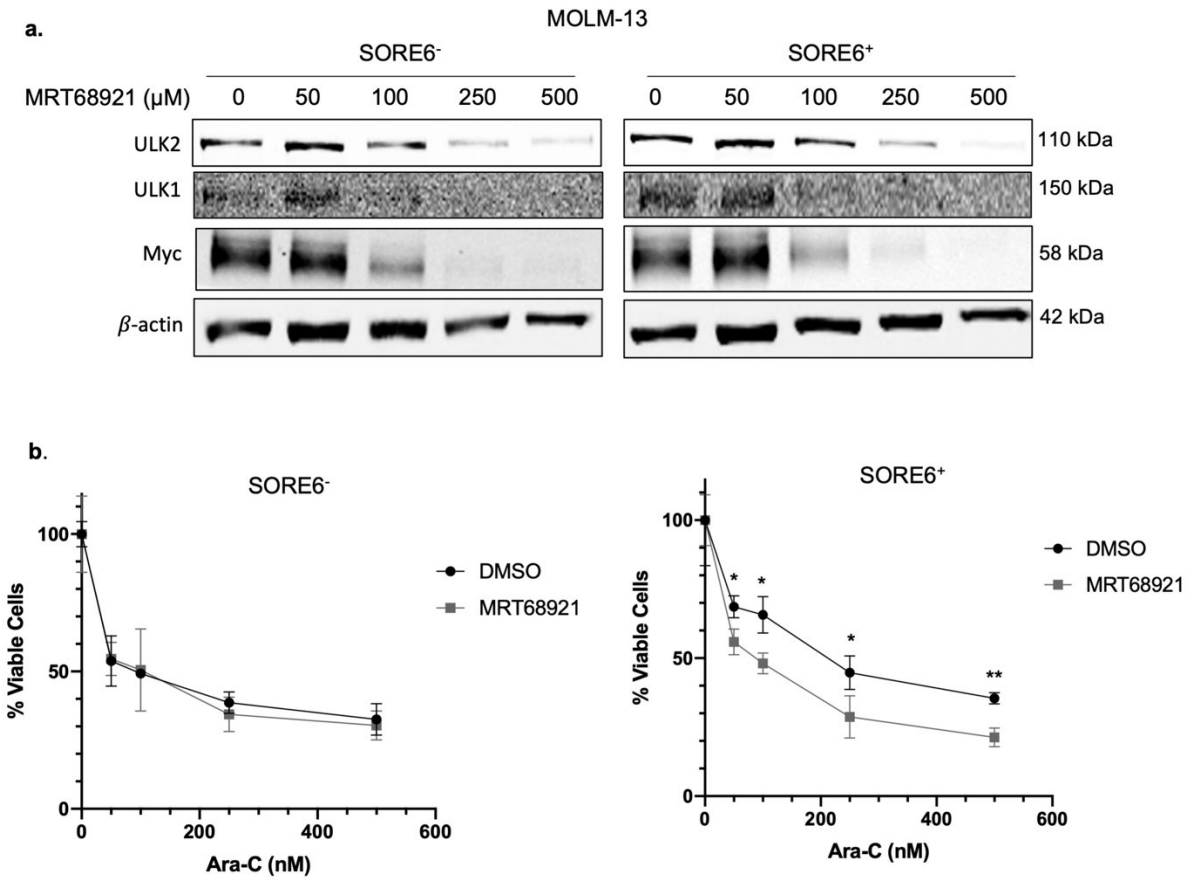

Figure 4.4. ULK1/2 inhibition sensitizes SORE6$^+$ cells to Ara-C treatment. (a) Western blot analysis of ULK2, ULK1 and Myc in SORE6$^-$ and SORE6$^+$ cells derived from MOLM-13 after treatment with 50-500 nM MRT68921 for 24 hours. (b) Cell viability of SORE6$^-$ and SORE6$^+$ subsets derived from MOLM-13 after treatment with 0, 50, 100, 250 or 500 nM Ara-C, either in the presence of 250 nM MRT68921 or DMSO, for 24 hours. Cell viability was normalized to the DMSO treatment group. Data is reported as mean ± standard deviation (triplicate experiments). *p<0.05, **p<0.01, student's t test.

4.3.6. ULK2 and Myc form a positive feedback loop

Since we recently found that the differential protein expression of Myc is a regulator of the phenotype of SORE6$^+$ cells (Chapter 2) we asked if the expression level of ULK2 is regulated by Myc. As shown in **Figure 4.5a**, pharmacological inhibition of Myc with 10058-F4 resulted in an appreciable decrease in the protein expression of ULK2. These results may explain the preferential high expression of ULK2 in SORE6$^+$ cells, since the high Myc protein level in these cells may directly contribute to the upregulation of ULK2. Similarly, knockdown of *Myc* using shRNA showed a dramatic decrease in ULK2 expression in SORE6$^+$ cells (**Figure 4.5b**).

As shown in **Figure 4.4a**, inhibition of ULK2 using MRT68921 substantially decreased Myc protein expression. In keeping with the concept that Myc is a key driver of the SORE6 activity in SORE6$^+$ cells, inhibition of ULK2 activity using MRT68921 in SORE6$^+$ cells showed a significant decrease in %SORE6$^+$ cells in a dose-dependent manner, from 94.0±4.2 to 78.5±2.5% when treated with 100 nM, 55.2±2.8% when treated with 250 nM, 46.6±5.1% when treated with 500 nM, and 41.3±1.8% when treated with 1000 nM (**Figure 4.5c**). Taken together, these results suggest that ULK2 and Myc form a positive feedback loop in *FLT3*-mutated AML cells.

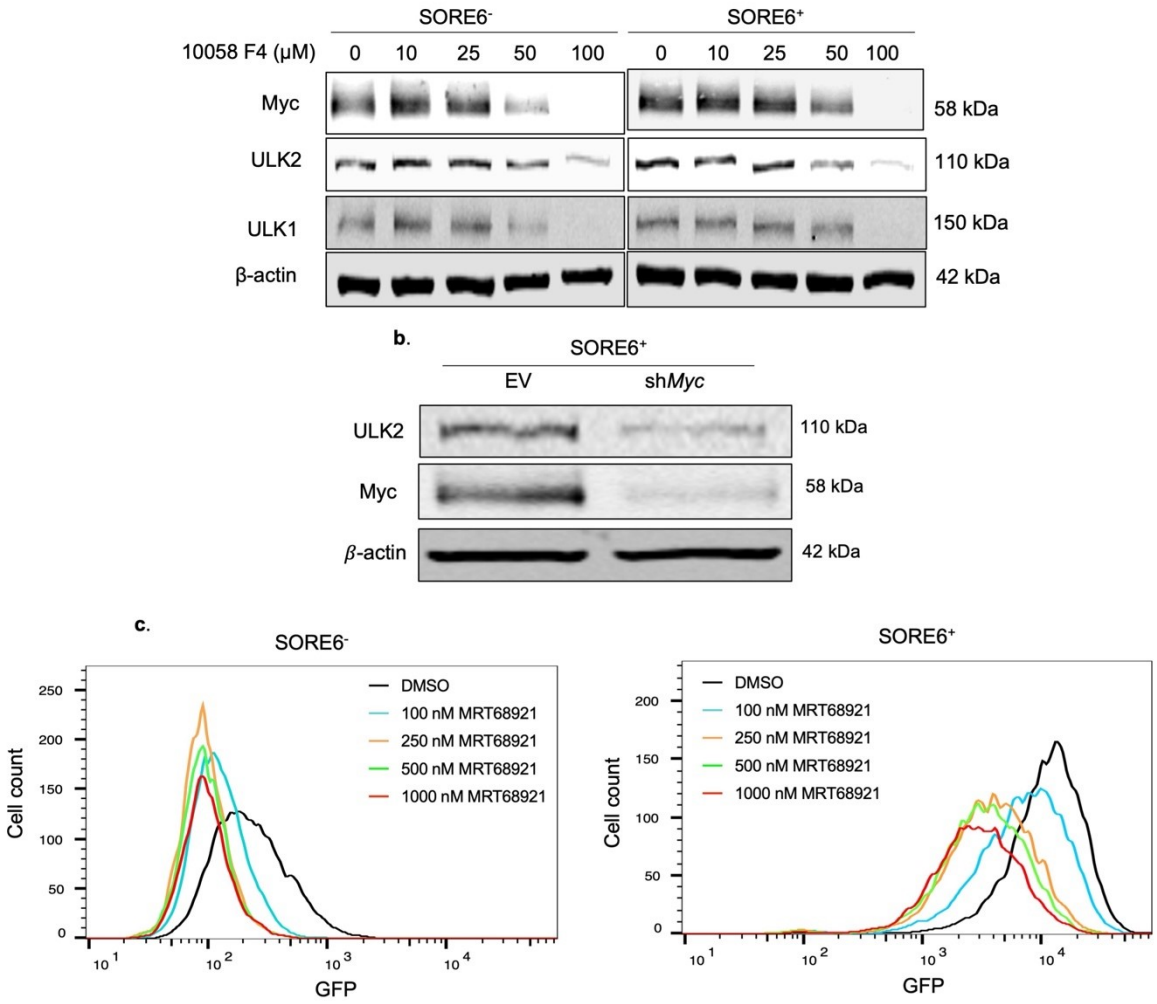

Figure 4.5. ULK2 and Myc form a positive feedback loop. (a) Western blot analysis of Myc, ULK2 and ULK1 in MOLM-13 SORE6$^-$ and SORE6$^+$ subsets after treatment with 10-100 μM of 10058-F4 for 24 hours. (b) Western blot analysis of ULK2 and Myc in MOLM-13 SORE6$^+$ cells transduced with shMyc or an empty vector (EV). (c) GFP levels, assessed by flow cytometry, of MOLM-13 SORE6$^+$ cells treated with increasing doses of MRT68921 for 24 hours.

4.3.7. ULK2 is critical for the regeneration of Ara-C treated cells

In light of our evidence that ULK2 is a key regulator of autophagic-induced chemoresistance of SORE6$^+$ cells, we asked if ULK2 plays an important role in the *in-vitro* relapse model. Firstly, we

examined the protein expression of ULK2 in MV4-11 regenerated cells. Cells pooled in a 9:1 ratio of SORE6$^-$:SORE6$^+$ subsets were subjected to Ara-C treatment. The cells achieved *in-vitro* relapse (IR) (i.e. achieved the same number of viable cells present at the start of the experiment) 14 days after reaching the '*in-vitro* remission'. As shown in **Figure 4.6a**, there was a substantial increase in ULK2 protein level in IR cells compared to cells collected pre-treatment, while no change was observed in ULK1.

Since ULK2 was elevated in IR cells, we asked whether inhibition of ULK2 would impede IR. We repeated our *in-vitro* relapse model with the ULK1/2 inhibitor MRT68921 in addition to Ara-C treatment. This combination treatment prevented IR, and no viable cells were detected at the end of the experiment, which was arbitrarily set at 32 days after the start of the experiment. In comparison, cells treated with Ara-C alone or MRT68921 alone both reached a pre-treatment level of viability 16-20 days after the start of the experiment (**Figure 4.6b**). Similar results were observed in MOLM-13 cells.

Given that ULK2 appears to be important in maintaining SORE6$^+$ cells, but not SORE6$^-$ cells, we asked whether IR cells regenerated from MRT68921 treatment alone were enriched with SORE6$^-$ cells. As shown in **Figure 4.6c**, IR cells after MRT68921 treatment were composed entirely of SORE6$^-$ cells. In contrast, IR cells after Ara-C treatment were enriched with SORE6$^+$ cells, consistent with our previous results. This finding may explain why IR was inhibited by combining MRT68921, as it targets the SORE6$^+$ cell subset, which is the major culprit of relapse in our *in-vitro* relapse model.

4.3.8. Relapsed bone marrow samples express higher ULK2 compared with initially diagnosed specimens

Given that a high expression of ULK2 was found to be important in the *in-vitro* relapse, we compared the expression of ULK2 in AML patient samples before treatment and at relapse. By western blot studies of bone marrow samples from the initially diagnosed and relapsed specimens from the same patient (n=2), we found that ULK2 was higher in the relapsed samples, after the normalization for the blast count was performed (**Figure 4.7**).

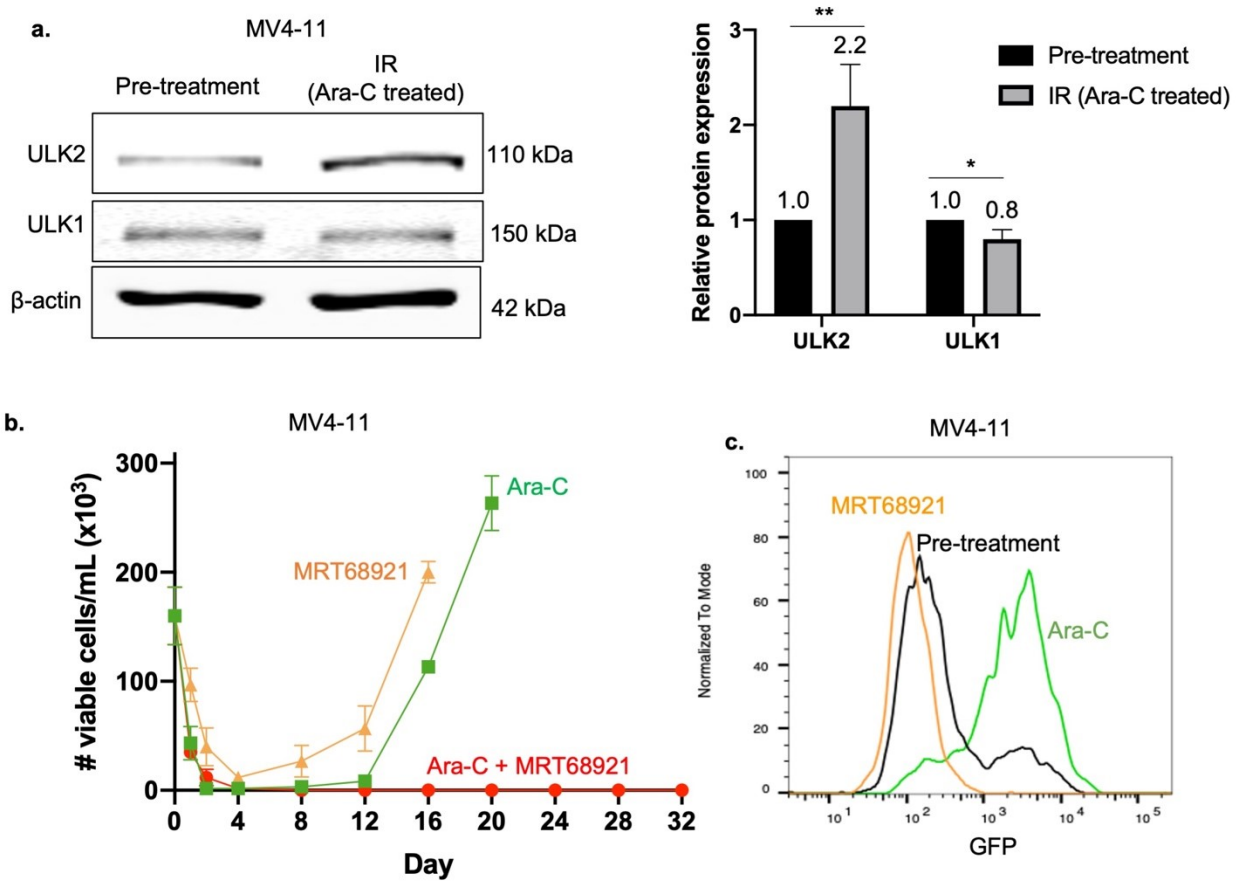

Figure 4.6. ULK2 contributes to the *in-vitro* relapse after Ara-C treatment. (a) Western blots of ULK1 and ULK2 in MV4-11 cells at *in-vitro* relapse (IR) after Ara-C treatment compared to cells at pre-treatment. Data from three independent experiments are shown in the bar graph. ULK2 and ULK1 expression were normalized to β-actin. * denotes $p<.05$, ** denotes $p<.01$, student's *t* test. (b) Cell viability assessed by trypan blue in MV4-11 cells subjected to the *in-vitro* relapse model treated with Ara-C alone, MRT68921 alone or combination of Ara-C + MRT68921. Three independent experiments were performed. (c) Flow cytometry analysis of GFP levels in IR cells from Ara-C treatment or MRT68921 treatment, compared to cells at pre-treatment.

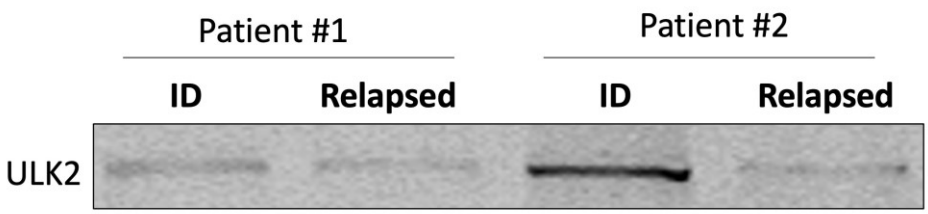

Densitometry	10.5	6.6	28.8	5.2
Blast count (%)	67	5	80	7
Densitometry normalized to blast count	15.7	132.2	36.0	73.8
Fold up-regulation in Relapsed vs. Initially Diagnosed	8.4		2.1	

Figure 4.7. Relapsed AML bone marrow specimens showed higher ULK2 expression compared to initially diagnosed bone marrow specimens. Results from Western blot studies and densitometry analysis of two paired patient samples with both initially diagnosed and relapsed specimens. The densitometry data of the ULK2 bands were normalized to the blast count, and the fold-upregulation was calculated for each patient.

4.4. Discussion

Cancer stem cells and CSL cells are believed to be the major contributors to cancer relapse (14). Thus, it is highly important and relevant to understand how cancer stemness is regulated. In recent years, there is accumulating evidence that autophagy is one of the important mechanisms in promoting cancer stemness. In support of this concept, several published studies have shown that inhibition of autophagy in cancer stem/CSL cells can effectively attenuate their stemness. For instance, inhibition of autophagy in primary ovarian cancer cells using chloroquine or ATG5 knockdown was shown to significantly decrease CSL features including spheroid formation, tumorigenicity and the expression of embryonic stem cell proteins (Sox2, Oct4 and Nanog) (9). Attenuation of CSL features resulting from autophagy blockade was also reported in pancreatic cancer and osteosarcoma model (15, 16). Results from our current study are also consistent with

the concept that autophagy is a key contributor to cancer stemness. Thus, inhibition of autophagy using chloroquine or the ULK1/2 inhibitor MRT68921 significantly decreased the chemoresistance to Ara-C in SORE6^{+} cells. The lack of a significant response in the SORE6^{-} cell population to chloroquine and MRT68921 increases the specificity of our findings.

Studies of cancer relapse have been highly challenging due to the relative paucity of *in-vitro* models and the difficulty in obtaining a sufficient number of cancer cells from patients during their remission. However, there has been evidence emerging from studies of AML that support the role of cancer stemness in relapse. For instance, one study showed a correlation between the cancer stem cell (CSC)-gene signature score of AML bone marrow specimens and relapse rate (17). Furthermore, several studies comparing initially diagnostic and relapsed bone marrow specimens have provided evidence that cancer stemness increases at relapse. Specifically, one study found that the percentage of CSCs, which were defined using an *in-vivo* limiting dilution assay, increased at relapse by 9- to 90- fold compared to diagnosis (18). Additionally, a study by Shlush et al. used whole genome sequencing of paired diagnosis and relapse blasts to track the origin of clones at relapse (19). Two major patterns of relapse were identified: one where the dominant relapse clone emerged from the CSC subset, and the other where relapse originated from bulk leukemic cells that carried a strong CSC-gene signature score. Although two different patterns of relapse emerged, both patterns highlighted the importance of stemness in this process. While these studies provide evidence that cancer stemness contributes to AML relapse, very little is known about the role of autophagy in AML relapse. However, there are a handful of studies on solid tumors providing correlational evidence to support the link between autophagy and cancer relapse. For instance, a high ULK1 protein expression detectable by immunohistochemistry in gastric carcinomas was found to significantly correlate with a high rate of disease relapse (20). Similarly, in a cohort of breast cancer patients, those with tumors carrying high *ULK1* mRNA expression were found to have a significantly shorter relapse-free survival (21). Leveraging the SORE6^{-}/SORE6^{+} dichotomy, we have recently generated an *in-vitro* AML relapse model which mimics the disease clinically. As mentioned in the introduction, regeneration of AML cells (i.e. *in-vitro* relapse) was identified under certain circumstances after a period of chemotherapy-induced *in-vitro* remission. Using molecular barcoding, we found that regenerated cells are enriched in SORE6^{+} cells at the expense of SORE6^{-} cells. In this current study, by employing this *in-vitro*

model, we have provided evidence that pharmacologic inhibition of autophagy using chloroquine or ULK1/2 inhibitor can effectively inhibit *in-vitro* relapse. This finding also correlates well with our finding that the ULK2 inhibitor MRT68921 can potently inhibit the expression of Myc, shown to be the key driver of the SORE6 reporter and the associated CSL phenotype. Taken together, it appears that autophagy maintains the stemness in the cancer stem/CSL cells, which are the contributors of cancer relapse. Accordingly, inhibition of autophagy, which attenuates cancer stemness, inhibits cancer relapse.

In our model, ULK2 but not ULK1 appears to contribute to the high autophagic flux in SORE6$^+$ cells. In the literature, ULK2 has been 'overshadowed' by its homologue ULK1, as the former has not been extensively studied. Nonetheless, it is known that the structures of both ULK1 and ULK2 are very similar, with a 98% query cover (22). Furthermore, both ULK1 and ULK2 contain a N-terminal serine/threonine kinase domain and a C-terminal interacting domain. ULK1 and ULK2 proteins also are known to have similar functions, as they are both capable of inducing autophagy by binding to Atg13 and FIP200 (22, 23), a process that can be inhibited by mTOR and increased by AMPK (24, 25). Accordingly, ULK1 and ULK2 are generally regarded as being functionally redundant, and evidence to support this redundancy has been shown in several studies. For instance, in mouse embryonic fibroblasts, disruption of autophagy occurred when both ULK1 and ULK2 were suppressed, but not when only either ULK1 or ULK2 was knocked out (26). Similarly, while ULK1/ULK2 double knockout mice die within one day after birth, single ULK1 or ULK2 knockout mice had normal survival (27-29). However, results from a few studies suggests that ULK1 and ULK2 may have non-redundant functions. For example, ULK2, but not ULK1, interacts with p62 and WIPI2, and transcriptional regulators (23). Another study found distinct function of ULK1 and ULK2 in lipid metabolism, as knockdown of *ULK1* inhibited fatty acid oxidation, while knockdown of *ULK2* increased it (30). Results from our current study have provided additional evidence that ULK2 carries functions distinct from ULK1. Based on the structural differences in the C-terminal interacting domain between the two ULK1/2 proteins (i.e. 55.1% shared sequence) (22), one may speculate that the non-redundant functions are related to the differences in their binding partners. Since ULK2 expression was not increased in SORE6$^-$ cells in our study, we would not have observed the importance of ULK2 without using the SORE6$^-$/SORE6$^+$ dichotomy, highlighting the importance of incorporating the concept of intra-tumoral heterogeneity into our

study model. One of the limitations of our study is that we did not specifically inhibit ULK2, as MRT68921 inhibited both ULK1 and ULK2 expression. Specific inhibition of ULK2 and ULK1 separately would produce more conclusive results that these two proteins act distinctly, and that the promotion of chemoresistance and *in-vitro* relapse is attributed to ULK2, rather than ULK1. However, since we found that the increase in expression after Ara-C treatment was exclusive to ULK2, and was not observed with ULK1, we believe this strongly supports that ULK1 and ULK2 are distinct.

In contrast with the 'general' autophagy inhibitors such as chloroquine and bafilomycin A1, MRT68921 was developed in 2015 as a more specific autophagy inhibitor which functions by targeting/suppressing the kinase activity of ULK1/2 proteins (13). Since MRT68921 was only developed relatively recently, clinical data about its therapeutic efficacy is not available. However, its potential therapeutic effects against cancers have been tested using *in-vivo* animal models. Specifically, mice xenografted with a gastric cancer cell line treated with MRT68921 had significantly lower tumor volume compared to DMSO treatment group (31). In view of the efficacy of chloroquine demonstrated in several clinical trials (32), we believe that MRT68921 holds promise as a useful anti-cancer agent, especially knowing that it can target CSL cells.

To conclude, our findings support that enhanced autophagy contributes to chemoresistance in $SORE6^{+}$ cells, which is not observed in $SORE6^{-}$ cells. This enhanced autophagy may contribute to AML relapse. ULK2 appears to be a key player in enhancing autophagy-mediated chemoresistance in $SORE6^{+}$ cells and may contribute to cancer stemness and relapse. Given our findings, targeting autophagy may be useful in the treatment of AML patients and may hinder relapses.

4.5. References

1. Vetrie D, Helgason GV, Copland M. The leukaemia stem cell: similarities, differences and clinical prospects in CML and AML. Nature reviewsCancer. 2020;20(3):158-73.

2. Ram R, Scheid C, Amit O, Chemnitz JM, Moshe Y, Hallek M, et al. Sequential therapy for patients with primary refractory acute myeloid leukemia: a historical prospective analysis of the German and Israeli experience. Haematologica. 2019;104(9):1798-803.
3. Dohner H, Weisdorf DJ, Bloomfield CD. Acute Myeloid Leukemia. N Engl J Med. 2015;373(12):1136-52.
4. Li X, Lewis MT, Huang J, Gutierrez C, Osborne CK, Wu MF, et al. Intrinsic resistance of tumorigenic breast cancer cells to chemotherapy. J Natl Cancer Inst. 2008;100(9):672-9.
5. Tang B, Raviv A, Esposito D, Flanders KC, Daniel C, Nghiem BT, et al. A flexible reporter system for direct observation and isolation of cancer stem cells. Stem Cell Reports. 2015;4(1):155-69.
6. Lai J, Brandwein J, Shang C, Chen W, Chu MP, Sandhu I, et al. The Application of the SORE6 Reporter in the Studies of Acute Myeloid Leukemia - a Novel Model for Disease Relapses. Blood. 2022;140(Supplement 1):9155-.
7. Vasconcelos FC, de Souza PS, Hancio T, de Faria FCC, Maia RC. Update on drug transporter proteins in acute myeloid leukemia: Pathological implication and clinical setting. Crit Rev Oncol Hematol. 2021;160:103281.
8. Lagadinou ED, Sach A, Callahan K, Rossi RM, Neering SJ, Minhajuddin M, et al. BCL-2 inhibition targets oxidative phosphorylation and selectively eradicates quiescent human leukemia stem cells. Cell Stem Cell. 2013;12(3):329-41.
9. Pagotto A, Pilotto G, Mazzoldi EL, Nicoletto MO, Frezzini S, Pasto A, et al. Autophagy inhibition reduces chemoresistance and tumorigenic potential of human ovarian cancer stem cells. Cell Death Dis. 2017;8(7):e2943.
10. Folkerts H, Hilgendorf S, Wierenga ATJ, Jaques J, Mulder AB, Coffer PJ, et al. Inhibition of autophagy as a treatment strategy for p53 wild-type acute myeloid leukemia. Cell Death Dis. 2017;8(7):e2927.
11. Jang JE, Eom JI, Jeung HK, Cheong JW, Lee JY, Kim JS, et al. AMPK-ULK1-Mediated Autophagy Confers Resistance to BET Inhibitor JQ1 in Acute Myeloid Leukemia Stem Cells. Clin Cancer Res. 2017;23(11):2781-94.
12. Mizushima N. The role of the Atg1/ULK1 complex in autophagy regulation. Curr Opin Cell Biol. 2010;22(2):132-9.

13. Petherick KJ, Conway OJ, Mpamhanga C, Osborne SA, Kamal A, Saxty B, et al. Pharmacological inhibition of ULK1 kinase blocks mammalian target of rapamycin (mTOR)-dependent autophagy. J Biol Chem. 2015;290(48):28726.
14. Marzagalli M, Fontana F, Raimondi M, Limonta P. Cancer Stem Cells-Key Players in Tumor Relapse. Cancers (Basel). 2021;13(3).
15. Yang MC, Wang HC, Hou YC, Tung HL, Chiu TJ, Shan YS. Blockade of autophagy reduces pancreatic cancer stem cell activity and potentiates the tumoricidal effect of gemcitabine. Mol Cancer. 2015;14:179.
16. Zhang D, Zhao Q, Sun H, Yin L, Wu J, Xu J, et al. Defective autophagy leads to the suppression of stem-like features of CD271(+) osteosarcoma cells. J Biomed Sci. 2016;23(1):82.
17. Ng SW, Mitchell A, Kennedy JA, Chen WC, McLeod J, Ibrahimova N, et al. A 17-gene stemness score for rapid determination of risk in acute leukaemia. Nature. 2016;540(7633):433-7.
18. Ho TC, LaMere M, Stevens BM, Ashton JM, Myers JR, O'Dwyer KM, et al. Evolution of acute myelogenous leukemia stem cell properties after treatment and progression. Blood. 2016;128(13):1671-8.
19. Shlush LI, Mitchell A, Heisler L, Abelson S, Ng SWK, Trotman-Grant A, et al. Tracing the origins of relapse in acute myeloid leukaemia to stem cells. Nature. 2017;547(7661):104-8.
20. Chen MB, Ji XZ, Liu YY, Zeng P, Xu XY, Ma R, et al. Ulk1 over-expression in human gastric cancer is correlated with patients' T classification and cancer relapse. Oncotarget. 2017;8(20):33704-12.
21. Pike LR, Singleton DC, Buffa F, Abramczyk O, Phadwal K, Li JL, et al. Transcriptional up-regulation of ULK1 by ATF4 contributes to cancer cell survival. Biochem J. 2013;449(2):389-400.
22. Wong PM, Puente C, Ganley IG, Jiang X. The ULK1 complex: sensing nutrient signals for autophagy activation. Autophagy. 2013;9(2):124-37.
23. Demeter A, Romero-Mulero MC, Csabai L, Olbei M, Sudhakar P, Haerty W, et al. ULK1 and ULK2 are less redundant than previously thought: computational analysis uncovers distinct regulation and functions of these autophagy induction proteins. Sci Rep. 2020;10(1):10940.
24. Alers S, Loffler AS, Wesselborg S, Stork B. The incredible ULKs. Cell Commun Signal. 2012;10(1):7.

25. Zachari M, Ganley IG. The mammalian ULK1 complex and autophagy initiation. Essays Biochem. 2017;61(6):585-96.
26. Lee EJ, Tournier C. The requirement of uncoordinated 51-like kinase 1 (ULK1) and ULK2 in the regulation of autophagy. Autophagy. 2011;7(7):689-95.
27. Cheong H, Lindsten T, Wu J, Lu C, Thompson CB. Ammonia-induced autophagy is independent of ULK1/ULK2 kinases. Proc Natl Acad Sci U S A. 2011;108(27):11121-6.
28. Kundu M, Lindsten T, Yang CY, Wu J, Zhao F, Zhang J, et al. Ulk1 plays a critical role in the autophagic clearance of mitochondria and ribosomes during reticulocyte maturation. Blood. 2008;112(4):1493-502.
29. Cheong H, Wu J, Gonzales LK, Guttentag SH, Thompson CB, Lindsten T. Analysis of a lung defect in autophagy-deficient mouse strains. Autophagy. 2014;10(1):45-56.
30. Ro SH, Jung CH, Hahn WS, Xu X, Kim YM, Yun YS, et al. Distinct functions of Ulk1 and Ulk2 in the regulation of lipid metabolism in adipocytes. Autophagy. 2013;9(12):2103-14.
31. Chen Y, Xie X, Wang C, Hu Y, Zhang H, Zhang L, et al. Dual targeting of NUAK1 and ULK1 using the multitargeted inhibitor MRT68921 exerts potent antitumor activities. Cell Death Dis. 2020;11(8):712.
32. Xu R, Ji Z, Xu C, Zhu J. The clinical value of using chloroquine or hydroxychloroquine as autophagy inhibitors in the treatment of cancers: A systematic review and meta-analysis. Medicine (Baltimore). 2018;97(46):e12912.

Chapter 5

Discussion

This Discussion is divided into three sections. In Section 5.1, I put forward a hypothetical model of AML relapse by incorporating several key observations from my studies with relevant concepts found in the literature. I will present arguments in support of the validity and usefulness of my *in-vitro* AML study model, with the acknowledgment that further validation is certainly warranted due to its intrinsic limitations. In Section 5.2, I will summarize my considerations regarding some of my experimental design and data interpretation, and by doing so, highlighting the potential pitfalls and weaknesses of my studies. Section 5.3 will include my suggestion of future studies.

5.1. My postulated hypothetical model for AML relapse

Despite the recent therapeutic advances for AML, disease relapse remains a significant clinical challenge and a major contributor of deaths in these patients. The main objective of my PhD studies is to extend our understanding of the biology of AML relapse, in the hope that this new knowledge can help design more effective therapeutic approaches for AML patients.

I believe that any valid conceptual model for AML relapse needs to include plausible explanations for two key phenomena. The first phenomenon is related to the extremely low number of AML cells that survive the high intensity of induction/consolidation chemotherapy. The persistence of such a small cell population during clinical remission strongly suggests that these leukemic cells possess highly unique biological characteristics. The second phenomenon that needs to be addressed is related to the relatively long latency before relapse (i.e. clinical remission), a phenomenon that cannot be easily explained by mechanisms commonly used for refractory disease, such as the lack of drug receptors, the use of alternative cellular pathways to bypass the site of pharmacologic blockade, or an increase in the drug export out of the cells. The concept of CSC/CSL cells has provided reasonable explanations to both of these two phenomena. Perhaps this is the reason why the concept of CSC/CSL cells is one of most frequently cited mechanisms in the literature to explain cancer relapse (including AML relapse). Thus, my research focus is related to the role and biology of CSC/CSL cells in the context of AML relapse.

In the remainder of this section, I will state my 5 key observations described in Chapters 2-4. In the last paragraph of this section, I postulate a hypothetical model for AML relapse (illustrated in **Figure 5.1**) based on these key observations, with reference to the relevant concepts found in the literature. My new perspective of the definition of CSC/CSL cells also will be discussed.

Observation #1 - the existence of two phenotypically and molecularly distinct cell subsets, SORE6$^-$ and SORE6$^+$ cells

It is logical to assume that the extremely low number of AML cells which survive induction/consolidation chemotherapy carry highly unique biological characteristics. As detailed in the Introduction, normal stem cells, including HSCs and embryonic stem cells (ESCs), possess many of these characteristics that are instrumental for survival and self-preservation in a highly hostile environment. In this regard, many published studies and reviews have highlighted these characteristics used by both normal stem cells and CSC/CSL cells, such as a superior ability of DNA repair as well as high levels of chemoresistance, tumorigenicity and autophagy (1-4). A handful of 'master' ESC proteins have been shown to maintain these stemness phenotypes in ESCs, and it is logical to assume that the same ESC proteins may play similar roles in CSC/CSL cells. This is the rationale behind the development of various reporters designed to detect the expression/transcriptional activity of these 'master' ESC proteins which include Myc, Sox2 and Oct4. Prior studies using these reporters applied to a variety of cancer cell types and experimental models have supported that this assumption is correct. Subsets of cancer cells, from both cell lines and primary patient samples, have been found to exhibit reporter activity, which correlates with high levels of stem-like features (5, 6).

At the beginning of my PhD studies, these ESC reporters had not been used in leukemia research. Shortly into my studies, I was able to identify and purify small subsets of cells in two AML cell lines using the SORE6 reporter. The dichotomy of the SORE6$^-$/SORE6$^+$ cell subsets in the two AML cell lines represents one of the basic elements of my experiments. Since these cell subsets represent subclones of cells derived from the same cell lines, their phenotypic differences exemplify a distinct level of intra-tumoral heterogeneity.

I then collected evidence to support that SORE6$^-$ and SORE6$^+$ cells are phenotypically and molecularly distinct based on several experimental approaches. As described in Chapter 2, these two subsets were found to display significant differences in chemoresistance and colony formation in the hanging drop assay. The expressions of Myc (an ESC protein), FLT3 and pSTAT5 were substantially higher in SORE6$^+$ cells. I also found that these two cell subsets behave differently in response to Ara-C, as the anti-apoptotic protein Bcl-2 was effectively downregulated in SORE6$^+$ but not SORE6$^-$ cells. As described in Chapter 4, SORE6$^-$ and SORE6$^+$ cells are different in their autophagic flux in response to Ara-C, and this difference correlates with an upregulation of ULK2 in SORE6$^+$ but not SORE6$^-$ cells. Lastly, I have provided evidence that autophagy provides cytoprotective effects against Ara-C in SORE6$^+$ but not SORE6$^-$ cells.

My review of the literature shows that intra-tumoral heterogeneity has not been a consideration in most published studies of AML. Incorporating the concept of intra-tumoral heterogeneity in any study will undoubtedly create further complexity in the experimental design and data interpretation, and this may explain why this factor has not been widely incorporated in most studies. Nonetheless, I believe that intra-tumoral heterogeneity cannot be ignored, since it is highly likely that different therapeutic strategies are needed to kill subclones of AML cells carrying different biochemical and phenotypic characteristics.

Observation #2 - both SORE6$^-$ and SORE6$^+$ cells can contribute to AML relapse

One of the most challenging aspects of my PhD studies is related to the definition of CSC/CSL cells. The use of the SORE6 reporter, and the pros and cons of this experimental strategy, will be further discussed in Section 5.2. Admittedly, there is no definitive proof that CSC/CSL cells have to be SORE6$^+$ cells and not SORE6$^-$ cells. Nonetheless, I believe that the use of the SORE6$^-$/SORE6$^+$ system did serve as a good starting point for my research.

Leveraging molecular barcoding, I was able to track SORE6$^-$ and SORE6$^+$ cells and determine their cell fate. Using the *in-vitro* relapse model, I found evidence that SORE6$^+$ cells are the major contributor of *in-vitro* relapse when AML cells were treated with Ara-C (Chapter 2). These

findings are in alignment with my initial hypothesis that SORE6 reporter activity is a marker of CSC/CSL cells, which are believed to be the contributors of AML relapse. However, results described in Chapter 3 have prompted me to re-evaluate this hypothesis, because of the observation that SORE6$^-$ but not SORE6$^+$ cells are the major contributors to the *in-vitro* relapse in AML cells treated with AZA and AZA+Ven. These findings suggest that subsets of SORE6$^-$ cells can behave like SORE6$^+$ cells treated with Ara-C. Thus, if one views CSC/CSL cells as the very small subset of cancer cells that can enter/exit a state of dormancy followed by clonal expansion (representing remission and relapse, respectively), perhaps these SORE6$^-$ cells are also CSC/CSL cells.

In most published studies of AML, CSC/CSL cells are defined by the expression of specific cell surface markers or occasionally cytoplasmic markers (7, 8). Less commonly, CSC/CSL cells are defined by the expression of a set of genes that are known to be highly expressed by relapsed tumors (9). Based on my experience with the *in-vitro* relapse model, I believe that the one of most defining features of CSC/CSL cells is related to their functional versatility. In view of their highly dynamic nature, defining these cells based on limited scopes of protein or gene expression may be rather counter-intuitive. My postulation regarding the definition of CSC/CSL cells in the context of AML relapse will be further discussed in the last paragraph of this section.

Observation #3 - Dormancy

Conceptually, AML relapse occurs after a period of dormancy, during which the very few surviving AML cells keep their metabolism at a minimum level. The nature of this dormancy has never been studied or understood. Not only do suitable *in-vitro*/*in-vivo* study models not exist, but it is also highly difficult to isolate a sufficient number of AML cells from patients in clinical remission for studies.

Using the *in-vitro* relapse model I generated, I attempted to explore the nature of this dormancy. As described in Chapter 2, I performed flow cytometry to analyze the cell culture during the '*in-vitro* remission' induced by Ara-C. Being a more sensitive method than the trypan blue assay, flow cytometry is expected to allow the quantification of the very small number of viable cells in cell culture with 'zero viability'. Indeed, I was able to consistently detect 200-500 cells/mL in these

samples, as compared to 150,000 cells/mL at the beginning of the experiments (i.e. 0.1-0.3% viability). Importantly, regular monitoring of the number of viable cells during the mean of 10 days of *in-vitro* remission showed no appreciable changes. Although these findings are rather preliminary and clinical validation has not been performed, I believe that these observations support the concept that Ara-C-induced dormancy is characterized by a state of quiescence (i.e. no cell proliferation), and that the transition between dormancy and relapse is likely a relatively abrupt event, possibly in response to specific signal(s) (i.e. a wake-up call).

Observation #4 - Dramatic changes in the metabolic profile during in-vitro relapse

It is perceivable that this transition into and out of dormancy requires a swift and dramatic biochemical program switch. For instance, autophagy, a process designed to recycle/scavenge internal organelles, is useful during the state of dormancy but probably not in alignment with the high cell proliferative state during disease relapse (10). In Chapter 3, I have presented data generated from large-scale metabolomic profiling to compare the pre-treatment AML cells and *in-vitro* relapse cells regenerated from Ara-C treatment. The pathway of ornithine/spermidine/spermine was highlighted. Interestingly, while I have found many significant differences between the two groups, there were relatively few differences in the metabolic profile between $SORE6^-$ and $SORE6^+$ cells at the steady state (i.e. no treatment). This finding suggests that the differences between $SORE6^-$ and $SORE6^+$ cells are less pronounced at steady state compared to with stimulation, and that $SORE6^+$ cells appear to have the ability to swiftly change their metabolic machinery in response to treatment. Taken together, AML relapse involves at least two dramatic but swift biochemical program switches, with the first being responsible for entering the state of dormancy and the second being responsible for exiting dormancy and entering a new phase of cell proliferation and clonal expansion. This superior ability of swiftly and massively switching the biochemical programs may well represent the most defining feature of CSC/CSL cells responsible for AML relapse.

My literature search revealed only two AML studies performing metabolomic analysis of relapsed patient samples and the paired pre-treatment samples (11, 12). While a list of metabolites and their associated metabolic pathways that are significantly different between the two groups are listed,

validation studies were not included in these studies. Nonetheless, the upregulation of ornithine identified in my study was also detected in the study by Kim *et al.* (13). Using western blots, I went on to confirm the upregulation of ODC proteins in the *in-vitro* relapse AML cells regenerated from Ara-C (Chapter 3).

Observation #5 - In-vitro relapsed SORE6$^+$ cells are biologically different from pre-treated SORE6$^+$ cells

Most of my experimental results are derived from the use of the *in-vitro* model in which AML cells were treated with Ara-C. In this experimental system, I consistently observed evidence that *in-vitro* relapse cells, which are predominantly SORE6$^+$ cells, are substantially different from the pre-treatment SORE6$^+$ cells. As discussed above (i.e. Observation #1), SORE6$^+$ cells at the steady state are more stem-like, with higher level of chemoresistance, autophagy and expressions of several key proteins such as Myc/FLT3/pSTAT5. These properties likely contribute to the survival of a subset of these cells during the first 2 days of Ara-C treatment, giving them time and opportunity to enter the dormancy state by executing the first biochemical program switch. After their exit of the dormancy state followed by clonal expansion, the *in-vitro* relapse cells retain their SORE6 activity, but these relapse SORE6$^+$ cells show several key differences. Firstly, they display even higher levels of chemoresistance than the pre-treatment SORE6$^+$ cells (Chapter 2). Secondly, their metabolite profile has been dramatically altered, as evidenced by our metabolomics studies described in Chapter *3*. Lastly, our glycomics scan has revealed a dramatic downregulation of lectin binding, indicating that there are profound alterations in the sialic acid composition/configuration on their cell surface.

These findings from my *in-vitro* studies are consistent with results of published studies comparing relapsed AML with pre-treatment AML. They are also in alignment with the clinical observation that relapsed AML tumors do not typically respond to the initial treatment. These changes may result from the second biochemical switch that is responsible for the onset of relapse from dormancy. These changes need to be further characterized and their significance should be determined.

A hypothetical model of AML relapse and a re-evaluation of the definition of CSC/CSL cells

Although the CSC/CSL concept has been frequently used to explain the mechanistic basis of AML relapse, the picture is incomplete. Based on the 5 key observations described above, I attempt to add more details to the model. Since most of my research data were derived from Ara-C treatment, my comments on how AML cells respond to other therapeutic agents are more speculative. This hypothetical model is explained as follows and is illustrated in **Figure 5.1**.

Intra-tumoral heterogeneity exists in AML. A small cell subset expresses an aberrantly high level of ESC proteins such as Myc, which is a key driver of a host of stem-like features (such as chemoresistance) in these cells. At least some of these cells are identified as SORE6$^+$ cells in my *in-vitro* model. In view of the known functional interplays among ESC proteins during normal development, it is likely that the degrees of cancer stemness vary within the SORE6$^+$ cell population, and it is possible that a small subset of SORE6$^-$ cells possess cancer stemness that is not detectable by using the SORE6 reporter. Nonetheless, SORE6$^+$ cells as a whole are more stem-like (Observation #1).

Upon Ara-C treatment, those carrying the highest level of cancer stemness within the SORE6$^+$ cell population, which represent 0.1-0.3% of the initial cell population, survive and they execute the first biochemical program switch that results in dormancy. The picture is slightly different when treatments, such as AZA+Ven, are used. In this scenario, the SORE6$^+$ cell population is effectively eliminated. The surviving cells come from a small subset of SORE6$^-$ cells, which may carry a high level of cancer stemness driven by ESC proteins not detectable by the SORE6 reporter or by entirely different mechanisms. These SORE6$^-$ cells are also able to enter the state of dormancy and are responsible for the subsequent relapse. It is perceivable that dormancy involves the selective use of metabolic pathways, heightened autophagy and a general metabolic slow-down. There is essentially no cell proliferation, and the number of viable cells is largely unchanged during this time period (***Observations #2 and 3***).

When appropriate signal(s) become available, there is a second biochemical program switch which gears up cell proliferation and clonal expansion. This second wave brings about dramatic changes

in the metabolism, which likely produce 'global' effects that have impacts on cell surface glycosylations. Certain stem-like features such as chemoresistance are elevated. This second biochemical program switch may also modulate various DNA repair mechanisms, such that the genome is more prone to errors and mutations. Consequently, additional gene mutations, commonly found in relapsed AML, are acquired during relapse (14).

With the background of this hypothetical model, I have re-evaluated my perspective of what CSC/CSL cells may represent in the context of AML relapse. Based on the hypothetical model illustrated in **Figure 5.1**, I am inclined to view CSC/CSL cells in at least three possible ways, dependent on the answers to certain unknowns:

1) AML relapse is entirely dependent on the existence of a small subset of cells that share many key biochemical programs with normal stem cells, and thus, they bear many phenotypic similarities with stem cells. While most of these cells can be identified as SORE6^{+} cells, a small subset of SORE6^{-} cells also carry the same characteristics, although they do not express SORE6 reporter activity for unknown reasons. In this scenario, CSC/CSL cells can be simply defined by their stem cell biochemical and phenotypic characteristics. If this scenario is true, one would expect that co-transfection of multiple reporters sensing the expression/activity of different ESC proteins should increase the sensitivity and probably specificity of these CSC/CSL cells.

2) Although CSC/CSL cells as defined in scenario #1 exist and play a key role in AML relapse, there are other small cell subsets, identified as SORE6^{-} cells, that can also survive the initial chemotherapy (e.g. AZA), and enter and exit the state of dormancy by executing two dramatic biochemical program switches. Unlike CSC/CSL cells defined in scenario #1, these SORE6^{-} cells are equipped with these abilities via mechanisms unrelated to ESC proteins. In this scenario, perhaps these highly unique SORE6^{-} cells should not be labeled CSC/CSL cells, as their uniqueness has nothing to do with the ESC programming. These cells need to be defined based on our understanding of the alternative mechanism(s) that enable them to enter/exit dormancy.

3) Regardless of the underlying mechanisms, cells that are responsible for AML relapse share their superior ability of swiftly modulating their biochemical programs. Perhaps this functionality can serve as the marker, and the concept of CSC/CSL cells needs to be de-emphasized.

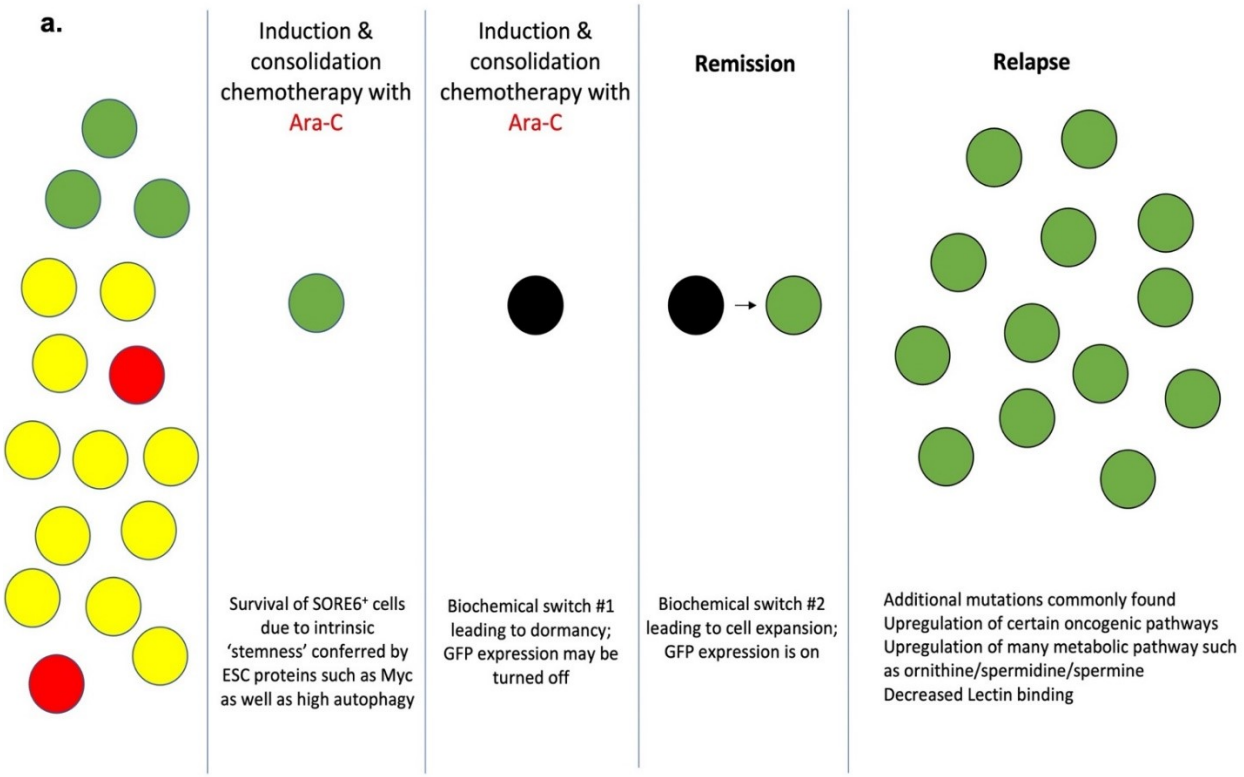

b.

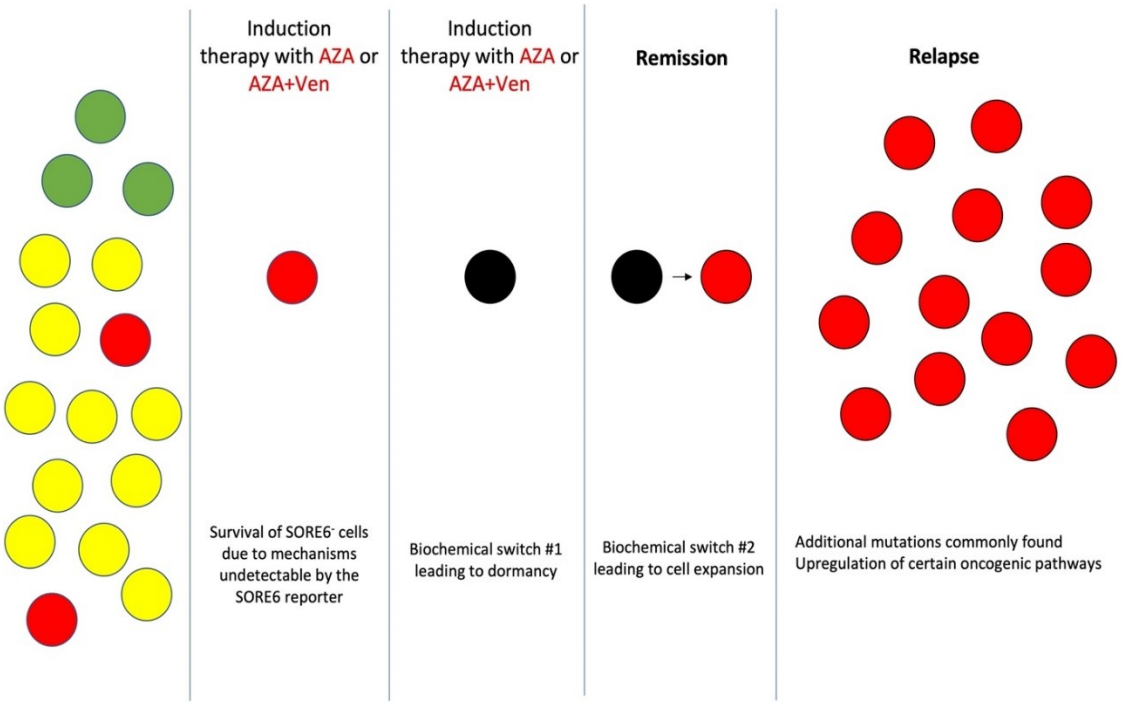

Figure 5.1. Hypothetical model of AML relapse. (a) At diagnosis, a small subset of stem-like cells exist that share phenotypic similarities with embryonic stem cells. These cells are mainly SORE6^{+} (in green), but a subset exist in the SORE6^{-} subset (in red), however, it is unknown why they do not express SORE6 reporter activity and their molecular differences from SORE6^{+} cells. Bulk cells, which make up the largest proportion of the cancer cell population, are shown in yellow. During Ara-C treatment, SORE6^{+} cells survive because of their stem-like features and ability to undergo a metabolic switch allowing them to achieve a state of dormancy. An unknown stimulus induces a metabolic switch out of dormancy, allowing the cells to proliferate once again. (b) After AZA or AZA+Ven treatment, the subset of SORE6^{-} cells carrying stem-like cells. After a metabolic switch, they experience a state of dormancy. A following metabolic switch reverses the dormancy, and they start proliferating again.

5.2. Experimental considerations and potential pitfalls

In this section, I will discuss the pros and cons of the *in-vitro* study model and SORE6 reporter system, both of which are key elements of my experimental studies.

The in-vitro study model for AML relapse

The first challenge of my PhD project was to develop a workable study model for AML relapse. This is probably the most pivotal point in my PhD studies because a failure of developing such a model would have necessitated a dramatic change in the direction (and probably the topics) of my research. Features that are important in the model include the following: 1) the use of AML cell lines rather than patient samples, such that my research would not be limited by the relative scarcity of these samples; 2) the induction of a period of chemotherapy-induced zero viability, where no viable cells could be detected based on a simple microscopic assessment, mimicking the clinical remission as defined by the identification of <5% blasts in the bone marrow biopsy by routine microscopic examination; 3) the occurrence of AML cell regeneration following the period of *in-vitro* remission, mimicking clinical relapse.

As detailed in Chapter 2, I was able to establish an experimental model which embodies these features. In addition to being simple and workable, this model was found to be highly consistent. Throughout my studies, the dosages of therapeutic agents required to induce the state of 'zero viability', the duration of the *in-vitro* remission and the time taken to achieve the IR were found to be highly consistent and reproducible for each of the combinations of AML cell lines/drugs I had tested. The importance of this consistency and reproducibility cannot be overstated; without this property, I would not have been able to use various parameters in this *in-vitro* model as my experimental readouts. For instance, in Chapter 3, I used the duration of *in-vitro* remission and time taken to reach IR as the key readouts when I compared the therapeutic efficacy of different therapeutic agents. In Chapter 4, the observation that pharmacologic inhibition of ULK2 significantly delayed *in-vitro* relapse has provided evidence in support of the role of ULK2 in AML relapse. The other advantage of this *in-vitro* model is related to its technical simplicity; it

can be easily adopted into any standard medical research laboratories, potentially allowing researchers from different parts of the world to compare their results. As both AML cell lines I tested were successfully incorporated into this model, it is likely that other AML cell lines and other cancer cell lines of different lineages can be used.

Similar to almost all of the other experimental models for cancer, this *in-vitro* model is not expected to be fully representative of the real disease. Perhaps the first obvious limitation of my model is that only *FLT3*-ITD AML cell lines were used. In fact, to avoid the molecular and biological diversity of AML as potential confounding factors, I intentionally chose to use the two *FLT3*-ITD AML cell lines (MOLM-13 and MV4-11) to be my key research tools.

Secondly, how much of the information generated through studies of this model is truly reflective of the diseases occurring in human bodies will always be an uncertainty. Whenever possible, generated findings and concepts need to be validated using patient samples. Recent advances in single cell studies will be highly relevant, especially in studies related to the state of dormancy when the number of cells studied is highly limited. That being said, I am cautiously optimistic about the degree of mimicry of this study model based on a number of observations. In my comparison between AZA versus AZA+Ven, I found a general agreement between the *in-vitro* efficacies of these agents and those of a clinical trial (15). Specifically, the AZA+Ven group had no *in-vitro* relapse at the optimal dose whereas the AZA group showed a relatively short period of *in-vitro* remission. Another support came from the metabolomics studies in which the upregulation of ODC after Ara-C treatment was validated in my *in-vitro* experiments. My preliminary validation studies using patient samples also showed some promising results; specifically, the group of relapsed AML samples showed significantly higher ODC protein expression than that of initial diagnostic samples.

Beyond doubt, the validity of this *in-vitro* model will become more apparent with more studies. Without this model, I would not have been able to generate a conceptual framework regarding the biology of AML relapse, as described in Section 5.1 and illustrated in **Figure 5.1**. Many aspects of this hypothetical model are testable. It is my hope that the undertaking of testing these aspects

of the hypothetical model will further advance our understanding of AML relapse, so that we are a step closer to finding a cure.

The use of the SORE6 reporter

One of the key questions at the beginning of my study was related to how CSC/CSL cells are to be defined, selected, and purified. This is a challenging question since the definition of CSCs has been largely operational. Specifically, cell populations enriched in CSCs, most commonly generated by sorting out subsets of cells based on their high expression of specific immunophenotypes (e.g. CD133 or $CD34^{+}CD38^{-}$), exhibit a significantly higher efficiency of forming tumors in SCID mice compared to the cell subset without these markers. As discussed in the Introduction, these cell surface antigens (e.g. CD133) typically do not bear any direct apparent biological link with cancer stemness. In the field of AML, a number of CSC markers have been reported but contradictory results have been reported. For instance, CD96 and CD200, both CSC markers in AML, have been found to enrich CSCs in several publications (8, 16). However, even these initial studies validating these markers have found these markers did not reliably identify CSCs in all cases. In my own experience, I found these immunophenotypic markers are not detectable in my two AML cell lines. Thus, the usefulness of these markers is highly dependent on cell type.

As mentioned in Section 5.1, specific gene expression patterns have also been used in some studies to define CSC/CSL cells. In this regard, I believe that this approach may not be optimal because CSC/CSL cells may dramatically change their biochemical properties as they enter/exit the state of dormancy and initiate clonal expansion. In one recent study, the authors generated a panel of CSC-related genes using RNA-sequencing of functionally defined CSCs (9). Many of these genes have no apparent relatedness to cancer stemness. This experimental approach also may suffer from the limitation that it is not clear if the gene signals are derived from a small subset of cells carrying high levels of expression of these genes or from a substantial proportion of the cell population.

Given the limitations of the mentioned markers, I decided to use a different approach to detect and identify CSL cells. Details of the SORE6 reporter have been described in the Introduction. I believe

that the use of SORE6 has several advantages over the use of cell surface markers such as $CD34^+/CD38^-$, CD96 or CD200. Firstly, in view of the important functions of ESC proteins, and the fact that expression of these proteins result in the dedifferentiation of somatic cells (17, 18), cells aberrantly expressing these ESC proteins are likely to be more 'stem-like'. Secondly, since the mechanisms underlying the SORE6 reporter are at least partially known, it becomes possible to design experiments that manipulate the reporter activity. In my studies, I have shown that inhibitors of Myc, FLT3, and ULK2 can downregulate the SORE6 reporter activity. Lastly, the use of the SORE6 reporter has been tested and reported in eight previous studies, both in solid cancer models and hematologic cancer models (5, 6, 19-24). Thus, the use of SORE6 is justified.

In view of the relative lack of Sox2 and Oct4 in the two AML cell lines used in this study, a Myc reporter might have been a better choice in retrospect. Nonetheless, in view of the high redundancy of the DNA binding sequences recognizable by embryonic stem cell proteins, it is highly likely that reporter systems designed to detect specific ESC transcriptional factors are intrinsically 'non-specific'. For instance, one previous study has shown that the promoter region of a Sox2 reporter can be recognized by 15 other transcriptional factors, most of which are known to play important roles in embryogenesis (25). I believe that this 'pitfall' is outweighed by the benefit of the SORE6 reporter, since SORE6 reporter activity as a marker of CSC/CSL cells has been documented in both solid tumor and hematologic cancers (5, 19, 20).

The use of flow cytometry/barcoding to assess $SORE6^-/SORE6^+$ conversion

Coupled with the molecular barcoding and flow cytometry to detect GFP expression (i.e. readout for the SORE6 reporter), I was able to accurately monitor the relative contribution of CSL cells to the regeneration during IR as well as the degree of $SORE6^-/SORE6^+$ phenotypic conversion (if any). Regarding the latter point, previous research using other cancer cell types and experimental models have shown that the $SORE6^-/SORE6^+$ conversion can occur. Karpas 299, a T-cell lymphoma cell line, has been reported to have two phenotypically distinct cell subsets separated by their Sox2 transcriptional activity (26). In this system, purifier Sox2-active cells with high stem-like features gradually and spontaneously lose Sox2 activity over a few weeks, reminiscent of

differentiation. In other cancer cell systems, it has been shown that Sox2-inactive cells can acquire Sox2 reporter activity upon oxidative or hypoxic stimulation (27). In my experimental system, the relative proportions of SORE6$^-$/SORE6$^+$ cells detectable by molecular barcoding and flow cytometry were generally concordant across all combinations of drugs/dosages, with the exception of Venetoclax-treated cells, suggesting that SORE6$^-$/SORE6$^+$ conversion does not play a substantial role in the *in-vitro* relapse. Nonetheless, I cannot exclude the possibility that the SORE6$^-$/SORE6$^+$ conversion may occur if there are additional signals, such as cytokines. If these additional signals are required, models based on cell lines will not show any conversion, and an *in-vivo* model may be required. Thus, further studies using xenograft mouse models may be helpful in addressing this question.

5.3. Future Studies

Similar to other research, I believe that results from my studies have generated more questions than answers, and these questions form the basis of future research and studies. Some of these questions are summarized and discussed as follows. Most of my suggested future studies are related to further clarifications and/testing of the hypothetical model illustrated in ***Figure 5.1.***

1) The biological characteristic of SORE6$^-$ cells expanded in IR

The nature of *in-vitro* relapse due to the expansion of SORE6$^-$ cells in the AZA and AZA+Ven groups is highly interesting. Depending on whether their uniqueness is driven by other ESC proteins or a completely different mechanism, the concept and definition of CSC/CSL cells may have to be modified. In order to evaluate the CSL characteristics of these SORE6$^-$ IR cells after AZA treatment, functional tests, including hanging drop and chemoresistance assays, can be performed. The presence of higher CSL features in these cells suggests that CSL cells can be found in the SORE6$^-$ fraction. Another possibility is that the SORE6$^-$ expansion at *in-vitro* relapse is through a completely different mechanism unrelated to cancer stemness. Large scale RNA sequencing and metabolomic analysis can be performed using pre-treatment and *in-vitro* relapse cells to determine pathways necessary for *in-vitro* relapse that are dependent on treatment type.

2) The nature and regulation of two biochemical program switches

As discussed above, my metabolomics studies did not reveal any substantial difference between SORE6^{-} and SORE6^{+} cells; however, *in-vitro* relapse compared to pre-treatment cells had substantial differences in their metabolic profiles. These finding strongly suggest that a biochemical program switch in CSL cells occurs after the initiation of the treatment.

Additionally, my preliminary data suggests that there may be two distinct biochemical switches, with the first occurring after treatment that maintains dormancy during remission, and the second occurring at the end of remission, providing a the 'wake-up' call that triggers the onset of relapse. Thus, understanding when these metabolic switches occur and the regulators involved can provide important insights into the biology of AML relapse. If this hypothetical model is correct, targeting the regulators responsible for the metabolic switches in Ara-C-treated cells should be expected to inhibit the expansion of CSL cells and AML relapse.

As mentioned previously, 200-500 viable cells/mL are present during the *in-vitro* remission stage of the model. Using these *in-vitro* remission cells, as well as cells at *in-vitro* relapse and at steady state/pre-treatment, large scale sequencing or metabolomic analysis in the *in-vitro* remission cells can be done to determine whether biochemical and metabolic differences exist between these three stages. Based on these analyses, the importance of identified pathways to the initiation of the *in-vitro* remission/dormancy stage and the *in-vitro* relapse/wake-up stage can be validated using pharmacologic inhibitors. If two distinct biochemical switches occur that use different biological pathways, then blocking specific pathways at different stages in the model should have different abilities to suppress IR. For instance, pathways that are important in providing the 'wake-up' call should prevent IR if the treatment is maintained throughout the experiment but should not prevent IR if the treatment is only administered at the beginning of the experiment before the 'wake-up' call is necessary.

3) The prognostic value of ODC and ULK2

Using the *in-vitro* relapse model, ODC and ULK2 have been identified as markers that may contribute to relapse. In this study, ODC and ULK2 were upregulated in a small cohort of relapsed patient samples. Future studies can correlate ODC and ULK2 expression with clinical characteristics to determine whether they predict likelihood of relapse, length of clinical remission, and survival.

5.4. References

1. Nathansen J, Meyer F, Muller L, Schmitz M, Borgmann K, Dubrovska A. Beyond the Double-Strand Breaks: The Role of DNA Repair Proteins in Cancer Stem-Cell Regulation. Cancers (Basel). 2021;13(19).
2. Maynard S, Swistowska AM, Lee JW, Liu Y, Liu ST, Da Cruz AB, et al. Human embryonic stem cells have enhanced repair of multiple forms of DNA damage. Stem Cells. 2008;26(9):2266-74.
3. Ishikawa F, Yoshida S, Saito Y, Hijikata A, Kitamura H, Tanaka S, et al. Chemotherapy-resistant human AML stem cells home to and engraft within the bone-marrow endosteal region. Nature biotechnology. 2007;25(11):1315-21.
4. Shang C, Hassan B, Haque M, Song Y, Li J, Liu D, et al. Crizotinib Resistance Mediated by Autophagy Is Higher in the Stem-Like Cell Subset in ALK-Positive Anaplastic Large Cell Lymphoma, and This Effect Is MYC-Dependent. Cancers (Basel). 2021;13(2).
5. Tang B, Raviv A, Esposito D, Flanders KC, Daniel C, Nghiem BT, et al. A flexible reporter system for direct observation and isolation of cancer stem cells. Stem Cell Reports. 2015;4(1):155-69.
6. Vaddi PK, Stamnes MA, Cao H, Chen S. Elimination of SOX2/OCT4-Associated Prostate Cancer Stem Cells Blocks Tumor Development and Enhances Therapeutic Response. Cancers (Basel). 2019;11(9).

7. Lapidot T, Sirard C, Vormoor J, Murdoch B, Hoang T, Caceres-Cortes J, et al. A cell initiating human acute myeloid leukaemia after transplantation into SCID mice. Nature; 1994. p. 4.
8. Ho JM, Dobson SM, Voisin V, McLeod J, Kennedy JA, Mitchell A, et al. CD200 expression marks leukemia stem cells in human AML. Blood advances. 2020;4(21):5402-13.
9. Ng SW, Mitchell A, Kennedy JA, Chen WC, McLeod J, Ibrahimova N, et al. A 17-gene stemness score for rapid determination of risk in acute leukaemia. Nature. 2016;540(7633):433-7.
10. Jung CH, Ro SH, Cao J, Otto NM, Kim DH. mTOR regulation of autophagy. FEBS Lett. 2010;584(7):1287-95.
11. Kim HK, Son SY, Oh JS, Song YN, Byun JM, Koh Y, et al. Metabolic Profiling during Acute Myeloid Leukemia Progression Using Paired Clinical Bone Marrow Serum Samples. Metabolites. 2021;11(9).
12. Culp-Hill R, Stevens BM, Jones CL, Pei S, Dzieciatkowska M, Minhajuddin M, et al. Therapy-Resistant Acute Myeloid Leukemia Stem Cells Are Resensitized to Venetoclax + Azacitidine by Targeting Fatty Acid Desaturases 1 and 2. Metabolites. 2023;13(4).
13. Duy C, Li M, Teater M, Meydan C, Garrett-Bakelman FE, Lee TC, et al. Chemotherapy Induces Senescence-Like Resilient Cells Capable of Initiating AML Recurrence. Cancer Discov. 2021;11(6):1542-61.
14. Kronke J, Bullinger L, Teleanu V, Tschurtz F, Gaidzik VI, Kuhn MW, et al. Clonal evolution in relapsed NPM1-mutated acute myeloid leukemia. Blood. 2013;122(1):100-8.
15. DiNardo CD, Jonas BA, Pullarkat V, Thirman MJ, Garcia JS, Wei AH, et al. Azacitidine and Venetoclax in Previously Untreated Acute Myeloid Leukemia. N Engl J Med. 2020;383(7):617-29.
16. Hosen N, Park CY, Tatsumi N, Oji Y, Sugiyama H, Gramatzki M, et al. CD96 is a leukemic stem cell-specific marker in human acute myeloid leukemia. Proc Natl Acad Sci U S A. 2007;104(26):11008-13.
17. Kopp JL, Ormsbee BD, Desler M, Rizzino A. Small increases in the level of Sox2 trigger the differentiation of mouse embryonic stem cells. Stem Cells. 2008;26(4):903-11.
18. Takahashi K, Tanabe K, Ohnuki M, Narita M, Ichisaka T, Tomoda K, et al. Induction of pluripotent stem cells from adult human fibroblasts by defined factors. Cell. 2007;131(5):861-72.

19. Pádua D, Barros R, Amaral AL, Mesquita P, Freire AF, Sousa M, et al. A SOX2 Reporter System Identifies Gastric Cancer Stem-Like Cells Sensitive to Monensin. Cancers (Basel). 2020;12(2):20.
20. Li J, Haque M, Shang C, Hassan B, Liu D, Chen W, et al. Identification and Characterization of Cancer Stem-Like Cells in ALK-Positive Anaplastic Large Cell Lymphoma Using the SORE6 Reporter. Curr Issues Mol Biol. 2021;43(2):543-57.
21. Menendez ST, Rey V, Martinez-Cruzado L, Gonzalez MV, Morales-Molina A, Santos L, et al. SOX2 Expression and Transcriptional Activity Identifies a Subpopulation of Cancer Stem Cells in Sarcoma with Prognostic Implications. Cancers (Basel). 2020;12(4).
22. Gao W, Wu D, Wang Y, Wang Z, Zou C, Dai Y, et al. Development of a novel and economical agar-based non-adherent three-dimensional culture method for enrichment of cancer stem-like cells. Stem Cell Res Ther. 2018;9(1):243.
23. Rosas-Cruz A, Salinas-Jazmin N, Valdes-Rives A, Velasco-Velazquez MA. DRD1 and DRD4 are differentially expressed in breast tumors and breast cancer stem cells: pharmacological implications. Transl Cancer Res. 2022;11(11):3941-50.
24. Bano A, Stevens JH, Modi PS, Gustafsson JA, Strom AM. Estrogen Receptor beta4 Regulates Chemotherapy Resistance and Induces Cancer Stem Cells in Triple Negative Breast Cancer. Int J Mol Sci. 2023;24(6).
25. Gupta N, Jung K, Wu C, Alshareef A, Alqahtani H, Damaraju S, et al. High Myc expression and transcription activity underlies intra-tumoral heterogeneity in triple-negative breast cancer. Oncotarget. 2017;8(17):28101-15.
26. Wu C, Zhang HF, Gupta N, Alshareef A, Wang Q, Huang YH, et al. A positive feedback loop involving the Wnt/beta-catenin/MYC/Sox2 axis defines a highly tumorigenic cell subpopulation in ALK-positive anaplastic large cell lymphoma. J Hematol Oncol. 2016;9(1):120.
27. Gopal K, Gupta N, Zhang H, Alshareef A, Alqahtani H, Bigras G, et al. Oxidative stress induces the acquisition of cancer stem-like phenotype in breast cancer detectable by using a Sox2 regulatory region-2 (SRR2) reporter. Oncotarget. 2016;7(3):3111-27.

Bibliography

Abu-Duhier, F. M., A. C. Goodeve, G. A. Wilson, R. S. Care, I. R. Peake and J. T. Reilly (2001). "Identification of novel FLT-3 Asp835 mutations in adult acute myeloid leukaemia." Br J Haematol 113(4): 983-988.

Aimiuwu, J., H. Wang, P. Chen, Z. Xie, J. Wang, S. Liu, R. Klisovic, A. Mims, W. Blum, G. Marcucci and K. K. Chan (2012). "RNA-dependent inhibition of ribonucleotide reductase is a major pathway for 5-azacytidine activity in acute myeloid leukemia." Blood 119(22): 5229-5238.

Akkoc, Y., N. Peker, A. Akcay and D. Gozuacik (2021). "Autophagy and Cancer Dormancy." Front Oncol 11: 627023.

Alers, S., A. S. Loffler, S. Wesselborg and B. Stork (2012). "The incredible ULKs." Cell Commun Signal 10(1): 7.

Anand, K., P. Niravath, T. Patel, J. Ensor, A. Rodriguez, T. Boone, S. T. Wong and J. C. Chang (2021). "A Phase II Study of the Efficacy and Safety of Chloroquine in Combination With Taxanes in the Treatment of Patients With Advanced or Metastatic Anthracycline-refractory Breast Cancer." Clin Breast Cancer 21(3): 199-204.

Arber, D. A., A. Orazi, R. Hasserjian, J. Thiele, M. J. Borowitz, M. M. Le Beau, C. D. Bloomfield, M. Cazzola and J. W. Vardiman (2016). "The 2016 revision to the World Health Organization classification of myeloid neoplasms and acute leukemia." Blood 127(20): 2391-2405.

Arnaout, A., S. J. Robertson, G. R. Pond, H. Lee, A. Jeong, L. Ianni, L. Kroeger, J. Hilton, S. Coupland, C. Gottlieb, B. Hurley, A. McCarthy and M. Clemons (2019). "A randomized, double-blind, window of opportunity trial evaluating the effects of chloroquine in breast cancer patients." Breast Cancer Res Treat 178(2): 327-335.

Bano, A., J. H. Stevens, P. S. Modi, J. A. Gustafsson and A. M. Strom (2023). "Estrogen Receptor beta4 Regulates Chemotherapy Resistance and Induces Cancer Stem Cells in Triple Negative Breast Cancer." Int J Mol Sci 24(6).

Bano, N., M. I. Ansari, K. M. Kainat, V. K. Singh and P. K. Sharma (2023). "Chloroquine synergizes doxorubicin efficacy in cervical cancer cells through flux impairment and down regulation of proteins involved in the fusion of autophagosomes to lysosomes." Biochem Biophys Res Commun 656: 131-138.

Beckmann, J., S. Scheitza, P. Wernet, J. C. Fischer and B. Giebel (2007). "Asymmetric cell division within the human hematopoietic stem and progenitor cell compartment: identification of asymmetrically segregating proteins." Blood 109(12): 5494-5501.

Beltran, A. S., A. G. Rivenbark, B. T. Richardson, X. Yuan, H. Quian, J. P. Hunt, E. Zimmerman, L. M. Graves and P. Blancafort (2011). "Generation of tumor-initiating cells by exogenous delivery of OCT4 transcription factor." Breast Cancer Res 13(5): R94.

Benderra, Z., A. M. Faussat, L. Sayada, J. Y. Perrot, D. Chaoui, J. P. Marie and O. Legrand (2004). "Breast cancer resistance protein and P-glycoprotein in 149 adult acute myeloid leukemias." Clin Cancer Res 10(23): 7896-7902.

Bennett, J. M., D. Catovsky, M. T. Daniel, G. Flandrin, D. A. Galton, H. R. Gralnick and C. Sultan (1976). "Proposals for the classification of the acute leukaemias. French-American-British (FAB) co-operative group." Br J Haematol 33(4): 451-458.

Betancourt-Garcia, R. D., J. Castro, A. C. Fernandez, A. Lopez-Enriquez, J. Fradera and E. Pacheco (2009). "Acquired acute myelogenous leukemia after therapy for acute promyelocytic leukemia with t(15;17): a case report and review of the literature." P R Health Sci J 28(2): 146-150.

Bewersdorf, J. P. and A. M. Zeidan (2020). "Hyperleukocytosis and Leukostasis in Acute Myeloid Leukemia: Can a Better Understanding of the Underlying Molecular Pathophysiology Lead to Novel Treatments?" Cells 9(10).

Bingol, K. (2018). "Recent Advances in Targeted and Untargeted Metabolomics by NMR and MS/NMR Methods." High Throughput 7(2).

Boettcher, S., P. G. Miller, R. Sharma, M. McConkey, M. Leventhal, A. V. Krivtsov, A. O. Giacomelli, W. Wong, J. Kim, S. Chao, K. J. Kurppa, X. Yang, K. Milenkowic, F. Piccioni, D. E. Root, F. G. Rucker, Y. Flamand, D. Neuberg, R. C. Lindsley, P. A. Janne, W. C. Hahn, T. Jacks, H. Dohner, S. A. Armstrong and B. L. Ebert (2019). "A dominant-negative effect drives selection of TP53 missense mutations in myeloid malignancies." Science 365(6453): 599-604.

Bolwell, B. J., P. A. Cassileth and R. P. Gale (1988). "High dose cytarabine: a review." Leukemia 2(5): 253-260.

Bonetti, P., T. Davoli, C. Sironi, B. Amati, P. G. Pelicci and E. Colombo (2008). "Nucleophosmin and its AML-associated mutant regulate c-Myc turnover through Fbw7 gamma." The Journal of cell biology 182(1): 19-26.

Borah, A., S. Raveendran, A. Rochani, T. Maekawa and D. S. Kumar (2015). "Targeting self-renewal pathways in cancer stem cells: clinical implications for cancer therapy." Oncogenesis 4(11): e177.

Borer, R. A., C. F. Lehner, H. M. Eppenberger and E. A. Nigg (1989). "Major nucleolar proteins shuttle between nucleus and cytoplasm." Cell 56(3): 379-390.

Bose, P., P. Vachhani and J. E. Cortes (2017). "Treatment of Relapsed/Refractory Acute Myeloid Leukemia." Curr Treat Options Oncol 18(3): 17.

Bosnjak, M., B. Ristic, K. Arsikin, A. Mircic, V. Suzin-Zivkovic, V. Perovic, A. Bogdanovic, V. Paunovic, I. Markovic, V. Bumbasirevic, V. Trajkovic and L. Harhaji-Trajkovic (2014). "Inhibition of mTOR-dependent autophagy sensitizes leukemic cells to cytarabine-induced apoptotic death." PLoS One 9(4): e94374.

Bourguignon, L. Y., K. Peyrollier, W. Xia and E. Gilad (2008). "Hyaluronan-CD44 interaction activates stem cell marker Nanog, Stat-3-mediated MDR1 gene expression, and ankyrin-regulated multidrug efflux in breast and ovarian tumor cells." J Biol Chem 283(25): 17635-17651.

Bousquet, G., M. El Bouchtaoui, T. Sophie, C. Leboeuf, C. de Bazelaire, P. Ratajczak, S. Giacchetti, A. de Roquancourt, P. Bertheau, L. Verneuil, J. P. Feugeas, M. Espie and A. Janin (2017). "Targeting autophagic cancer stem-cells to reverse chemoresistance in human triple negative breast cancer." Oncotarget 8(21): 35205-35221.

Bracker, T. U., B. Giebel, J. Spanholtz, U. R. Sorg, L. Klein-Hitpass, T. Moritz and J. Thomale (2006). "Stringent regulation of DNA repair during human hematopoietic differentiation: a gene expression and functional analysis." Stem Cells 24(3): 722-730.

Bradley, T. R. and D. Metcalf (1966). "The growth of mouse bone marrow cells in vitro." Aust J Exp Biol Med Sci 44(3): 287-299.

Breems, D. A., W. L. Van Putten, P. C. Huijgens, G. J. Ossenkoppele, G. E. Verhoef, L. F. Verdonck, E. Vellenga, G. E. De Greef, E. Jacky, J. Van der Lelie, M. A. Boogaerts and B. Lowenberg (2005). "Prognostic index for adult patients with acute myeloid leukemia in first relapse." J Clin Oncol 23(9): 1969-1978.

Bursch, W., A. Ellinger, H. Kienzl, L. Torok, S. Pandey, M. Sikorska, R. Walker and R. S. Hermann (1996). "Active cell death induced by the anti-estrogens tamoxifen and ICI 164 384 in human mammary carcinoma cells (MCF-7) in culture: the role of autophagy." Carcinogenesis 17(8): 1595-1607.

Caldwell, J. T., Y. Ge and J. W. Taub (2014). "Prognosis and management of acute myeloid leukemia in patients with Down syndrome." Expert Rev Hematol 7(6): 831-840.

Campisi, J. (2001). "Cellular senescence as a tumor-suppressor mechanism." Trends Cell Biol 11(11): S27-31.

Chan, E. Y., A. Longatti, N. C. McKnight and S. A. Tooze (2009). "Kinase-inactivated ULK proteins inhibit autophagy via their conserved C-terminal domains using an Atg13-independent mechanism." Mol Cell Biol 29(1): 157-171.

Chang, H., J. Brandwein, Q. L. Yi, K. Chun, B. Patterson and B. Brien (2004). "Extramedullary infiltrates of AML are associated with CD56 expression, 11q23 abnormalities and inferior clinical outcome." Leuk Res 28(10): 1007-1011.

Chavez-Dominguez, R., M. Perez-Medina, J. S. Lopez-Gonzalez, M. Galicia-Velasco and D. Aguilar-Cazares (2020). "The Double-Edge Sword of Autophagy in Cancer: From Tumor Suppression to Pro-tumor Activity." Front Oncol 10: 578418.

Chen, M. B., X. Z. Ji, Y. Y. Liu, P. Zeng, X. Y. Xu, R. Ma, Z. D. Guo, J. W. Lu and J. F. Feng (2017). "Ulk1 over-expression in human gastric cancer is correlated with patients' T classification and cancer relapse." Oncotarget 8(20): 33704-33712.

Chen, W. L., J. H. Wang, A. H. Zhao, X. Xu, Y. H. Wang, T. L. Chen, J. M. Li, J. Q. Mi, Y. M. Zhu, Y. F. Liu, Y. Y. Wang, J. Jin, H. Huang, D. P. Wu, Y. Li, X. J. Yan, J. S. Yan, J. Y. Li, S. Wang, X. J. Huang, B. S. Wang, Z. Chen, S. J. Chen and W. Jia (2014). "A distinct glucose metabolism signature of acute myeloid leukemia with prognostic value." Blood 124(10): 1645-1654.

Chen, Y., X. Xie, C. Wang, Y. Hu, H. Zhang, L. Zhang, S. Tu, Y. He and Y. Li (2020). "Dual targeting of NUAK1 and ULK1 using the multitargeted inhibitor MRT68921 exerts potent antitumor activities." Cell Death Dis 11(8): 712.

Cheong, H., T. Lindsten, J. Wu, C. Lu and C. B. Thompson (2011). "Ammonia-induced autophagy is independent of ULK1/ULK2 kinases." Proc Natl Acad Sci U S A 108(27): 11121-11126.

Cheong, H., J. Wu, L. K. Gonzales, S. H. Guttentag, C. B. Thompson and T. Lindsten (2014). "Analysis of a lung defect in autophagy-deficient mouse strains." Autophagy 10(1): 45-56.

Cheson, B. D., J. M. Bennett, K. J. Kopecky, T. Buchner, C. L. Willman, E. H. Estey, C. A. Schiffer, H. Doehner, M. S. Tallman, T. A. Lister, F. Lo-Coco, R. Willemze, A. Biondi, W. Hiddemann, R. A. Larson, B. Lowenberg, M. A. Sanz, D. R. Head, R. Ohno, C. D. Bloomfield, S. o. R. C. T. O. International Working Group for Diagnosis and L. Reporting Standards for Therapeutic Trials in Acute Myeloid (2003). "Revised recommendations of the International Working Group for Diagnosis, Standardization of Response Criteria, Treatment Outcomes, and Reporting Standards for Therapeutic Trials in Acute Myeloid Leukemia." J Clin Oncol 21(24): 4642-4649.

Cheung, A. M., T. S. Wan, J. C. Leung, L. Y. Chan, H. Huang, Y. L. Kwong, R. Liang and A. Y. Leung (2007). "Aldehyde dehydrogenase activity in leukemic blasts defines a subgroup of acute myeloid leukemia with adverse prognosis and superior NOD/SCID engrafting potential." Leukemia 21(7): 1423-1430.

Chou, S. H., B. S. Ko, J. S. Chiou, Y. C. Hsu, M. H. Tsai, Y. C. Chiu, I. S. Yu, S. W. Lin, H. A. Hou, Y. Y. Kuo, H. M. Lin, M. F. Wu, W. C. Chou and H. F. Tien (2012). "A knock-in Npm1 mutation in mice results in myeloproliferation and implies a perturbation in hematopoietic microenvironment." PloS one 7(11): e49769.

Chute, J. P., G. G. Muramoto, J. Whitesides, M. Colvin, R. Safi, N. J. Chao and D. P. McDonnell (2006). "Inhibition of aldehyde dehydrogenase and retinoid signaling induces the expansion of human hematopoietic stem cells." Proc Natl Acad Sci U S A 103(31): 11707-11712.

Clark, D. W. and K. Palle (2016). "Aldehyde dehydrogenases in cancer stem cells: potential as therapeutic targets." Ann Transl Med 4(24): 518.

Cocciardi, S., A. Dolnik, S. Kapp-Schwoerer, F. G. Rucker, S. Lux, T. J. Blatte, S. Skambraks, J. Kronke, F. H. Heidel, T. M. Schnoder, A. Corbacioglu, V. I. Gaidzik, P. Paschka, V. Teleanu, G. Gohring, F. Thol, M. Heuser, A. Ganser, D. Weber, E. Strang, H. A. Kestler, H. Dohner, L. Bullinger and K. Dohner (2019). "Clonal evolution patterns in acute myeloid leukemia with NPM1 mutation." Nat Commun 10(1): 2031.

Colombo, E., P. Martinelli, R. Zamponi, D. C. Shing, P. Bonetti, L. Luzi, S. Volorio, L. Bernard, G. Pruneri, M. Alcalay and P. G. Pelicci (2006). "Delocalization and destabilization of the Arf tumor suppressor by the leukemia-associated NPM mutant." Cancer research 66(6): 3044-3050.

Cripe, L. D., H. Uno, E. M. Paietta, M. R. Litzow, R. P. Ketterling, J. M. Bennett, J. M. Rowe, H. M. Lazarus, S. Luger and M. S. Tallman (2010). "Zosuquidar, a novel modulator of P-glycoprotein, does not improve the outcome of older patients with newly diagnosed acute myeloid leukemia: a randomized, placebo-controlled trial of the Eastern Cooperative Oncology Group 3999." Blood 116(20): 4077-4085.

Culp-Hill, R., B. M. Stevens, C. L. Jones, S. Pei, M. Dzieciatkowska, M. Minhajuddin, C. T. Jordan and A. D'Alessandro (2023). "Therapy-Resistant Acute Myeloid Leukemia Stem Cells Are Resensitized to Venetoclax + Azacitidine by Targeting Fatty Acid Desaturases 1 and 2." Metabolites 13(4).

Dan, H. C., A. Ebbs, M. Pasparakis, T. Van Dyke, D. S. Basseres and A. S. Baldwin (2014). "Akt-dependent activation of mTORC1 complex involves phosphorylation of mTOR

(mammalian target of rapamycin) by IkappaB kinase alpha (IKKalpha)." J Biol Chem 289(36): 25227-25240.

Daver, N., R. F. Schlenk, N. H. Russell and M. J. Levis (2019). "Targeting FLT3 mutations in AML: review of current knowledge and evidence." Leukemia 33(2): 299-312.

de Figueiredo-Pontes, L. L., M. C. Pintao, L. C. Oliveira, L. F. Dalmazzo, R. H. Jacomo, A. B. Garcia, R. P. Falcao and E. M. Rego (2008). "Determination of P-glycoprotein, MDR-related protein 1, breast cancer resistance protein, and lung-resistance protein expression in leukemic stem cells of acute myeloid leukemia." Cytometry B Clin Cytom 74(3): 163-168.

De Kouchkovsky, I. and M. Abdul-Hay (2016). "Acute myeloid leukemia: a comprehensive review and 2016 update." Blood cancer journal (New York) 6(7): e441.

Deeg, H. J. and B. M. Sandmaier (2010). "Who is fit for allogeneic transplantation?" Blood 116(23): 4762-4770.

Degenhardt, K., R. Mathew, B. Beaudoin, K. Bray, D. Anderson, G. Chen, C. Mukherjee, Y. Shi, C. Gelinas, Y. Fan, D. A. Nelson, S. Jin and E. White (2006). "Autophagy promotes tumor cell survival and restricts necrosis, inflammation, and tumorigenesis." Cancer Cell 10(1): 51-64.

Dembinski, J. L. and S. Krauss (2009). "Characterization and functional analysis of a slow cycling stem cell-like subpopulation in pancreas adenocarcinoma." Clin Exp Metastasis 26(7): 611-623.

Demeter, A., M. C. Romero-Mulero, L. Csabai, M. Olbei, P. Sudhakar, W. Haerty and T. Korcsmaros (2020). "ULK1 and ULK2 are less redundant than previously thought: computational analysis uncovers distinct regulation and functions of these autophagy induction proteins." Sci Rep 10(1): 10940.

DeWolf, S. and M. S. Tallman (2020). "How I treat relapsed or refractory AML." Blood 136(9): 1023-1032.

DiNardo, C. D. and J. E. Cortes (2016). "Mutations in AML: prognostic and therapeutic implications." Hematology Am Soc Hematol Educ Program 2016(1): 348-355.

DiNardo, C. D., B. A. Jonas, V. Pullarkat, M. J. Thirman, J. S. Garcia, A. H. Wei, M. Konopleva, H. Dohner, A. Letai, P. Fenaux, E. Koller, V. Havelange, B. Leber, J. Esteve, J. Wang, V. Pejsa, R. Hajek, K. Porkka, A. Illes, D. Lavie, R. M. Lemoli, K. Yamamoto, S. S. Yoon, J. H. Jang, S. P. Yeh, M. Turgut, W. J. Hong, Y. Zhou, J. Potluri and K. W. Pratz (2020). "Azacitidine and Venetoclax in Previously Untreated Acute Myeloid Leukemia." N Engl J Med 383(7): 617-629.

Dohner, H., E. Estey, D. Grimwade, S. Amadori, F. R. Appelbaum, T. Buchner, H. Dombret, B. L. Ebert, P. Fenaux, R. A. Larson, R. L. Levine, F. Lo-Coco, T. Naoe, D. Niederwieser, G. J. Ossenkoppele, M. Sanz, J. Sierra, M. S. Tallman, H. F. Tien, A. H. Wei, B. Lowenberg and C. D. Bloomfield (2017). "Diagnosis and management of AML in adults: 2017 ELN recommendations from an international expert panel." Blood 129(4): 424-447.

Dohner, H., A. H. Wei, F. R. Appelbaum, C. Craddock, C. D. DiNardo, H. Dombret, B. L. Ebert, P. Fenaux, L. A. Godley, R. P. Hasserjian, R. A. Larson, R. L. Levine, Y. Miyazaki, D. Niederwieser, G. Ossenkoppele, C. Rollig, J. Sierra, E. M. Stein, M. S. Tallman, H. F. Tien, J. Wang, A. Wierzbowska and B. Lowenberg (2022). "Diagnosis and management of AML in adults: 2022 recommendations from an international expert panel on behalf of the ELN." Blood 140(12): 1345-1377.

Dohner, H., D. J. Weisdorf and C. D. Bloomfield (2015). "Acute Myeloid Leukemia." N Engl J Med 373(12): 1136-1152.

Dombret, H., J. F. Seymour, A. Butrym, A. Wierzbowska, D. Selleslag, J. H. Jang, R. Kumar, J. Cavenagh, A. C. Schuh, A. Candoni, C. Recher, I. Sandhu, T. Bernal del Castillo, H. K. Al-Ali,

G. Martinelli, J. Falantes, R. Noppeney, R. M. Stone, M. D. Minden, H. McIntyre, S. Songer, L. M. Lucy, C. L. Beach and H. Dohner (2015). "International phase 3 study of azacitidine vs conventional care regimens in older patients with newly diagnosed AML with >30% blasts." Blood 126(3): 291-299.

Dovey, O. M., J. L. Cooper, A. Mupo, C. S. Grove, C. Lynn, N. Conte, R. M. Andrews, S. Pacharne, K. Tzelepis, M. S. Vijayabaskar, P. Green, R. Rad, M. Arends, P. Wright, K. Yusa, A. Bradley, I. Varela and G. S. Vassiliou (2017). Molecular synergy underlies the co-occurrence patterns and phenotype of NPM1-mutant acute myeloid leukemia. 130: 1911.

Duy, C., M. Li, M. Teater, C. Meydan, F. E. Garrett-Bakelman, T. C. Lee, C. R. Chin, C. Durmaz, K. C. Kawabata, E. Dhimolea, C. S. Mitsiades, H. Doehner, R. J. D'Andrea, M. W. Becker, E. M. Paietta, C. E. Mason, M. Carroll and A. M. Melnick (2021). "Chemotherapy Induces Senescence-Like Resilient Cells Capable of Initiating AML Recurrence." Cancer Discov 11(6): 1542-1561.

Egan, D., J. Kim, R. J. Shaw and K. L. Guan (2011). "The autophagy initiating kinase ULK1 is regulated via opposing phosphorylation by AMPK and mTOR." Autophagy 7(6): 643-644.
Emadi, A. and J. E. Karp (2012). "The clinically relevant pharmacogenomic changes in acute myelogenous leukemia." Pharmacogenomics 13(11): 1257-1269.

Estey, E. and H. Dohner (2006). "Acute myeloid leukaemia." Lancet 368(9550): 1894-1907.
Facchino, S., M. Abdouh, W. Chatoo and G. Bernier (2010). "BMI1 confers radioresistance to normal and cancerous neural stem cells through recruitment of the DNA damage response machinery." J Neurosci 30(30): 10096-10111.

Fajardo-Orduna, G. R., E. Ledesma-Martinez, I. Aguiniga-Sanchez, M. L. Mora-Garcia, B. Weiss-Steider and E. Santiago-Osorio (2021). "Inhibitors of Chemoresistance Pathways in Combination with Ara-C to Overcome Multidrug Resistance in AML. A Mini Review." Int J Mol Sci 22(9).

Falini, B., L. Brunetti, P. Sportoletti and M. P. Martelli (2020). "NPM1-mutated acute myeloid leukemia: from bench to bedside." Blood 136(15): 1707-1721.

Falini, B., C. Mecucci, E. Tiacci, M. Alcalay, R. Rosati, L. Pasqualucci, R. La Starza, D. Diverio, E. Colombo, A. Santucci, B. Bigerna, R. Pacini, A. Pucciarini, A. Liso, M. Vignetti, P. Fazi, N. Meani, V. Pettirossi, G. Saglio, F. Mandelli, F. Lo-Coco, P. G. Pelicci, M. F. Martelli and G. A. L. W. Party (2005). "Cytoplasmic nucleophosmin in acute myelogenous leukemia with a normal karyotype." N Engl J Med 352(3): 254-266.

Fan, X., L. Khaki, T. S. Zhu, M. E. Soules, C. E. Talsma, N. Gul, C. Koh, J. Zhang, Y. M. Li, J. Maciaczyk, G. Nikkhah, F. Dimeco, S. Piccirillo, A. L. Vescovi and C. G. Eberhart (2010). "NOTCH pathway blockade depletes CD133-positive glioblastoma cells and inhibits growth of tumor neurospheres and xenografts." Stem Cells 28(1): 5-16.

Feng, Y., D. He, Z. Yao and D. J. Klionsky (2014). "The machinery of macroautophagy." Cell Res 24(1): 24-41.

Fernandez, H. F., Z. Sun, X. Yao, M. R. Litzow, S. M. Luger, E. M. Paietta, J. Racevskis, G. W. Dewald, R. P. Ketterling, J. M. Bennett, J. M. Rowe, H. M. Lazarus and M. S. Tallman (2009). "Anthracycline dose intensification in acute myeloid leukemia." N Engl J Med 361(13): 1249-1259.

Fircanis, S., P. Merriam, N. Khan and J. J. Castillo (2014). "The relation between cigarette smoking and risk of acute myeloid leukemia: an updated meta-analysis of epidemiological studies." Am J Hematol 89(8): E125-132.

Fischer, K. R., A. Durrans, S. Lee, J. Sheng, F. Li, S. T. Wong, H. Choi, T. El Rayes, S. Ryu, J. Troeger, R. F. Schwabe, L. T. Vahdat, N. K. Altorki, V. Mittal and D. Gao (2015). "Epithelial-to-mesenchymal transition is not required for lung metastasis but contributes to chemoresistance." Nature 527(7579): 472-476.

Folkerts, H., S. Hilgendorf, A. T. J. Wierenga, J. Jaques, A. B. Mulder, P. J. Coffer, J. J. Schuringa and E. Vellenga (2017). "Inhibition of autophagy as a treatment strategy for p53 wild-type acute myeloid leukemia." Cell Death Dis 8(7): e2927.

Foty, R. (2011). "A simple hanging drop cell culture protocol for generation of 3D spheroids." J Vis Exp(51).

Frohling, S., R. F. Schlenk, J. Breitruck, A. Benner, S. Kreitmeier, K. Tobis, H. Dohner, K. Dohner and A. M. L. S. G. U. A. m. leukemia (2002). "Prognostic significance of activating FLT3 mutations in younger adults (16 to 60 years) with acute myeloid leukemia and normal cytogenetics: a study of the AML Study Group Ulm." Blood 100(13): 4372-4380.

Gangemi, R. M., F. Griffero, D. Marubbi, M. Perera, M. C. Capra, P. Malatesta, G. L. Ravetti, G. L. Zona, A. Daga and G. Corte (2009). "SOX2 silencing in glioblastoma tumor-initiating cells causes stop of proliferation and loss of tumorigenicity." Stem Cells 27(1): 40-48.

Ganzel, C., Z. Sun, L. D. Cripe, H. F. Fernandez, D. Douer, J. M. Rowe, E. M. Paietta, R. Ketterling, M. J. O'Connell, P. H. Wiernik, J. M. Bennett, M. R. Litzow, S. M. Luger, H. M. Lazarus and M. S. Tallman (2018). "Very poor long-term survival in past and more recent studies for relapsed AML patients: The ECOG-ACRIN experience." Am J Hematol 93(8): 1074-1081.

Gao, M. Q., Y. P. Choi, S. Kang, J. H. Youn and N. H. Cho (2010). "CD24+ cells from hierarchically organized ovarian cancer are enriched in cancer stem cells." Oncogene 29(18): 2672-2680.

Gao, W., D. Wu, Y. Wang, Z. Wang, C. Zou, Y. Dai, C. F. Ng, J. Y. Teoh and F. L. Chan (2018). "Development of a novel and economical agar-based non-adherent three-dimensional culture method for enrichment of cancer stem-like cells." Stem Cell Res Ther 9(1): 243.

Garg, M., Y. Nagata, D. Kanojia, A. Mayakonda, K. Yoshida, S. Haridas Keloth, Z. J. Zang, Y. Okuno, Y. Shiraishi, K. Chiba, H. Tanaka, S. Miyano, L. W. Ding, T. Alpermann, Q. Y. Sun, D. C. Lin, W. Chien, V. Madan, L. Z. Liu, K. T. Tan, A. Sampath, S. Venkatesan, K. Inokuchi, S. Wakita, H. Yamaguchi, W. J. Chng, S. K. Kham, A. E. Yeoh, M. Sanada, J. Schiller, K. A. Kreuzer, S. M. Kornblau, H. M. Kantarjian, T. Haferlach, M. Lill, M. C. Kuo, L. Y. Shih, I. W. Blau, O. Blau, H. Yang, S. Ogawa and H. P. Koeffler (2015). "Profiling of somatic mutations in acute myeloid leukemia with FLT3-ITD at diagnosis and relapse." Blood 126(22): 2491-2501.

Gheytanchi, E., M. Naseri, F. Karimi-Busheri, F. Atyabi, E. S. Mirsharif, M. Bozorgmehr, R. Ghods and Z. Madjd (2021). "Morphological and molecular characteristics of spheroid formation in HT-29 and Caco-2 colorectal cancer cell lines." Cancer Cell Int 21(1): 204.

Ghosh, S., S. C. Shinde, G. S. Kumaran, R. S. Sapre, S. R. Dhond, Y. Badrinath, R. Ansari, A. Kumar, S. Mahadik, A. B. Chougule and C. N. Nair (2003). "Haematologic and immunophenotypic profile of acute myeloid leukemia: an experience of Tata Memorial Hospital." Indian J Cancer 40(2): 71-76.

Goldman, A., B. Majumder, A. Dhawan, S. Ravi, D. Goldman, M. Kohandel, P. K. Majumder and S. Sengupta (2015). "Temporally sequenced anticancer drugs overcome adaptive resistance by targeting a vulnerable chemotherapy-induced phenotypic transition." Nat Commun 6: 6139.

Gopal, K., N. Gupta, H. Zhang, A. Alshareef, H. Alqahtani, G. Bigras, J. Lewis, D. Douglas, N. Kneteman, A. Lavasanifar and R. Lai (2016). "Oxidative stress induces the acquisition of cancer stem-like phenotype in breast cancer detectable by using a Sox2 regulatory region-2 (SRR2) reporter." Oncotarget 7(3): 3111-3127.

Greif, P. A., L. Hartmann, S. Vosberg, S. M. Stief, R. Mattes, I. Hellmann, K. H. Metzeler, T. Herold, S. A. Bamopoulos, P. Kerbs, V. Jurinovic, D. Schumacher, F. Pastore, K. Braundl, E. Zellmeier, B. Ksienzyk, N. P. Konstandin, S. Schneider, A. Graf, S. Krebs, H. Blum, M. Neumann, C. D. Baldus, S. K. Bohlander, S. Wolf, D. Gorlich, W. E. Berdel, B. J. Wormann, W. Hiddemann and K. Spiekermann (2018). "Evolution of Cytogenetically Normal Acute Myeloid

Leukemia During Therapy and Relapse: An Exome Sequencing Study of 50 Patients." Clin Cancer Res 24(7): 1716-1726.

Greif, P. A., N. P. Konstandin, K. H. Metzeler, T. Herold, Z. Pasalic, B. Ksienzyk, A. Dufour, F. Schneider, S. Schneider, P. M. Kakadia, J. Braess, M. C. Sauerland, W. E. Berdel, T. Buchner, B. J. Woermann, W. Hiddemann, K. Spiekermann and S. K. Bohlander (2012). "RUNX1 mutations in cytogenetically normal acute myeloid leukemia are associated with a poor prognosis and up-regulation of lymphoid genes." Haematologica 97(12): 1909-1915.

Grisolano, J. L., J. O'Neal, J. Cain and M. H. Tomasson (2003). "An activated receptor tyrosine kinase, TEL/PDGFbetaR, cooperates with AML1/ETO to induce acute myeloid leukemia in mice." Proc Natl Acad Sci U S A 100(16): 9506-9511.

Grob, T., A. S. A. Al Hinai, M. A. Sanders, F. G. Kavelaars, M. Rijken, P. L. Gradowska, B. J. Biemond, D. A. Breems, J. Maertens, M. van Marwijk Kooy, T. Pabst, O. de Weerdt, G. J. Ossenkoppele, A. A. van de Loosdrecht, G. A. Huls, J. J. Cornelissen, H. B. Beverloo, B. Lowenberg, M. Jongen-Lavrencic and P. J. M. Valk (2022). "Molecular characterization of mutant TP53 acute myeloid leukemia and high-risk myelodysplastic syndrome." Blood 139(15): 2347-2354.

Guerra, V. A., C. DiNardo and M. Konopleva (2019). "Venetoclax-based therapies for acute myeloid leukemia." Best Pract Res Clin Haematol 32(2): 145-153.

Guo, J. Y., G. Karsli-Uzunbas, R. Mathew, S. C. Aisner, J. J. Kamphorst, A. M. Strohecker, G. Chen, S. Price, W. Lu, X. Teng, E. Snyder, U. Santanam, R. S. Dipaola, T. Jacks, J. D. Rabinowitz and E. White (2013). "Autophagy suppresses progression of K-ras-induced lung tumors to oncocytomas and maintains lipid homeostasis." Genes Dev 27(13): 1447-1461.

Gupta, N., K. Jung, C. Wu, A. Alshareef, H. Alqahtani, S. Damaraju, J. R. Mackey, S. Ghosh, S. Sabri, B. S. Abdulkarim, G. Bigras and R. Lai (2017). "High Myc expression and transcription

activity underlies intra-tumoral heterogeneity in triple-negative breast cancer." Oncotarget 8(17): 28101-28115.

Hanahan, D. (2022). "Hallmarks of Cancer: New Dimensions." Cancer Discov 12(1): 31-46.
Hanekamp, D., J. Cloos and G. J. Schuurhuis (2017). Leukemic stem cells: identification and clinical application, Springer Science and Business Media LLC. 105: 549.

Haraguchi, N., H. Ishii, K. Mimori, F. Tanaka, M. Ohkuma, H. M. Kim, H. Akita, D. Takiuchi, H. Hatano, H. Nagano, G. F. Barnard, Y. Doki and M. Mori (2010). "CD13 is a therapeutic target in human liver cancer stem cells." J Clin Invest 120(9): 3326-3339.

Hardie, D. G., F. A. Ross and S. A. Hawley (2012). "AMPK: a nutrient and energy sensor that maintains energy homeostasis." Nat Rev Mol Cell Biol 13(4): 251-262.

Harir, N., C. Pecquet, M. Kerenyi, K. Sonneck, B. Kovacic, R. Nyga, M. Brevet, I. Dhennin, V. Gouilleux-Gruart, H. Beug, P. Valent, K. Lassoued, R. Moriggl and F. Gouilleux (2007). "Constitutive activation of Stat5 promotes its cytoplasmic localization and association with PI3-kinase in myeloid leukemias." Blood 109(4): 1678-1686.

Hayakawa, F., M. Towatari, H. Kiyoi, M. Tanimoto, T. Kitamura, H. Saito and T. Naoe (2000). "Tandem-duplicated Flt3 constitutively activates STAT5 and MAP kinase and introduces autonomous cell growth in IL-3-dependent cell lines." Oncogene 19(5): 624-631.

He, W., K. Li, F. Wang, Y. R. Qin and Q. X. Fan (2012). "Expression of OCT4 in human esophageal squamous cell carcinoma is significantly associated with poorer prognosis." World J Gastroenterol 18(7): 712-719.

Heath, E. M., S. M. Chan, M. D. Minden, T. Murphy, L. I. Shlush and A. D. Schimmer (2017). "Biological and clinical consequences of NPM1 mutations in AML." Leukemia 31(4): 798-807.
Herreros-Villanueva, M., J. S. Zhang, A. Koenig, E. V. Abel, T. C. Smyrk, W. R. Bamlet, A. A. de Narvajas, T. S. Gomez, D. M. Simeone, L. Bujanda and D. D. Billadeau (2013). "SOX2

promotes dedifferentiation and imparts stem cell-like features to pancreatic cancer cells." Oncogenesis 2(8): e61.

Heydt, Q., C. Larrue, E. Saland, S. Bertoli, J. E. Sarry, A. Besson, S. Manenti, C. Joffre and V. Mansat-De Mas (2018). "Oncogenic FLT3-ITD supports autophagy via ATF4 in acute myeloid leukemia." Oncogene 37(6): 787-797.

Hills, R. K., S. Castaigne, F. R. Appelbaum, J. Delaunay, S. Petersdorf, M. Othus, E. H. Estey, H. Dombret, S. Chevret, N. Ifrah, J. Y. Cahn, C. Recher, L. Chilton, A. V. Moorman and A. K. Burnett (2014). "Addition of gemtuzumab ozogamicin to induction chemotherapy in adult patients with acute myeloid leukaemia: a meta-analysis of individual patient data from randomised controlled trials." Lancet Oncol 15(9): 986-996.

Hirschmann-Jax, C., A. E. Foster, G. G. Wulf, J. G. Nuchtern, T. W. Jax, U. Gobel, M. A. Goodell and M. K. Brenner (2004). "A distinct "side population" of cells with high drug efflux capacity in human tumor cells." Proc Natl Acad Sci U S A 101(39): 14228-14233.

Ho, J. M., S. M. Dobson, V. Voisin, J. McLeod, J. A. Kennedy, A. Mitchell, L. Jin, K. Eppert, G. Bader, M. D. Minden, J. E. Dick and J. C. Y. Wang (2020). "CD200 expression marks leukemia stem cells in human AML." Blood advances 4(21): 5402-5413.

Ho, T. C., M. LaMere, B. M. Stevens, J. M. Ashton, J. R. Myers, K. M. O'Dwyer, J. L. Liesveld, J. H. Mendler, M. Guzman, J. D. Morrissette, J. Zhao, E. S. Wang, M. Wetzler, C. T. Jordan and M. W. Becker (2016). "Evolution of acute myelogenous leukemia stem cell properties after treatment and progression." Blood 128(13): 1671-1678.

Hollein, A., M. Meggendorfer, F. Dicker, S. Jeromin, N. Nadarajah, W. Kern, C. Haferlach and T. Haferlach (2018). "NPM1 mutated AML can relapse with wild-type NPM1: persistent clonal hematopoiesis can drive relapse." Blood Adv 2(22): 3118-3125.

Hosen, N., C. Y. Park, N. Tatsumi, Y. Oji, H. Sugiyama, M. Gramatzki, A. M. Krensky and I. L. Weissman (2007). "CD96 is a leukemic stem cell-specific marker in human acute myeloid leukemia." Proc Natl Acad Sci U S A 104(26): 11008-11013.

Hu, L., C. McArthur and R. B. Jaffe (2010). "Ovarian cancer stem-like side-population cells are tumourigenic and chemoresistant." Br J Cancer 102(8): 1276-1283.

Huang, E. H., M. J. Hynes, T. Zhang, C. Ginestier, G. Dontu, H. Appelman, J. Z. Fields, M. S. Wicha and B. M. Boman (2009). "Aldehyde dehydrogenase 1 is a marker for normal and malignant human colonic stem cells (SC) and tracks SC overpopulation during colon tumorigenesis." Cancer Res 69(8): 3382-3389.

Ishiguro, T., H. Ohata, A. Sato, K. Yamawaki, T. Enomoto and K. Okamoto (2017). "Tumor-derived spheroids: Relevance to cancer stem cells and clinical applications." Cancer Sci 108(3): 283-289.

Ishikawa, F., S. Yoshida, Y. Saito, A. Hijikata, H. Kitamura, S. Tanaka, R. Nakamura, T. Tanaka, H. Tomiyama, N. Saito, M. Fukata, T. Miyamoto, B. Lyons, K. Ohshima, N. Uchida, S. Taniguchi, O. Ohara, K. Akashi, M. Harada and L. D. Shultz (2007). "Chemotherapy-resistant human AML stem cells home to and engraft within the bone-marrow endosteal region." Nature biotechnology 25(11): 1315-1321.

Issa, G. C. and C. D. DiNardo (2021). "Acute myeloid leukemia with IDH1 and IDH2 mutations: 2021 treatment algorithm." Blood Cancer J 11(6): 107.

Jang, J. E., J. I. Eom, H. K. Jeung, J. W. Cheong, J. Y. Lee, J. S. Kim and Y. H. Min (2017). "AMPK-ULK1-Mediated Autophagy Confers Resistance to BET Inhibitor JQ1 in Acute Myeloid Leukemia Stem Cells." Clin Cancer Res 23(11): 2781-2794.

Janiszewska, M., M. L. Suva, N. Riggi, R. H. Houtkooper, J. Auwerx, V. Clement-Schatlo, I. Radovanovic, E. Rheinbay, P. Provero and I. Stamenkovic (2012). "Imp2 controls oxidative

phosphorylation and is crucial for preserving glioblastoma cancer stem cells." Genes Dev 26(17): 1926-1944.

Jeon, H. M. and J. Lee (2017). "MET: roles in epithelial-mesenchymal transition and cancer stemness." Ann Transl Med 5(1): 5.

Jeter, C. R., M. Badeaux, G. Choy, D. Chandra, L. Patrawala, C. Liu, T. Calhoun-Davis, H. Zaehres, G. Q. Daley and D. G. Tang (2009). "Functional evidence that the self-renewal gene NANOG regulates human tumor development." Stem Cells 27(5): 993-1005.

Jiang, F., Q. Qiu, A. Khanna, N. W. Todd, J. Deepak, L. Xing, H. Wang, Z. Liu, Y. Su, S. A. Stass and R. L. Katz (2009). "Aldehyde dehydrogenase 1 is a tumor stem cell-associated marker in lung cancer." Mol Cancer Res 7(3): 330-338.

Jin, L., E. M. Lee, H. S. Ramshaw, S. J. Busfield, A. G. Peoppl, L. Wilkinson, M. A. Guthridge, D. Thomas, E. F. Barry, A. Boyd, D. P. Gearing, G. Vairo, A. F. Lopez, J. E. Dick and R. B. Lock (2009). "Monoclonal antibody-mediated targeting of CD123, IL-3 receptor alpha chain, eliminates human acute myeloid leukemic stem cells." Cell Stem Cell 5(1): 31-42.

Jones, C. L., B. M. Stevens, A. D'Alessandro, J. A. Reisz, R. Culp-Hill, T. Nemkov, S. Pei, N. Khan, B. Adane, H. Ye, A. Krug, D. Reinhold, C. Smith, J. DeGregori, D. A. Pollyea and C. T. Jordan (2018). "Inhibition of Amino Acid Metabolism Selectively Targets Human Leukemia Stem Cells." Cancer Cell 34(5): 724-740 e724.

Jung, C. H., C. B. Jun, S. H. Ro, Y. M. Kim, N. M. Otto, J. Cao, M. Kundu and D. H. Kim (2009). "ULK-Atg13-FIP200 complexes mediate mTOR signaling to the autophagy machinery." Mol Biol Cell 20(7): 1992-2003.

Jung, C. H., S. H. Ro, J. Cao, N. M. Otto and D. H. Kim (2010). "mTOR regulation of autophagy." FEBS Lett 584(7): 1287-1295.

Jung, K., N. Gupta, P. Wang, J. T. Lewis, K. Gopal, F. Wu, X. Ye, A. Alshareef, B. S. Abdulkarim, D. N. Douglas, N. M. Kneteman and R. Lai (2015). "Triple negative breast cancers comprise a highly tumorigenic cell subpopulation detectable by its high responsiveness to a Sox2 regulatory region 2 (SRR2) reporter." Oncotarget 6(12): 10366-10373.

Kamel-Reid, S. and J. E. Dick (1988). "Engraftment of immune-deficient mice with human hematopoietic stem cells." Science 242(4886): 1706-1709.

Kang, M. R., M. S. Kim, J. E. Oh, Y. R. Kim, S. Y. Song, S. S. Kim, C. H. Ahn, N. J. Yoo and S. H. Lee (2009). "Frameshift mutations of autophagy-related genes ATG2B, ATG5, ATG9B and ATG12 in gastric and colorectal cancers with microsatellite instability." J Pathol 217(5): 702-706.

Kazi, J. U. and L. Ronnstrand (2019). "FMS-like Tyrosine Kinase 3/FLT3: From Basic Science to Clinical Implications." Physiol Rev 99(3): 1433-1466.

Kern, W., T. Haferlach, S. Schnittger, W. D. Ludwig, W. Hiddemann and C. Schoch (2002). "Karyotype instability between diagnosis and relapse in 117 patients with acute myeloid leukemia: implications for resistance against therapy." Leukemia 16(10): 2084-2091.

Kersey, J. H., D. Wang and M. Oberto (1998). "Resistance of t(4;11) (MLL-AF4 fusion gene) leukemias to stress-induced cell death: possible mechanism for extensive extramedullary accumulation of cells and poor prognosis." Leukemia 12(10): 1561-1564.

Keysar, S. B. and A. Jimeno (2010). "More than markers: biological significance of cancer stem cell-defining molecules." Mol Cancer Ther 9(9): 2450-2457.

Khoury, J. D., E. Solary, O. Abla, Y. Akkari, R. Alaggio, J. F. Apperley, R. Bejar, E. Berti, L. Busque, J. K. C. Chan, W. Chen, X. Chen, W. J. Chng, J. K. Choi, I. Colmenero, S. E. Coupland, N. C. P. Cross, D. De Jong, M. T. Elghetany, E. Takahashi, J. F. Emile, J. Ferry, L. Fogelstrand, M. Fontenay, U. Germing, S. Gujral, T. Haferlach, C. Harrison, J. C. Hodge, S. Hu, J. H. Jansen,

R. Kanagal-Shamanna, H. M. Kantarjian, C. P. Kratz, X. Q. Li, M. S. Lim, K. Loeb, S. Loghavi, A. Marcogliese, S. Meshinchi, P. Michaels, K. N. Naresh, Y. Natkunam, R. Nejati, G. Ott, E. Padron, K. P. Patel, N. Patkar, J. Picarsic, U. Platzbecker, I. Roberts, A. Schuh, W. Sewell, R. Siebert, P. Tembhare, J. Tyner, S. Verstovsek, W. Wang, B. Wood, W. Xiao, C. Yeung and A. Hochhaus (2022). "The 5th edition of the World Health Organization Classification of Haematolymphoid Tumours: Myeloid and Histiocytic/Dendritic Neoplasms." Leukemia 36(7): 1703-1719.

Kim, E. S. (2017). "Enasidenib: First Global Approval." Drugs 77(15): 1705-1711.

Kim, H. K., S. Y. Son, J. S. Oh, Y. N. Song, J. M. Byun, Y. Koh, J. Hong, S. S. Yoon, C. H. Lee, D. Y. Shin and M. R. Lee (2021). "Metabolic Profiling during Acute Myeloid Leukemia Progression Using Paired Clinical Bone Marrow Serum Samples." Metabolites 11(9).

Kindler, T., D. B. Lipka and T. Fischer (2010). "FLT3 as a therapeutic target in AML: still challenging after all these years." Blood 116(24): 5089-5102.

Kiyoi, H., N. Kawashima and Y. Ishikawa (2020). "FLT3 mutations in acute myeloid leukemia: Therapeutic paradigm beyond inhibitor development." Cancer Sci 111(2): 312-322.

Knapper, S., K. I. Mills, A. F. Gilkes, S. J. Austin, V. Walsh and A. K. Burnett (2006). "The effects of lestaurtinib (CEP701) and PKC412 on primary AML blasts: the induction of cytotoxicity varies with dependence on FLT3 signaling in both FLT3-mutated and wild-type cases." Blood 108(10): 3494-3503.

Kobyakova, M., Y. Lomovskaya, A. Senotov, A. Lomovsky, V. Minaychev, I. Fadeeva, D. Shtatnova, K. Krasnov, A. Zvyagina, I. Odinokova, V. Akatov and R. Fadeev (2022). "The Increase in the Drug Resistance of Acute Myeloid Leukemia THP-1 Cells in High-Density Cell Culture Is Associated with Inflammatory-like Activation and Anti-Apoptotic Bcl-2 Proteins." Int J Mol Sci 23(14).

Konopleva, M., D. A. Pollyea, J. Potluri, B. Chyla, L. Hogdal, T. Busman, E. McKeegan, A. H. Salem, M. Zhu, J. L. Ricker, W. Blum, C. D. DiNardo, T. Kadia, M. Dunbar, R. Kirby, N. Falotico, J. Leverson, R. Humerickhouse, M. Mabry, R. Stone, H. Kantarjian and A. Letai (2016). "Efficacy and Biological Correlates of Response in a Phase II Study of Venetoclax Monotherapy in Patients with Acute Myelogenous Leukemia." Cancer Discov 6(10): 1106-1117.

Kopp, J. L., B. D. Ormsbee, M. Desler and A. Rizzino (2008). "Small increases in the level of Sox2 trigger the differentiation of mouse embryonic stem cells." Stem Cells 26(4): 903-911.

Kottaridis, P. D., R. E. Gale, M. E. Frew, G. Harrison, S. E. Langabeer, A. A. Belton, H. Walker, K. Wheatley, D. T. Bowen, A. K. Burnett, A. H. Goldstone and D. C. Linch (2001). "The presence of a FLT3 internal tandem duplication in patients with acute myeloid leukemia (AML) adds important prognostic information to cytogenetic risk group and response to the first cycle of chemotherapy: analysis of 854 patients from the United Kingdom Medical Research Council AML 10 and 12 trials." Blood 98(6): 1752-1759.

Kroemer, G. (2015). "Autophagy: a druggable process that is deregulated in aging and human disease." J Clin Invest 125(1): 1-4.

Kronke, J., L. Bullinger, V. Teleanu, F. Tschurtz, V. I. Gaidzik, M. W. Kuhn, F. G. Rucker, K. Holzmann, P. Paschka, S. Kapp-Schworer, D. Spath, T. Kindler, M. Schittenhelm, J. Krauter, A. Ganser, G. Gohring, B. Schlegelberger, R. F. Schlenk, H. Dohner and K. Dohner (2013). "Clonal evolution in relapsed NPM1-mutated acute myeloid leukemia." Blood 122(1): 100-108.

Kundu, M., T. Lindsten, C. Y. Yang, J. Wu, F. Zhao, J. Zhang, M. A. Selak, P. A. Ney and C. B. Thompson (2008). "Ulk1 plays a critical role in the autophagic clearance of mitochondria and ribosomes during reticulocyte maturation." Blood 112(4): 1493-1502.

Lagadec, C., E. Vlashi, L. Della Donna, C. Dekmezian and F. Pajonk (2012). "Radiation-induced reprogramming of breast cancer cells." Stem Cells 30(5): 833-844.

Lagadinou, E. D., A. Sach, K. Callahan, R. M. Rossi, S. J. Neering, M. Minhajuddin, J. M. Ashton, S. Pei, V. Grose, K. M. O'Dwyer, J. L. Liesveld, P. S. Brookes, M. W. Becker and C. T. Jordan (2013). "BCL-2 inhibition targets oxidative phosphorylation and selectively eradicates quiescent human leukemia stem cells." Cell Stem Cell 12(3): 329-341.

Lagunas-Rangel, F. A. and V. Chavez-Valencia (2017). "FLT3-ITD and its current role in acute myeloid leukaemia." Med Oncol 34(6): 114.

Lai, J., J. Brandwein, C. Shang, W. Chen, M. P. Chu, I. Sandhu, R. Lai and P. Wang (2022). "The Application of the SORE6 Reporter in the Studies of Acute Myeloid Leukemia - a Novel Model for Disease Relapses." Blood 140(Supplement 1): 9155-9155.

Lapidot, T., C. Sirard, J. Vormoor, B. Murdoch, T. Hoang, J. Caceres-Cortes, M. Mindent, B. Paterson, M. A. Caligiuri and J. E. Dick (1994). A cell initiating human acute myeloid leukaemia after transplantation into SCID mice, Nature. 367: 4.

Lee, E. J. and C. Tournier (2011). "The requirement of uncoordinated 51-like kinase 1 (ULK1) and ULK2 in the regulation of autophagy." Autophagy 7(7): 689-695.

Leis, O., A. Eguiara, E. Lopez-Arribillaga, M. J. Alberdi, S. Hernandez-Garcia, K. Elorriaga, A. Pandiella, R. Rezola and A. G. Martin (2012). "Sox2 expression in breast tumours and activation in breast cancer stem cells." Oncogene 31(11): 1354-1365.

Leung, K. K., A. Nguyen, T. Shi, L. Tang, X. Ni, L. Escoubet, K. J. MacBeth, J. DiMartino and J. A. Wells (2019). "Multiomics of azacitidine-treated AML cells reveals variable and convergent targets that remodel the cell-surface proteome." Proc Natl Acad Sci U S A 116(2): 695-700.

Levine, B. and G. Kroemer (2008). "Autophagy in the pathogenesis of disease." Cell 132(1): 27-42.

Levine, B. and J. Yuan (2005). "Autophagy in cell death: an innocent convict?" J Clin Invest 115(10): 2679-2688.

Ley, T. J., L. Ding, M. J. Walter, M. D. McLellan, T. Lamprecht, D. E. Larson, C. Kandoth, J. E. Payton, J. Baty, J. Welch, C. C. Harris, C. F. Lichti, R. R. Townsend, R. S. Fulton, D. J. Dooling, D. C. Koboldt, H. Schmidt, Q. Zhang, J. R. Osborne, L. Lin, M. O'Laughlin, J. F. McMichael, K. D. Delehaunty, S. D. McGrath, L. A. Fulton, V. J. Magrini, T. L. Vickery, J. Hundal, L. L. Cook, J. J. Conyers, G. W. Swift, J. P. Reed, P. A. Alldredge, T. Wylie, J. Walker, J. Kalicki, M. A. Watson, S. Heath, W. D. Shannon, N. Varghese, R. Nagarajan, P. Westervelt, M. H. Tomasson, D. C. Link, T. A. Graubert, J. F. DiPersio, E. R. Mardis and R. K. Wilson (2010). "DNMT3A mutations in acute myeloid leukemia." N Engl J Med 363(25): 2424-2433.

Li, J., M. Haque, C. Shang, B. Hassan, D. Liu, W. Chen and R. Lai (2021). "Identification and Characterization of Cancer Stem-Like Cells in ALK-Positive Anaplastic Large Cell Lymphoma Using the SORE6 Reporter." Curr Issues Mol Biol 43(2): 543-557.

Li, L., O. Piloto, H. B. Nguyen, K. Greenberg, K. Takamiya, F. Racke, D. Huso and D. Small (2008). "Knock-in of an internal tandem duplication mutation into murine FLT3 confers myeloproliferative disease in a mouse model." Blood 111(7): 3849-3858.

Li, S., L. Chen, W. Jin, X. Ma, Y. Ma, F. Dong, H. Zhu, J. Li and K. Wang (2017). "Influence of body mass index on incidence and prognosis of acute myeloid leukemia and acute promyelocytic leukemia: A meta-analysis." Sci Rep 7(1): 17998.

Li, W. W., J. Li and J. K. Bao (2012). "Microautophagy: lesser-known self-eating." Cell Mol Life Sci 69(7): 1125-1136.

Li, X., M. T. Lewis, J. Huang, C. Gutierrez, C. K. Osborne, M. F. Wu, S. G. Hilsenbeck, A. Pavlick, X. Zhang, G. C. Chamness, H. Wong, J. Rosen and J. C. Chang (2008). "Intrinsic resistance of tumorigenic breast cancer cells to chemotherapy." J Natl Cancer Inst 100(9): 672-679.

Liang, X. H., S. Jackson, M. Seaman, K. Brown, B. Kempkes, H. Hibshoosh and B. Levine (1999). "Induction of autophagy and inhibition of tumorigenesis by beclin 1." Nature 402(6762): 672-676.

Lin, C. L., M. Sojitra, E. J. Carpenter, E. S. Hayhoe, S. Sarkar, E. A. Volker, C. Wang, D. T. Bui, L. Yang, J. S. Klassen, P. Wu, M. S. Macauley, T. L. Lowary and R. Derda (2023). "Chemoenzymatic synthesis of genetically-encoded multivalent liquid N-glycan arrays." Nat Commun 14(1): 5237.

Liu, G., X. Yuan, Z. Zeng, P. Tunici, H. Ng, I. R. Abdulkadir, L. Lu, D. Irvin, K. L. Black and J. S. Yu (2006). "Analysis of gene expression and chemoresistance of CD133+ cancer stem cells in glioblastoma." Mol Cancer 5: 67.

Liu, T., W. Cheng, D. Lai, Y. Huang and L. Guo (2010). "Characterization of primary ovarian cancer cells in different culture systems." Oncol Rep 23(5): 1277-1284.

Loke, J., R. Buka and C. Craddock (2021). "Allogeneic Stem Cell Transplantation for Acute Myeloid Leukemia: Who, When, and How?" Front Immunol 12: 659595.

Lomonaco, S. L., S. Finniss, C. Xiang, A. Decarvalho, F. Umansky, S. N. Kalkanis, T. Mikkelsen and C. Brodie (2009). "The induction of autophagy by gamma-radiation contributes to the radioresistance of glioma stem cells." Int J Cancer 125(3): 717-722.

Luo, W., S. Li, B. Peng, Y. Ye, X. Deng and K. Yao (2013). "Embryonic stem cells markers SOX2, OCT4 and Nanog expression and their correlations with epithelial-mesenchymal transition in nasopharyngeal carcinoma." PLoS One 8(2): e56324.

Ma, I. and A. L. Allan (2011). "The role of human aldehyde dehydrogenase in normal and cancer stem cells." Stem Cell Rev Rep 7(2): 292-306.

Mackarehtschian, K., J. D. Hardin, K. A. Moore, S. Boast, S. P. Goff and I. R. Lemischka (1995). "Targeted disruption of the flk2/flt3 gene leads to deficiencies in primitive hematopoietic progenitors." Immunity 3(1): 147-161.

Marinello, J., M. Delcuratolo and G. Capranico (2018). "Anthracyclines as Topoisomerase II Poisons: From Early Studies to New Perspectives." Int J Mol Sci 19(11).

Marzagalli, M., F. Fontana, M. Raimondi and P. Limonta (2021). "Cancer Stem Cells-Key Players in Tumor Relapse." Cancers (Basel) 13(3).

Mathew, R., S. Kongara, B. Beaudoin, C. M. Karp, K. Bray, K. Degenhardt, G. Chen, S. Jin and E. White (2007). "Autophagy suppresses tumor progression by limiting chromosomal instability." Genes Dev 21(11): 1367-1381.

Mauthe, M., I. Orhon, C. Rocchi, X. Zhou, M. Luhr, K. J. Hijlkema, R. P. Coppes, N. Engedal, M. Mari and F. Reggiori (2018). "Chloroquine inhibits autophagic flux by decreasing autophagosome-lysosome fusion." Autophagy 14(8): 1435-1455.

Maynard, S., A. M. Swistowska, J. W. Lee, Y. Liu, S. T. Liu, A. B. Da Cruz, M. Rao, N. C. de Souza-Pinto, X. Zeng and V. A. Bohr (2008). "Human embryonic stem cells have enhanced repair of multiple forms of DNA damage." Stem Cells 26(9): 2266-2274.

McMahon, C. M., T. Ferng, J. Canaani, E. S. Wang, J. J. D. Morrissette, D. J. Eastburn, M. Pellegrino, R. Durruthy-Durruthy, C. D. Watt, S. Asthana, E. A. Lasater, R. DeFilippis, C. A. C. Peretz, L. H. F. McGary, S. Deihimi, A. C. Logan, S. M. Luger, N. P. Shah, M. Carroll, C. C. Smith and A. E. Perl (2019). "Clonal Selection with RAS Pathway Activation Mediates Secondary Clinical Resistance to Selective FLT3 Inhibition in Acute Myeloid Leukemia." Cancer Discov 9(8): 1050-1063.

Meacham, C. E. and S. J. Morrison (2013). "Tumour heterogeneity and cancer cell plasticity." Nature 501(7467): 328-337.

Medeiros, B. C., A. T. Fathi, C. D. DiNardo, D. A. Pollyea, S. M. Chan and R. Swords (2017). "Isocitrate dehydrogenase mutations in myeloid malignancies." Leukemia 31(2): 272-281.

Menendez, S. T., V. Rey, L. Martinez-Cruzado, M. V. Gonzalez, A. Morales-Molina, L. Santos, V. Blanco, C. Alvarez, O. Estupinan, E. Allonca, J. P. Rodrigo, J. Garcia-Castro, J. M. Garcia-Pedrero and R. Rodriguez (2020). "SOX2 Expression and Transcriptional Activity Identifies a Subpopulation of Cancer Stem Cells in Sarcoma with Prognostic Implications." Cancers (Basel) 12(4).

Mihalyova, J., T. Jelinek, K. Growkova, M. Hrdinka, M. Simicek and R. Hajek (2018). "Venetoclax: A new wave in hematooncology." Exp Hematol 61: 10-25.

Mill, C. P., W. Fiskus, C. D. DiNardo, C. Birdwell, J. A. Davis, T. M. Kadia, K. Takahashi, N. Short, N. Daver, M. Ohanian, G. Borthakur, S. M. Kornblau, M. R. Green, Y. Qi, X. Su, J. D. Khoury and K. N. Bhalla (2022). "Effective therapy for AML with RUNX1 mutation by cotreatment with inhibitors of protein translation and BCL2." Blood 139(6): 907-921.

Mitrea, D. M. and R. W. Kriwacki (2018). "On the relationship status for Arf and NPM1 - it's complicated." FEBS J 285(5): 828-831.

Mizushima, N. (2010). "The role of the Atg1/ULK1 complex in autophagy regulation." Curr Opin Cell Biol 22(2): 132-139.

Mizushima, N., Y. Ohsumi and T. Yoshimori (2002). "Autophagosome formation in mammalian cells." Cell Struct Funct 27(6): 421-429.

Modjtahedi, H., S. Ali and S. Essapen (2012). "Therapeutic application of monoclonal antibodies in cancer: advances and challenges." Br Med Bull 104: 41-59.

Mohsen, S., P. T. Sobash, G. F. Algwaiz, N. Nasef, S. A. Al-Zeidaneen and N. A. Karim (2022). "Autophagy Agents in Clinical Trials for Cancer Therapy: A Brief Review." Curr Oncol 29(3): 1695-1708.

Murayama, T. and N. Gotoh (2019). "Drug resistance mechanisms of cancer stem-like cells and their therapeutic potential as drug targets." Cancer Drug Resist 2(3): 457-470.

Musharraf, S. G., A. J. Siddiqui, T. Shamsi, M. I. Choudhary and A. U. Rahman (2016). "Serum metabonomics of acute leukemia using nuclear magnetic resonance spectroscopy." Sci Rep 6: 30693.

Nathansen, J., F. Meyer, L. Muller, M. Schmitz, K. Borgmann and A. Dubrovska (2021). "Beyond the Double-Strand Breaks: The Role of DNA Repair Proteins in Cancer Stem-Cell Regulation." Cancers (Basel) 13(19).

National Cancer Institute (2023). "SEER cancer stat facts: leukemia – acute myeloid leukemia (AML)." Retrieved October 10, 2023, from https://seer.cancer.gov/statfacts/html/amyl.html.

Ng, S. W., A. Mitchell, J. A. Kennedy, W. C. Chen, J. McLeod, N. Ibrahimova, A. Arruda, A. Popescu, V. Gupta, A. D. Schimmer, A. C. Schuh, K. W. Yee, L. Bullinger, T. Herold, D. Gorlich, T. Buchner, W. Hiddemann, W. E. Berdel, B. Wormann, M. Cheok, C. Preudhomme, H. Dombret, K. Metzeler, C. Buske, B. Lowenberg, P. J. Valk, P. W. Zandstra, M. D. Minden, J. E. Dick and J. C. Wang (2016). "A 17-gene stemness score for rapid determination of risk in acute leukaemia." Nature 540(7633): 433-437.

Norsworthy, K. J., L. Luo, V. Hsu, R. Gudi, S. E. Dorff, D. Przepiorka, A. Deisseroth, Y. L. Shen, C. M. Sheth, R. Charlab, G. M. Williams, K. B. Goldberg, A. T. Farrell and R. Pazdur (2019). "FDA Approval Summary: Ivosidenib for Relapsed or Refractory Acute Myeloid Leukemia with an Isocitrate Dehydrogenase-1 Mutation." Clin Cancer Res 25(11): 3205-3209.

Ohanian, M., U. Rozovski, R. Kanagal-Shamanna, L. V. Abruzzo, S. Loghavi, T. Kadia, A. Futreal, K. Bhalla, Z. Zuo, Y. O. Huh, S. M. Post, P. Ruvolo, G. Garcia-Manero, M. Andreeff, S. Kornblau, G. Borthakur, P. Hu, L. J. Medeiros, K. Takahashi, M. J. Hornbaker, J. Zhang, G. M. Nogueras-Gonzalez, X. Huang, S. Verstovsek, Z. Estrov, S. Pierce, F. Ravandi, H. M. Kantarjian, C. E. Bueso-Ramos and J. E. Cortes (2019). "MYC protein expression is an important prognostic factor in acute myeloid leukemia." Leuk Lymphoma 60(1): 37-48.

Oran, B. and D. J. Weisdorf (2012). "Survival for older patients with acute myeloid leukemia: a population-based study." Haematologica 97(12): 1916-1924.

Pabst, T., L. Kortz, G. M. Fiedler, U. Ceglarek, J. R. Idle and D. Beyoğlu (2017). "The plasma lipidome in acute myeloid leukemia at diagnosis in relation to clinical disease features." BBA Clinical 7: 105-114.

Pádua, D., R. Barros, A. L. Amaral, P. Mesquita, A. F. Freire, M. Sousa, A. F. Maia, I. Caiado, H. Fernandes, A. Pombinho, C. F. Pereira and R. Almeida (2020). "A SOX2 Reporter System Identifies Gastric Cancer Stem-Like Cells Sensitive to Monensin." Cancers (Basel) 12(2): 20.

Pagotto, A., G. Pilotto, E. L. Mazzoldi, M. O. Nicoletto, S. Frezzini, A. Pasto and A. Amadori (2017). "Autophagy inhibition reduces chemoresistance and tumorigenic potential of human ovarian cancer stem cells." Cell Death Dis 8(7): e2943.

Panda, P. K., S. Mukhopadhyay, D. N. Das, N. Sinha, P. P. Naik and S. K. Bhutia (2015). "Mechanism of autophagic regulation in carcinogenesis and cancer therapeutics." Semin Cell Dev Biol 39: 43-55.

Pang, W. W., E. A. Price, D. Sahoo, I. Beerman, W. J. Maloney, D. J. Rossi, S. L. Schrier and I. L. Weissman (2011). "Human bone marrow hematopoietic stem cells are increased in frequency and myeloid-biased with age." Proc Natl Acad Sci U S A 108(50): 20012-20017.

Park, C. Y., D. Tseng and I. L. Weissman (2009). "Cancer stem cell-directed therapies: recent data from the laboratory and clinic." Mol Ther 17(2): 219-230.

Pattingre, S., A. Tassa, X. Qu, R. Garuti, X. H. Liang, N. Mizushima, M. Packer, M. D. Schneider and B. Levine (2005). "Bcl-2 antiapoptotic proteins inhibit Beclin 1-dependent autophagy." Cell 122(6): 927-939.

Pavlovsky, S., M. Eppinger-Helft and F. Sackmann Muriel (1973). "Factors that influence the appearance of central nervous system leukemia." Blood 42(6): 935-938.

Pelcovits, A. and R. Niroula (2020). "Acute Myeloid Leukemia: A Review." R I Med J (2013) 103(3): 38-40.

Pemmaraju, N., H. Kantarjian, F. Ravandi and J. Cortes (2011). "FLT3 inhibitors in the treatment of acute myeloid leukemia: the start of an era?" Cancer 117(15): 3293-3304.

Peng, S., N. J. Maihle and Y. Huang (2010). "Pluripotency factors Lin28 and Oct4 identify a sub-population of stem cell-like cells in ovarian cancer." Oncogene 29(14): 2153-2159.

Perl, A. E., G. Martinelli, J. E. Cortes, A. Neubauer, E. Berman, S. Paolini, P. Montesinos, M. R. Baer, R. A. Larson, C. Ustun, F. Fabbiano, H. P. Erba, A. Di Stasi, R. Stuart, R. Olin, M. Kasner, F. Ciceri, W. C. Chou, N. Podoltsev, C. Recher, H. Yokoyama, N. Hosono, S. S. Yoon, J. H. Lee, T. Pardee, A. T. Fathi, C. Liu, N. Hasabou, X. Liu, E. Bahceci and M. J. Levis (2019). "Gilteritinib or Chemotherapy for Relapsed or Refractory FLT3-Mutated AML." N Engl J Med 381(18): 1728-1740.

Petherick, K. J., O. J. Conway, C. Mpamhanga, S. A. Osborne, A. Kamal, B. Saxty and I. G. Ganley (2015). "Pharmacological inhibition of ULK1 kinase blocks mammalian target of rapamycin (mTOR)-dependent autophagy." J Biol Chem 290(48): 28726.

Phi, L. T. H., I. N. Sari, Y. G. Yang, S. H. Lee, N. Jun, K. S. Kim, Y. K. Lee and H. Y. Kwon (2018). "Cancer Stem Cells (CSCs) in Drug Resistance and their Therapeutic Implications in Cancer Treatment." Stem Cells Int 2018: 5416923.

Pike, L. R., D. C. Singleton, F. Buffa, O. Abramczyk, K. Phadwal, J. L. Li, A. K. Simon, J. T. Murray and A. L. Harris (2013). "Transcriptional up-regulation of ULK1 by ATF4 contributes to cancer cell survival." Biochem J 449(2): 389-400.

Piloto, O., M. Wright, P. Brown, K. T. Kim, M. Levis and D. Small (2007). "Prolonged exposure to FLT3 inhibitors leads to resistance via activation of parallel signaling pathways." Blood 109(4): 1643-1652.

Pinho, S. S. and C. A. Reis (2015). "Glycosylation in cancer: mechanisms and clinical implications." Nat Rev Cancer 15(9): 540-555.

Pinz, S., S. Unser and A. Rascle (2016). "Signal transducer and activator of transcription STAT5 is recruited to c-Myc super-enhancer." BMC Mol Biol 17: 10.

Pluquet, O., C. Abbadie and O. Coqueret (2019). "Connecting cancer relapse with senescence." Cancer Lett 463: 50-58.

Poitras, J. L., D. Heiser, L. Li, B. Nguyen, K. Nagai, A. S. Duffield, C. Gamper and D. Small (2016). "Dnmt3a deletion cooperates with the Flt3/ITD mutation to drive leukemogenesis in a murine model." Oncotarget 7(43): 69124-69135.

Pollyea, D. A., B. M. Stevens, C. L. Jones, A. Winters, S. Pei, M. Minhajuddin, A. D'Alessandro, R. Culp-Hill, K. A. Riemondy, A. E. Gillen, J. R. Hesselberth, D. Abbott, D. Schatz, J. A. Gutman, E. Purev, C. Smith and C. T. Jordan (2018). "Venetoclax with azacitidine disrupts energy metabolism and targets leukemia stem cells in patients with acute myeloid leukemia." Nat Med 24(12): 1859-1866.

Qadir, M. A., B. Kwok, W. H. Dragowska, K. H. To, D. Le, M. B. Bally and S. M. Gorski (2008). "Macroautophagy inhibition sensitizes tamoxifen-resistant breast cancer cells and enhances mitochondrial depolarization." Breast Cancer Res Treat 112(3): 389-403.

Qu, X., J. Yu, G. Bhagat, N. Furuya, H. Hibshoosh, A. Troxel, J. Rosen, E. L. Eskelinen, N. Mizushima, Y. Ohsumi, G. Cattoretti and B. Levine (2003). "Promotion of tumorigenesis by heterozygous disruption of the beclin 1 autophagy gene." J Clin Invest 112(12): 1809-1820.

Quentmeier, H., J. Reinhardt, M. Zaborski and H. G. Drexler (2003). "FLT3 mutations in acute myeloid leukemia cell lines." Leukemia 17(1): 120-124.

Raaijmakers, M. H., E. P. de Grouw, L. H. Heuver, B. A. van der Reijden, J. H. Jansen, R. J. Scheper, G. L. Scheffer, T. J. de Witte and R. A. Raymakers (2005). "Breast cancer resistance protein in drug resistance of primitive CD34+38- cells in acute myeloid leukemia." Clin Cancer Res 11(6): 2436-2444.

Ram, R., C. Scheid, O. Amit, J. M. Chemnitz, Y. Moshe, M. Hallek, D. Wolf, I. Avivi and U. Holtick (2019). "Sequential therapy for patients with primary refractory acute myeloid leukemia: a historical prospective analysis of the German and Israeli experience." Haematologica 104(9): 1798-1803.

Randhawa, R., M. Sehgal, T. R. Singh, A. Duseja and H. Changotra (2015). "Unc-51 like kinase 1 (ULK1) in silico analysis for biomarker identification: a vital component of autophagy." Gene 562(1): 40-49.

Rix, B., A. H. Maduro, K. S. Bridge and W. Grey (2022). "Markers for human haematopoietic stem cells: The disconnect between an identification marker and its function." Front Physiol 13: 1009160.

Ro, S. H., C. H. Jung, W. S. Hahn, X. Xu, Y. M. Kim, Y. S. Yun, J. M. Park, K. H. Kim, M. Seo, T. Y. Ha, E. A. Arriaga, D. A. Bernlohr and D. H. Kim (2013). "Distinct functions of Ulk1 and Ulk2 in the regulation of lipid metabolism in adipocytes." Autophagy 9(12): 2103-2114.

Rocha, C. R. R., L. K. Lerner, O. K. Okamoto, M. C. Marchetto and C. F. M. Menck (2013). "The role of DNA repair in the pluripotency and differentiation of human stem cells." Mutat Res 752(1): 25-35.

Rosas-Cruz, A., N. Salinas-Jazmin, A. Valdes-Rives and M. A. Velasco-Velazquez (2022). "DRD1 and DRD4 are differentially expressed in breast tumors and breast cancer stem cells: pharmacological implications." Transl Cancer Res 11(11): 3941-3950.

Saha, M. and S. Das (2021). "Free radical induced activity of an anthracycline analogue and its Mn(II) complex on biological targets through in situ electrochemical generation of semiquinone." Heliyon 7(8): e07746.

Saillard, C., M. Darmon, M. Bisbal, A. Sannini, L. Chow-Chine, M. Faucher, E. Lengline, N. Vey, D. Blaise, E. Azoulay, D. Mokart and d. O.-H. on behalf the Groupe de Recherche en Reanimation Respiratoire du patient (2018). "Critically ill allogenic HSCT patients in the intensive care unit: a systematic review and meta-analysis of prognostic factors of mortality." Bone Marrow Transplant 53(10): 1233-1241.

Saleh, T., L. Tyutyunyk-Massey, G. F. Murray, M. R. Alotaibi, A. S. Kawale, Z. Elsayed, S. C. Henderson, V. Yakovlev, L. W. Elmore, A. Toor, H. Harada, J. Reed, J. W. Landry and D. A. Gewirtz (2019). "Tumor cell escape from therapy-induced senescence." Biochem Pharmacol 162: 202-212.

Samaras, P., M. Tusup, T. D. L. Nguyen-Kim, B. Seifert, H. Bachmann, R. von Moos, A. Knuth and S. Pascolo (2017). "Phase I study of a chloroquine-gemcitabine combination in patients with metastatic or unresectable pancreatic cancer." Cancer Chemother Pharmacol 80(5): 1005-1012.

Samra, B., G. Richard-Carpentier, T. M. Kadia, F. Ravandi, N. Daver, C. D. DiNardo, G. C. Issa, P. Bose, M. Y. Konopleva, M. Yilmaz, M. Ohanian, G. Borthakur, G. Garcia-Manero, S. Pierce, J. E. Cortes, H. Kantarjian and N. J. Short (2020). "Characteristics and outcomes of patients with therapy-related acute myeloid leukemia with normal karyotype." Blood Cancer J 10(5): 47.

Sato, T., X. Yang, S. Knapper, P. White, B. D. Smith, S. Galkin, D. Small, A. Burnett and M. Levis (2011). "FLT3 ligand impedes the efficacy of FLT3 inhibitors in vitro and in vivo." Blood 117(12): 3286-3293.

Saultz, J. N. and R. Garzon (2016). "Acute Myeloid Leukemia: A Concise Review." J Clin Med 5(3).

Scarpa, M., P. Singh, C. M. Bailey, J. K. Lee, S. Kapoor, R. G. Lapidus, S. Niyongere, J. Sangodkar, Y. Wang, D. Perrotti, G. Narla and M. R. Baer (2021). "PP2A-activating Drugs Enhance FLT3 Inhibitor Efficacy through AKT Inhibition-Dependent GSK-3beta-Mediated c-Myc and Pim-1 Proteasomal Degradation." Mol Cancer Ther 20(4): 676-690.

Schaich, M., S. Soucek, C. Thiede, G. Ehninger, T. Illmer and S. A. S. Group (2005). "MDR1 and MRP1 gene expression are independent predictors for treatment outcome in adult acute myeloid leukaemia." Br J Haematol 128(3): 324-332.

Scholl, S., M. Fleischmann, U. Schnetzke and F. H. Heidel (2020). "Molecular Mechanisms of Resistance to FLT3 Inhibitors in Acute Myeloid Leukemia: Ongoing Challenges and Future Treatments." Cells 9(11).

Seedhouse, C. H., M. Pallis, M. Grundy, S. Shang and N. H. Russell (2009). "FLT3-ITD expression levels and their effect on STAT5 in AML with and without NPM mutations." Br J Haematol 147(5): 653-661.

Seigel, G. M., L. M. Campbell, M. Narayan and F. Gonzalez-Fernandez (2005). "Cancer stem cell characteristics in retinoblastoma." Mol Vis 11: 729-737.

Shan, X., J. J. Fung, A. Kosaka, G. Danet-Desnoyers and B. Reproducibility Project: Cancer (2017). "Replication Study: Inhibition of BET recruitment to chromatin as an effective treatment for MLL-fusion leukaemia." Elife 6.

Shang, C., B. Hassan, M. Haque, Y. Song, J. Li, D. Liu, E. Lipke, W. Chen, S. Giuriato and R. Lai (2021). "Crizotinib Resistance Mediated by Autophagy Is Higher in the Stem-Like Cell Subset in ALK-Positive Anaplastic Large Cell Lymphoma, and This Effect Is MYC-Dependent." Cancers (Basel) 13(2).

Shantz, L. M. and A. E. Pegg (1999). "Translational regulation of ornithine decarboxylase and other enzymes of the polyamine pathway." Int J Biochem Cell Biol 31(1): 107-122.

Sharma, S. V., D. Y. Lee, B. Li, M. P. Quinlan, F. Takahashi, S. Maheswaran, U. McDermott, N. Azizian, L. Zou, M. A. Fischbach, K. K. Wong, K. Brandstetter, B. Wittner, S. Ramaswamy, M. Classon and J. Settleman (2010). "A chromatin-mediated reversible drug-tolerant state in cancer cell subpopulations." Cell 141(1): 69-80.

Shim, D., L. Duan and C. G. Maki (2021). "P53-regulated autophagy and its impact on drug resistance and cell fate." Cancer Drug Resist 4(1): 85-95.

Shin, S. H., E. J. Lee, J. Chun, S. Hyun and S. S. Kang (2015). "ULK2 Ser 1027 Phosphorylation by PKA Regulates Its Nuclear Localization Occurring through Karyopherin Beta 2 Recognition of a PY-NLS Motif." PLoS One 10(6): e0127784.

Shlush, L. I., A. Mitchell, L. Heisler, S. Abelson, S. W. K. Ng, A. Trotman-Grant, J. J. F. Medeiros, A. Rao-Bhatia, I. Jaciw-Zurakowsky, R. Marke, J. L. McLeod, M. Doedens, G. Bader, V. Voisin, C. Xu, J. D. McPherson, T. J. Hudson, J. C. Y. Wang, M. D. Minden and J. E. Dick (2017). "Tracing the origins of relapse in acute myeloid leukaemia to stem cells." Nature 547(7661): 104-108.

Sholl, L. M., J. A. Barletta, B. Y. Yeap, L. R. Chirieac and J. L. Hornick (2010). "Sox2 protein expression is an independent poor prognostic indicator in stage I lung adenocarcinoma." Am J Surg Pathol 34(8): 1193-1198.

Singh, S. S., S. Vats, A. Y. Chia, T. Z. Tan, S. Deng, M. S. Ong, F. Arfuso, C. T. Yap, B. C. Goh, G. Sethi, R. Y. Huang, H. M. Shen, R. Manjithaya and A. P. Kumar (2018). "Dual role of autophagy in hallmarks of cancer." Oncogene 37(9): 1142-1158.

Skvortsov, S., P. Debbage, P. Lukas and I. Skvortsova (2015). "Crosstalk between DNA repair and cancer stem cell (CSC) associated intracellular pathways." Semin Cancer Biol 31: 36-42.

Smith, A. G. and K. F. Macleod (2019). "Autophagy, cancer stem cells and drug resistance." J Pathol 247(5): 708-718.

Smith, C. C., Q. Wang, C. S. Chin, S. Salerno, L. E. Damon, M. J. Levis, A. E. Perl, K. J. Travers, S. Wang, J. P. Hunt, P. P. Zarrinkar, E. E. Schadt, A. Kasarskis, J. Kuriyan and N. P. Shah (2012). "Validation of ITD mutations in FLT3 as a therapeutic target in human acute myeloid leukaemia." Nature 485(7397): 260-263.

Sood, R., N. F. Hansen, F. X. Donovan, B. Carrington, D. Bucci, B. Maskeri, A. Young, N. S. Trivedi, J. Kohlschmidt, R. M. Stone, M. A. Caligiuri, S. C. Chandrasekharappa, G. Marcucci, J. C. Mullikin, C. D. Bloomfield and P. Liu (2016). "Somatic mutational landscape of AML with inv(16) or t(8;21) identifies patterns of clonal evolution in relapse leukemia." Leukemia 30(2): 501-504.

Spiekermann, K., K. Bagrintseva, R. Schwab, K. Schmieja and W. Hiddemann (2003). "Overexpression and constitutive activation of FLT3 induces STAT5 activation in primary acute myeloid leukemia blast cells." Clin Cancer Res 9(6): 2140-2150.

Stanisic, S. and M. Kalaycio (2002). "Treatment of refractory and relapsed acute myelogenous leukemia." Expert Rev Anticancer Ther 2(3): 287-295.

Stone, R. M., S. J. Mandrekar, B. L. Sanford, K. Laumann, S. Geyer, C. D. Bloomfield, C. Thiede, T. W. Prior, K. Dohner, G. Marcucci, F. Lo-Coco, R. B. Klisovic, A. Wei, J. Sierra, M. A. Sanz, J. M. Brandwein, T. de Witte, D. Niederwieser, F. R. Appelbaum, B. C. Medeiros, M. S. Tallman, J. Krauter, R. F. Schlenk, A. Ganser, H. Serve, G. Ehninger, S. Amadori, R. A. Larson and H. Dohner (2017). "Midostaurin plus Chemotherapy for Acute Myeloid Leukemia with a FLT3 Mutation." N Engl J Med 377(5): 454-464.

Storms, R. W., A. P. Trujillo, J. B. Springer, L. Shah, O. M. Colvin, S. M. Ludeman and C. Smith (1999). "Isolation of primitive human hematopoietic progenitors on the basis of aldehyde dehydrogenase activity." Proc Natl Acad Sci U S A 96(16): 9118-9123.

Strickland, S. A. and N. Vey (2022). "Diagnosis and treatment of therapy-related acute myeloid leukemia." Crit Rev Oncol Hematol 171: 103607.

Takahashi, K., K. Tanabe, M. Ohnuki, M. Narita, T. Ichisaka, K. Tomoda and S. Yamanaka (2007). "Induction of pluripotent stem cells from adult human fibroblasts by defined factors." Cell 131(5): 861-872.

Tamamyan, G., T. Kadia, F. Ravandi, G. Borthakur, J. Cortes, E. Jabbour, N. Daver, M. Ohanian, H. Kantarjian and M. Konopleva (2017). "Frontline treatment of acute myeloid leukemia in adults." Crit Rev Oncol Hematol 110: 20-34.

Tang, B., A. Raviv, D. Esposito, K. C. Flanders, C. Daniel, B. T. Nghiem, S. Garfield, L. Lim, P. Mannan, A. I. Robles, W. I. Smith, Jr., J. Zimmerberg, R. Ravin and L. M. Wakefield (2015). "A flexible reporter system for direct observation and isolation of cancer stem cells." Stem Cell Reports 4(1): 155-169.

Tasdemir, E., M. C. Maiuri, L. Galluzzi, I. Vitale, M. Djavaheri-Mergny, M. D'Amelio, A. Criollo, E. Morselli, C. Zhu, F. Harper, U. Nannmark, C. Samara, P. Pinton, J. M. Vicencio, R. Carnuccio, U. M. Moll, F. Madeo, P. Paterlini-Brechot, R. Rizzuto, G. Szabadkai, G. Pierron, K.

Blomgren, N. Tavernarakis, P. Codogno, F. Cecconi and G. Kroemer (2008). "Regulation of autophagy by cytoplasmic p53." Nat Cell Biol 10(6): 676-687.

Taussig, D. C., F. Miraki-Moud, F. Anjos-Afonso, D. J. Pearce, K. Allen, C. Ridler, D. Lillington, H. Oakervee, J. Cavenagh, S. G. Agrawal, T. A. Lister, J. G. Gribben and D. Bonnet (2008). "Anti-CD38 antibody-mediated clearance of human repopulating cells masks the heterogeneity of leukemia-initiating cells." Blood 112(3): 568-575.

Taussig, D. C., J. Vargaftig, F. Miraki-Moud, E. Griessinger, K. Sharrock, T. Luke, D. Lillington, H. Oakervee, J. Cavenagh, S. G. Agrawal, T. A. Lister, J. G. Gribben and D. Bonnet (2010). "Leukemia-initiating cells from some acute myeloid leukemia patients with mutated nucleophosmin reside in the CD34(-) fraction." Blood 115(10): 1976-1984.

Tenold, M. E., B. N. Moskoff, D. J. Benjamin, R. T. Hoeg, A. S. Rosenberg, M. Abedi, J. M. Tuscano and B. A. Jonas (2021). "Outcomes of Adults With Relapsed/Refractory Acute Myeloid Leukemia Treated With Venetoclax Plus Hypomethylating Agents at a Comprehensive Cancer Center." Front Oncol 11: 649209.

Thol, F. and A. Ganser (2020). "Treatment of Relapsed Acute Myeloid Leukemia." Curr Treat Options Oncol 21(8): 66.

Thol, F., R. F. Schlenk, M. Heuser and A. Ganser (2015). "How I treat refractory and early relapsed acute myeloid leukemia." Blood 126(3): 319-327.

To, K., A. Fotovati, K. M. Reipas, J. H. Law, K. Hu, J. Wang, A. Astanehe, A. H. Davies, L. Lee, A. L. Stratford, A. Raouf, P. Johnson, I. M. Berquin, H. D. Royer, C. J. Eaves and S. E. Dunn (2010). "Y-box binding protein-1 induces the expression of CD44 and CD49f leading to enhanced self-renewal, mammosphere growth, and drug resistance." Cancer Res 70(7): 2840-2851.

Tomic, B., T. Smoljo, H. Lalic, V. Dembitz, J. Batinic, D. Batinic, A. Bedalov and D. Visnjic (2022). "Cytarabine-induced differentiation of AML cells depends on Chk1 activation and shares the mechanism with inhibitors of DHODH and pyrimidine synthesis." Sci Rep 12(1): 11344.

Tothova, E., M. Fricova, N. Stecova, A. Kafkova and A. Elbertova (2002). "High expression of Bcl-2 protein in acute myeloid leukemia cells is associated with poor response to chemotherapy." Neoplasma 49(3): 141-144.

Tsai, R. J., S. E. Luckhaupt, P. Schumacher, R. D. Cress, D. M. Deapen and G. M. Calvert (2014). "Acute myeloid leukemia risk by industry and occupation." Leuk Lymphoma 55(11): 2584-2591.

Vaddi, P. K., M. A. Stamnes, H. Cao and S. Chen (2019). "Elimination of SOX2/OCT4-Associated Prostate Cancer Stem Cells Blocks Tumor Development and Enhances Therapeutic Response." Cancers (Basel) 11(9).

Vasconcelos, F. C., P. S. de Souza, T. Hancio, F. C. C. de Faria and R. C. Maia (2021). "Update on drug transporter proteins in acute myeloid leukemia: Pathological implication and clinical setting." Crit Rev Oncol Hematol 160: 103281.

Vassiliou, G. S., J. L. Cooper, R. Rad, J. Li, S. Rice, A. Uren, L. Rad, P. Ellis, R. Andrews, R. Banerjee, C. Grove, W. Wang, P. Liu, P. Wright, M. Arends and A. Bradley (2011). "Mutant nucleophosmin and cooperating pathways drive leukemia initiation and progression in mice." Nature genetics 43(5): 470-475.

Venditti, A., G. Del Poeta, L. Maurillo, F. Buccisano, M. I. Del Principe, C. Mazzone, A. Tamburini, C. Cox, P. Panetta, B. Neri, L. Ottaviani and S. Amadori (2004). "Combined analysis of bcl-2 and MDR1 proteins in 256 cases of acute myeloid leukemia." Haematologica 89(8): 934-939.

Venugopal, S., K. Takahashi, N. Daver, A. Maiti, G. Borthakur, S. Loghavi, N. J. Short, M. Ohanian, L. Masarova, G. Issa, X. Wang, B. R. Carlos, M. Yilmaz, T. Kadia, M. Andreeff, F. Ravandi, M. Konopleva, H. M. Kantarjian and C. D. DiNardo (2022). "Efficacy and safety of enasidenib and azacitidine combination in patients with IDH2 mutated acute myeloid leukemia and not eligible for intensive chemotherapy." Blood Cancer J 12(1): 10.

Vessoni, A. T., E. C. Filippi-Chiela, C. F. Menck and G. Lenz (2013). "Autophagy and genomic integrity." Cell Death Differ 20(11): 1444-1454.

Vetrie, D., G. V. Helgason and M. Copland (2020). "The leukaemia stem cell: similarities, differences and clinical prospects in CML and AML." Nature reviews.Cancer 20(3): 158-173.

Viale, A., P. Pettazzoni, C. A. Lyssiotis, H. Ying, N. Sanchez, M. Marchesini, A. Carugo, T. Green, S. Seth, V. Giuliani, M. Kost-Alimova, F. Muller, S. Colla, L. Nezi, G. Genovese, A. K. Deem, A. Kapoor, W. Yao, E. Brunetto, Y. Kang, M. Yuan, J. M. Asara, Y. A. Wang, T. P. Heffernan, A. C. Kimmelman, H. Wang, J. B. Fleming, L. C. Cantley, R. A. DePinho and G. F. Draetta (2014). "Oncogene ablation-resistant pancreatic cancer cells depend on mitochondrial function." Nature 514(7524): 628-632.

Vincent, Z., K. Urakami, K. Maruyama, K. Yamaguchi and M. Kusuhara (2014). "CD133-positive cancer stem cells from Colo205 human colon adenocarcinoma cell line show resistance to chemotherapy and display a specific metabolomic profile." Genes Cancer 5(7-8): 250-260.

Vosberg, S. and P. A. Greif (2019). "Clonal evolution of acute myeloid leukemia from diagnosis to relapse." Genes Chromosomes Cancer 58(12): 839-849.

Walker, M. R., H. L. Goel, D. Mukhopadhyay, P. Chhoy, E. R. Karner, J. L. Clark, H. Liu, R. Li, J. L. Zhu, S. Chen, L. K. Mahal, B. A. Bensing and A. M. Mercurio (2022). "O-linked alpha2,3 sialylation defines stem cell populations in breast cancer." Sci Adv 8(1): eabj9513.

Wang, B., R. Iyengar, X. Li-Harms, J. H. Joo, C. Wright, A. Lavado, L. Horner, M. Yang, J. L. Guan, S. Frase, D. R. Green, X. Cao and M. Kundu (2018). "The autophagy-inducing kinases, ULK1 and ULK2, regulate axon guidance in the developing mouse forebrain via a noncanonical pathway." Autophagy 14(5): 796-811.

Wang, Y., L. Zhang, W. L. Chen, J. H. Wang, N. Li, J. M. Li, J. Q. Mi, W. N. Zhang, Y. Li, S. F. Wu, J. Jin, Y. G. Wang, H. Huang, Z. Chen, S. J. Chen and H. Tang (2013). "Rapid diagnosis and prognosis of de novo acute myeloid leukemia by serum metabonomic analysis." J Proteome Res 12(10): 4393-4401.

Warburg, O. (1956). "On the origin of cancer cells." Science 123(3191): 309-314.
Wassenberg, D., W. Liebl and R. Jaenicke (2000). "Maltose-binding protein from the hyperthermophilic bacterium Thermotoga maritima: stability and binding properties." J Mol Biol 295(2): 279-288.

Wei, A. H., P. Montesinos, V. Ivanov, C. D. DiNardo, J. Novak, K. Laribi, I. Kim, D. A. Stevens, W. Fiedler, M. Pagoni, O. Samoilova, Y. Hu, A. Anagnostopoulos, J. Bergeron, J. Z. Hou, V. Murthy, T. Yamauchi, A. McDonald, B. Chyla, S. Gopalakrishnan, Q. Jiang, W. Mendes, J. Hayslip and P. Panayiotidis (2020). "Venetoclax plus LDAC for newly diagnosed AML ineligible for intensive chemotherapy: a phase 3 randomized placebo-controlled trial." Blood 135(24): 2137-2145.

Wei, H., S. Wei, B. Gan, X. Peng, W. Zou and J. L. Guan (2011). "Suppression of autophagy by FIP200 deletion inhibits mammary tumorigenesis." Genes Dev 25(14): 1510-1527.

Wei, Y., S. Pattingre, S. Sinha, M. Bassik and B. Levine (2008). "JNK1-mediated phosphorylation of Bcl-2 regulates starvation-induced autophagy." Mol Cell 30(6): 678-688.

Wolpin, B. M., D. A. Rubinson, X. Wang, J. A. Chan, J. M. Cleary, P. C. Enzinger, C. S. Fuchs, N. J. McCleary, J. A. Meyerhardt, K. Ng, D. Schrag, A. L. Sikora, B. A. Spicer, L. Killion, H. Mamon and A. C. Kimmelman (2014). "Phase II and pharmacodynamic study of autophagy

inhibition using hydroxychloroquine in patients with metastatic pancreatic adenocarcinoma." Oncologist 19(6): 637-638.

Wong, P. M., C. Puente, I. G. Ganley and X. Jiang (2013). "The ULK1 complex: sensing nutrient signals for autophagy activation." Autophagy 9(2): 124-137.

Wu, C., N. Gupta, Y. H. Huang, H. F. Zhang, A. Alshareef, A. Chow and R. Lai (2018). "Oxidative stress enhances tumorigenicity and stem-like features via the activation of the Wnt/beta-catenin/MYC/Sox2 axis in ALK-positive anaplastic large-cell lymphoma." BMC Cancer 18(1): 361.

Wu, C., H. F. Zhang, N. Gupta, A. Alshareef, Q. Wang, Y. H. Huang, J. T. Lewis, D. N. Douglas, N. M. Kneteman and R. Lai (2016). "A positive feedback loop involving the Wnt/beta-catenin/MYC/Sox2 axis defines a highly tumorigenic cell subpopulation in ALK-positive anaplastic large cell lymphoma." J Hematol Oncol 9(1): 120.

Wu, Y. T., H. L. Tan, G. Shui, C. Bauvy, Q. Huang, M. R. Wenk, C. N. Ong, P. Codogno and H. M. Shen (2010). "Dual role of 3-methyladenine in modulation of autophagy via different temporal patterns of inhibition on class I and III phosphoinositide 3-kinase." J Biol Chem 285(14): 10850-10861.

Wuchter, C., K. Leonid, V. Ruppert, M. Schrappe, T. Buchner, C. Schoch, T. Haferlach, J. Harbott, R. Ratei, B. Dorken and W. D. Ludwig (2000). "Clinical significance of P-glycoprotein expression and function for response to induction chemotherapy, relapse rate and overall survival in acute leukemia." Haematologica 85(7): 711-721.

Xie, Y., J. Li, R. Kang and D. Tang (2020). "Interplay Between Lipid Metabolism and Autophagy." Front Cell Dev Biol 8: 431.

Xu, C. X., M. Xu, L. Tan, H. Yang, J. Permuth-Wey, P. A. Kruk, R. M. Wenham, S. V. Nicosia, J. M. Lancaster, T. A. Sellers and J. Q. Cheng (2012). "MicroRNA miR-214 regulates ovarian cancer cell stemness by targeting p53/Nanog." J Biol Chem 287(42): 34970-34978.

Xu, R., Z. Ji, C. Xu and J. Zhu (2018). "The clinical value of using chloroquine or hydroxychloroquine as autophagy inhibitors in the treatment of cancers: A systematic review and meta-analysis." Medicine (Baltimore) 97(46): e12912.

Yada, M., S. Hatakeyama, T. Kamura, M. Nishiyama, R. Tsunematsu, H. Imaki, N. Ishida, F. Okumura, K. Nakayama and K. I. Nakayama (2004). "Phosphorylation-dependent degradation of c-Myc is mediated by the F-box protein Fbw7." EMBO J 23(10): 2116-2125.

Yamauchi, T., Y. Matsuda, T. Tasaki, E. Negoro, S. Ikegaya, K. Takagi, A. Yoshida, Y. Urasaki and T. Ueda (2012). "Induction of DNA strand breaks is critical to predict the cytotoxicity of gemtuzumab ozogamicin against leukemic cells." Cancer Sci 103(9): 1722-1729.

Yang, L., R. Rau and M. A. Goodell (2015). "DNMT3A in haematological malignancies." Nat Rev Cancer 15(3): 152-165.

Yang, M. C., H. C. Wang, Y. C. Hou, H. L. Tung, T. J. Chiu and Y. S. Shan (2015). "Blockade of autophagy reduces pancreatic cancer stem cell activity and potentiates the tumoricidal effect of gemcitabine." Mol Cancer 14: 179.

Yang, S., X. Wang, G. Contino, M. Liesa, E. Sahin, H. Ying, A. Bause, Y. Li, J. M. Stommel, G. Dell'antonio, J. Mautner, G. Tonon, M. Haigis, O. S. Shirihai, C. Doglioni, N. Bardeesy and A. C. Kimmelman (2011). "Pancreatic cancers require autophagy for tumor growth." Genes Dev 25(7): 717-729.

Yang, Z. and D. J. Klionsky (2009). "An overview of the molecular mechanism of autophagy." Curr Top Microbiol Immunol 335: 1-32.

Yilmaz, M., F. Wang, S. Loghavi, C. Bueso-Ramos, C. Gumbs, L. Little, X. Song, J. Zhang, T. Kadia, G. Borthakur, E. Jabbour, N. Pemmaraju, N. Short, G. Garcia-Manero, Z. Estrov, H. Kantarjian, A. Futreal, K. Takahashi and F. Ravandi (2019). "Late relapse in acute myeloid leukemia (AML): clonal evolution or therapy-related leukemia?" Blood Cancer J 9(2): 7.

Yoo, S. H., Y. G. Yoon, J. S. Lee, Y. S. Song, J. S. Oh, B. S. Park, T. K. Kwon, C. Park, Y. H. Choi and Y. H. Yoo (2012). "Etoposide induces a mixed type of programmed cell death and overcomes the resistance conferred by Bcl-2 in Hep3B hepatoma cells." Int J Oncol 41(4): 1443-1454.

Yoshimoto, G., T. Miyamoto, S. Jabbarzadeh-Tabrizi, T. Iino, J. L. Rocnik, Y. Kikushige, Y. Mori, T. Shima, H. Iwasaki, K. Takenaka, K. Nagafuji, S. Mizuno, H. Niiro, G. D. Gilliland and K. Akashi (2009). "FLT3-ITD up-regulates MCL-1 to promote survival of stem cells in acute myeloid leukemia via FLT3-ITD-specific STAT5 activation." Blood 114(24): 5034-5043.

Zachari, M. and I. G. Ganley (2017). "The mammalian ULK1 complex and autophagy initiation." Essays Biochem 61(6): 585-596.

Zbinden, M., A. Duquet, A. Lorente-Trigos, S. N. Ngwabyt, I. Borges and A. Ruiz i Altaba (2010). "NANOG regulates glioma stem cells and is essential in vivo acting in a cross-functional network with GLI1 and p53." EMBO J 29(15): 2659-2674.

Zeidan, A. M., D. A. Pollyea, U. Borate, A. Vasconcelos, R. Potluri, D. Rotter, Z. Kiendrebeogo, L. Gaugler, T. Prebet, M. Strocchia, G. Bonifacio and C. Chen (2023). "Venetoclax plus azacitidine compared with intensive chemotherapy as induction for patients with acute myeloid leukemia: retrospective analysis of an electronic medical record database in the United States." Ann Hematol 102(4): 749-754.

Zeng, J., O. S. Shirihai and M. W. Grinstaff (2020). "Modulating lysosomal pH: a molecular and nanoscale materials design perspective." J Life Sci (Westlake Village) 2(4): 25-37.

Zhang, D., Q. Zhao, H. Sun, L. Yin, J. Wu, J. Xu, T. He, C. Yang and C. Liang (2016). "Defective autophagy leads to the suppression of stem-like features of CD271(+) osteosarcoma cells." J Biomed Sci 23(1): 82.

Zhang, H. F., C. Wu, A. Alshareef, N. Gupta, Q. Zhao, X. E. Xu, J. W. Jiao, E. M. Li, L. Y. Xu and R. Lai (2016). "The PI3K/AKT/c-MYC Axis Promotes the Acquisition of Cancer Stem-Like Features in Esophageal Squamous Cell Carcinoma." Stem Cells 34(8): 2040-2051.

Zhao, J. C., S. Agarwal, H. Ahmad, K. Amin, J. P. Bewersdorf and A. M. Zeidan (2021). "A review of FLT3 inhibitors in acute myeloid leukemia." Blood Rev: 100905.

Zhu, P., Y. Wang, L. He, G. Huang, Y. Du, G. Zhang, X. Yan, P. Xia, B. Ye, S. Wang, L. Hao, J. Wu and Z. Fan (2015). "ZIC2-dependent OCT4 activation drives self-renewal of human liver cancer stem cells." J Clin Invest 125(10): 3795-3808.

Zhu, Y., S. Huang, S. Chen, J. Chen, Z. Wang, Y. Wang and H. Zheng (2021). "SOX2 promotes chemoresistance, cancer stem cells properties, and epithelial-mesenchymal transition by beta-catenin and Beclin1/autophagy signaling in colorectal cancer." Cell Death Dis 12(5): 449.